SUPPORTING INFORMATION

Synthesis of enantiomerically pure ring-substituted L-pyridylalanines by biocatalytic hydroamination

Syed T. Ahmed, Fabio Parmeggiani, Nicholas J. Weise, Sabine L. Flitsch, Nicholas J. Turner*

School of Chemistry, The University of Manchester, Manchester Institute of Biotechnology (MIB), 131 Princess Street, M1 7DN, Manchester, United Kingdom

Table of Contents **Page**

* Corresponding author. E-mail address: nicholas.turner@manchester.ac.uk

General methods

Chemicals and enzymes

Analytical grade reagents, solvents and heteroaromatic aldehydes were obtained from Sigma-Aldrich, Alfa-Aesar or Fluorochem and have been used without further purification. D-amino acid oxidase (DAAO) from porcine kidney and L-amino acid oxidase (LAAO) from *Crotalus adamanteus* were purchased from Sigma-Aldrich.

NMR spectroscopy

^{1}H and ^{13}C NMR spectra were recorded on a Bruker Avance 400 spectrometer (400 MHz) at 298 K without additional internal standard. Chemical shifts are reported as δ in parts per million (ppm) and are calibrated against residual solvent signal. A water suppression method was used to obtain the ^{1}H NMR spectra in water, with D_2O as the residual solvent peak (^{1}H NMR: D_2O = 4.79 ppm). ^{1}H NMR data were analysed on MestreNova and are reported as follows: chemical shift (ppm), multiplicity (s = singlet, d = doublet, dd = doublet of doublets, t = triplet, m = multiplet), coupling constants (Hz) and integration. ^{13}C NMR data for compounds **4b, 4d** and **5e** were recorded on a Bruker Avance III 500 spectrometer (500 MHz).

High-resolution mass spectrometry

HRMS analysis was performed using a Waters LCT time-of-flight mass spectrometer connected to a Waters Alliance LC (Waters, Milford, MA, USA). For halogen-substituted compounds, only the ion containing the most abundant isotope was reported (^{79}Br and ^{35}Cl).

Molecular biology protocols

Strains and plasmids

E. coli BL21(DE3) was used as an expression host for protein production. The pET16b-AvPAL plasmid containing *Anabaena variabilis* (codon-optimised for *E. coli*) was obtained as described previously.[1]

Standard LB medium was used for cell growth, with the addition of ampicillin (Amp) to a final concentration of 100 μg mL^{-1}. Solid media were prepared by addition of agar (1.5% w/v) to liquid media.

Transformation into competent cells

Competent cells (50 μL aliquot) were thawed on ice for 15 min, transferred to a pre-chilled tube containing plasmid DNA (20-50 ng). The tubes were gently flicked for mixing, incubated in ice for 30 min, heat-shocked at 42°C for 30 s and transferred back to ice for 5 min. SOC medium (900 μL) was added to the tube under sterile conditions and incubated at 37°C, 250 rpm for 1 h. The culture was then concentrated to 100 μL (by centrifugation and resuspension) and spread across an LB plate containing ampicillin, under sterile condition. Plates were incubated overnight at 37°C and stored at 4˚C.

Biocatalyst production

A single colony of *E. coli* BL21(DE3) carrying the pET16b-AvPAL plasmid was used to inoculate LB medium (8 mL) supplemented with ampicillin, which was grown overnight at 37°C and 220 rpm. The starter culture was used to inoculate LB-based auto-induction medium[2] (800 mL, Formedium) containing ampicillin and glycerol (0.5% v/v) which was incubated at 18°C and 250 rpm for 4 days. The cells (approximately 5 g) were harvested by centrifugation (5,000 rpm, 20 min, 4°C) and flash frozen in liquid nitrogen. Frozen cells were lyophilized under high vacuum overnight to yield the powdered formulation of the biocatalyst which was stored at –20°C.

NMR time-course experiment

Conversion for compounds **3g-l** were obtained by ^{1}H NMR, monitoring the appearance of the ABX system corresponding to the aliphatic portion of the amino acid and the disappearance of the acrylic acid doublets. A sample of the crude biotransformation mixture (600 µL) was added to D_2O (200 µL), thoroughly mixed and centrifuged to remove whole cell components and insoluble solids. The supernatant was then analysed by NMR with suppression of the residual water signal. Representative spectra are shown in the following.

3h

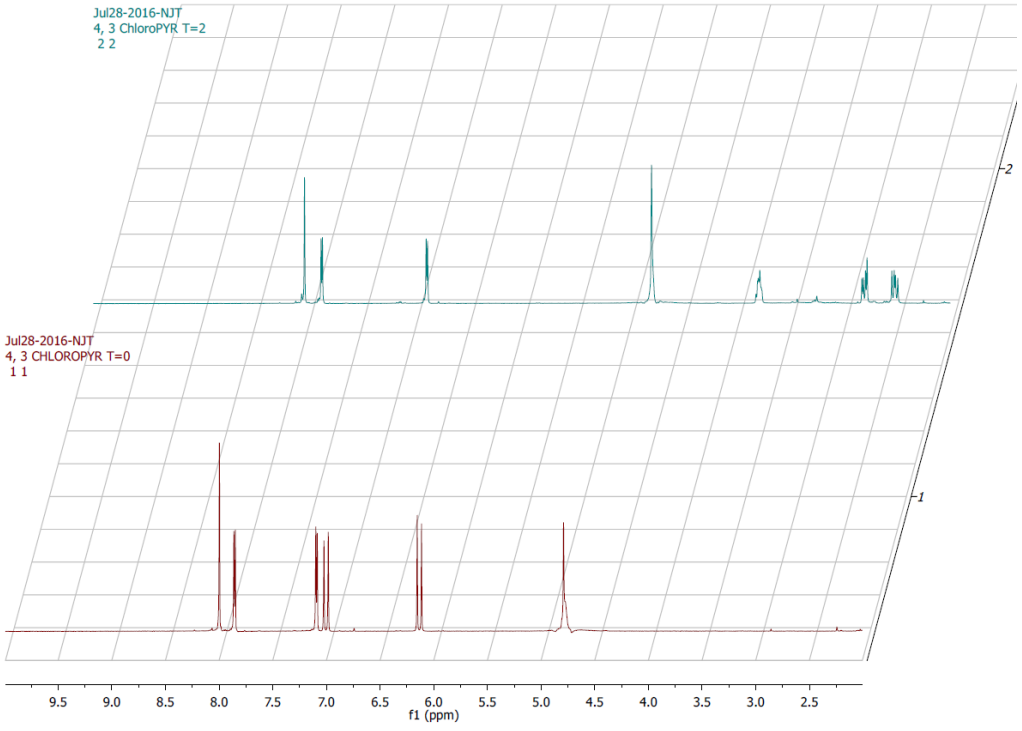

3i

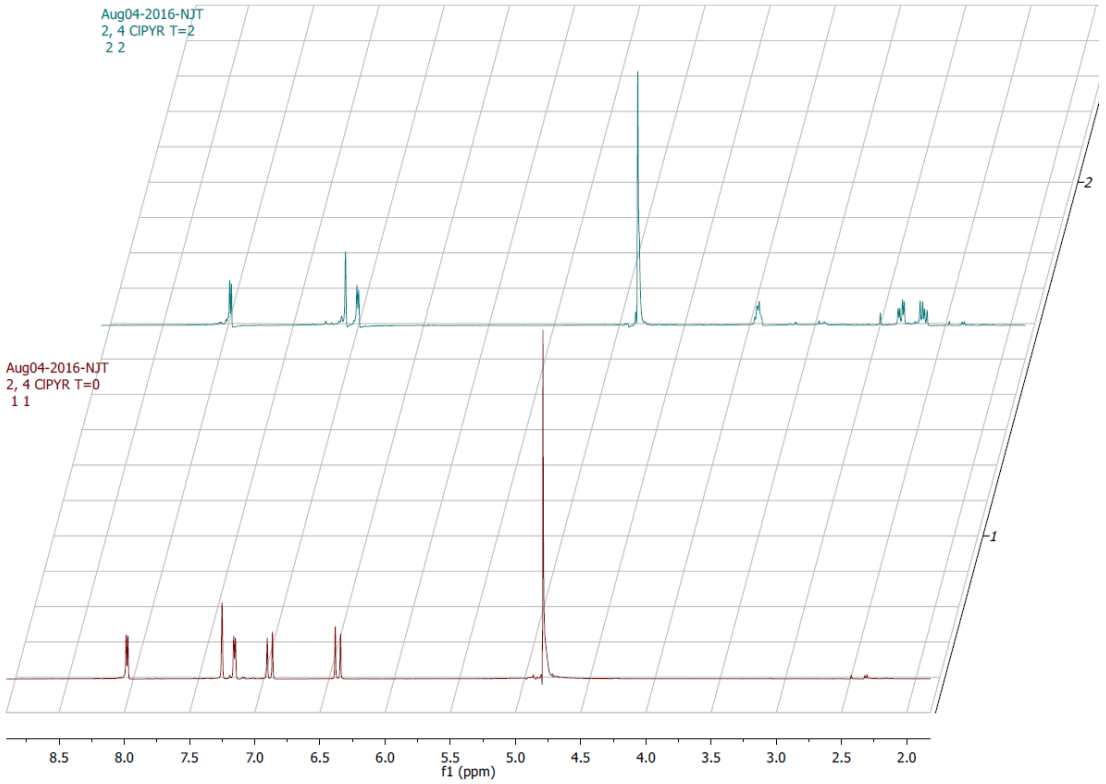
Aug04-2016-NJT
2, 4 ClPYR T=2
2 2
Aug04-2016-NJT
2, 4 ClPYR T=0
1 1
2
1
8.5
8.0
7.5
7.0
6.5
6.0
5.5
5.0
4.5
4.0
3.5
3.0
2.5
2.0
f1 (ppm)

3j

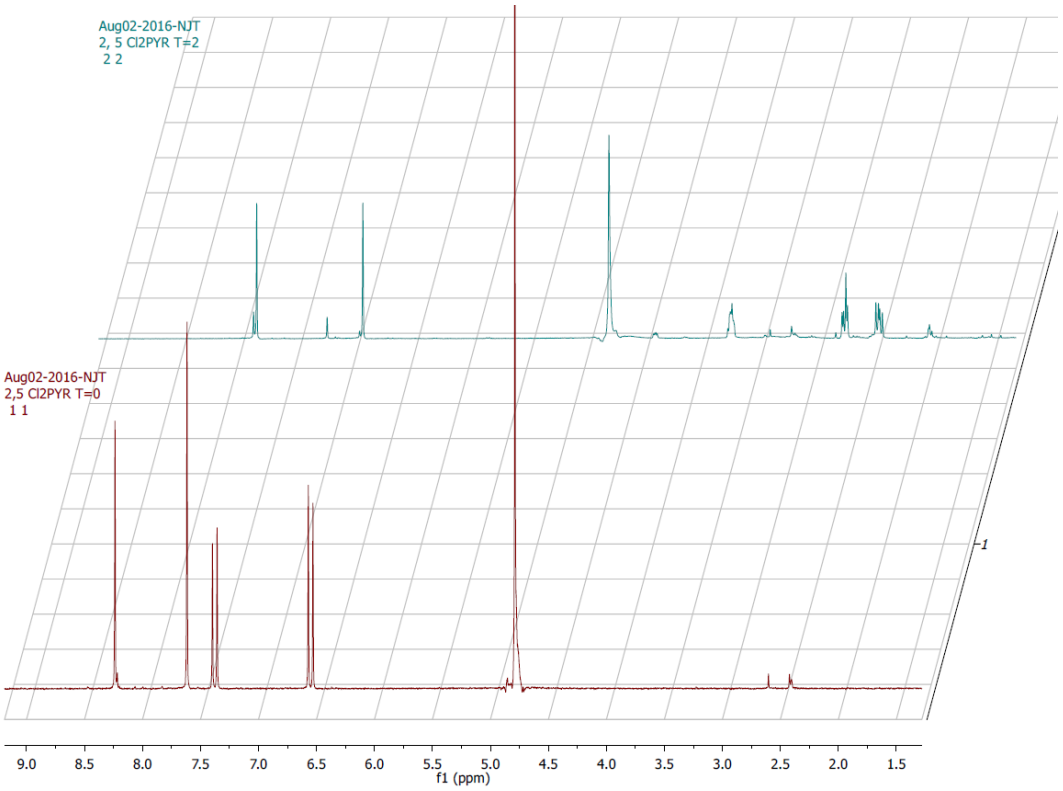
Aug02-2016-NJT
2, 5 Cl2PYR T=2
2 2
Aug02-2016-NJT
2,5 Cl2PYR T=0
1 1
1
9.0
8.5
8.0
7.5
7.0
6.5
6.0
5.5
5.0
4.5
4.0
3.5
3.0
2.5
2.0
1.5
f1 (ppm)

3k

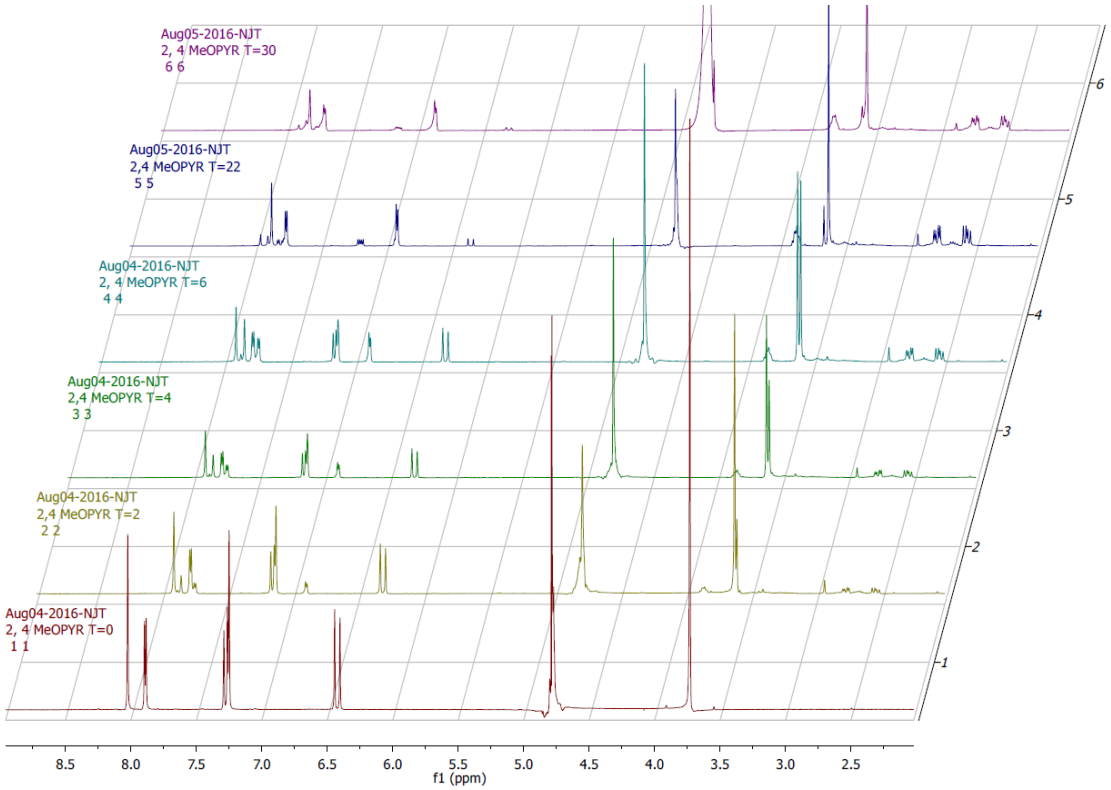
Aug05-2016-NJT
2, 4 MeOPYR T=30
6 6
Aug05-2016-NJT
2,4 MeOPYR T=22
5 5
Aug04-2016-NJT
2, 4 MeOPYR T=6
4 4
Aug04-2016-NJT
2,4 MeOPYR T=4
3 3
Aug04-2016-NJT
2,4 MeOPYR T=2
2 2
Aug04-2016-NJT
2, 4 MeOPYR T=0
1 1
8.5 8.0 7.5 7.0 6.5 6.0 5.5 5.0 4.5 4.0 3.5 3.0 2.5
f1 (ppm)

3l

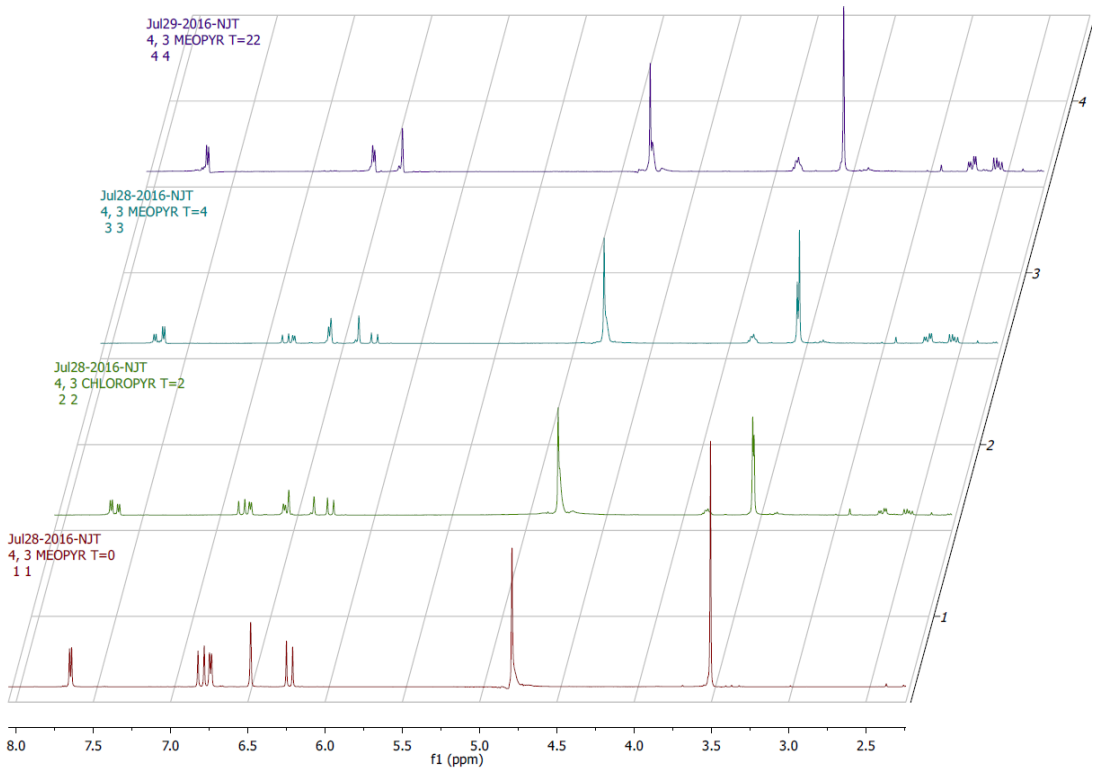
Jul29-2016-NJT
4, 3 MEOPYR T=22
4 4
Jul28-2016-NJT
4, 3 MEOPYR T=4
3 3
Jul28-2016-NJT
4, 3 CHLOROPYR T=2
2 2
Jul28-2016-NJT
4, 3 MEOPYR T=0
1 1
8.0 7.5 7.0 6.5 6.0 5.5 5.0 4.5 4.0 3.5 3.0 2.5
f1 (ppm)

5a

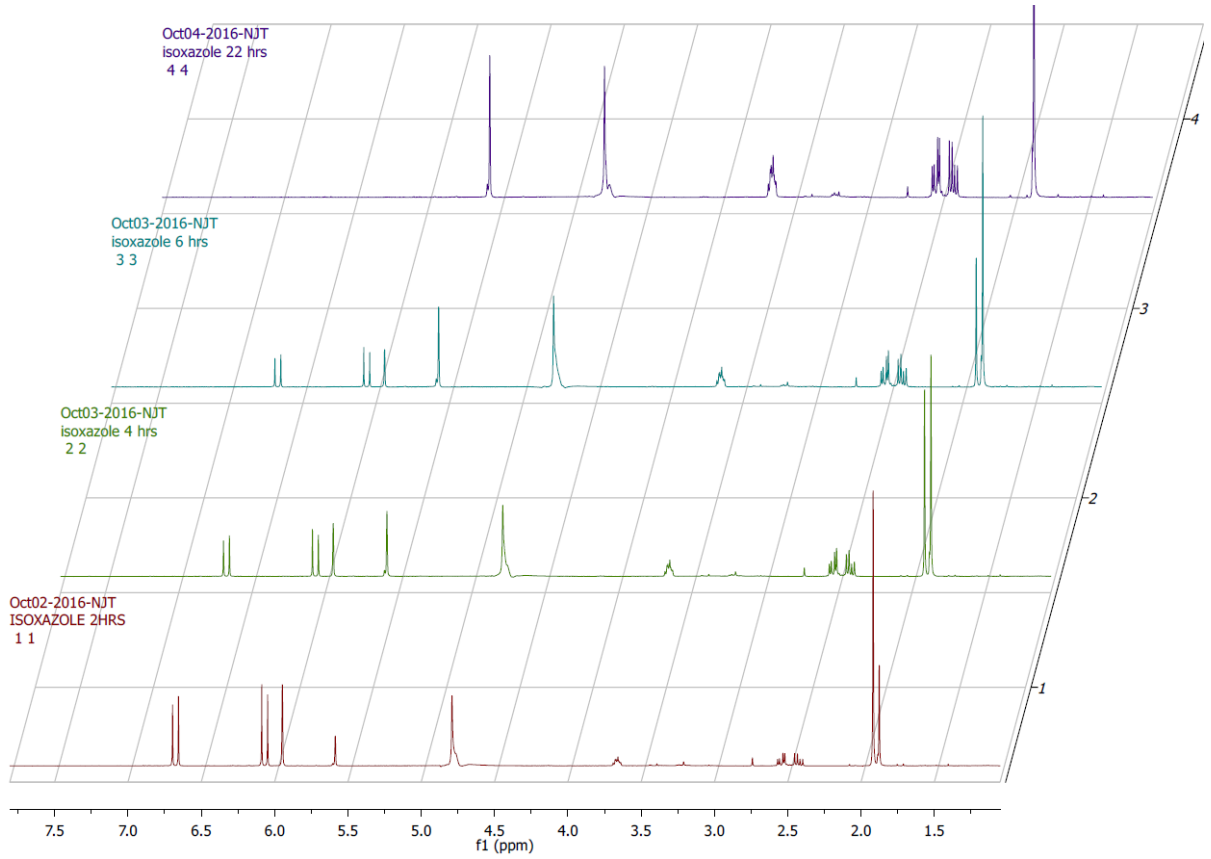
Oct04-2016-NJT
isoxazole 22 hrs
4 4
Oct03-2016-NJT
isoxazole 6 hrs
3 3
Oct03-2016-NJT
isoxazole 4 hrs
2 2
Oct02-2016-NJT
ISOXAZOLE 2HRS
1 1
4
3
2
1
7.5
7.0
6.5
6.0
5.5
5.0
4.5
4.0
3.5
3.0
2.5
2.0
1.5
f1 (ppm)

5b

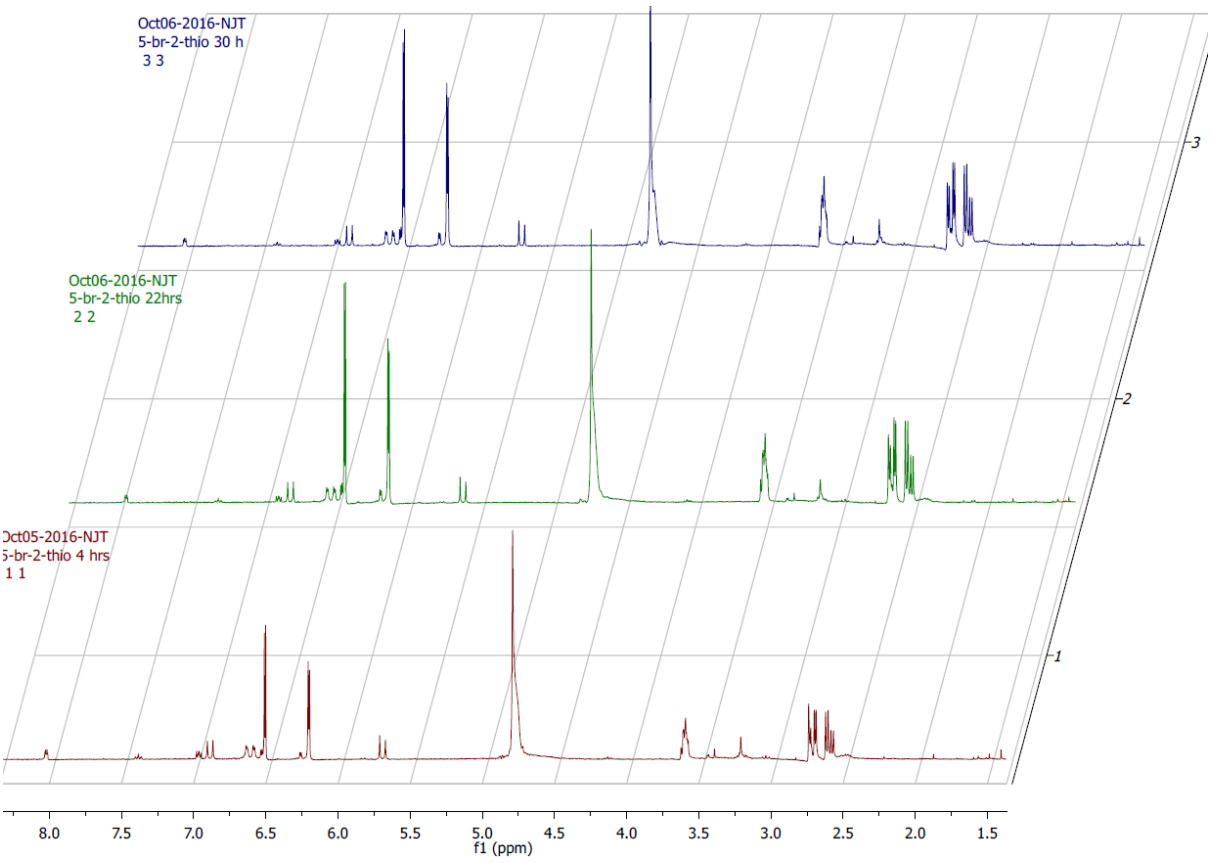
Oct06-2016-NJT
5-br-2-thio 30 h
3 3
Oct06-2016-NJT
5-br-2-thio 22hrs
2 2
Oct05-2016-NJT
5-br-2-thio 4 hrs
1 1
3
2
1
8.0
7.5
7.0
6.5
6.0
5.5
5.0
4.5
4.0
3.5
3.0
2.5
2.0
1.5
f1 (ppm)

5c

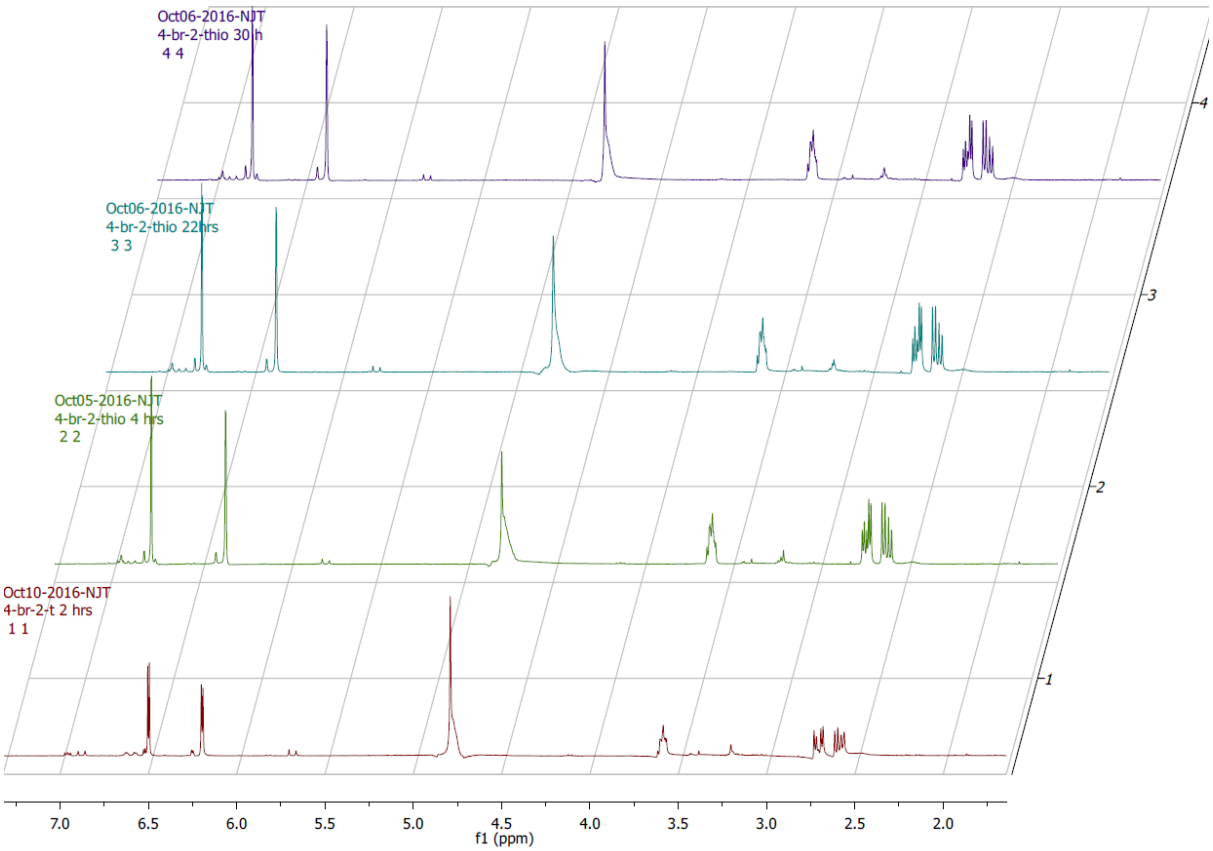
Oct06-2016-NJT
4-br-2-thio 30 h
4 4
Oct06-2016-NJT
4-br-2-thio 22hrs
3 3
Oct05-2016-NJT
4-br-2-thio 4 hrs
2 2
Oct10-2016-NJT
4-br-2-t 2 hrs
1 1
4
3
2
1
7.0
6.5
6.0
5.5
5.0
4.5
4.0
3.5
3.0
2.5
2.0
f1 (ppm)

5d

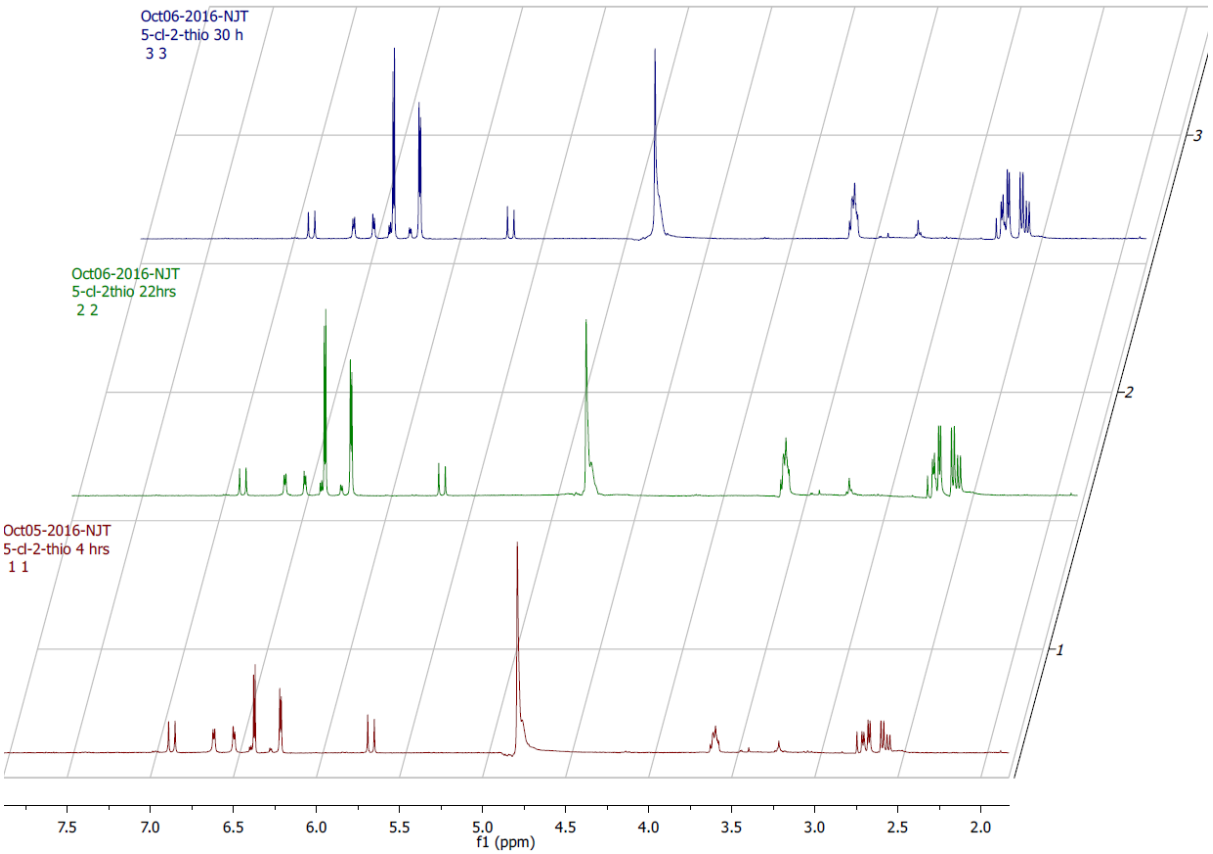
Oct06-2016-NJT
5-cl-2-thio 30 h
3 3
Oct06-2016-NJT
5-cl-2thio 22hrs
2 2
Oct05-2016-NJT
5-cl-2-thio 4 hrs
1 1
3
2
1
7.5
7.0
6.5
6.0
5.5
5.0
4.5
4.0
3.5
3.0
2.5
2.0
f1 (ppm)

5e

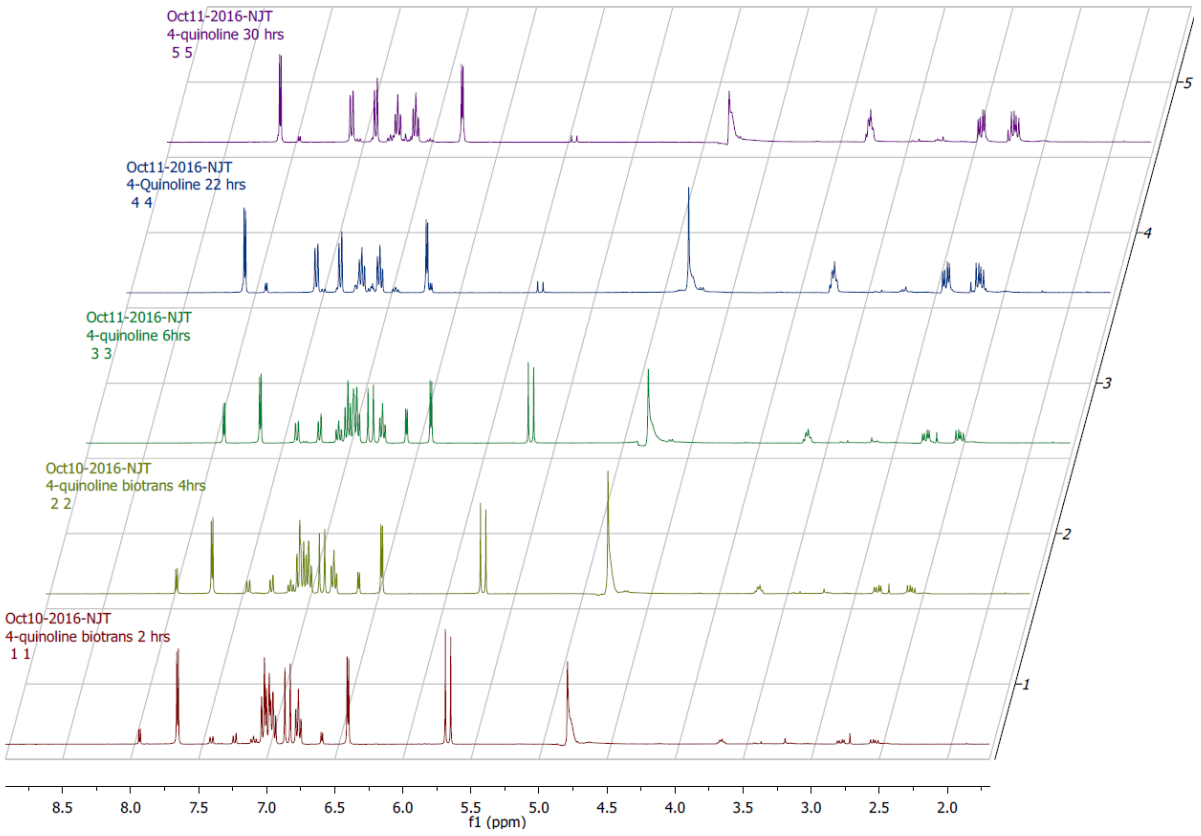
Oct11-2016-NJT
4-quinoline 30 hrs
5 5
Oct11-2016-NJT
4-Quinoline 22 hrs
4 4
Oct11-2016-NJT
4-quinoline 6hrs
3 3
Oct10-2016-NJT
4-quinoline biotrans 4hrs
2 2
Oct10-2016-NJT
4-quinoline biotrans 2 hrs
1 1
5
4
3
2
1
8.5
8.0
7.5
7.0
6.5
6.0
5.5
5.0
4.5
4.0
3.5
3.0
2.5
2.0
f1 (ppm)

Telescopic synthesis of L-5a-f

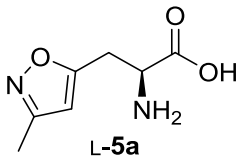

L-**5a**

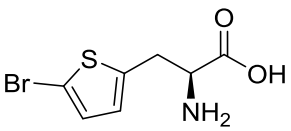

L-**5b**

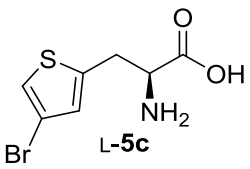

L-**5c**

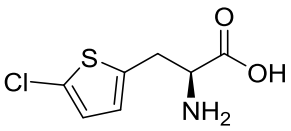

L-**5d**

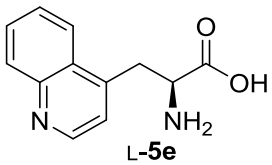

L-**5e**

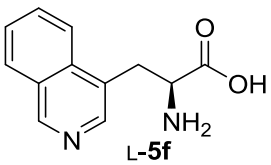

L-**5f**

Prod.	Time (h)	Conv. (%)	ee (%)	Isol. yield (%)
5a	22	>99	>99	40
5b	4	88	>99	35
5c	4	95	>99	54
5d	4	80	>99	44
5e	22	93	>99	37
5f	30	<5	–	–

Unsuccessful biotransformations/syntheses

(*E*)-3-(6-methoxypyridin-3-yl) acrylic acid (**2m**) was synthesized and tested with AvPAL. No conversion was observed after 30 h incubation.

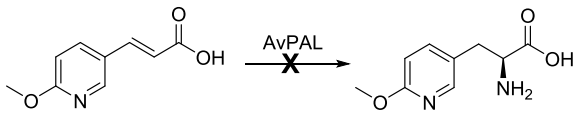

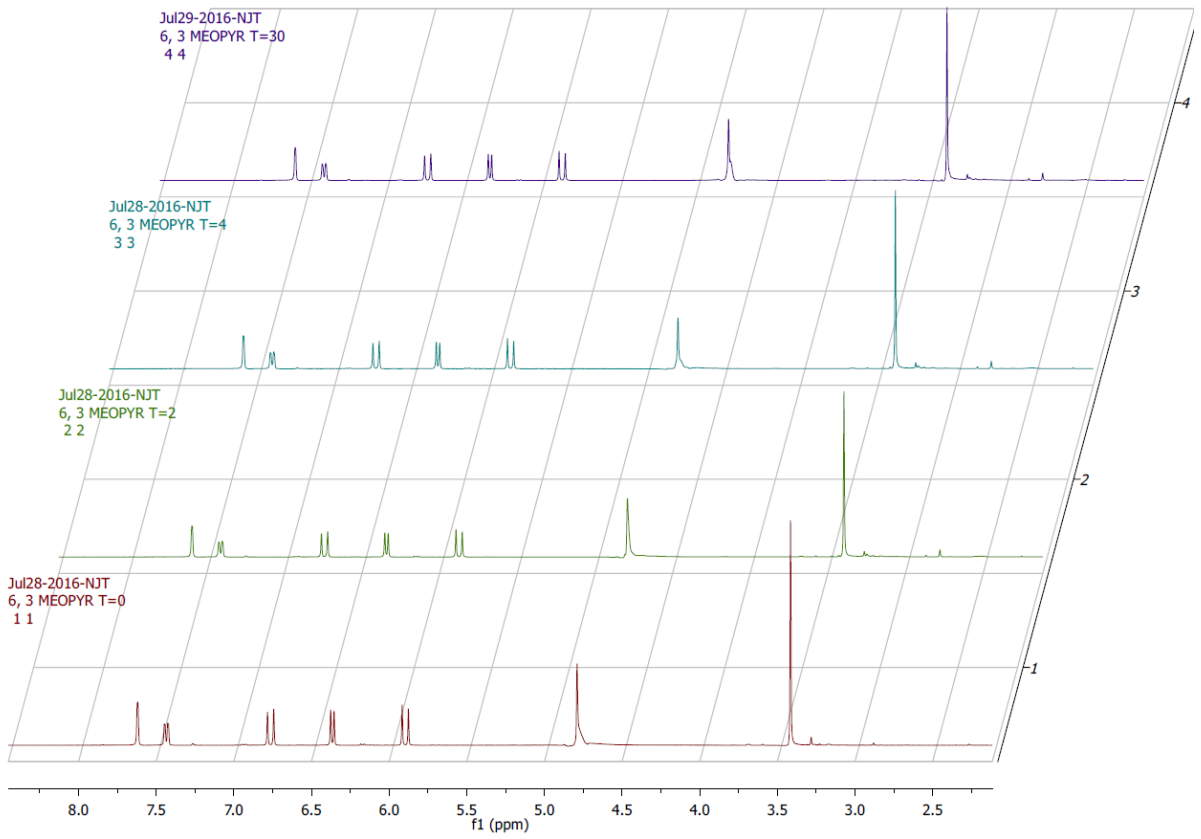

Also, the synthesis and isolation of (*E*)-3-(2-bromopyridin-3-yl)acrylic acid (**2n**) was unsuccessful, with no trace of the acrylic acid doublets present whilst following the reaction by NMR. The reaction mixture turned black (as opposed to being colorless to pale yellow) yielding a black/grey solid.

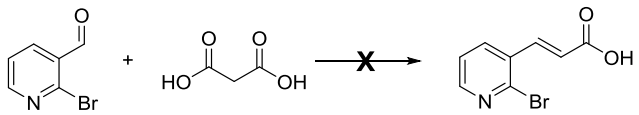

(E)-3-(isoquinolin-4-yl)acrylic acid (**4f**) was synthesized successfully and tested with AvPAL yielding no conversion after 30 h incubation.

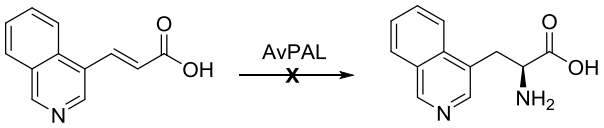

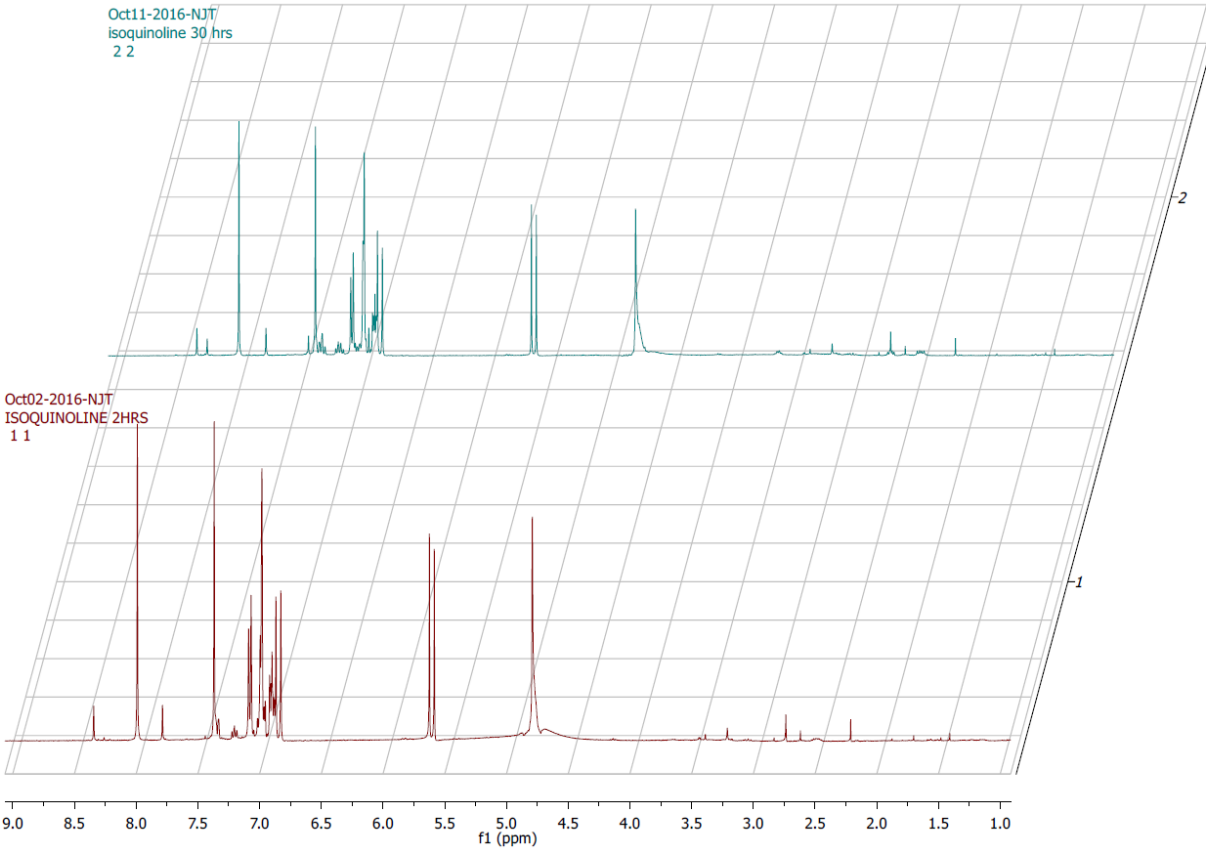

HPLC methods

Conversion

The conversion of compounds **2a-f** to **3a-f** was measured on a non-chiral reverse-phase Zorbax C-18 Extend column (50 mm x 4.5 µm, Agilent). Mobile phase aq. NH_4OH 0.1 M pH 10 / MeOH 90:10 (12 min), flow rate 1 mL min^{-1}, temperature 40°C, detection wavelength 210 nm (retention time are reported below).

	Retention time (t_R) [min]	
	3	**2**
a	2.30	5.00
b	2.37	5.35
c	2.65	7.01
d	3.17	8.53
e	1.80	3.40
f	1.90	3.16

Enantiomeric excess

The optical purity of amino acid products **3a-j** and **5a-e** was measured on a reverse-phase Crownpak CR(+) column (150 mm x 4 mm x 3.5 µm, Daicel). Mobile phase aq. $HClO_4$ 1.14% w/v / MeOH 96:4, flow rate 1.0 mL min^{-1}, temperature 40°C, detection wavelength 210 nm. The optical purity of amino acid products **3k-l** was measured on a reverse-phase Chirobiotic T column (250 mm x 46 mm x 5 µM, Supelco). Mobile phase H_2O/MeOH 60:40, flow rate 0.8 mL min^{-1}, temperature 40°C, detection wavelength 210 nm (retention times are reported below).

	Retention time (t_R) [min]	
	D-**3**	L-**3**
a	5.45	7.20
b	3.58	4.28
c	7.45	9.76
d	7.57	9.06
e	4.01	5.56
f	1.93	2.14
g	3.23	6.79
h	1.84	2.06
i	3.35	4.55
j	6.94	9.21
k	–[a]	8.65
l	6.16	5.59

[a]D-**3k** could not be produced with the method described below.

	Retention time (t_R) [min]	
	D-**5**	L-**5**
a	2.17	2.54
b	19.80	26.25
c	16.15	22.80
d	14.00	18.50
e	–[a]	2.10

[a]D-**5e** could not be produced with the method described below.

Compounds **3a**, **g**, **k**, **l** gave >99% L-enantiomer in all cases. In order to verify the separation capability of the column employed, a deracemisation was performed to produce a small but measurable amount of the D-enantiomer. This was done with a chemo-enzymatic cascade identical to the one described in the paper for the chiral polishing of the L-enantiomer (as shown in the scheme below), but using in this case L-amino acid oxidase (LAAO) instead of DAAO.

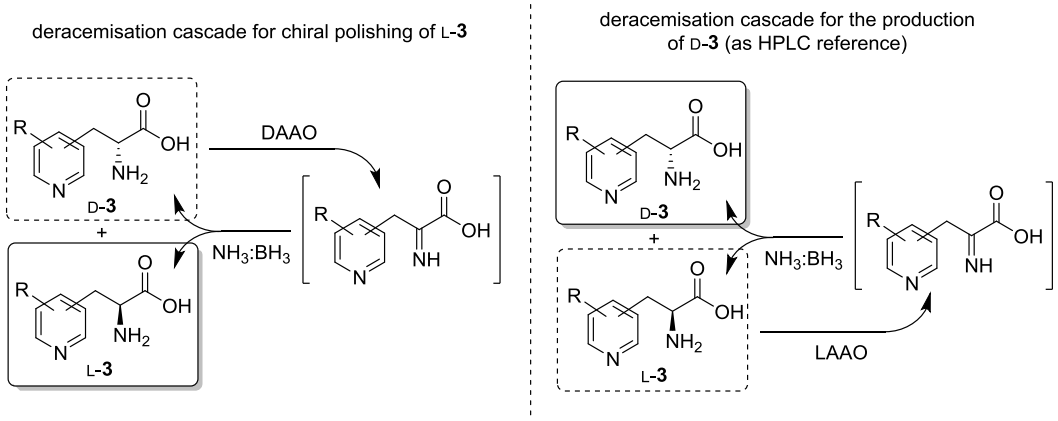

Chiral HPLC chromatograms

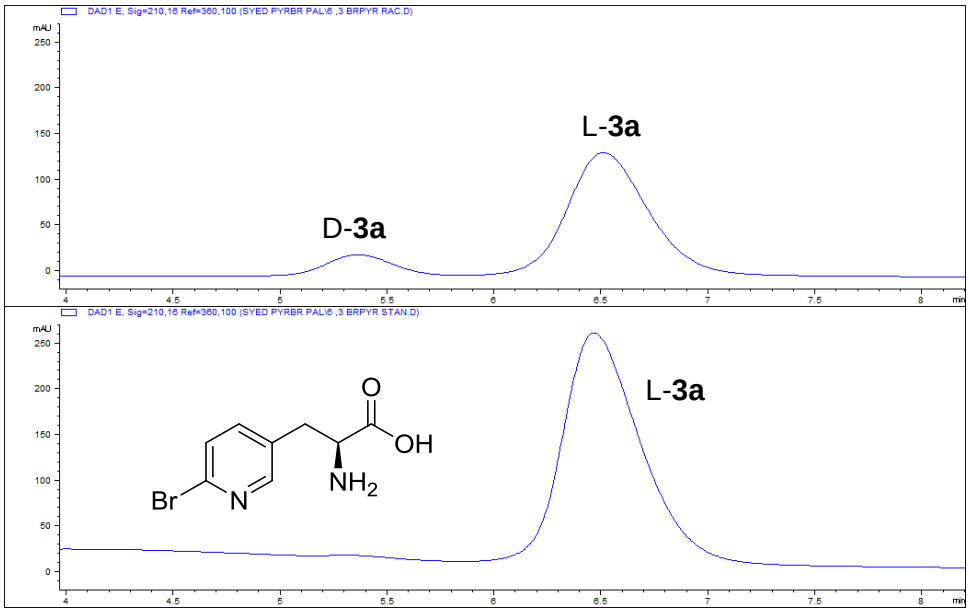

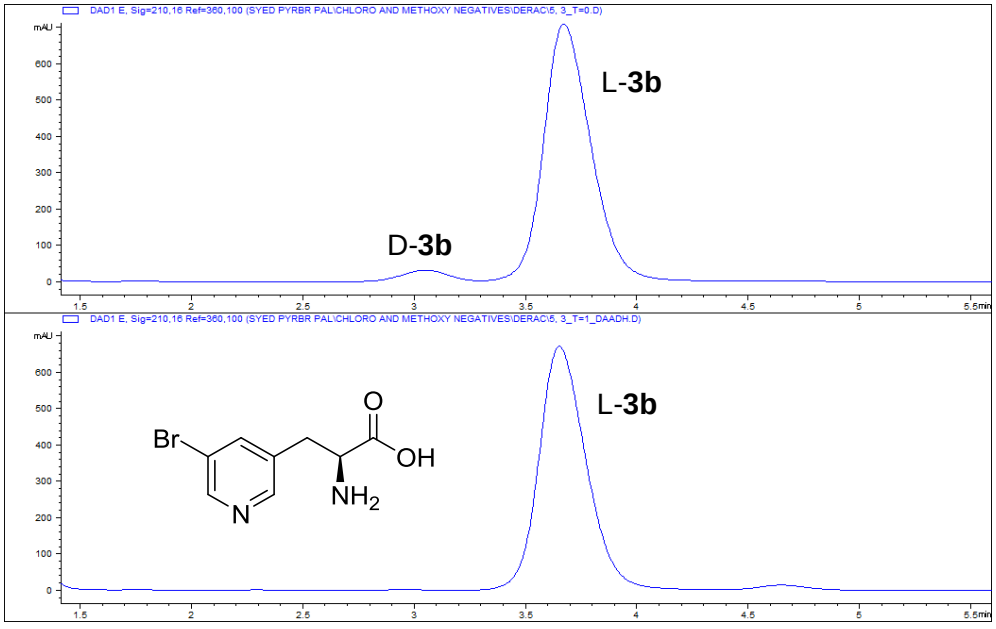

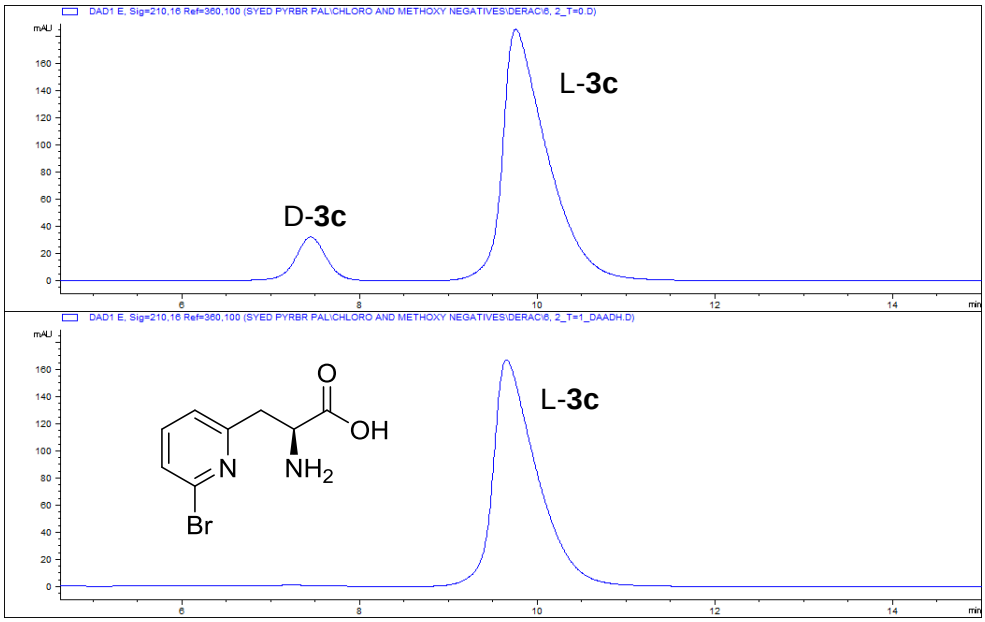
DAD1 E, Sig=210,16 Ref=360,100 (SYED PYRBR PAL\CHLORO AND METHOXY NEGATIVES\DERAC\5, 2_T=0.D)
mAU
D-3c
L-3c
min
DAD1 E, Sig=210,16 Ref=360,100 (SYED PYRBR PAL\CHLORO AND METHOXY NEGATIVES\DERAC\5, 2_T=1_DAADH.D)
mAU
L-3c
O
OH
N
NH2
Br
min

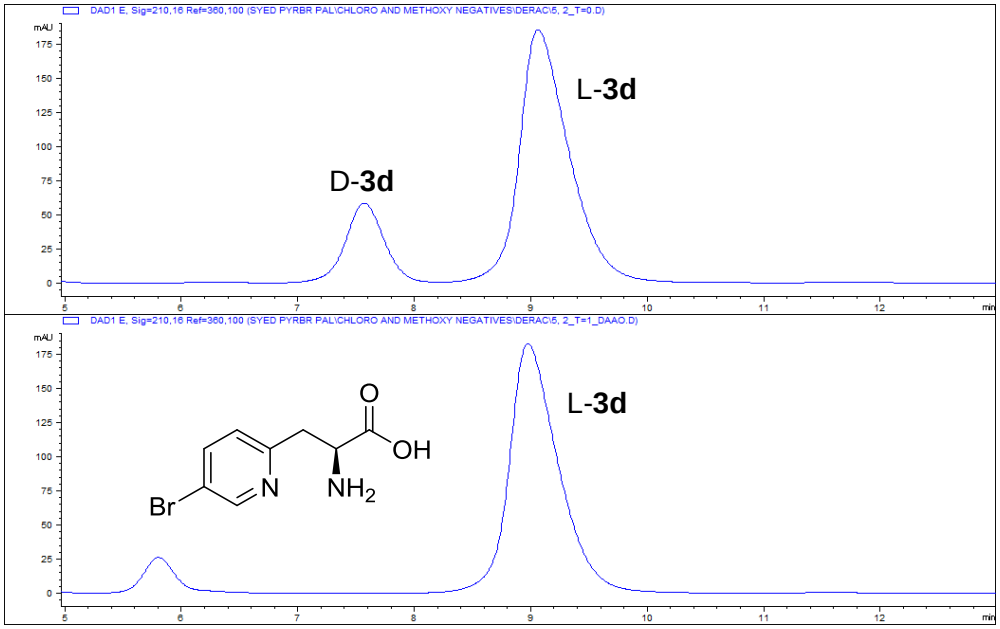
DAD1 E, Sig=210,16 Ref=360,100 (SYED PYRBR PAL\CHLORO AND METHOXY NEGATIVES\DERAC\5, 2_T=0.D)
mAU
D-3d
L-3d
min
DAD1 E, Sig=210,16 Ref=360,100 (SYED PYRBR PAL\CHLORO AND METHOXY NEGATIVES\DERAC\5, 2_T=1_DAAO.D)
mAU
L-3d
O
OH
Br
N
NH2
min

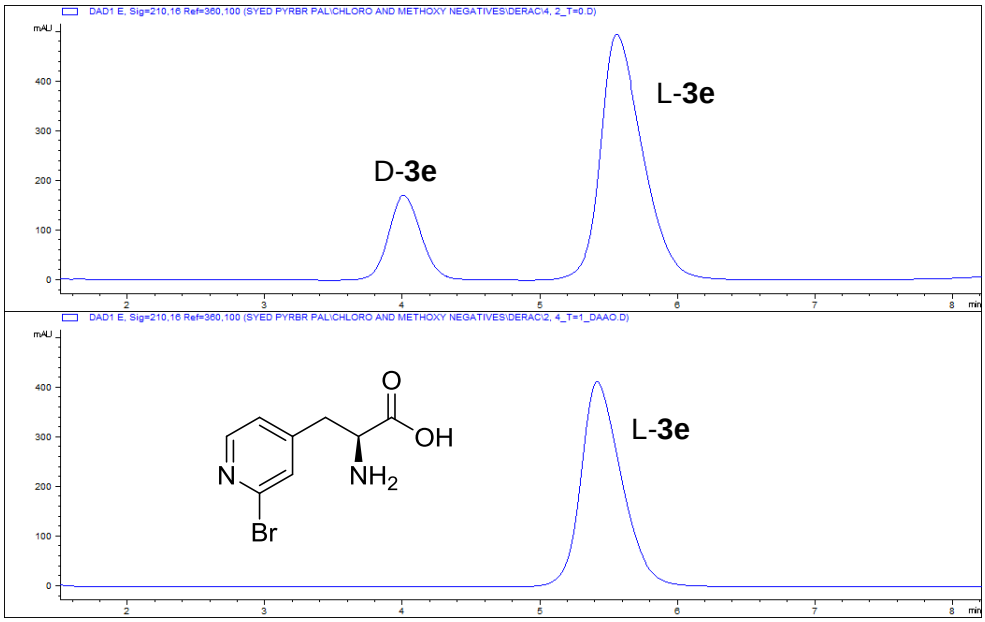
DAD1 E, Sig=210,16 Ref=360,100 (SYED PYRBR PAL\CHLORO AND METHOXY NEGATIVES\DERAC\4, 2_T=0.D)
mAU
D-3e
L-3e
min
DAD1 E, Sig=210,16 Ref=360,100 (SYED PYRBR PAL\CHLORO AND METHOXY NEGATIVES\DERAC\2, 4_T=1_DAAO.D)
O
OH
N
NH2
Br
L-3e

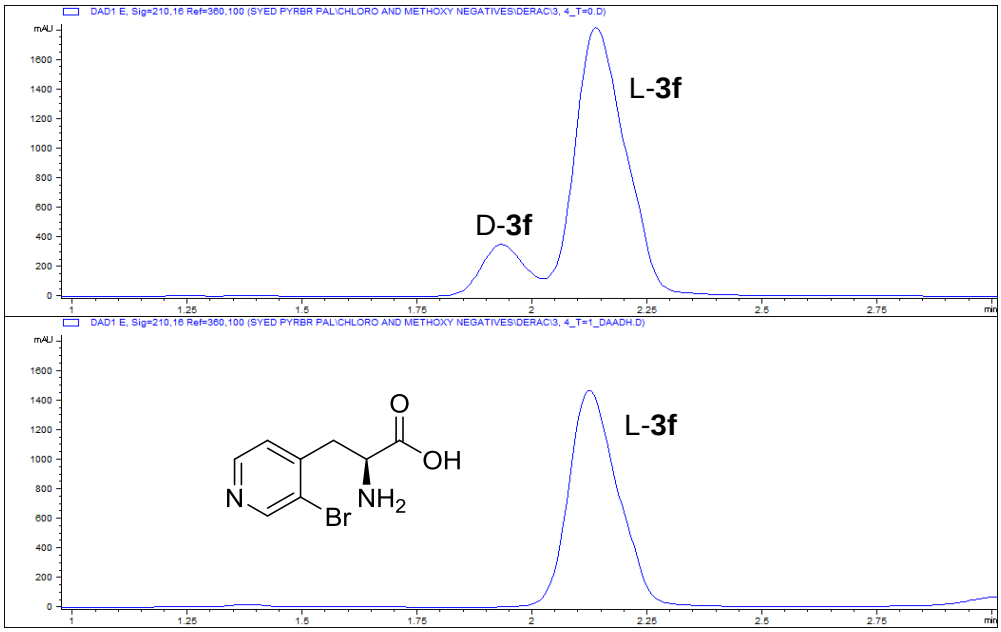
DAD1 E, Sig=210,16 Ref=360,100 (SYED PYRBR PAL\CHLORO AND METHOXY NEGATIVES\DERAC\3, 4_T=0.D)
mAU
L-3f
D-3f
min
DAD1 E, Sig=210,16 Ref=360,100 (SYED PYRBR PAL\CHLORO AND METHOXY NEGATIVES\DERAC\3, 4_T=1_DAADH.D)
O
OH
N
NH2
Br
L-3f

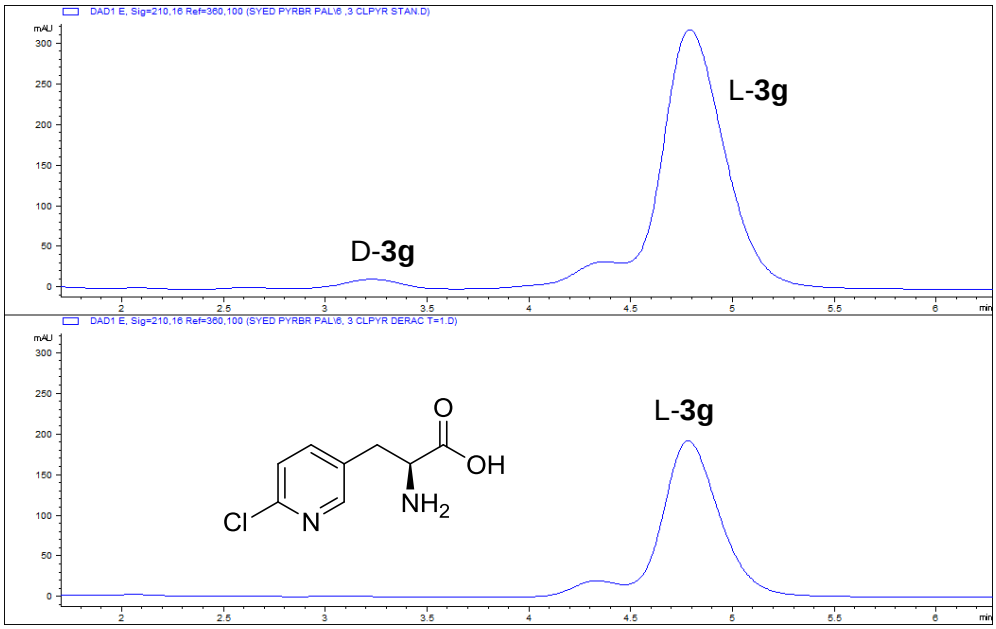
DAD1 E, Sig=210,16 Ref=360,100 (SYED PYRBR PAL\6 ,3 CLPYR STAN.D)
mAU
L-3g
D-3g
DAD1 E, Sig=210,16 Ref=360,100 (SYED PYRBR PAL\6, 3 CLPYR DERAC T=1.D)
L-3g
O
OH
NH2
Cl
N
min

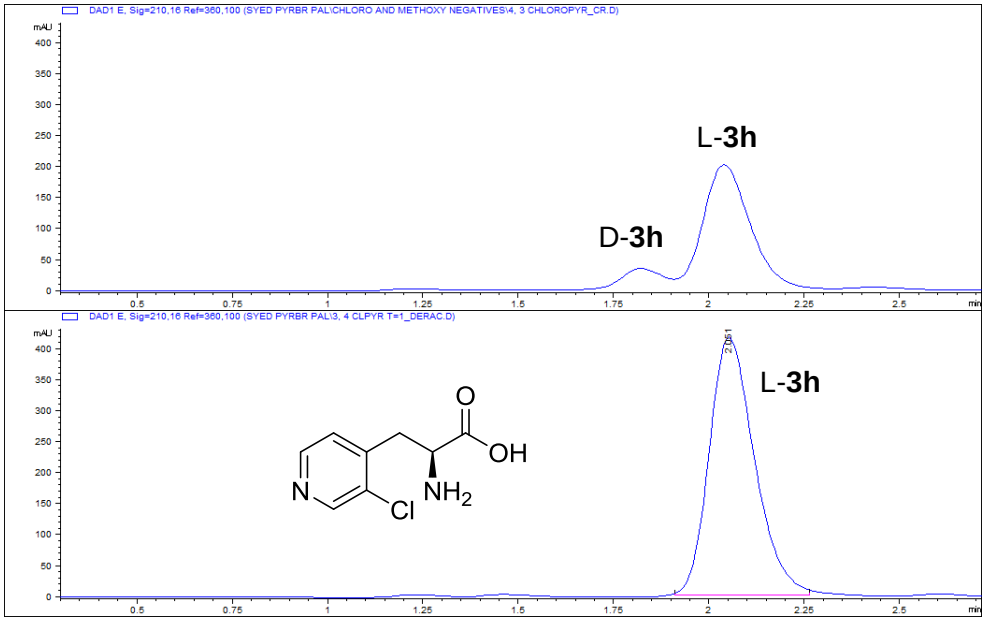
DAD1 E, Sig=210,16 Ref=360,100 (SYED PYRBR PAL\CHLORO AND METHOXY NEGATIVES\4, 3 CHLOROPYR_CR.D)
mAU
L-3h
D-3h
DAD1 E, Sig=210,16 Ref=360,100 (SYED PYRBR PAL\3, 4 CLPYR T=1_DERAC.D)
L-3h
O
OH
NH2
N
Cl
min

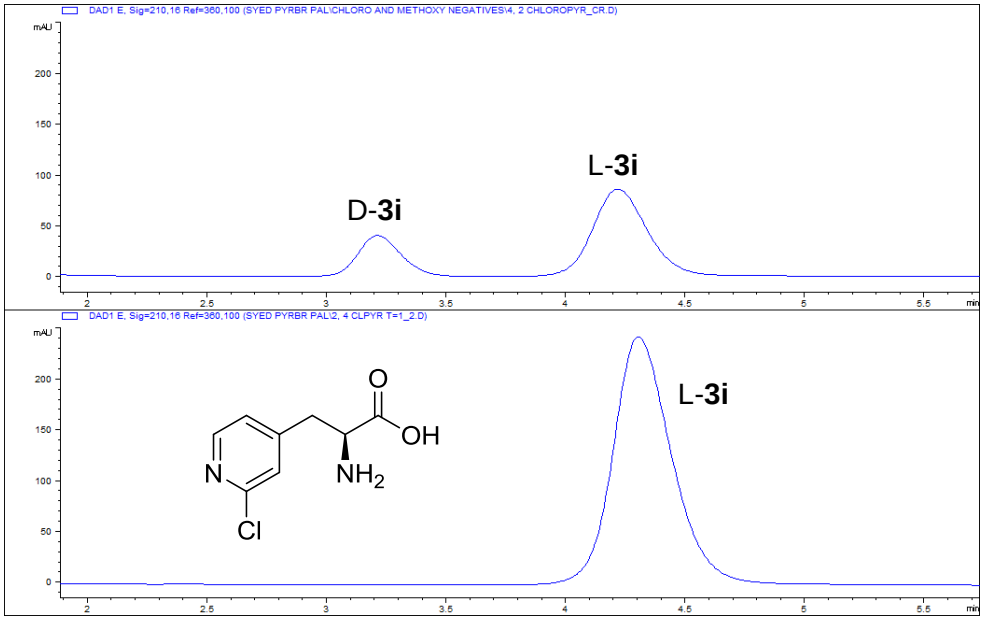
DAD1 E, Sig=210,16 Ref=360,100 (SYED PYRBR PAL\CHLORO AND METHOXY NEGATIVES\4, 2 CHLOROPYR_CR.D)
mAU
D-3i
L-3i
min
DAD1 E, Sig=210,16 Ref=360,100 (SYED PYRBR PAL\2, 4 CLPYR T=1_2.D)
mAU
L-3i
O
OH
N
NH2
Cl
min

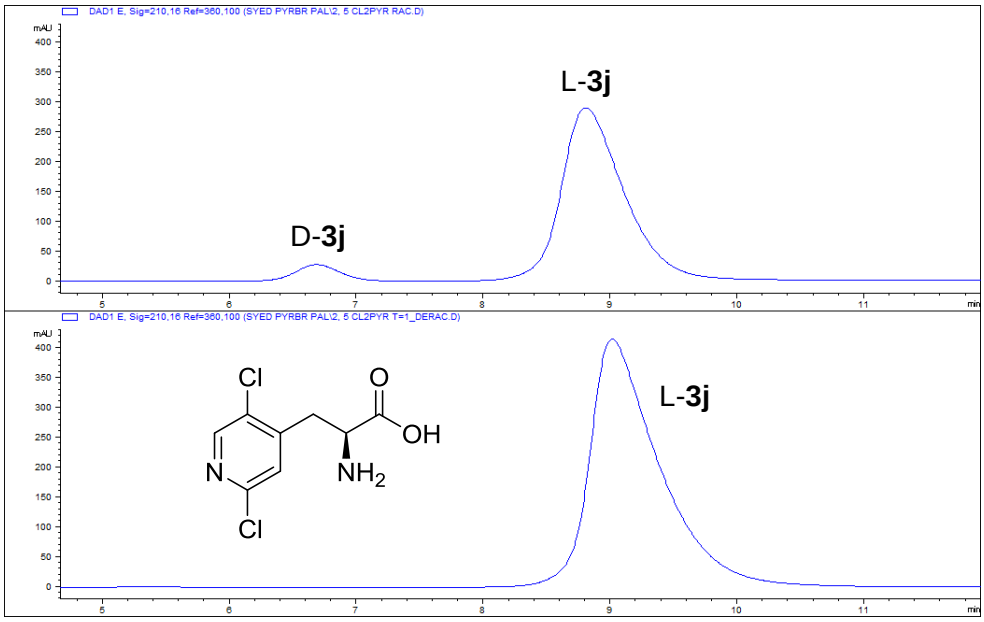
DAD1 E, Sig=210,16 Ref=360,100 (SYED PYRBR PAL\2, 5 CL2PYR RAC.D)
mAU
L-3j
D-3j
min
DAD1 E, Sig=210,16 Ref=360,100 (SYED PYRBR PAL\2, 5 CL2PYR T=1_DERAC.D)
mAU
L-3j
Cl
O
OH
N
NH2
Cl
min

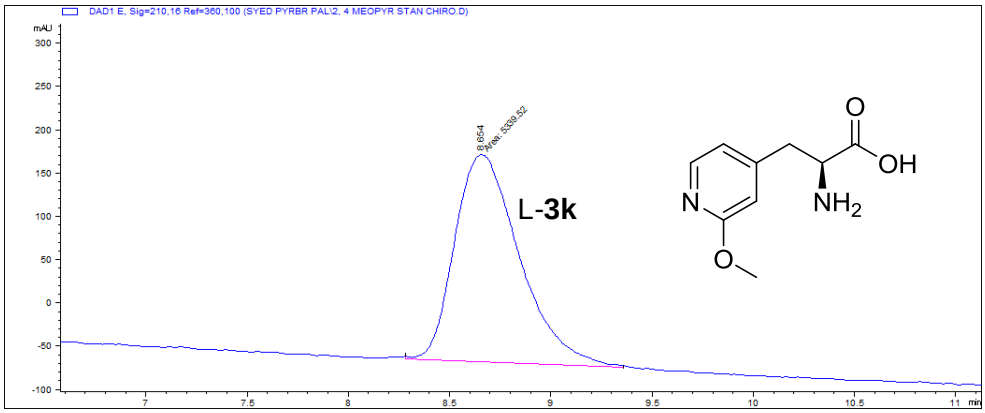
DAD1 E, Sig=210,16 Ref=360,100 (SYED PYRBR PAL\2, 4 MEOPYR STAN CHIRO.D)
mAU
8.654
Area: 5339.52
L-3k
O
OH
NH2
N
O

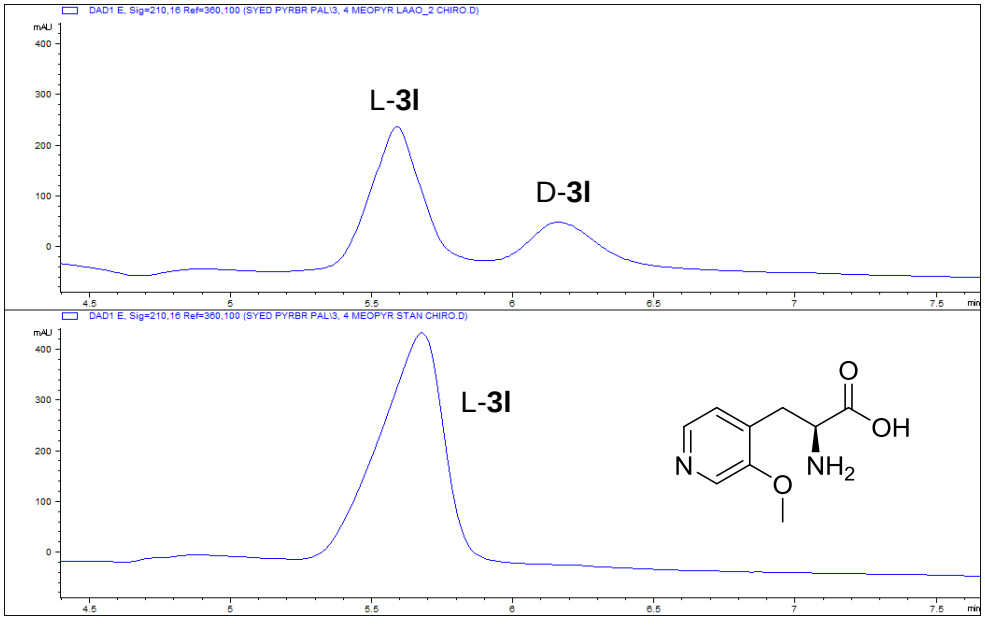
DAD1 E, Sig=210,16 Ref=360,100 (SYED PYRBR PAL\3, 4 MEOPYR LAAO_2 CHIRO.D)
mAU
L-3l
D-3l
min
DAD1 E, Sig=210,16 Ref=360,100 (SYED PYRBR PAL\3, 4 MEOPYR STAN CHIRO.D)
mAU
L-3l
O
OH
NH2
N
O
min

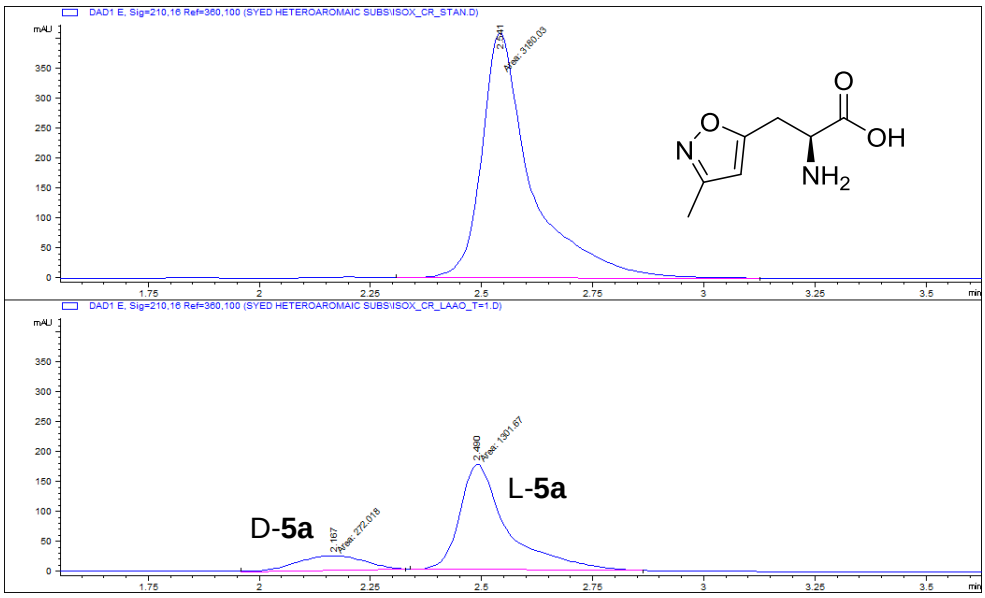
DAD1 E, Sig=210,16 Ref=360,100 (SYED HETEROAROMAIC SUBS\ISOX_CR_STAN.D)
mAU
2.541
Area: 3160.03
O
OH
N
O
NH2
DAD1 E, Sig=210,16 Ref=360,100 (SYED HETEROAROMAIC SUBS\ISOX_CR_LAAO_T=1.D)
2.490
Area: 1301.67
L-5a
D-5a
2.167
Area: 272.018
min

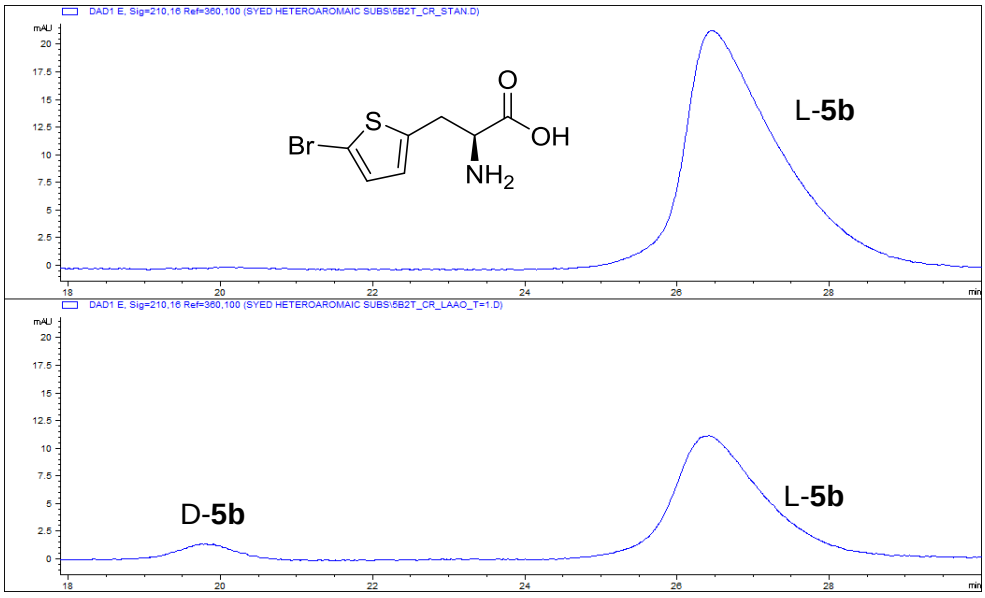
DAD1 E, Sig=210,16 Ref=360,100 (SYED HETEROAROMAIC SUBS\5B2T_CR_STAN.D)
mAU
O
S
OH
Br
NH2
L-5b
DAD1 E, Sig=210,16 Ref=360,100 (SYED HETEROAROMAIC SUBS\5B2T_CR_LAAO_T=1.D)
D-5b
L-5b
min

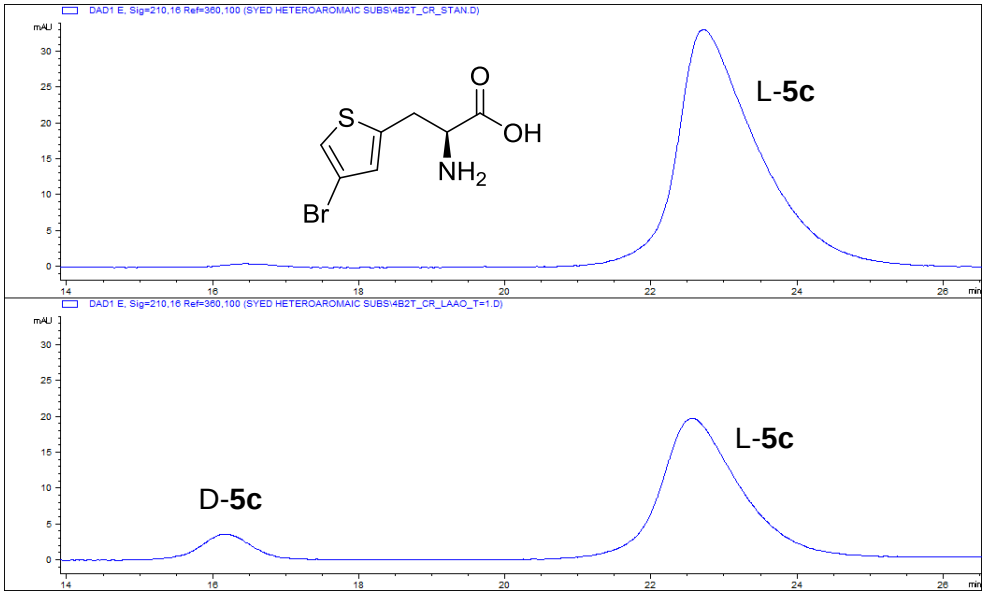
DAD1 E, Sig=210,16 Ref=360,100 (SYED HETEROAROMAIC SUBS\4B2T_CR_STAN.D)
mAU
O
S
OH
NH2
Br
L-5c
DAD1 E, Sig=210,16 Ref=360,100 (SYED HETEROAROMAIC SUBS\4B2T_CR_LAAO_T=1.D)
L-5c
D-5c
min

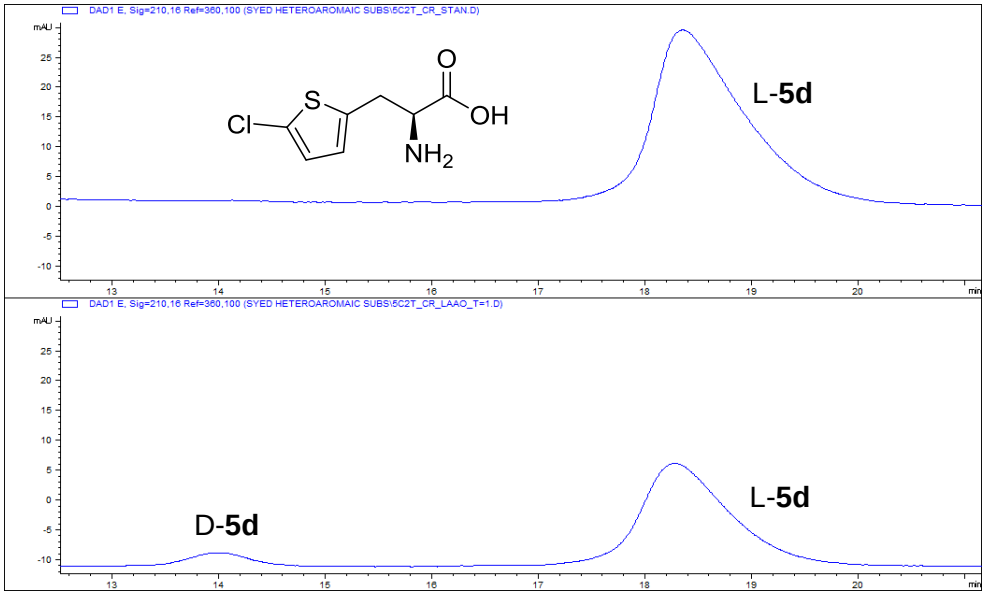
DAD1 E, Sig=210,16 Ref=360,100 (SYED HETEROAROMAIC SUBS\5C2T_CR_STAN.D)
mAU
O
S
Cl
OH
NH2
L-5d
DAD1 E, Sig=210,16 Ref=360,100 (SYED HETEROAROMAIC SUBS\5C2T_CR_LAAO_T=1.D)
L-5d
D-5d
min

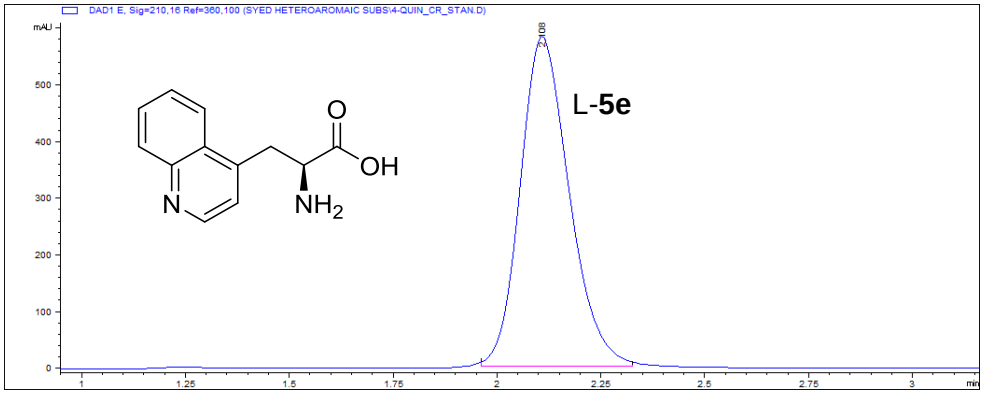
DAD1 E, Sig=210,16 Ref=360,100 (SYED HETEROAROMAIC SUBS\4-QUIN_CR_STAN.D)
mAU
500
400
300
200
100
0
1
1.25
1.5
1.75
2
2.25
2.5
2.75
3
min
O
OH
N
NH2
L-5e

Synthetic procedures and biotransformation protocols

Knoevenegel-Doebner synthesis of acrylic acids 2a-l and 4a-f

The suitable aldehyde (1 mmol) and malonic acid (3 mmol) were added to DMSO (1 mL). The mixture (final conc. 1 M aldehyde) was stirred until complete dissolution of the starting materials. Piperidine (2 mol%) was added, followed by heating at 100°C for 16 h. The mixture was cooled to room temperature and quenched with distilled water (5 mL) resulting in the precipitation of the acrylic acid. The solid was centrifuged and the water removed by decanting. The acrylic acid was washed 3 times by re-suspending in distilled water (5 mL) with decanting the liquid each time. Methanol (10 mL) was added to transfer the solid to a round-bottomed flask, followed by concentrating the sample *in vacuo* to give the title compound as a white solid.

Telescopic synthesis of amino acids 3a-l and 5a-f

The crude condensation mixture (500 µL) was added to a saturated solution of ammonium carbamate (9.5 mL) to give a final concentration of 50 mM acrylic acid. Lyophilized cells producing AvPAL (250 mg, 25 mg mL^{-1}) were added and the mixture was shaken until complete resuspension of the biocatalyst. The suspension was incubated at 37°C, 180 rpm for 2-30 h. Once the biotransformation reached full conversion (by HPLC and/or ^{1}H NMR), the mixture was centrifuged (4000 rpm, 10 min, 4°C) and the supernatant collected for purification. To follow the reaction by HPLC analysis, a sample of the biotransformation mixture (50 µL) was added to MeOH (450 µL), thoroughly mixed and centrifuged (13000 rpm, 1 min, 4°C). The supernatant was transferred to a filter vial and used directly for analysis.

Purification of amino acids 3a-l and 5a-f

Supernatant from the reaction mixture was acidified to pH < 2.0 by addition of aqueous H_2SO_4 (10% w/v) and centrifuged (4000 rpm, 10 min, 4°C) to remove cells and insoluble components. Dowex® 50WX8 hydrogen form (2.5 g) was washed with deionised water (50 mL) and aqueous H_2SO_4 (25 mL, 10% w/v). The acidified supernatant from the biotransformation was loaded onto the resin (1 mL min^{-1}). The resin was washed repeatedly with deionised water (until pH ~ 7) and the product was eluted with aqueous NH_4OH (30 mL, 10% w/v). Fractions containing the product were pooled and evaporated in a centrifugal evaporator, to afford amino acids L-**3a-l**.

Deracemisation cascade of compounds 3a-l using DAAO

Amino acid **3a-l** (10 mM) and borane-ammonia complex (50 mM) were dissolved in phosphate buffer (2 mL, 100 mM, pH 8.0). DAAO (1 mg mL^{-1}) was added to start the reaction and the mixture was incubated at 37°C for 1-3 h. To monitor the reaction, samples (200 uL) were taken at regular intervals, diluted with methanol (200 uL), centrifuged (13000 rpm, 1 min, 4°C) and the supernatant analysed by HPLC on a chiral stationary phase.[3] The same method (using LAAO instead of DAAO) was used to produce HPLC standards of the D-enantiomers of compounds that were obtained enantiomerically pure from the biotransformations.

Characterisation data of compounds 2a-l, 3a-l, 4a-f and 5a-e

(*E*)-3-(6-bromopyridin-3-yl) acrylic acid (2a)

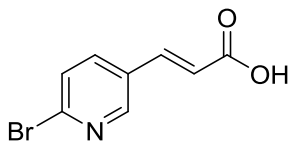

White solid (91 mg, 40%); **^{1}H NMR** (400 MHz, D_2O+NaOH) δ 8.22 (s, 1H), 7.72 (d, *J* = 8 Hz, 1H), 7.47 (d, *J* = 8 Hz, 1H), 7.14 (d, *J* = 16 Hz, 1H), 6.45 (d, *J* = 16 Hz, 1H); **^{13}C NMR** (100 MHz, D_2O+NaOH) δ 174.58, 148.72, 140.85, 137.38, 135.24, 130.86, 128.48, 127.34; **HRMS-ESI** (m/z) $[M+H]^+$ Calcd for $C_8H_6BrNO_2$: 227.9655; found, 227.9652.

(*E*)-3-(5-bromopyridin-3-yl) acrylic acid (2b)

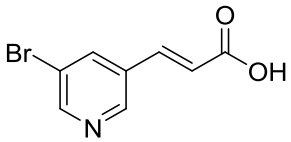

White solid (50 mg, 22%); **^{1}H NMR** (400 MHz, D_2O+NaOH) δ 8.37 (s, 2H), 8.00 (s, 1H), 7.10 (d, *J* = 16 Hz, 1H), 6.43 (d, *J* = 16 Hz, 1H); **^{13}C NMR** (100 MHz, D_2O+NaOH) δ 174.32, 149.56, 146.28, 137.22, 134.87, 133.00, 128.04, 120.68; **HRMS-ESI** (m/z) $[M+H]^+$ Calcd for $C_8H_6BrNO_2$: 227.9655; found, 227.9652.

(*E*)-3-(6-bromopyridin-2-yl) acrylic acid (2c)

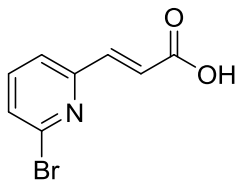

White solid (52 mg, 23%); **^{1}H NMR** (400 MHz, D_2O+NaOH) δ 7.58 (t, *J* = 8 Hz, 1H) 7.40-7.45 (m, 2H), 7.03 (d, *J* = 16 Hz, 1H), 6.56 (d, *J* = 16 Hz, 1H); **^{13}C NMR** (100 MHz, D_2O+NaOH) δ 174.32, 154.84, 141.10, 104.19, 137.21, 129.77, 128.21, 122.23; **HRMS-ESI** (m/z) $[M+H]^+$ Calcd for $C_8H_6BrNO_2$: 227.9655; found, 227.9649.

(*E*)-3-(5-bromopyridin-2-yl) acrylic acid (2d)

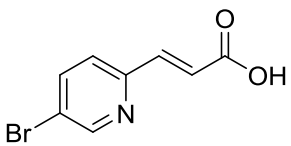

Pale yellow solid (59 mg, 26%); **^{1}H NMR** (400 MHz, D_2O+NaOH) δ 8.46 (s, 1H), 7.89 (d, *J* = 8 Hz, 1H), 7.42 (d, *J* = 8 Hz, 2H), 7.16 (d, *J* = 16 Hz, 1H), 6.62 (d, *J* = 16 Hz, 1H); **^{13}C NMR** (100 MHz, D_2O+NaOH) δ 174.62, 151.94, 150.01, 140.48, 137.63, 129.22, 124.53, 120.39; **HRMS-ESI** (m/z) $[M+H]^+$ Calcd for $C_8H_6BrNO_2$: 227.9655; found, 227.9652.

(*E*)-3-(2-bromopyridin-4-yl) acrylic acid (2e)

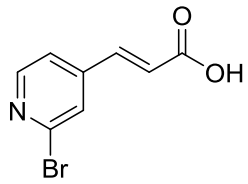

White solid (224 mg, 99%); **^{1}H NMR** (400 MHz, D_2O+NaOH) δ 8.11 (d, *J* = 8 Hz, 1H), 7.53 (s, 1H), 7.33 (d, *J* = 4 Hz, 1H), 7.04 (s, *J* = 16 Hz, 1H), 6.55 (d, *J* = 16 Hz, 1H); **^{13}C NMR** (100 MHz, D_2O+NaOH) δ 174.00, 149.65, 146.60, 141.28, 135.64, 130.70, 126.17, 121.37; **HRMS-ESI** (m/z) $[M+H]^+$ Calcd for $C_8H_6BrNO_2$: 227.9655; found, 227.9650.

(*E*)-3-(3-bromopyridin-4-yl) acrylic acid (2f)

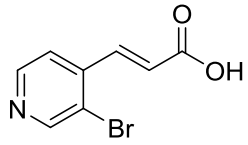

White solid (158 mg, 70%); **^{1}H NMR** (400 MHz, D_2O+NaOH) δ 8.50 (s, 1H), 8.25 (d, *J* = 4 Hz, 1H), 7.45 (d, *J* = 4 Hz, 1H), 7.37 (d, *J* = 16 Hz, 1H), 6.51 (d, *J* = 16 Hz, 1H); **^{13}C NMR** (100 MHz, D_2O+NaOH) δ 173.85, 151.31, 147.28, 143.38, 135.48, 131.38, 121.85, 121.78; **HRMS-ESI** (m/z) $[M+H]^+$ Calcd for $C_8H_6BrNO_2$: 227.9655; found, 227.9651.

(*E*)-3-(6-chloropyridin-3-yl) acrylic acid (2g)

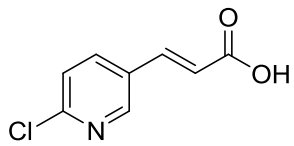

White solid (92 mg, 50%); **^{1}H NMR** (400 MHz, D_2O+NaOH) δ 8.36 (s, 1H), 7.94 (d, *J* = 4 Hz, 1H), 7.41 (d, *J* = 4 Hz, 1H), 7.24 (d, *J* = 16 Hz, 1H), 6.49 (d, *J* = 16 Hz, 1H); **^{13}C NMR** (100 MHz, D_2O+NaOH) δ 174.73, 150.37, 148.43, 137.90, 135.35, 130.68, 127.19, 124.72; **HRMS-ESI** (m/z) $[M+H]^+$ Calcd for $C_8H_6ClNO_2$: 184.0160; found, 184.0158.

(*E*)-3-(3-chloropyridin-4-yl) acrylic acid (2h)

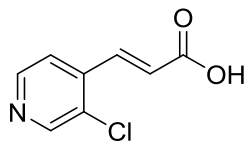

White solid (81 mg, 44%); **^{1}H NMR** (400 MHz, D_2O+NaOH) δ 8.39 (s, 1H), 8.25 (d, *J* = 8 Hz, 1H), 7.49 (d, *J* = 8 Hz, 1H), 7.44 (d, *J* = 16 Hz, 1H), 6.55 (d, *J* = 16 Hz, 1H); **^{13}C NMR** (100 MHz, D_2O+NaOH) δ 173.93, 148.84, 146.77, 141.61, 132.89, 131.33, 131.04, 121.43; **HRMS-ESI** (m/z) $[M+H]^+$ Calcd for $C_8H_6ClNO_2$: 184.0160; found, 184.0158.

(*E*)-3-(2-chloropyridin-4-yl) acrylic acid (2i)

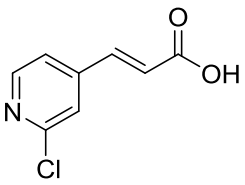

White solid (79 mg, 43%); **^{1}H NMR** (400 MHz, D_2O+NaOH) δ 8.19 (s, *J* = 8 Hz, 1H), 7.47 (s, 1H), 7.37 (d, *J* = 8 Hz, 1H), 7.12 (d, *J* = 16 Hz, 1H), 6.60 (d, *J* = 16 Hz, 1H); **^{13}C NMR** (100 MHz, D_2O+NaOH) δ 174.10, 150.80, 149.21, 147.04, 135.80, 130.61, 122.49, 121.05; **HRMS-ESI** (m/z) $[M+H]^+$ Calcd for $C_8H_6ClNO_2$: 184.0160; found, 184.0157.

(*E*)-3-(2,5-dichloropyridin-4-yl) acrylic acid (2j)

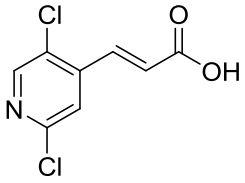

White crystals (69 mg, 32%); **^{1}H NMR** (400 MHz, D_2O+NaOH) δ 8.26 (s, 1H), 7.64 (s, 1H), 7.41 (d, *J* = 16 Hz, 1H), 6.60 (d, *J* = 16 Hz, 1H); **^{13}C NMR** (100 MHz, D_2O+NaOH) δ 173.59, 148.84, 148.78, 144.42, 132.56, 131.92, 130.05, 121.71; **HRMS-ESI** (m/z) $[M+H]^+$ Calcd for $C_8H_5Cl_2NO_2$: 217.9770; found, 217.9793

(*E*)-3-(2-methoxypyridin-4-yl) acrylic acid (2k)

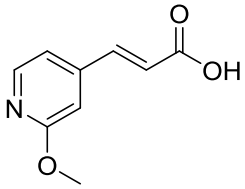

White solid (72 mg, 40%); **^{1}H NMR** (400 MHz, D_2O+NaOH) δ 8.00 (s, 1H), 7.90 (d, *J* = 8 Hz, 1H), 7.27 (d, *J* = 16 Hz, 1H), 7.20 (d, *J* = 4 Hz, 1H), 6.45 (d, *J* = 16 Hz, 1H), 3.79 (s, 3H); **^{13}C NMR** (100 MHz, D_2O+NaOH) δ 174.68, 152.86, 141.39, 133.24, 132.18, 132.86, 129.53, 121.51, 56.19; **HRMS-ESI** (m/z) $[M+H]^+$ Calcd for $C_9H_9NO_3$: 180.0655; found, 180.0663.

(*E*)-3-(3-methoxypyridin-4-yl) acrylic acid (2l)

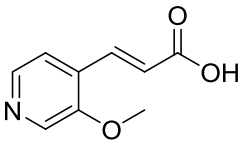

White solid (91 mg, 51%); **^{1}H NMR** (400 MHz, D_2O+NaOH) δ 7.86 (d, *J* = 4 Hz, 1H), 7.05 (d, *J* = 16 Hz, 1H), 6.96 (d, *J* = 4 Hz, 1H), 6.98 (s, 1H), 6.48 (d, *J* = 16 Hz, 1H), 3.77 (s, 3H); **^{13}C NMR** (100 MHz, D_2O+NaOH) δ 173.80, 163.47, 146.10, 145.76, 136.45, 128.58, 114.74, 107.83, 53.42; **HRMS-ESI** (m/z) $[M+H]^+$ Calcd for $C_9H_9NO_3$: 180.0655; found, 180.0663.

(*E*)-3-(6-methoxypyridin-3-yl) acrylic acid (2m)

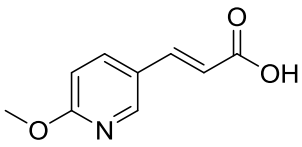

White solid (86 mg, 48%); **^{1}H NMR** (400 MHz, D_2O+NaOH) δ 8.03 (s, 1H), 7.85 (d, *J* = 8 Hz, 1H), 7.19 (d, *J* = 16 Hz, 1H), 6.76 (d, *J* = 12 Hz, 1H), 6.32 (d, *J* = 16 Hz, 1H), 3.83 (s, 3H); **^{13}C NMR** (100 MHz, D_2O+NaOH) δ 175.30, 164.11, 146.52, 137.75, 136.66, 125.10, 123.73, 110.60: **HRMS-ESI** (m/z) $[M+H]^+$ Calcd for $C_9H_9NO_3$: 180.0655; found, 180.0654.

(*S*)-2-amino-3-(6-bromopyridin-3-yl) propanoic acid (3a)

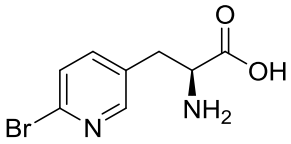

White solid (62 mg, 51%); **^{1}H NMR** (400 MHz, D_2O+NaOH) δ 8.12 (s, 1H), 7.51-7.58 (m, 2H), 3.48 (t, *J* = 8 Hz, 1H), 2.88-2.93 (dd, *J* = 16, 8 Hz, 1H), 2.80-2.85 (dd, *J* = 12, 8 Hz, 1H); **^{13}C NMR** (100 MHz, D_2O+NaOH) δ 181.18, 149.98, 140.79, 138.82, 133.75, 128.18, 56.90, 37.02; **HRMS-ESI** (m/z) $[M+H]^+$ Calcd for $C_8H_9BrN_2O_2$: 244.9920; found, 244.9785.

(*S*)-2-amino-3-(5-bromopyridin-3-yl) propanoic acid (3b)

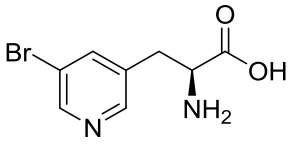

White solid (57 mg, 47%); **^{1}H NMR** (400 MHz, D_2O+NaOH) δ 8.36 (s, 1H), 8.18 (s, 1H), 7.78 (s, 1H), 3.35-3.38 (dd, *J* = 8, 4 Hz, 1H), 2.80-2.85 (dd, *J* = 16, 8Hz, 1H), 2.69-2.75 (dd, *J* = 16, 8Hz, 1H); **^{13}C NMR** (100 MHz, D_2O+NaOH) δ 181.43, 147.90, 147.65, 140.50, 136.50, 120.30, 57.07, 37.56; **HRMS-ESI** (m/z) $[M+H]^+$ Calcd for $C_8H_9BrN_2O_2$: 244.9920; found, 244.9923.

(*S*)-2-amino-3-(6-bromopyridin-2-yl) propanoic acid (3c)

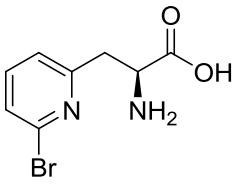

White solid (64 mg, 53%); **^{1}H NMR** (400 MHz, D_2O+NaOH) δ 7.51 (t, *J* = 8 Hz, 1H), 7.35 (d, *J* = 8 Hz, 1H), 7.16 (d, *J* = 8 Hz), 3.42-3.46 (dd, *J* = 8, 8 Hz, 1H), 2.93-2.98 (dd, *J* = 16, 8 Hz, 1H), 2.69-2.75 (dd, *J* = 16, 8 Hz, 1H); **^{13}C NMR** (100 MHz, D_2O+NaOH) δ 181.60, 159.94, 140.37, 140.18, 126.40, 123.43, 56.79, 42.37; **HRMS-ESI** (m/z) $[M+H]^+$ Calcd for $C_8H_9BrN_2O_2$: 244.9920; found, 244.9901.

(*S*)-2-amino-3-(5-bromopyridin-2-yl) propanoic acid (3d)

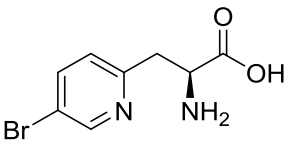

White solid (53 mg, 44%); **^{1}H NMR** (400 MHz, D_2O+NaOH) δ 8.50 (s, 1H), 7.90 (d, *J* = 8 Hz, 1H), 7.21 (d, *J* = 8 Hz, 1H), 3.53-3.57 (dd, *J* = 8, 8 Hz, 1H), 3.03-3.08 (dd, *J* = 16, 8 Hz, 1H), 2.83-2.88 (dd, *J* = 12, 8 Hz, 1H); **^{13}C NMR** (100 MHz, D_2O+NaOH) δ 181.73, 156.76, 149.33, 140.31, 125.81, 118.40, 56.74, 42.05; **HRMS-ESI** (m/z) $[M+H]^+$ Calcd for $C_8H_9BrN_2O_2$: 244.9920; found, 244.9871.

(*S*)-2-amino-3-(2-bromopyridin-4-yl) propanoic acid (3e)

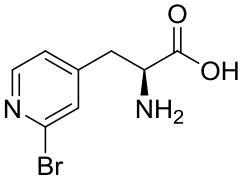

White solid (63 mg, 52%); **^{1}H NMR** (400 MHz, D_2O+NaOH) δ 8.09 (d, *J* = 8 Hz, 1H), 7.40 (s, 1H), 7.17 (d, *J* = 8 Hz, 1H), 3.39-3.42 (dd, *J* = 8, 4 Hz, 1H), 2.69-2.75 (dd, *J* = 16, 8 Hz, 1H); **^{13}C NMR** (100 MHz, D_2O+NaOH) δ 181. 27, 152.20, 149.26, 140.80, 129.06, 124.42, 56.73, 39.94; **HRMS-ESI** (m/z) $[M+H]^+$ Calcd for $C_8H_9BrN_2O_2$: 244.9920; found, 246.9985.

(*S*)-2-amino-3-(3-bromopyridin-4-yl) propanoic acid (3f)

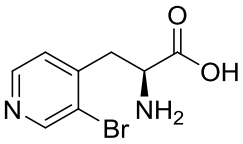

White solid (58 mg, 48%); **^{1}H NMR** (400 MHz, D_2O+NaOH) δ 8.57 (s, 1H), 8.30 (d, *J* = 4 Hz, 1H), 7.29 (d, *J* = 4 Hz, 1H), 3.55 (t, *J* = 8 Hz, 1H), 3.04-3.09 (dd, *J* = 16, 8 Hz, 1H), 2.90-2.95 (dd, *J* = 12, 8 Hz, 1H); **^{13}C NMR** (100 MHz, D_2O+NaOH) δ 181.46, 150.74, 148.41, 147.14, 126.64, 123.20, 55.97, 40.39: **HRMS-ESI** (m/z) $[M+H]^+$ Calcd for $C_8H_9BrN_2O_2$: 244.9920; found, 244.9871.

(*S*)-2-amino-3-(6-chloropyridin-3-yl) propanoic acid (3g)

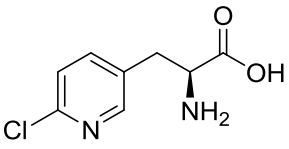

White solid (45mg, 45%); **^{1}H NMR** (400 MHz, D_2O+NaOH) δ 8.15 (s, 1H), 7.67 (d, *J* = 8 Hz, 1H), 7.40 (d, *J* = 8 Hz, 1H), 3.46 (t, *J* = 8 Hz, 1H), 2.89-2.94 (dd, *J* = 16, 8 Hz, 1H), 2.81-2.87 (dd, *J* = 16, 8 Hz, 1H); **^{13}C NMR** (100 MHz, D_2O+NaOH) δ 181.12, 149.37, 148.52, 141.04, 133.31, 124.38, 56.95, 36.90; **HRMS-ESI** (m/z) $[M+H]^+$ Calcd for $C_8H_9ClN_2O_2$: 201.0425; found, 201.0422.

(*S*)-2-amino-3-(3-chloropyridin-4-yl) propanoic acid (3h)

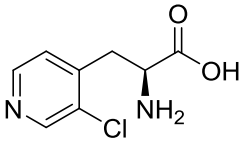

White solid (40 mg, 40%); **^{1}H NMR** (400 MHz, D_2O+NaOH) δ 8.36 (s, 1H), 8.19 (d, *J* = 4 Hz, 1H), 7.21 (d, *J* = 4 Hz, 1H), 3.46 (t, *J* = 8 Hz, 1H), 2.96-3.01 (dd, *J* = 12, 8 Hz, 1H), 2.82-2.88 (dd, *J* = 16, 8 Hz, 1H); **^{13}C NMR** (100 MHz, D_2O+NaOH) δ 181.46, 148.13, 146.60, 132.47, 126.42, 55.87, 37.93; **HRMS-ESI** (m/z) $[M+H]^+$ Calcd for $C_8H_9ClN_2O_2$: 201.0425; found, 201.0421.

(*S*)-2-amino-3-(2-chloropyridin-4-yl) propanoic acid (3i)

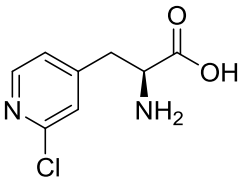

White solid (60 mg, 50%); **^{1}H NMR** (400 MHz, D_2O+NaOH) δ 8.09 (d, *J* = 4 Hz, 1H), 7.23 (s, 1H), 7.12 (d, *J* = 4 Hz, 1H), 3.42 (t, J = 8 Hz, 1H), 2.84-2.89 (dd, *J* = 16, 8 Hz, 1H), 2.71-2.77 (dd, *J* = 16, 8 Hz, 1H); **^{13}C NMR** (100 MHz, D_2O+NaOH) δ 181.07, 152.36, 150.23, 148.73, 125.24, 124.04, 56.66, 39.86; **HRMS-ESI** (m/z) $[M+H]^+$ Calcd for $C_8H_9ClN_2O_2$: 201.0425; found, 201.0421.

(*S*)-2-amino-3-(2,5-dichloropyridin-4-yl) propanoic acid (3j)

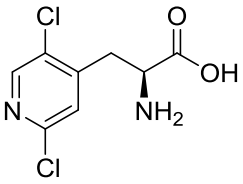

White solid (32 mg, 32%); **^{1}H NMR** (400 MHz, D_2O+NaOH) δ 8.18 (s, 0.5H), 7.29 (s, 1H), 3.44 (t, *J* = 8 Hz, 1H), 2.94-2.96 (dd, *J* = 16, 8 Hz, 1H), 2.78-2.84 (dd, *J* = 16, 8 Hz, 1H); **^{13}C NMR** (100 MHz, D_2O+NaOH) δ 181.17, 149.66, 148.37, 148.07, 131.53, 126.41, 55.71, 37.99; **HRMS-ESI** (m/z) $[M+H]^+$ Calcd for $C_8H_8Cl_2N_2O_2$: 235.0036; found, 235.0063.

(*S*)-2-amino-3-(2-methoxypyridin-4-yl) propanoic acid (3k)

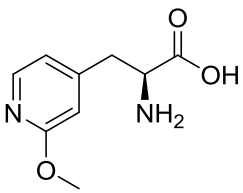

White solid (45 mg, 46%); **^{1}H NMR** (400 MHz, D_2O+NaOH) δ 8.03 (s, 1H), 7.93 (d, *J* = 8 Hz, 1H), 7.07 (d, *J* = 4 Hz, 1H), 3.78 (s, 3H), 3.43 (t, J = 8 Hz, 1H), 2.84-2.89 (dd, *J* = 12, 8 Hz, 1H), 2.69-2.74 (dd, *J* = 12, 8 Hz, 1H); **^{13}C NMR** (100 MHz, D_2O+NaOH) δ 181.43, 154.44, 141.44, 136.69, 132.23, 125.89, 55.97, 55.76, 34.58; **HRMS-ESI** (m/z) $[M+H]^+$ Calcd for $C_9H_{12}N_2O_3$: 197.0921; found, 197.0920.

(*S*)-2-amino-3-(3-methoxypyridin-4-yl) propanoic acid (3l)

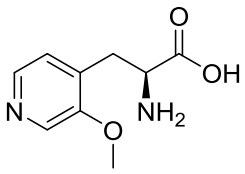

White solid (55 mg, 56%); **^{1}H NMR** (400 MHz, D_2O+NaOH) δ 7.94 (d, *J* = 4 Hz, 1H), 6.87 (d, *J* = 8 Hz, 1H), 6.68 (s, 1H), 3.83 (s, 3H), 3.59 (t, *J* = 8 Hz, 1H), 2.95-2.99 (dd, *J* = 12, 4 Hz, 1H), 2.81-2.86 (dd, *J* = 12, 8 Hz, 1H); **^{13}C NMR** (100 MHz, D_2O+NaOH) δ 179.63, 163.91, 151.24, 146.17, 117.65, 110.48, 56.26, 53.99, 39.12; **HRMS-ESI** (m/z) $[M+H]^+$ Calcd for $C_9H_{12}N_2O_3$: 197.0921; found, 197.0919.

(*E*)-3-(3-methylisoxazol-5-yl)acrylic acid (4a)

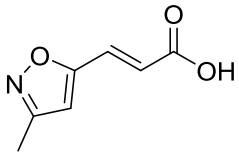

White solid (460mg, 66%) **^{1}H NMR** (400 MHz, DMSO-d_6) δ 7.39 (d, *J* = 16 Hz, 1H), 6.74 (s, 1H), 6.66 (d, *J* = 16 Hz, 1H), 2.41 (s, 3H); **^{13}C NMR** (100 MHz, D_2O+NaOH) δ 170.33, 166.55, 159.79, 130.77, 126.94, 99.88, 11.75; **HRMS-ESI** (m/z) $[M+H]^+$ Calcd for $C_7H_7NO_3$: 154.0504; found, 154.0507.

(*E*)-3-(5-bromothiophen-2-yl)acrylic acid (4b)

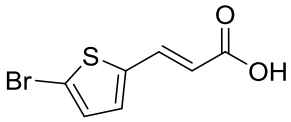

White solid (265 mg, 57%) **^{1}H NMR** (400 MHz, D_2O+NaOH) δ 7.33 (d, *J* = 16 Hz, 1H), 7.05 (d, *J* = 4 Hz, 1H), 7.00 (d, *J* = 4 Hz, 1H), 6.14 (d, *J* = 16 Hz, 1H); **^{13}C NMR** (100 MHz, D_2O+NaOH) δ 175.12, 141.74, 132.94, 131.26, 130.32, 123.25, 113.78 ; **HRMS-ESI** (m/z) $[M+H]^+$ Calcd for $C_7H_5BrO_2S$: 232.9272; found, 232.9265.

(*E*)-3-(4-bromothiophen-2-yl)acrylic acid (4c)

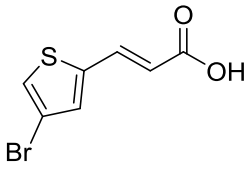

White solid (180 mg, 39%) **^{1}H NMR** (400 MHz, D_2O+NaOH) δ 7.36 (s, 1H), 7.34 (d, *J* = 16 Hz, 1H), 7.18 (s, 1H), 6.25 (d, *J* = 16 Hz, 1H); **^{13}C NMR** (100 MHz, D_2O+NaOH) δ 174.92, 140.97, 132.30, 131.11, 124.61, 124.08, 109.88; **HRMS-ESI** (m/z) $[M+H]^+$ Calcd for $C_7H_5BrO_2S$: 232.9272; found, 232.9262.

(*E*)-3-(5-chlorothiophen-2-yl)acrylic acid (4d)

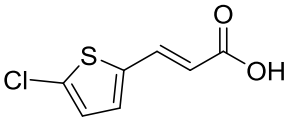

White solid (132 mg, 36%) **^{1}H NMR** (400 MHz, D_2O+NaOH) δ 7.31 (d, *J* = 16 Hz, 1H), 7.03 (d, *J* = 4 Hz, 1H), 6.91 (d, *J* = 4 Hz, 1H), 6.11 (d, *J* = 16 Hz, 1H); **^{13}C NMR** (100 MHz, D_2O+NaOH) δ 175.11, 138.92, 133.19, 130.99, 129.57, 127.52, 122.94; **HRMS-ESI** (m/z) $[M+H]^+$ Calcd for $C_7H_5ClO_2S$: 188.9777; found, 188.9764.

(*E*)-3-(quinolin-4-yl)acrylic acid (4e)

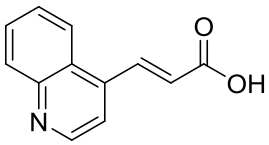

White solid (257 mg, 65%) **^{1}H NMR** (400 MHz, D_2O+NaOH) δ 819 (d, *J* = 4 Hz, 1H), 7.57 (t, *J* = 8 Hz, 2H), 7.48 (t, *J* = 8 Hz, 1H), 7.41 (d, *J* = 16 Hz, 1H), 7.31 (t, *J* = 8 Hz, 1H), 6.98 (d, *J* = 4 Hz, 1H), 6.22 (d, *J* = 16 Hz, 1H); **^{13}C NMR** (100 MHz, D_2O+NaOH) δ 174.21, 148.79, 146.01, 141.09, 133.50, 130.53, 129.90, 127.41, 127.01, 125.19, 123.13, 117.38; **HRMS-ESI** (m/z) $[M+H]^+$ Calcd for $C_{12}H_9NO_2$: 200.0712; found, 200.0736.

(*E*)-3-(isoquinolin-4-yl)acrylic acid (4f)

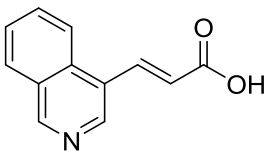

White solid (257 mg, 65%) **^{1}H NMR** (400 MHz, D_2O+NaOH) δ 8.44 (s, 1H), 7.81 (s, 1H), 7.53 (d, *J* = 8 Hz, 1H), 7.41-7.48 (m, 2H), 7.28-7.37 (m, 2H), 6.04 (d, *J* = 16 Hz, 1H); **^{13}C NMR** (100 MHz, D_2O+NaOH) δ 174.72, 151.68, 138.21, 133.66, 132.76, 131.44, 128.04, 127.72, 127.61, 127.13, 126.05, 121.92; **HRMS-ESI** (m/z) $[M+H]^+$ Calcd for $C_{12}H_9NO_2$: 200.0712; found, 200.0735.

(*S*)-2-amino-3-(3-methylisoxazol-5-yl)propanoic acid (5a)

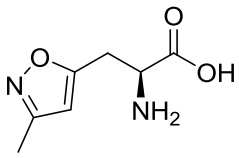

White solid (68 mg, 40%); **^{1}H NMR** (400 MHz, D_2O+NaOH) δ 6.05 (s, 1H), 3.57-3.60 (dd, *J* = 8, 4 Hz, 1H), 2.96-3.01 (dd, *J* = 12, 4 Hz, 1H), 2.86-2.91 (dd, *J* = 16, 8 Hz, 1H), 2.35 (s, 3H); **^{13}C NMR** (100 MHz, D_2O+NaOH) δ 180.08, 171.03, 161.68, 102.09, 54.66, 30.53, 11.32; **HRMS-ESI** (m/z) $[M+H]^+$ Calcd for $C_7H_{10}N_2O_3$: 171.0770; found, 171.0751.

(*S*)-2-amino-3-(5-bromothiophen-2-yl)propanoic acid (5b)

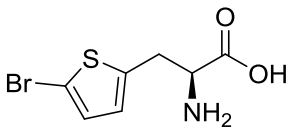

White solid (56 mg, 35%); **^{1}H NMR** (400 MHz, D_2O+NaOH) δ 6.86 (d, *J* = 4 Hz, 1H), 6.57 (d, *J* = 4 Hz, 1H), 3.34 (t, *J* = 8 Hz, 1H), 2.96 (d, *J* = 8 Hz, 2H); **^{13}C NMR** (100 MHz, D_2O+NaOH) δ 181.53, 141.94, 130.07, 127.02, 109.38, 56.90, 35.16; **HRMS-ESI** (m/z) $[M+H]^+$ Calcd for $C_7H_8BrNO_2S$: 249.9537; found, 249.9534.

(*S*)-2-amino-3-(4-bromothiophen-2-yl)propanoic acid (5c)

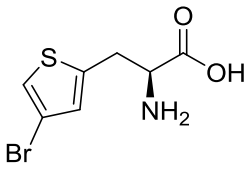

White solid (90 mg, 54%); **^{1}H NMR** (400 MHz, D_2O+NaOH) δ 7.13 (s, 1H), 6.75 (s, 1H), 3.36 (t, *J* = 8 Hz, 1H), 2.99 (d, *J* = 8 Hz, 2H); **^{13}C NMR** (100 MHz, D_2O+NaOH) δ 181.45, 141.69, 128.66, 122.02, 108.48, 56.97, 34.85; **HRMS-ESI** (m/z) $[M+H]^+$ Calcd for $C_7H_8BrNO_2S$: 249.9537; found, 249.9537.

(*S*)-2-amino-3-(5-chlorothiophen-2-yl)propanoic acid (5d)

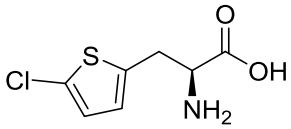

White solid (87 mg, 44%); **^{1}H NMR** (400 MHz, D_2O+NaOH) δ 6.82 (d, *J* = 4 Hz, 1H), 6.68 (d, *J* = 4 Hz, 1H), 3.52 (t, *J* = 4 Hz, 1H), 2.96 (d, *J* = 4 Hz, 2H); **^{13}C NMR** (100 MHz, D_2O+NaOH) δ 179.99, 138.32, 127.41, 126.31, 126.24, 56.63, 34.38; **HRMS-ESI** (m/z) $[M+H]^+$ Calcd for $C_7H_8ClNO_2S$: 206.0043; found, 206.0047.

(*S*)-2-amino-3-(quinolin-4-yl)propanoic acid (5e)

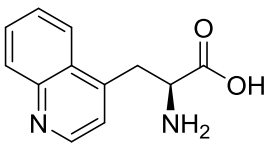

White solid (80 mg, 37%); **^{1}H NMR** (400 MHz, D_2O+NaOH) δ 8.50 (d, *J* = 4 Hz, 1H), 8.00 (d, *J* = 8 Hz, 1H), 7.83 (d, *J* = 8 Hz, 1H), 7.63 (t, *J* = 8 Hz, 1H), 7.50 (t, *J* = 8 Hz, 1H), 7.18 (d, *J* = 4 Hz, 1H), 3.46-3.50 (dd, *J* = 8, 8 Hz, 1H), 3.25-3.30 (dd, *J* = 16, 8 Hz, 1H), 3.01-3.07 (dd, *J* = 16, 8 Hz, 1H); **^{13}C NMR** (100 MHz, D_2O+NaOH) δ 181.64, 149.51, 146.53, 146.24, 129.87, 127.97, 127.35, 126.89, 124.00, 122.36, 56.90, 37.33; **HRMS-ESI** (m/z) $[M+H]^+$ Calcd for $C_{12}H_{12}N_2O_2$: 217.0977; found, 217.0973.

^{1}H NMR, ^{13}C NMR and HRMS spectra

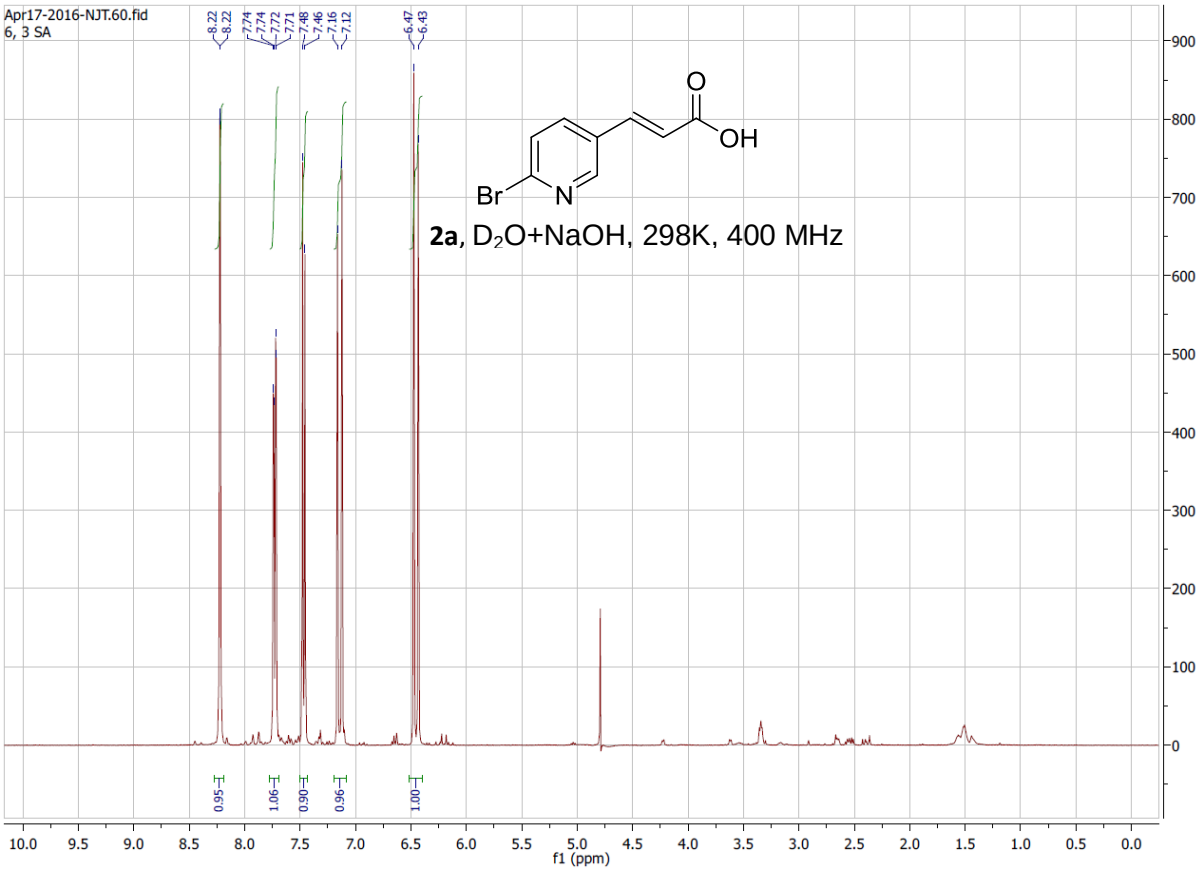

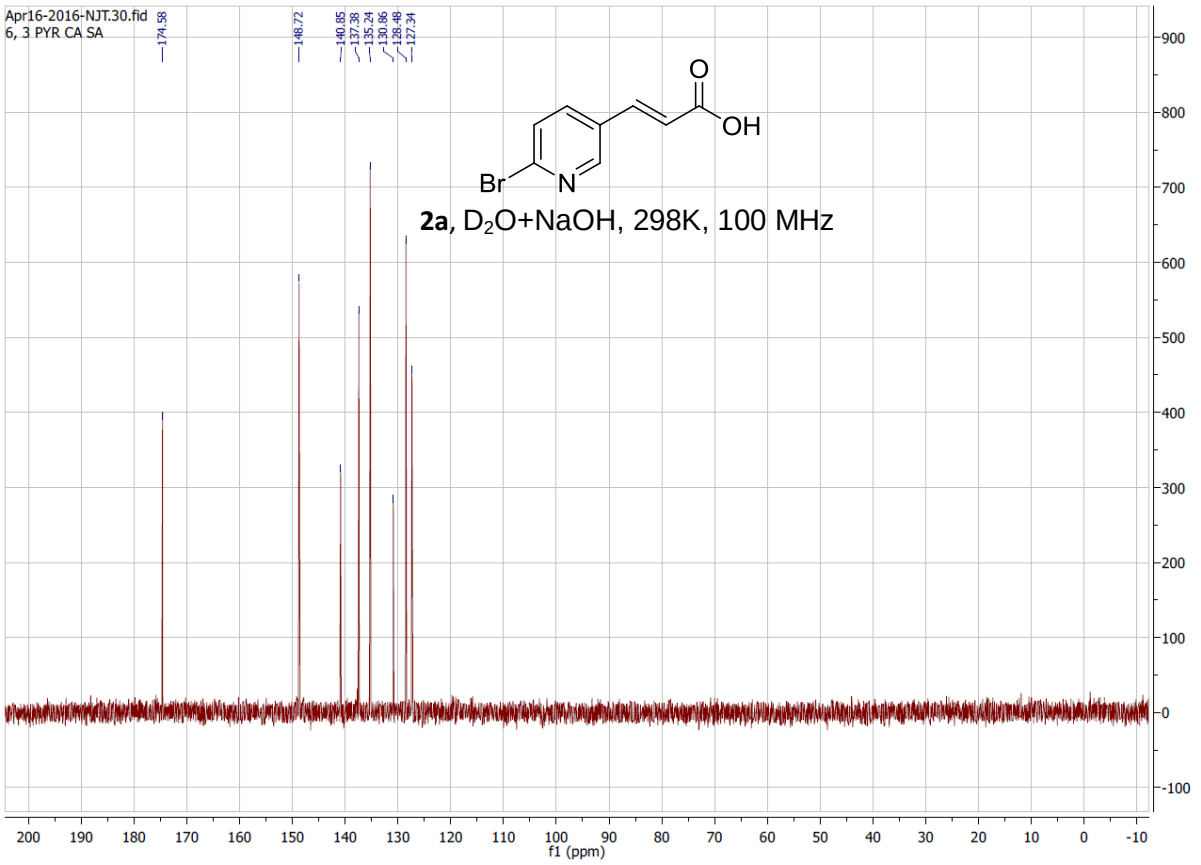

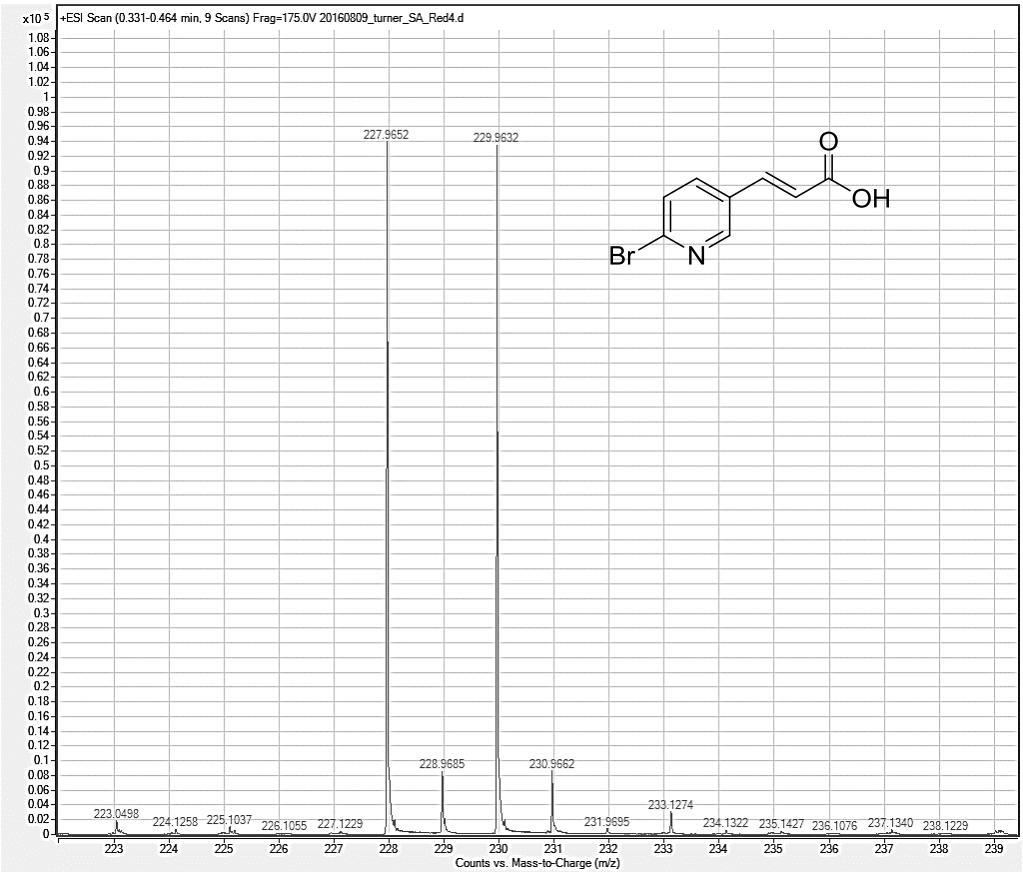
+ESI Scan (0.331-0.464 min, 9 Scans) Frag=175.0V 20160809_turner_SA_Red4.d
x10 5
227.9652
229.9632
228.9685
230.9662
233.1274
223.0498
224.1258
225.1037
226.1055
227.1229
231.9695
234.1322
235.1427
236.1076
237.1340
238.1229
Counts vs. Mass-to-Charge (m/z)
O
OH
Br
N

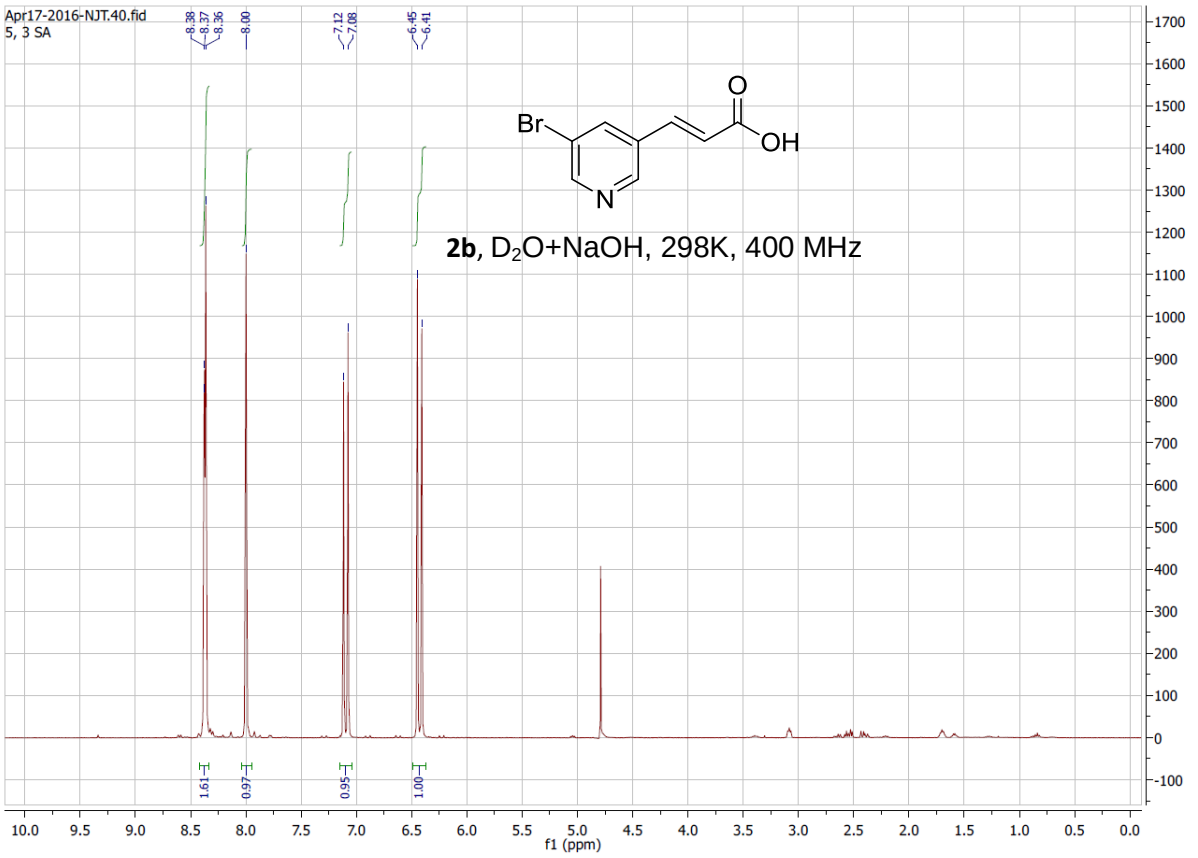

2b, D_2O+NaOH, 298K, 400 MHz

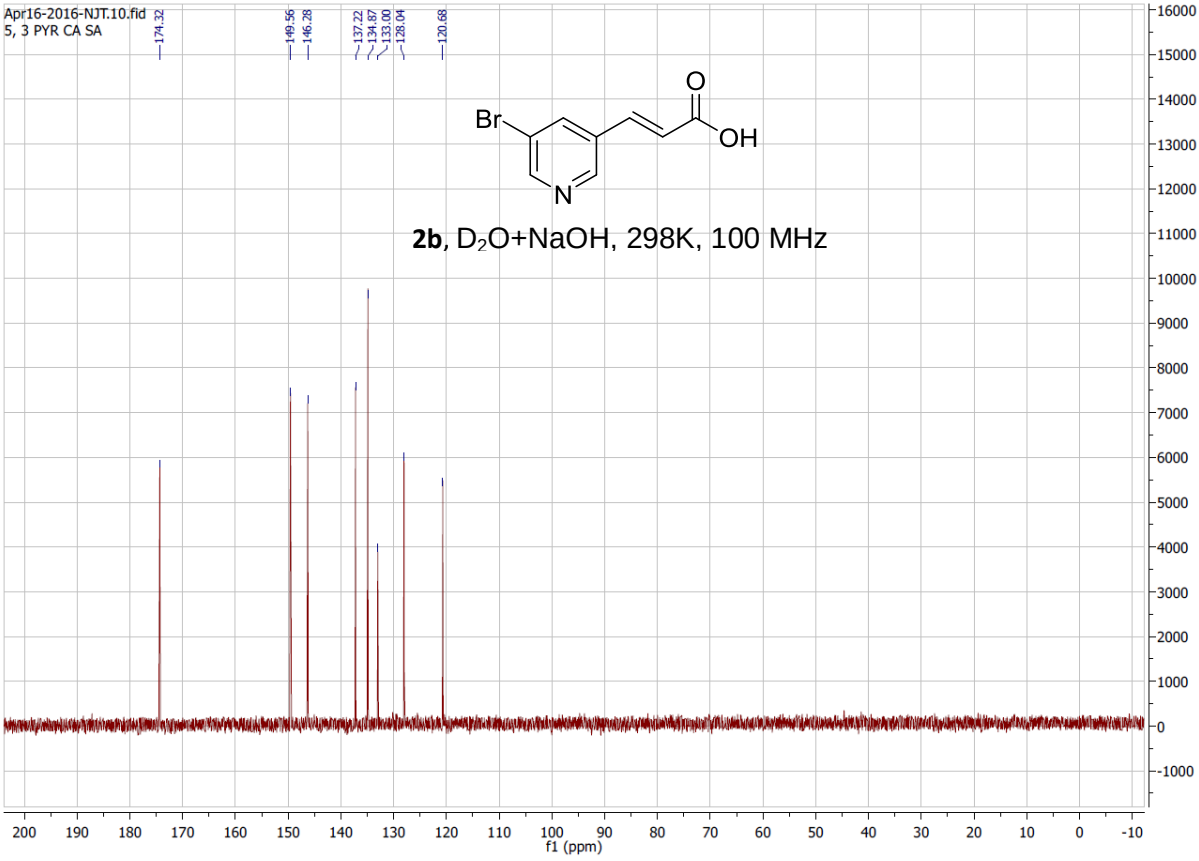

2b, D_2O+NaOH, 298K, 100 MHz

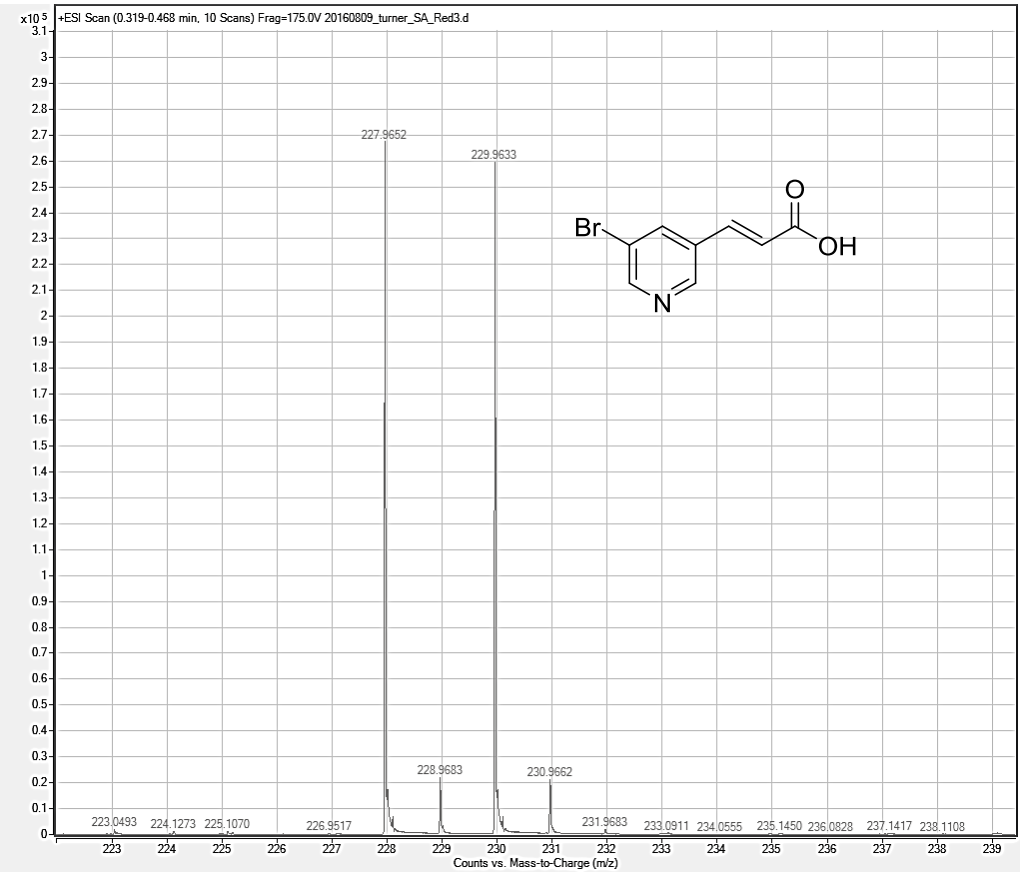
+ESI Scan (0.319-0.468 min, 10 Scans) Frag=175.0V 20160809_turner_SA_Red3.d
x10 5
227.9652
229.9633
228.9683
230.9662
223.0493
224.1273
225.1070
226.9517
231.9683
233.0911
234.0555
235.1450
236.0828
237.1417
238.1108
Br
O
OH
N
Counts vs. Mass-to-Charge (m/z)

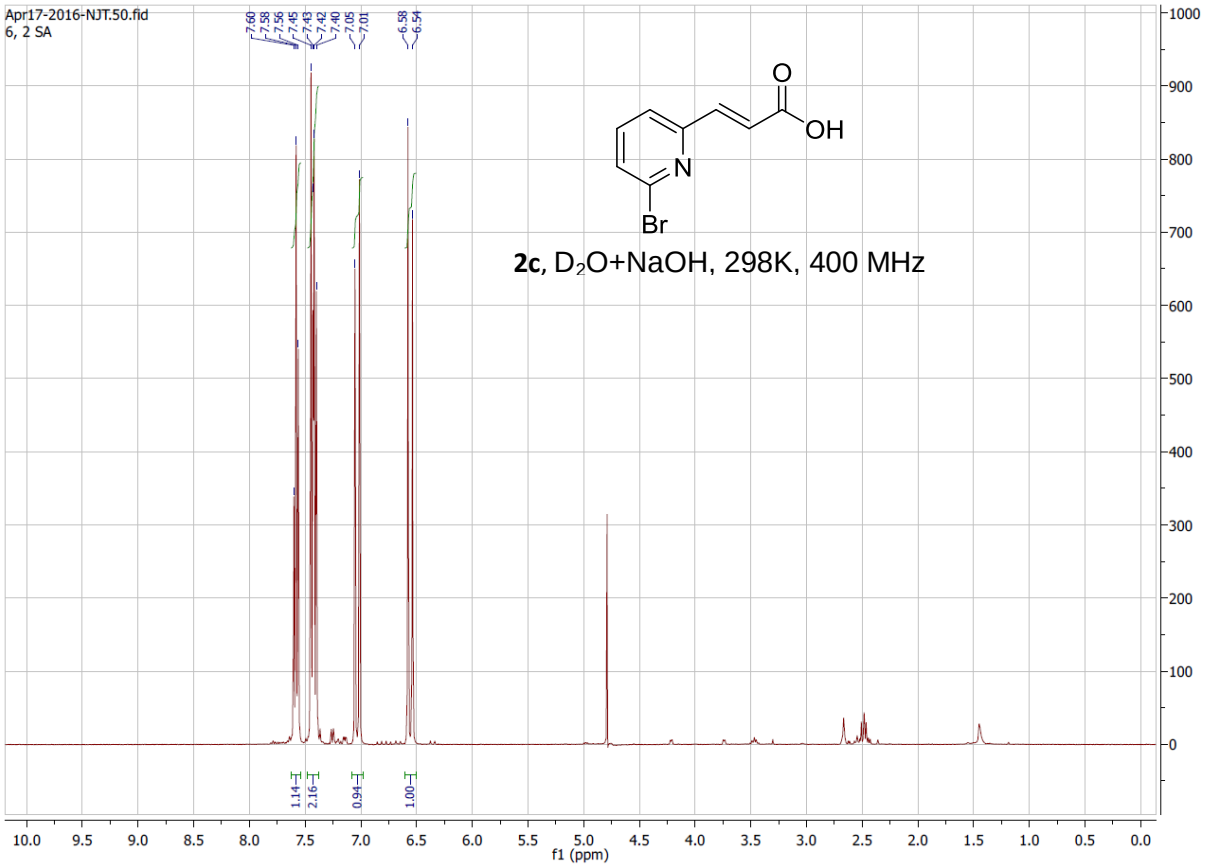

2c, D_2O+NaOH, 298K, 400 MHz

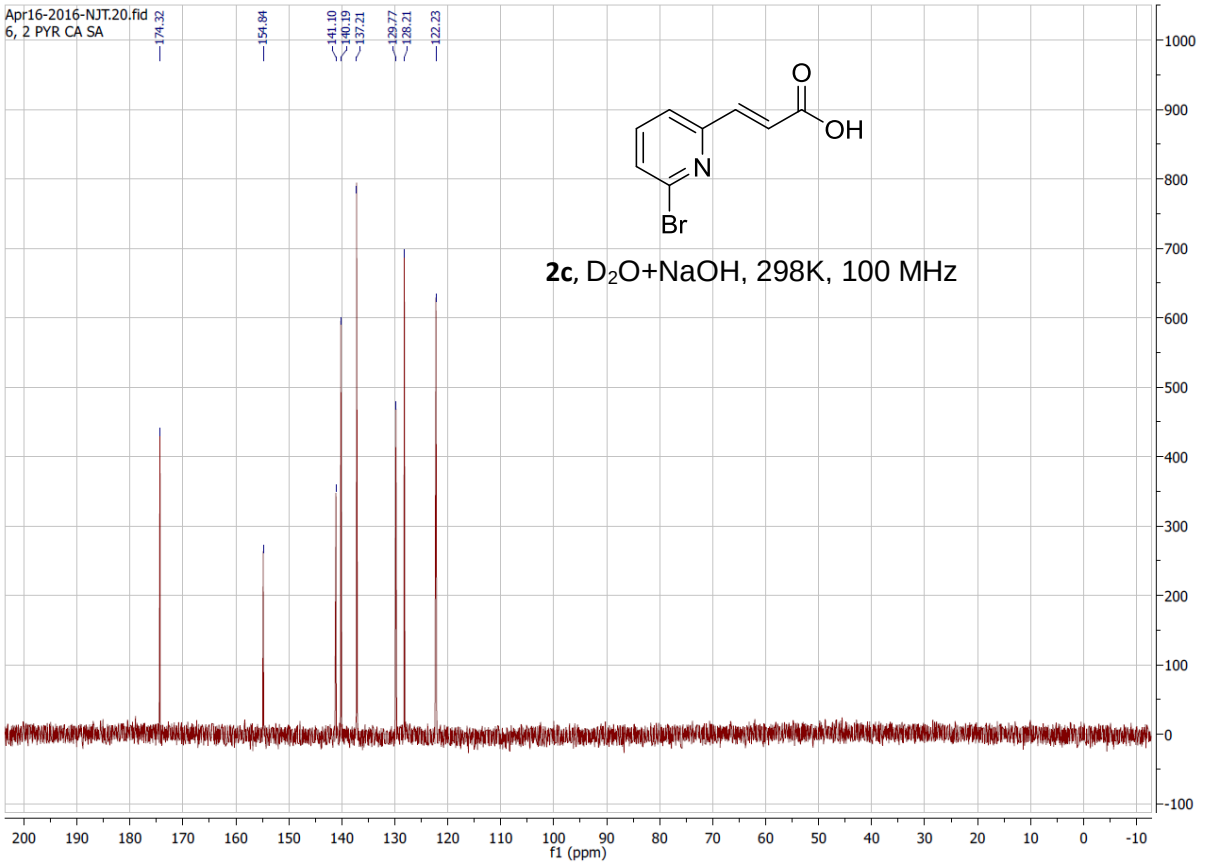

2c, D_2O+NaOH, 298K, 100 MHz

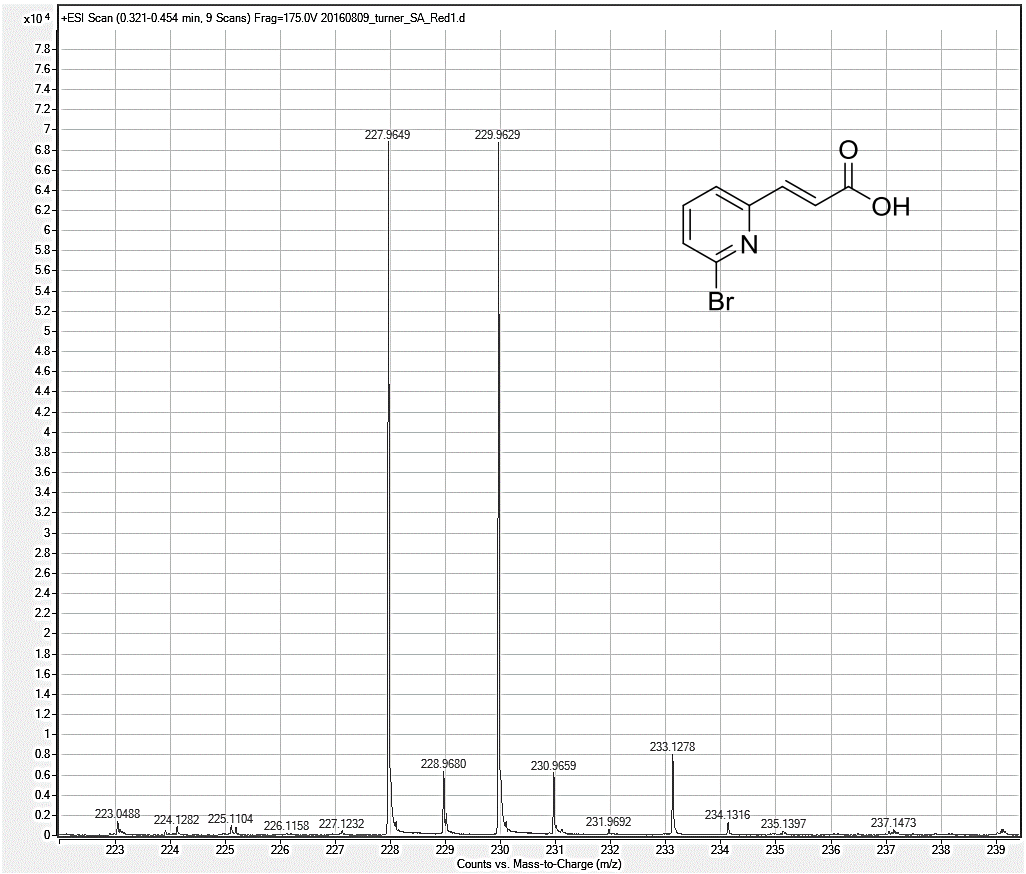
x10 4
+ESI Scan (0.321-0.454 min, 9 Scans) Frag=175.0V 20160809_turner_SA_Red1.d
227.9649
229.9629
228.9680
230.9659
233.1278
223.0488
224.1282
225.1104
226.1158
227.1232
231.9692
234.1316
235.1397
237.1473
O
OH
N
Br
Counts vs. Mass-to-Charge (m/z)

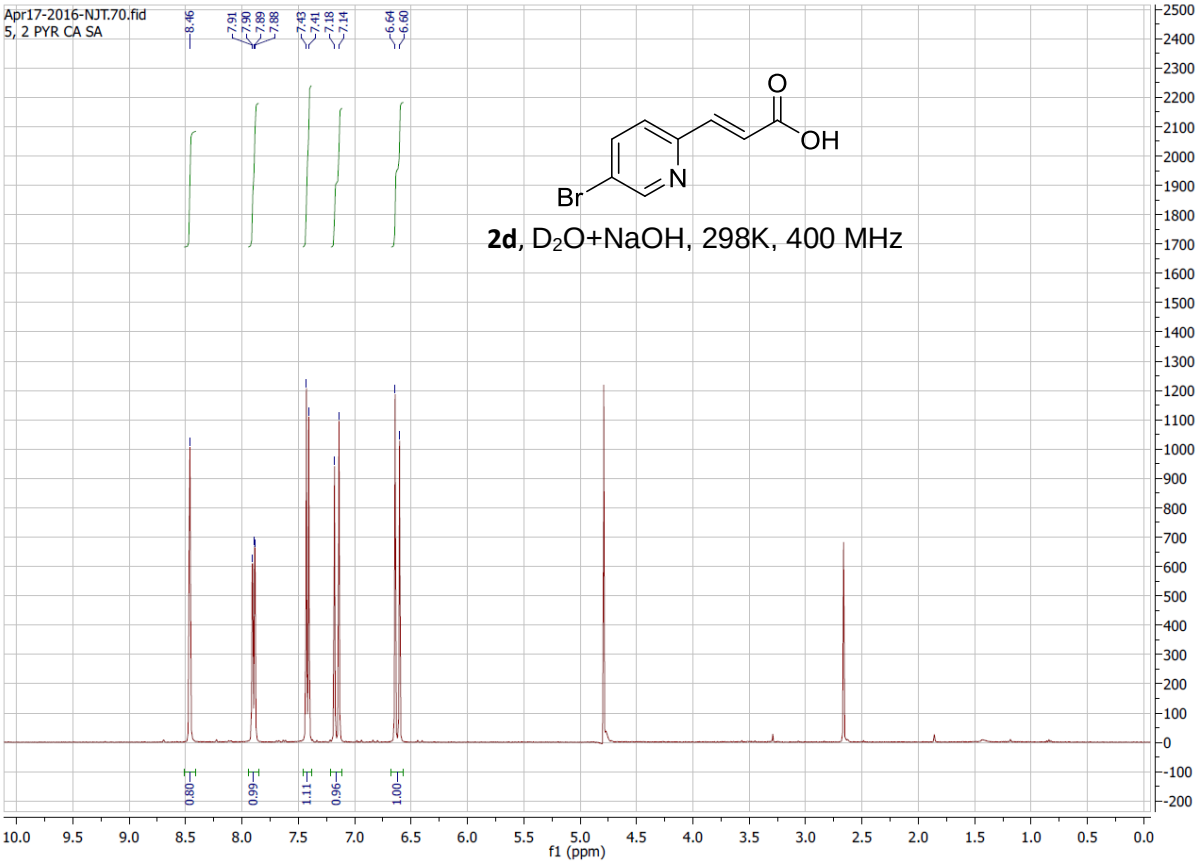

2d, D_2O+NaOH, 298K, 400 MHz

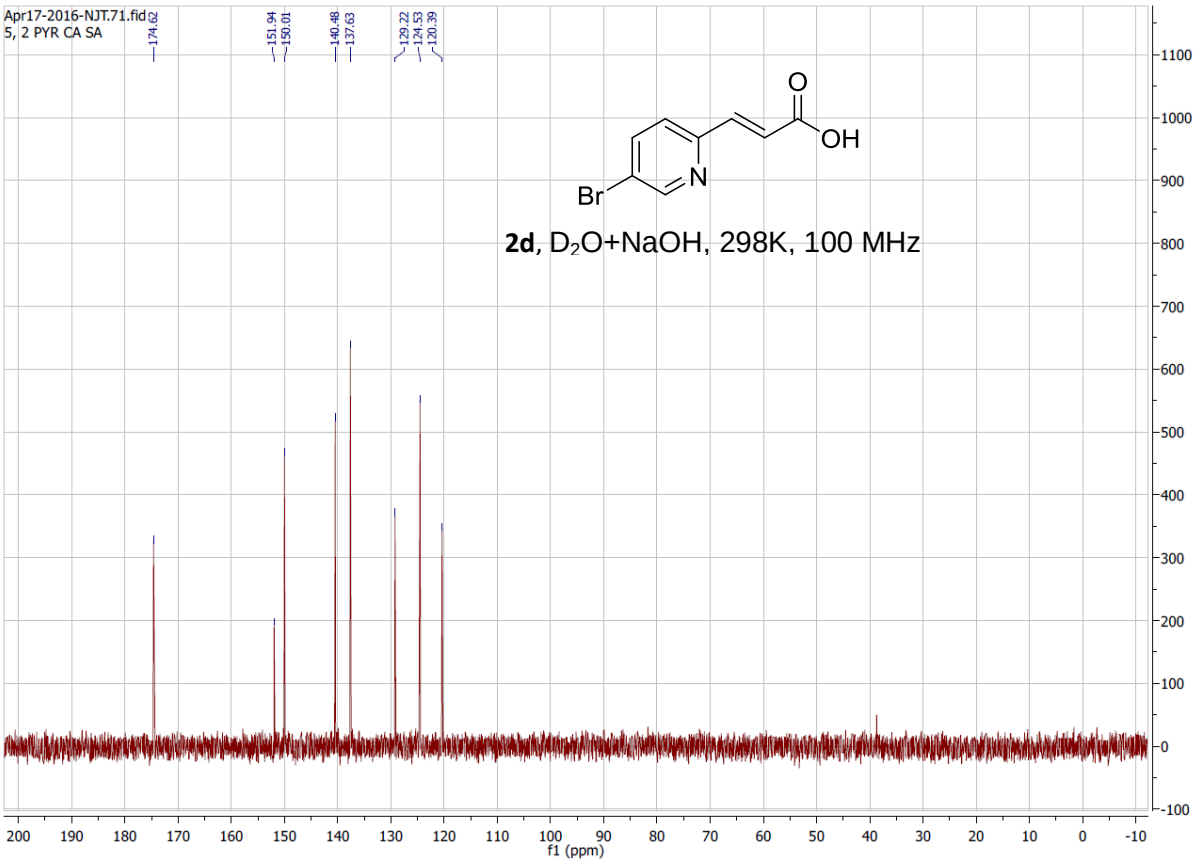

2d, D_2O+NaOH, 298K, 100 MHz

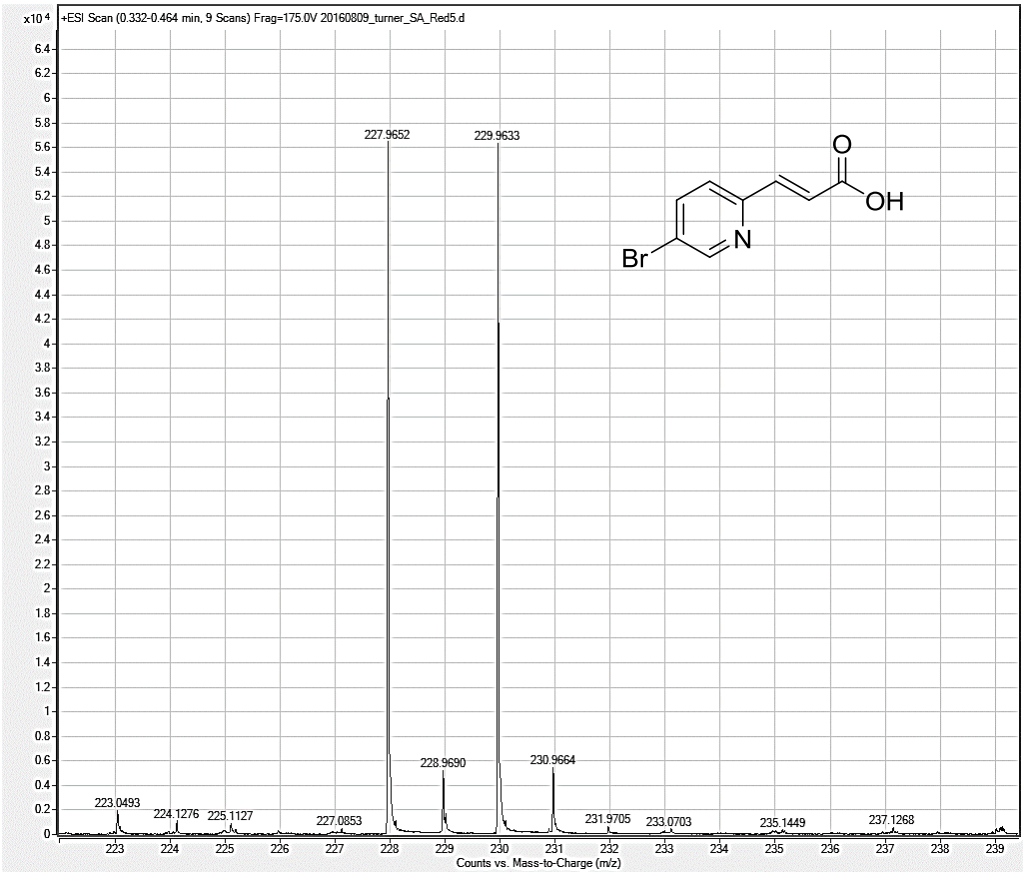
x10 4
+ESI Scan (0.332-0.464 min, 9 Scans) Frag=175.0V 20160809_turner_SA_Red5.d
227.9652
229.9633
228.9690
230.9664
223.0493
224.1276
225.1127
227.0853
231.9705
233.0703
235.1449
237.1268
O
OH
N
Br
Counts vs. Mass-to-Charge (m/z)

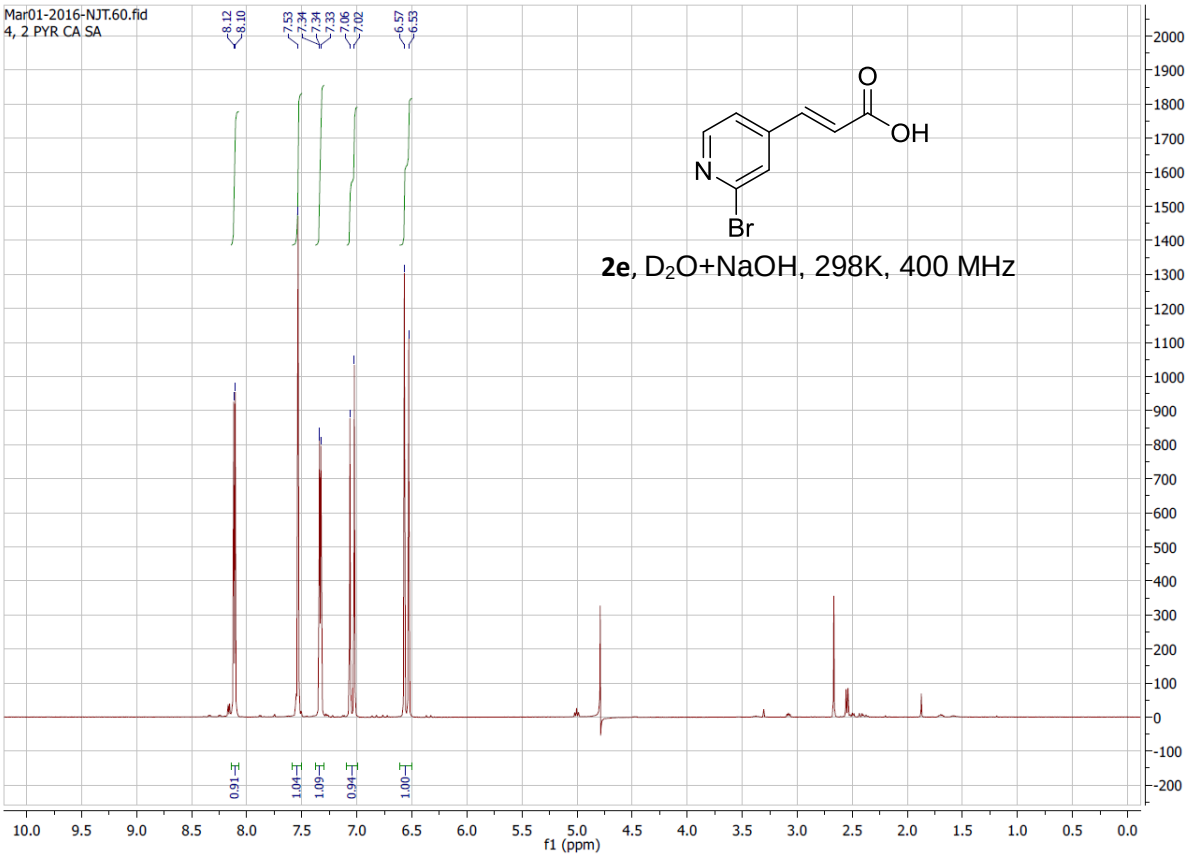

2e, D_2O+NaOH, 298K, 400 MHz

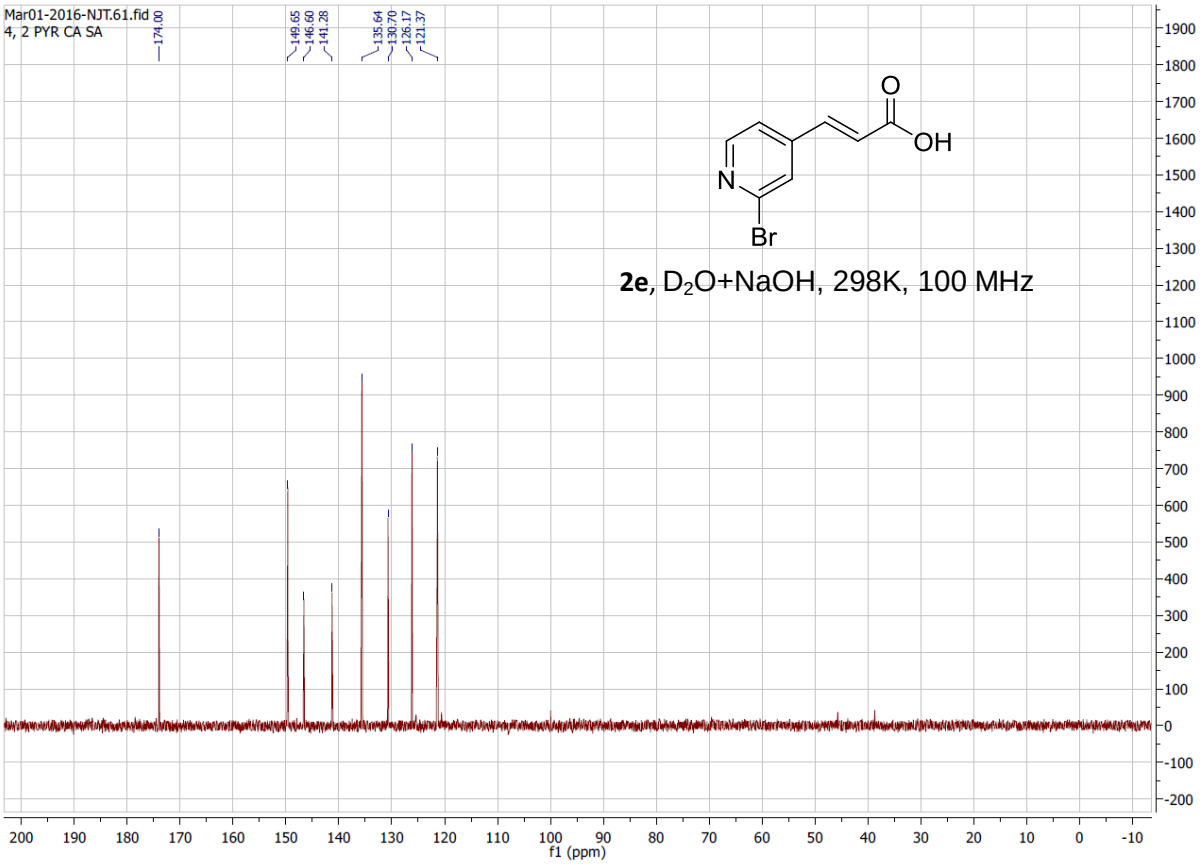

2e, D_2O+NaOH, 298K, 100 MHz

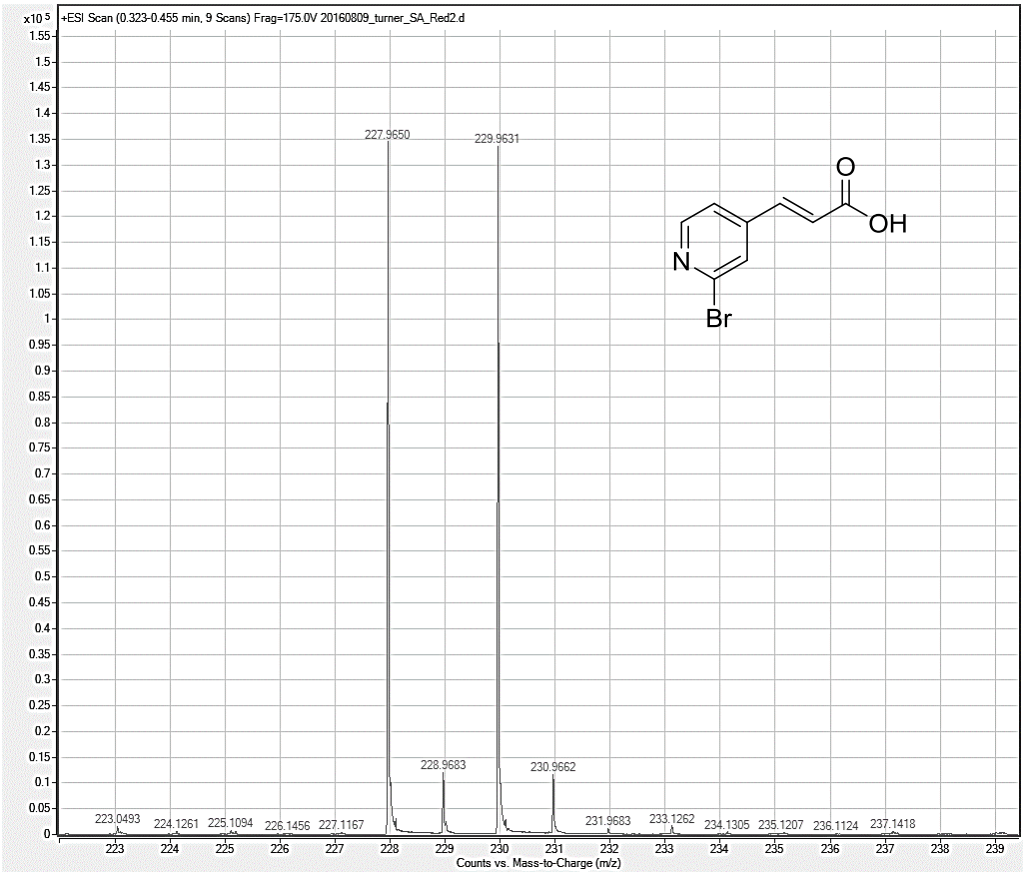
x10 5
+ESI Scan (0.323-0.455 min, 9 Scans) Frag=175.0V 20160809_turner_SA_Red2.d
227.9650
229.9631
228.9683
230.9662
223.0493
224.1261
225.1094
226.1456
227.1167
231.9683
233.1262
234.1305
235.1207
236.1124
237.1418
O
OH
N
Br
Counts vs. Mass-to-Charge (m/z)

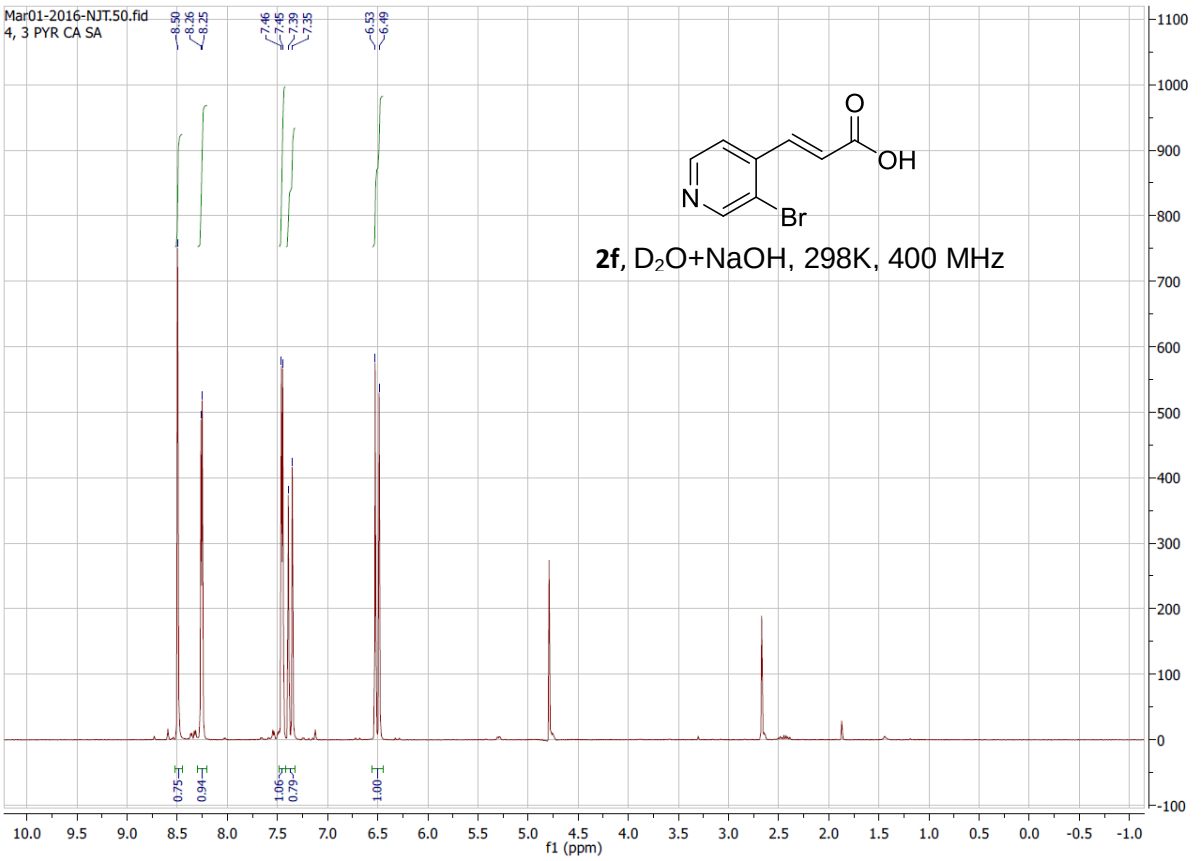

2f, D_2O+NaOH, 298K, 400 MHz

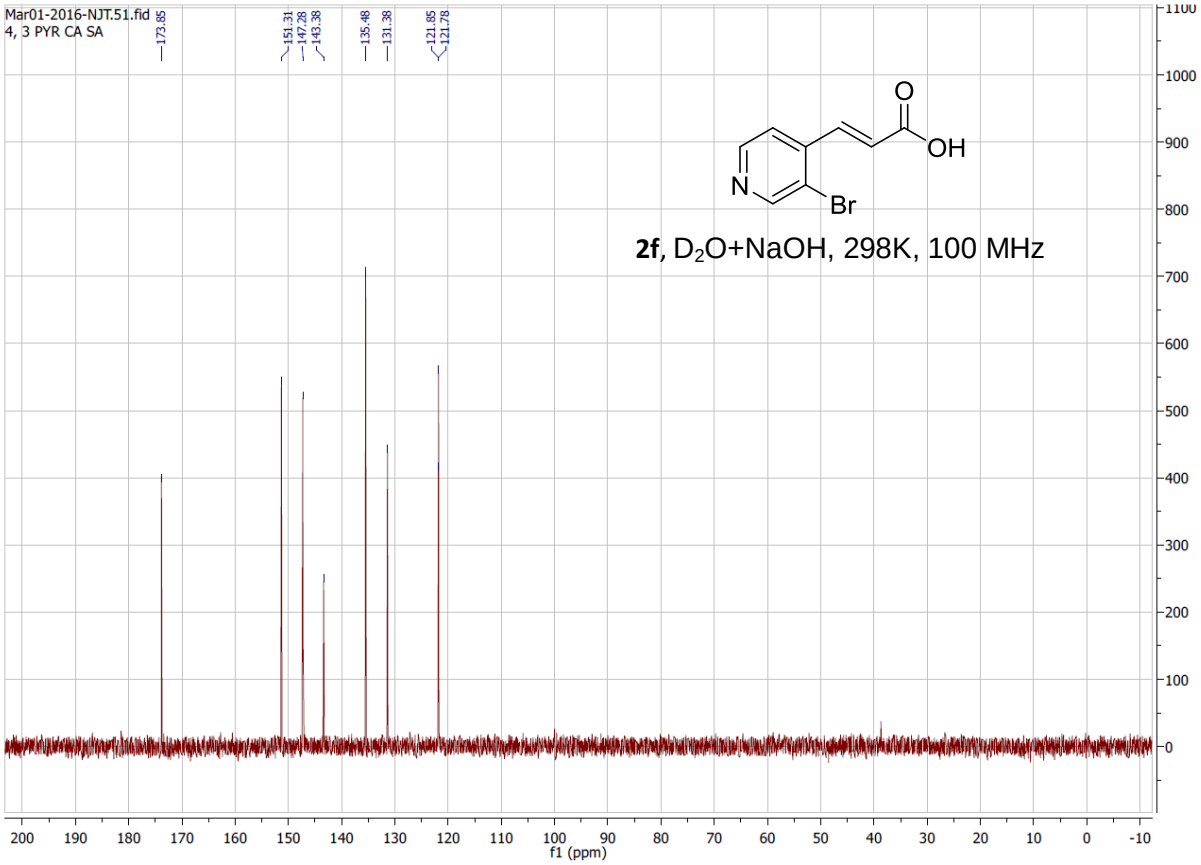

2f, D_2O+NaOH, 298K, 100 MHz

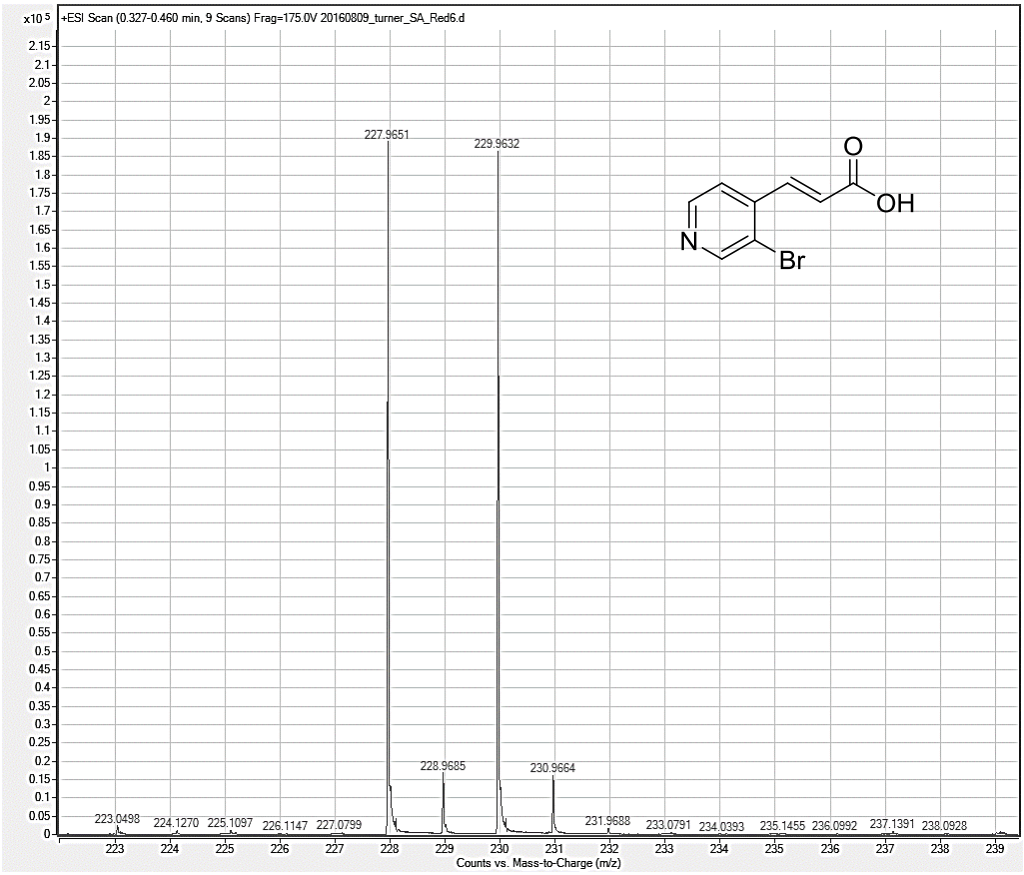
x10 5
+ESI Scan (0.327-0.460 min, 9 Scans) Frag=175.0V 20160809_turner_SA_Red6.d
227.9651
229.9632
228.9685
230.9664
223.0498
224.1270
225.1097
226.1147
227.0799
231.9688
233.0791
234.0393
235.1455
236.0992
237.1391
238.0928
O
OH
N
Br
Counts vs. Mass-to-Charge (m/z)

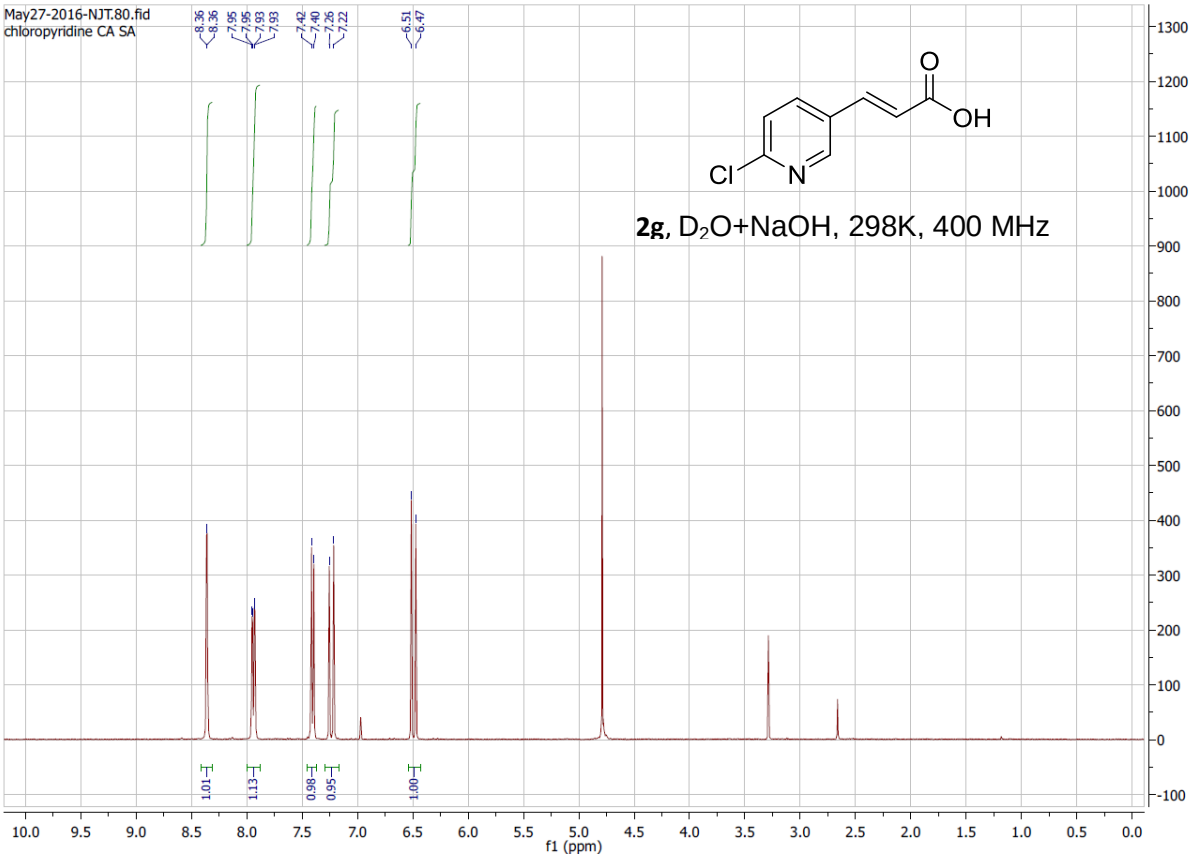
May27-2016-NJT.80.fid
chloropyridine CA SA
8.36
8.36
7.95
7.95
7.93
7.93
7.42
7.40
7.26
7.22
6.51
6.47
1.01
1.13
0.98
0.95
1.00
O
OH
Cl
N
2g, D2O+NaOH, 298K, 400 MHz
f1 (ppm)

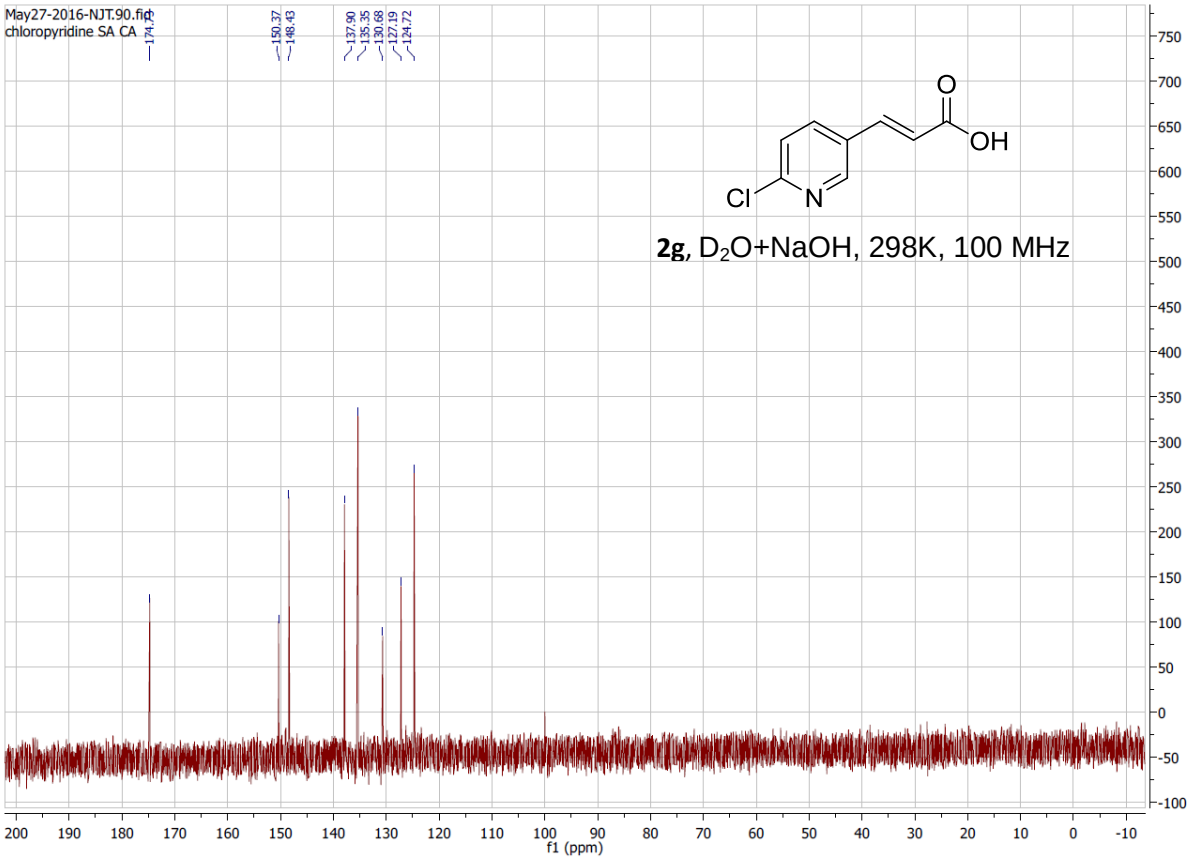
May27-2016-NJT.90.fid
chloropyridine SA CA
174.42
150.37
148.43
137.90
135.35
130.68
127.19
124.72
O
OH
Cl
N
2g, D2O+NaOH, 298K, 100 MHz
f1 (ppm)

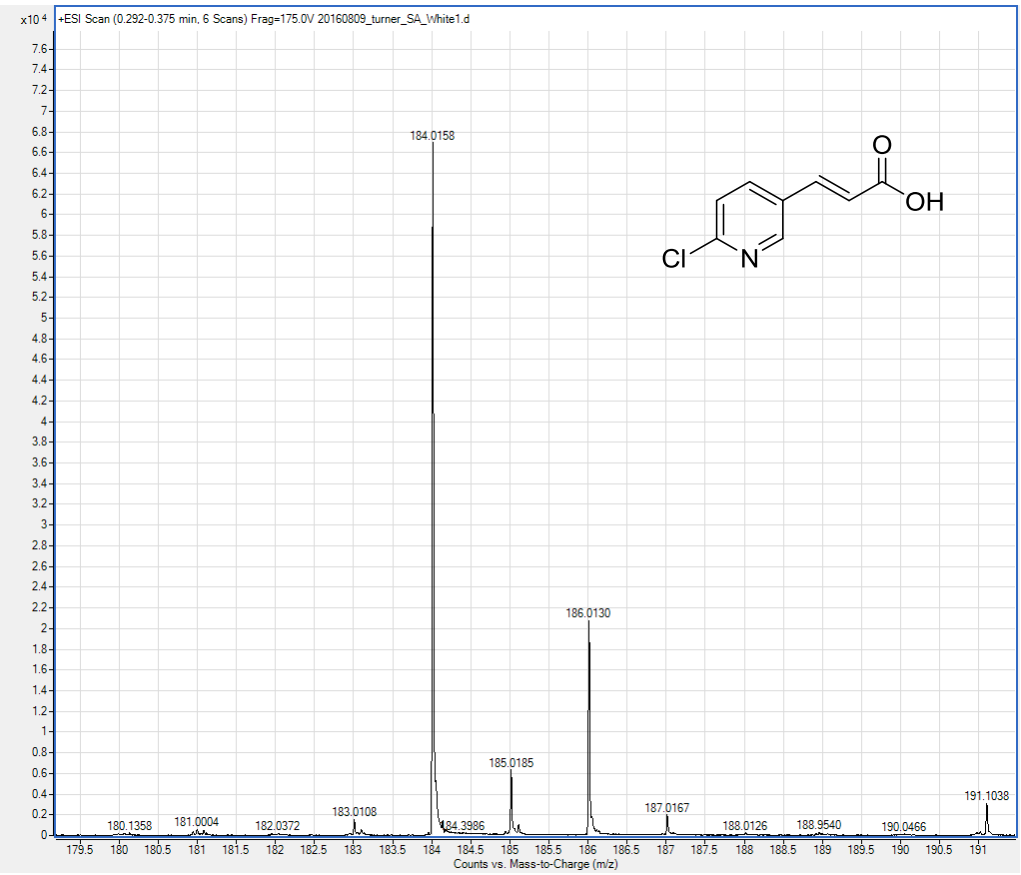
x10 4
+ESI Scan (0.292-0.375 min, 6 Scans) Frag=175.0V 20160809_turner_SA_White1.d
184.0158
186.0130
185.0185
187.0167
191.1038
183.0108
180.1358
181.0004
182.0372
184.3986
188.0126
188.9540
190.0466
O
OH
Cl
N
Counts vs. Mass-to-Charge (m/z)

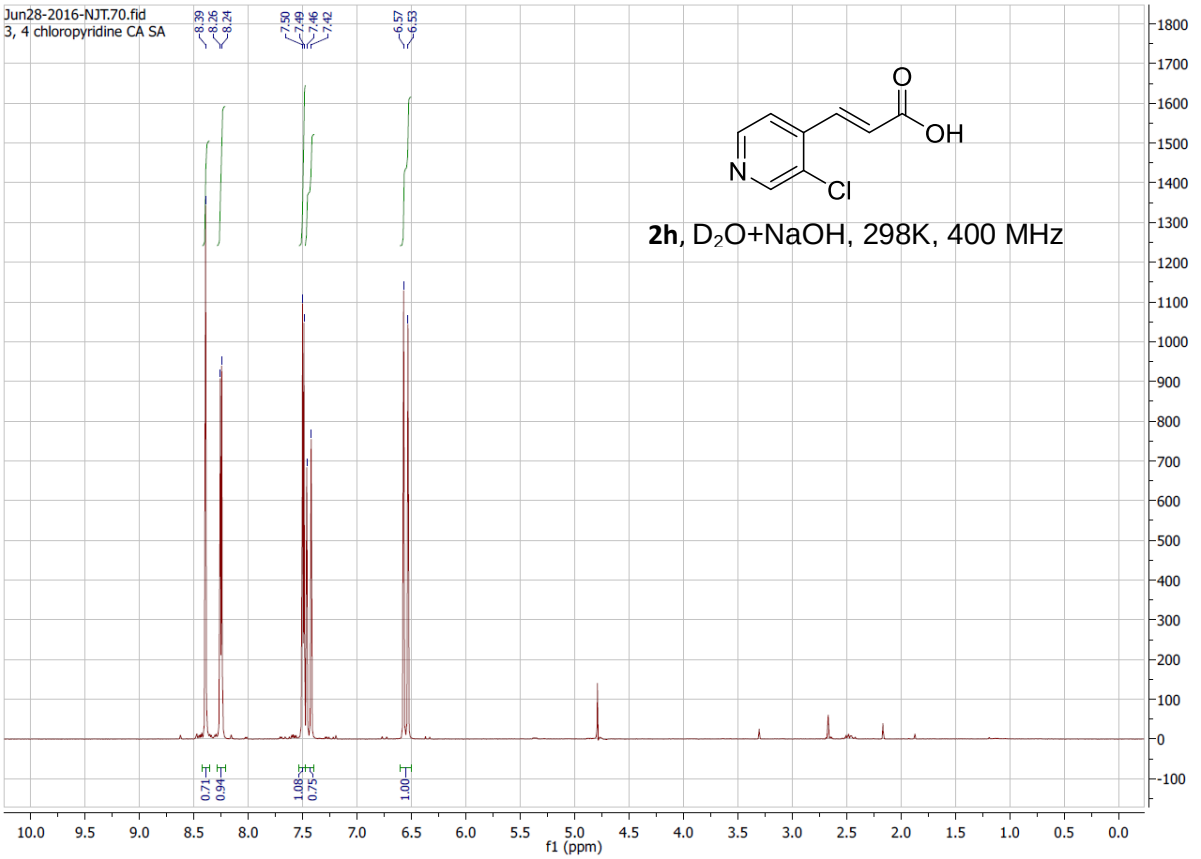

2h, D_2O+NaOH, 298K, 400 MHz

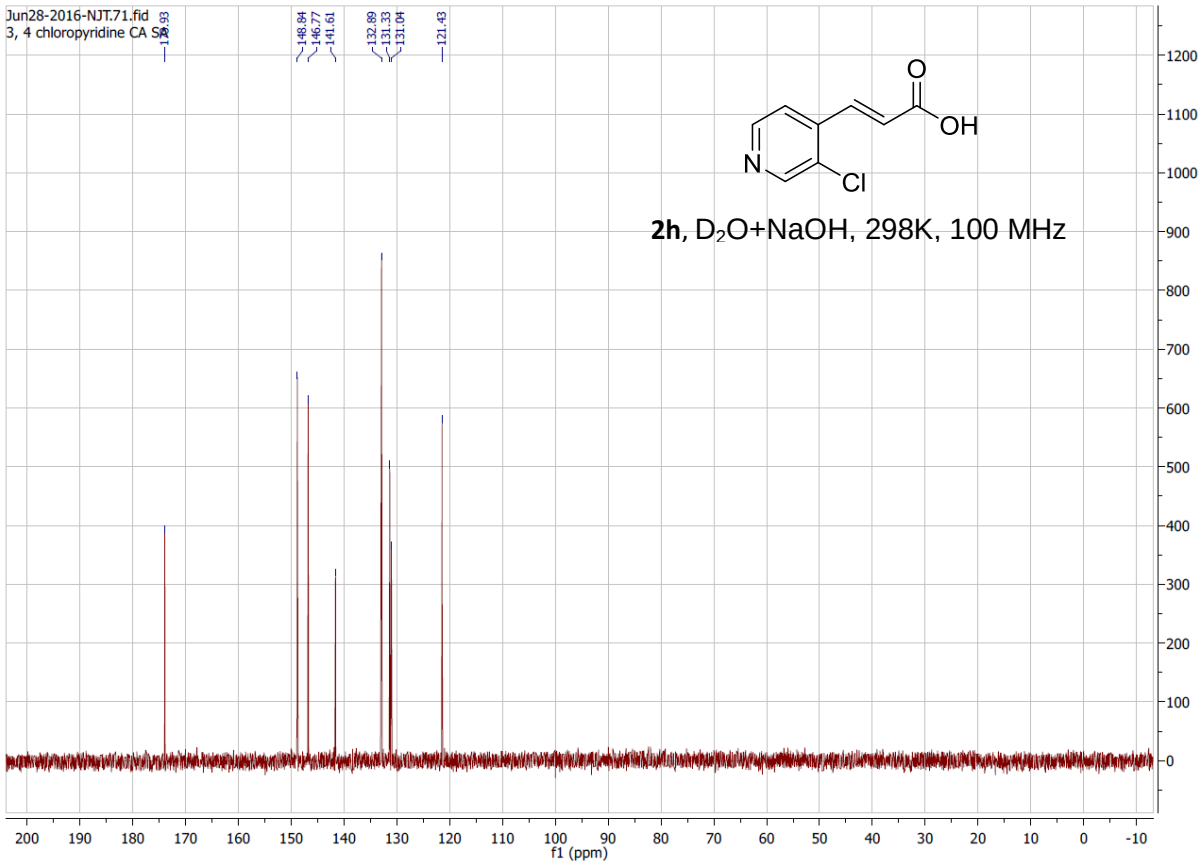

2h, D_2O+NaOH, 298K, 100 MHz

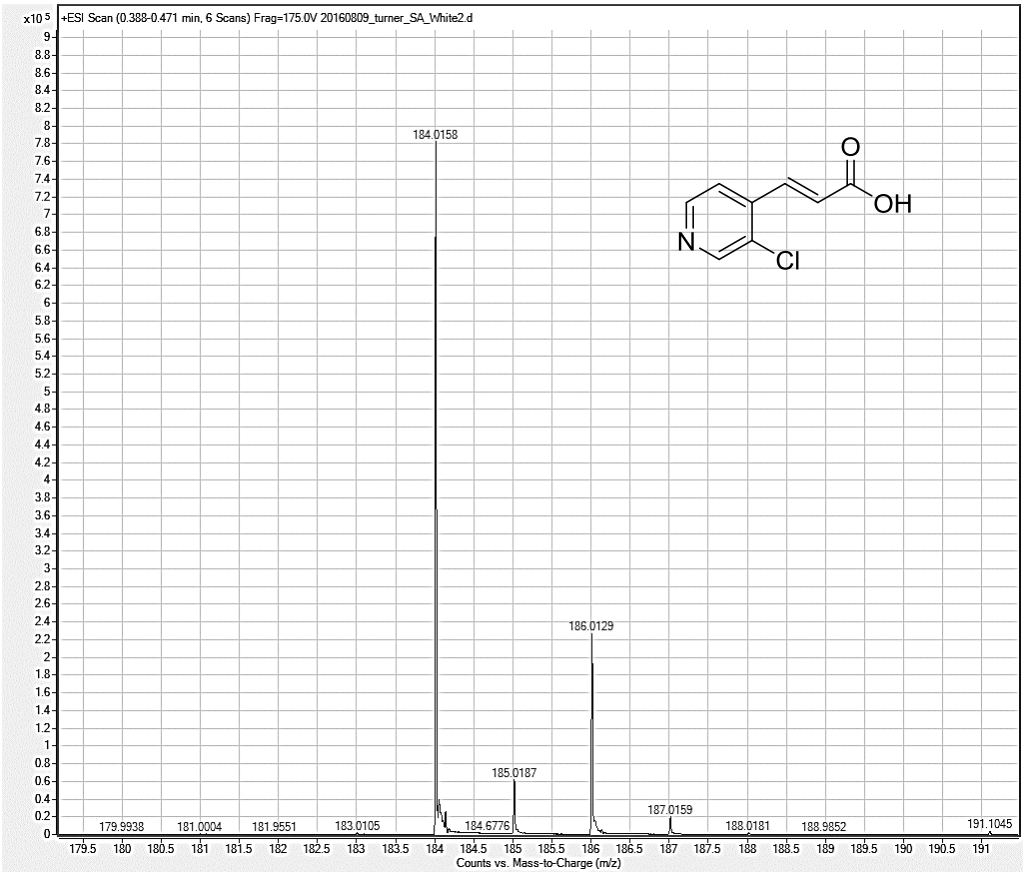
+ESI Scan (0.388-0.471 min, 6 Scans) Frag=175.0V 20160809_turner_SA_White2.d
x10 5
184.0158
186.0129
185.0187
187.0159
179.9938
181.0004
181.9551
183.0105
184.6776
188.0181
188.9852
191.1045
O
OH
N
Cl
Counts vs. Mass-to-Charge (m/z)

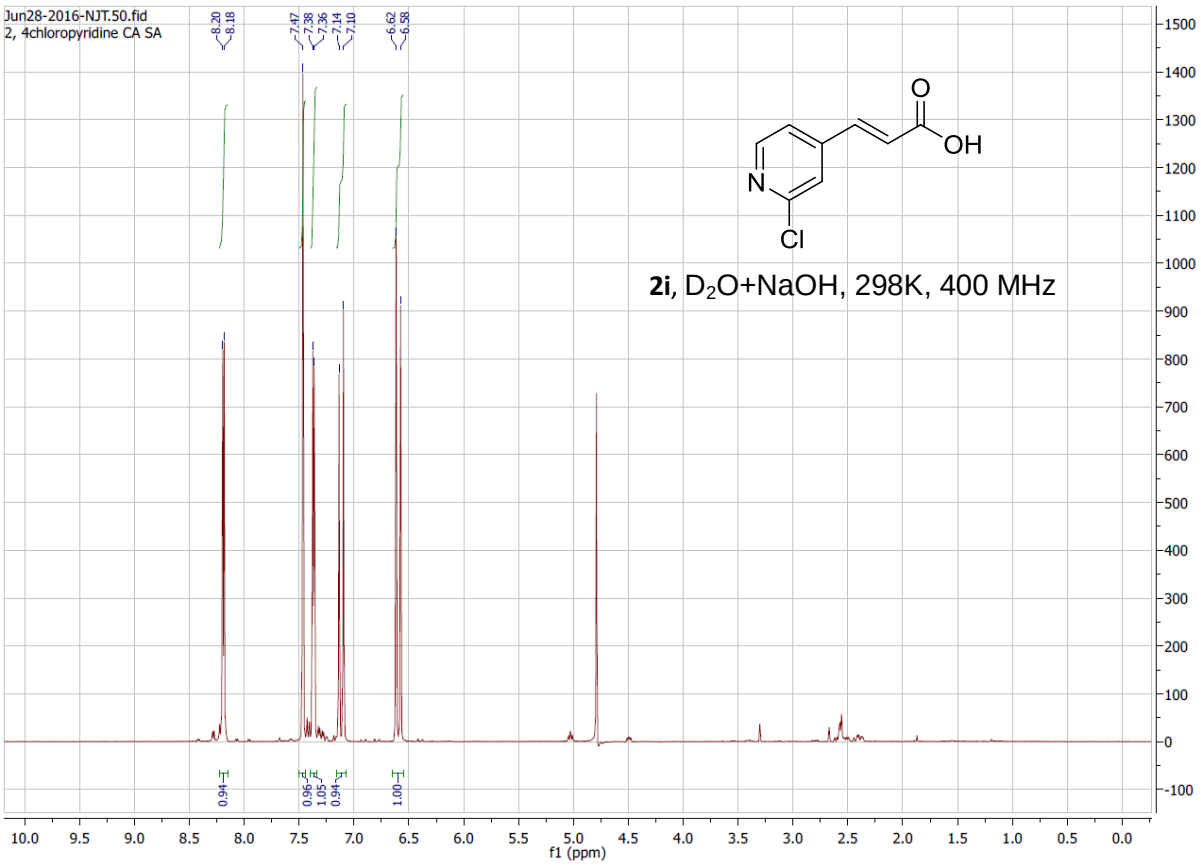

2i, D_2O+NaOH, 298K, 400 MHz

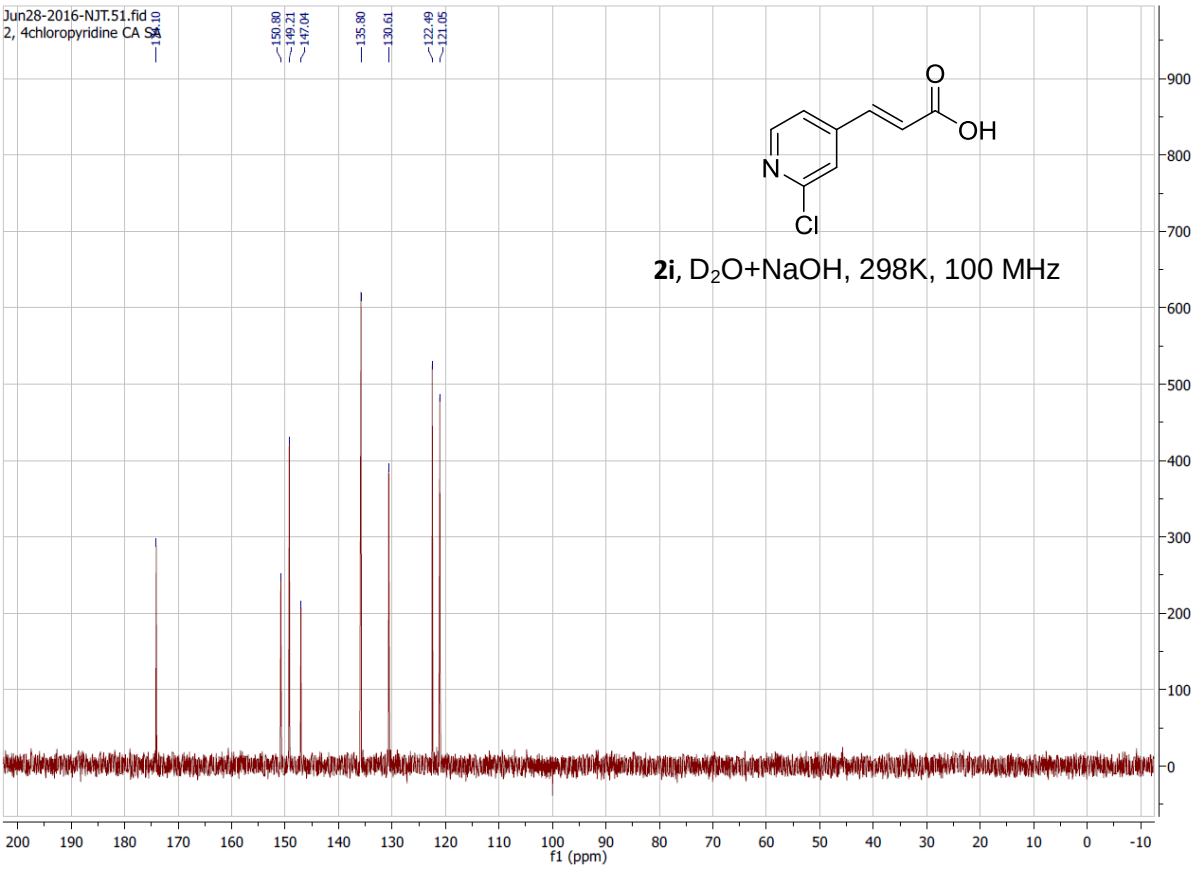

2i, D_2O+NaOH, 298K, 100 MHz

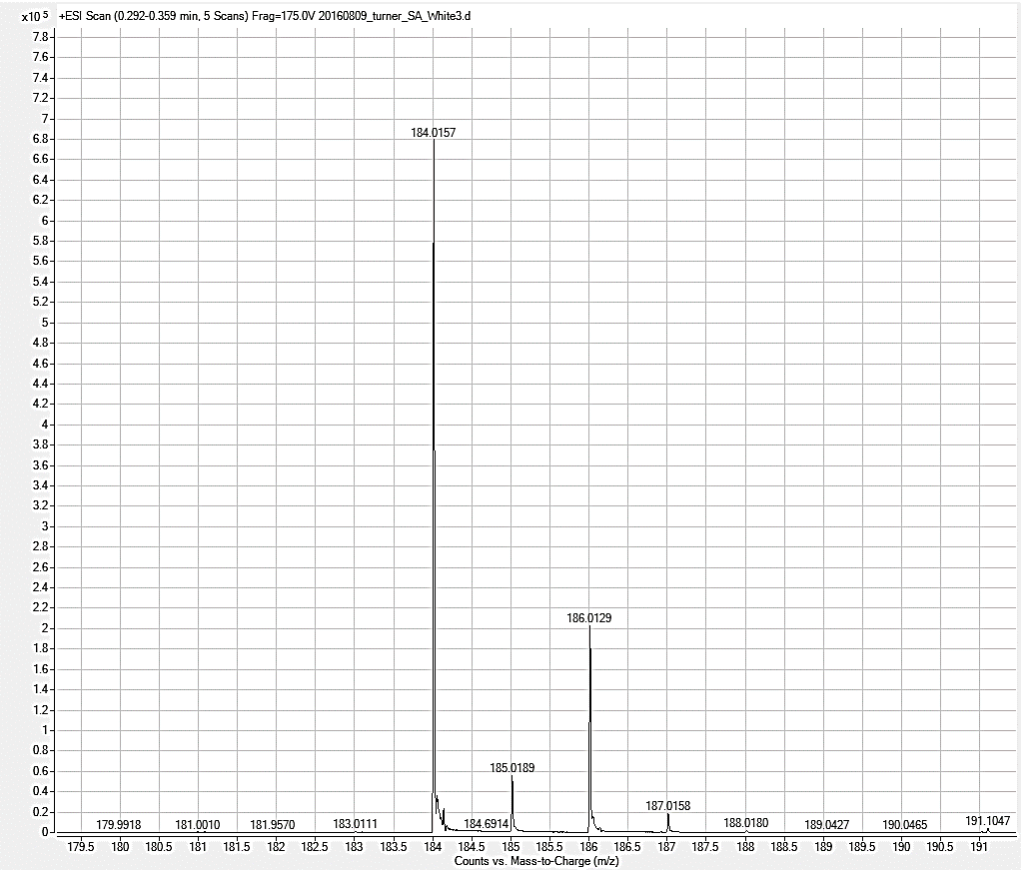
x10 5 +ESI Scan (0.292-0.359 min, 5 Scans) Frag=175.0V 20160809_turner_SA_White3.d
184.0157
186.0129
185.0189
187.0158
179.9918
181.0010
181.9570
183.0111
184.6914
188.0180
189.0427
190.0465
191.1047
Counts vs. Mass-to-Charge (m/z)

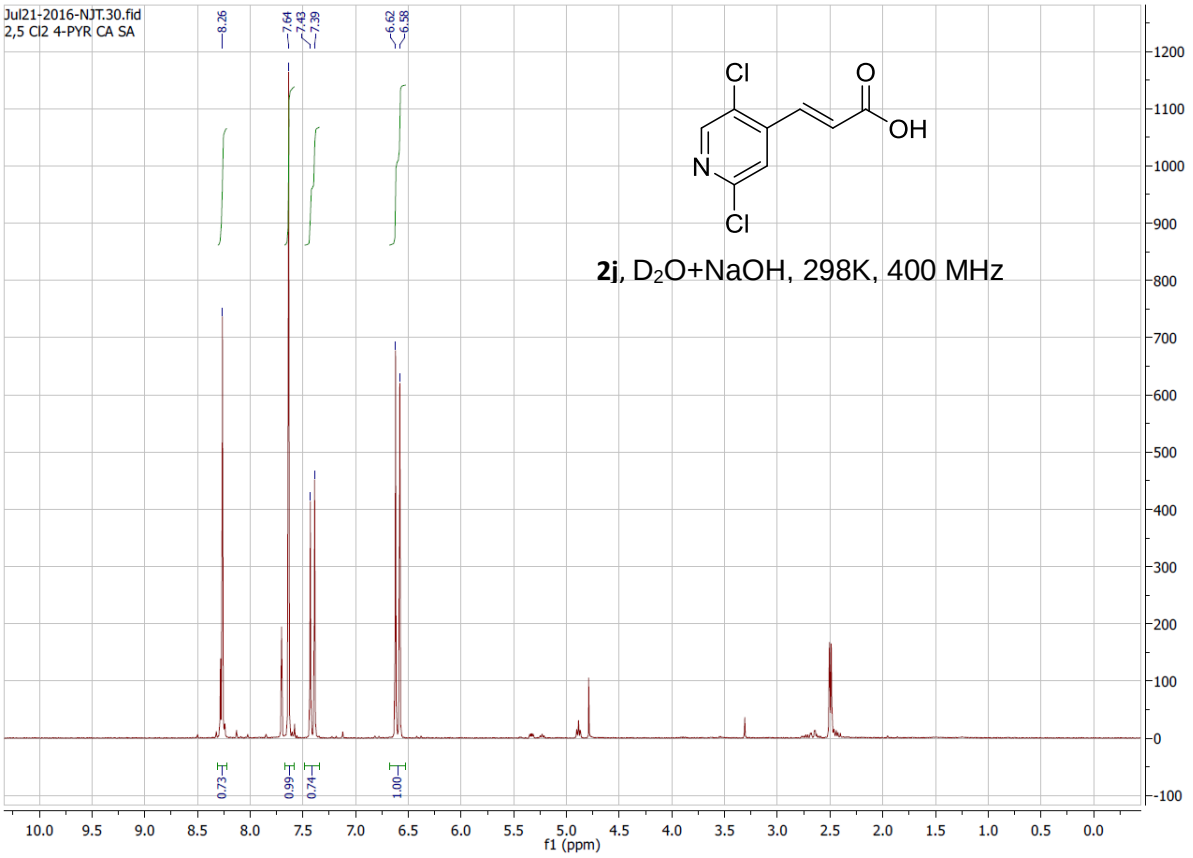

2j, D_2O+NaOH, 298K, 400 MHz

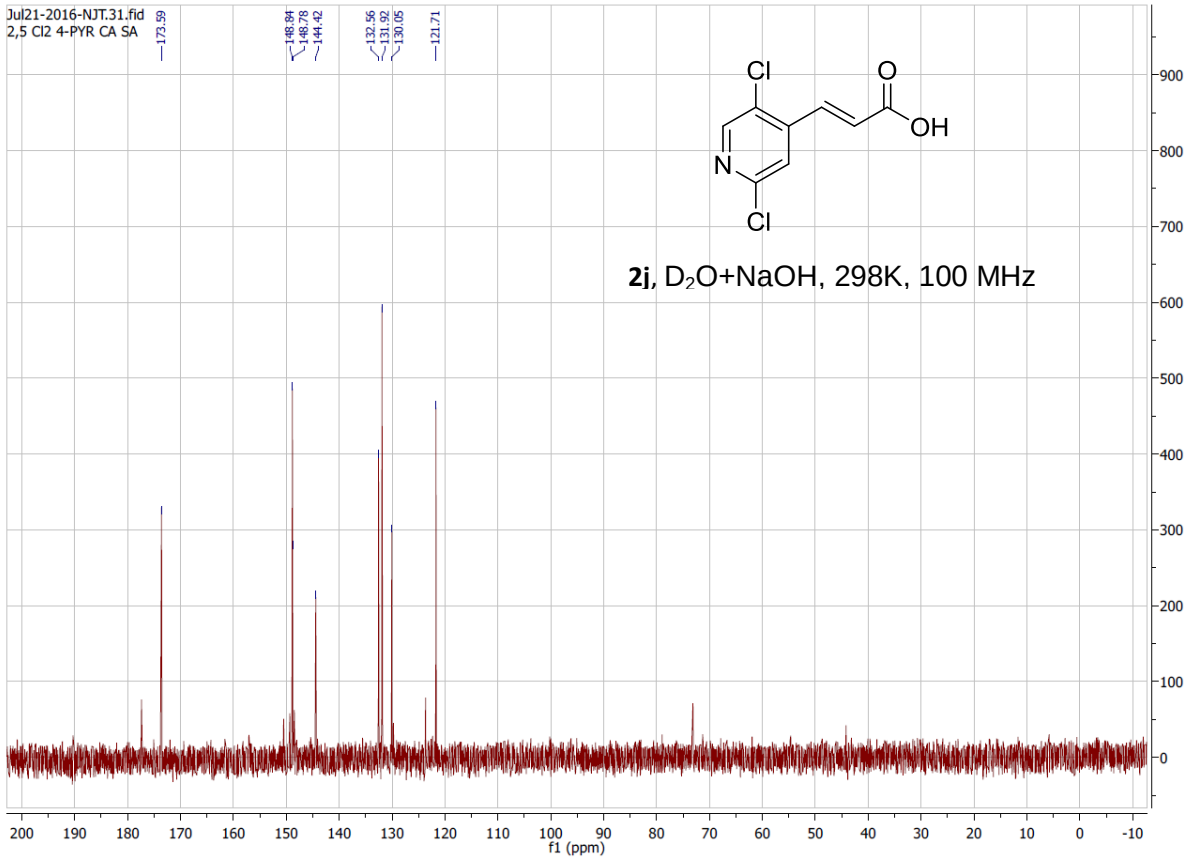

2j, D_2O+NaOH, 298K, 100 MHz

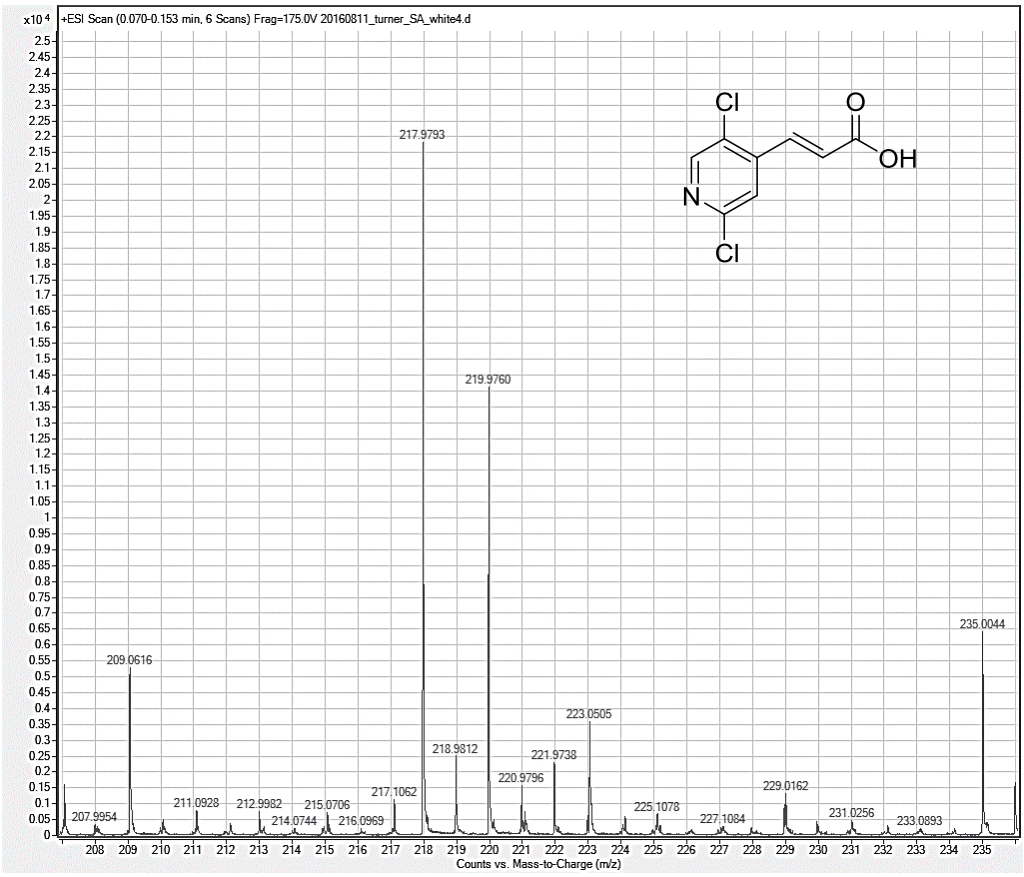
+ESI Scan (0.070-0.153 min, 6 Scans) Frag=175.0V 20160811_turner_SA_white4.d
x10 4
Cl
O
OH
N
Cl
217.9793
219.9760
235.0044
209.0616
223.0505
218.9812
221.9738
220.9796
229.0162
217.1062
211.0928
212.9982
215.0706
231.0256
225.1078
207.9954
214.0744
216.0969
227.1084
233.0893
Counts vs. Mass-to-Charge (m/z)

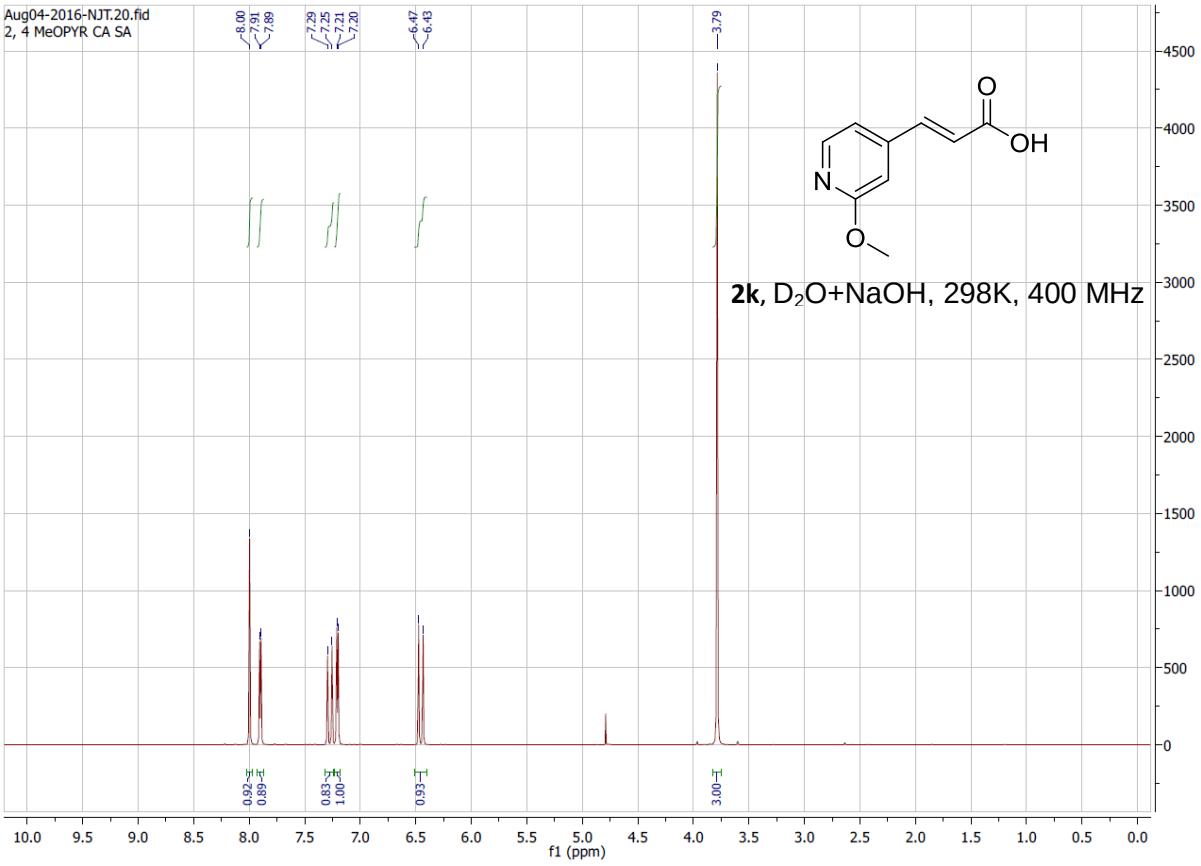
Aug04-2016-NJT.20.fid
2, 4 MeOPYR CA SA
8.00
7.91
7.89
7.29
7.25
7.21
7.20
6.47
6.43
3.79
0.92
0.89
0.83
1.00
0.93
3.00
f1 (ppm)
O
OH
N
O
2k, D2O+NaOH, 298K, 400 MHz

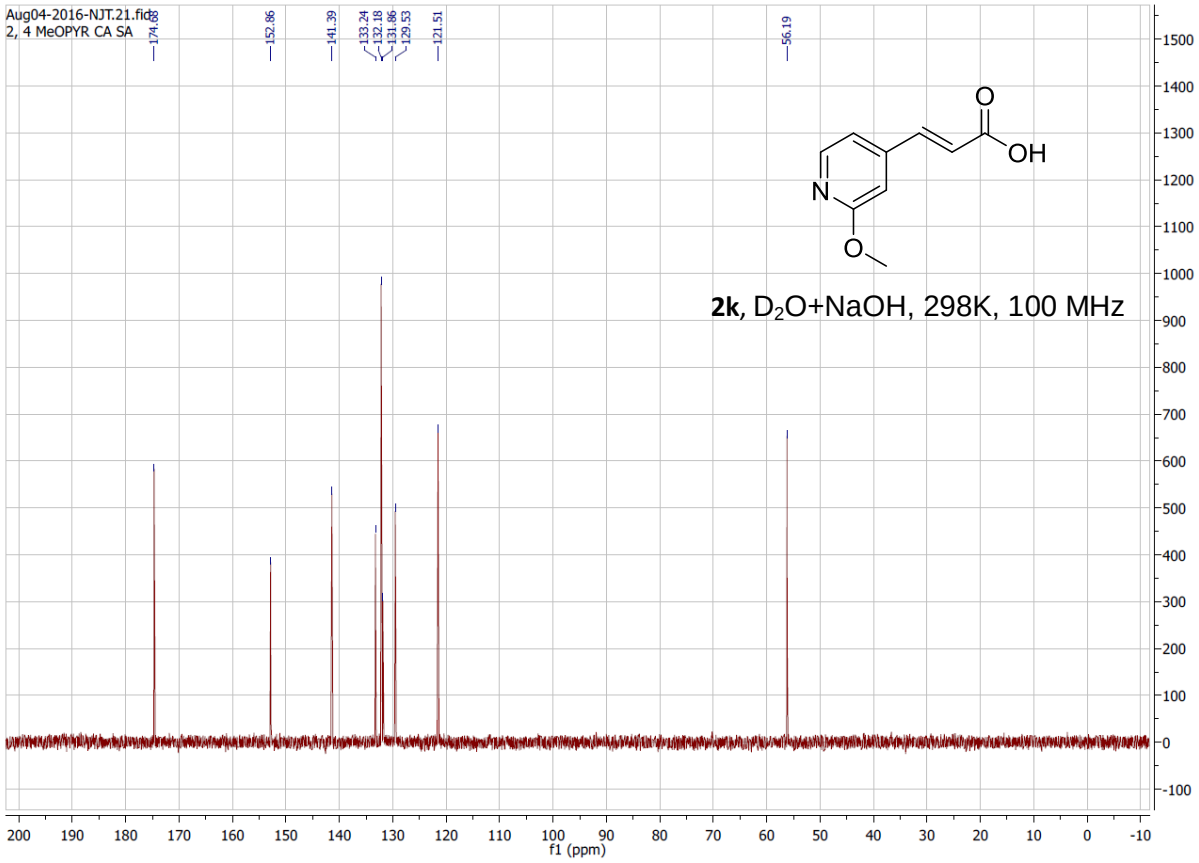
Aug04-2016-NJT.21.fid
2, 4 MeOPYR CA SA
174.88
152.86
141.39
133.24
132.18
131.86
129.53
121.51
56.19
f1 (ppm)
O
OH
N
O
2k, D2O+NaOH, 298K, 100 MHz

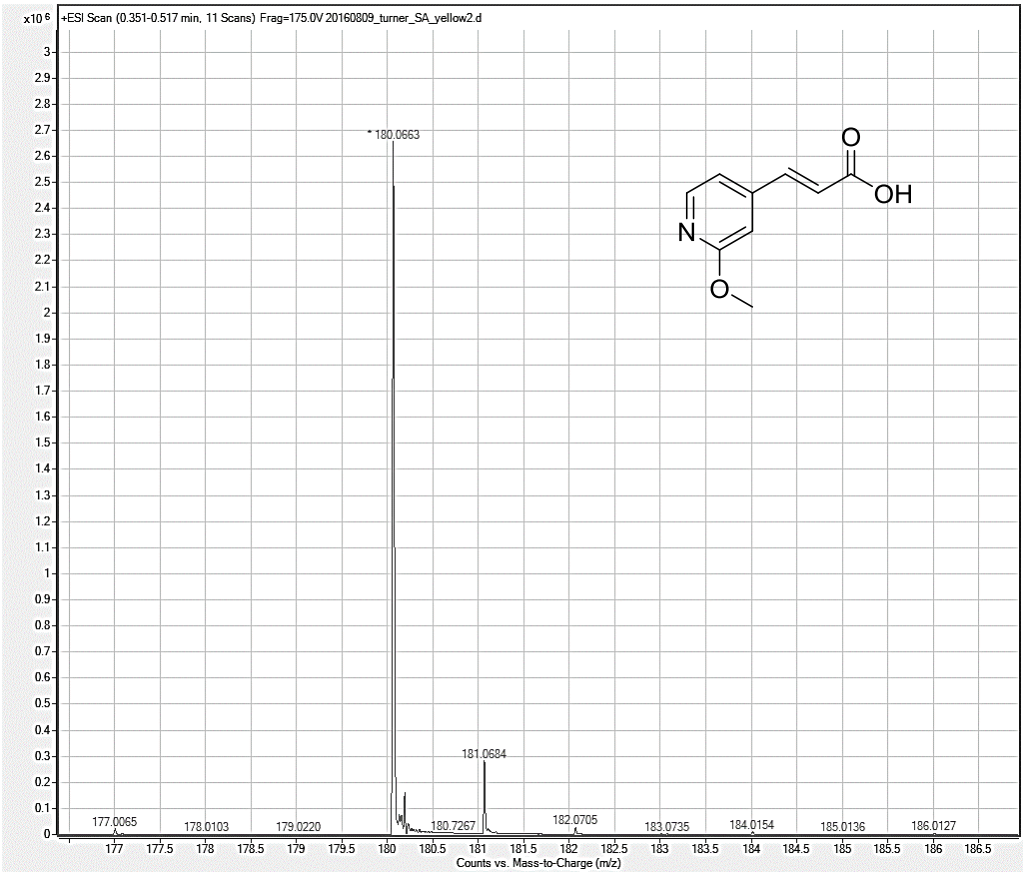
x10 6
+ESI Scan (0.351-0.517 min, 11 Scans) Frag=175.0V 20160809_turner_SA_yellow2.d
* 180.0663
181.0684
177.0065
178.0103
179.0220
180.7267
182.0705
183.0735
184.0154
185.0136
186.0127
Counts vs. Mass-to-Charge (m/z)
O
OH
N
O

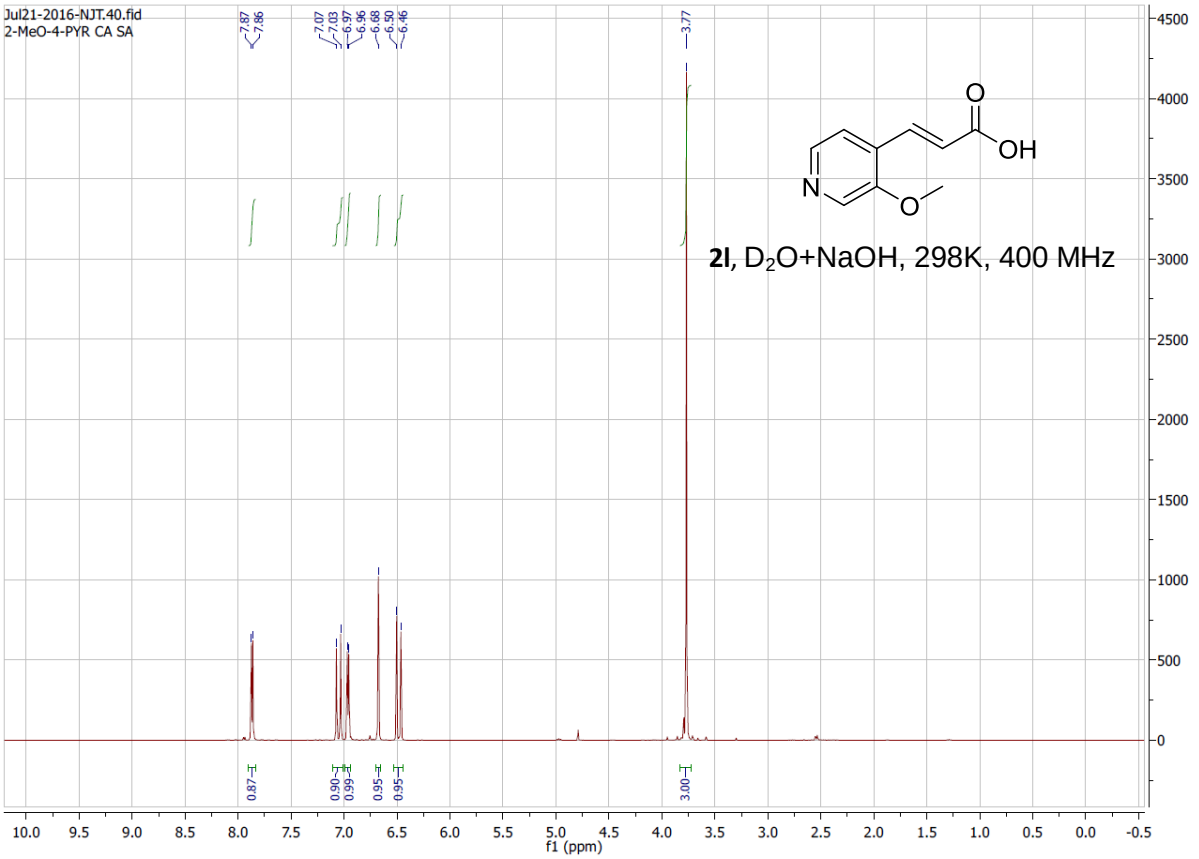

2l, D_2O+NaOH, 298K, 400 MHz

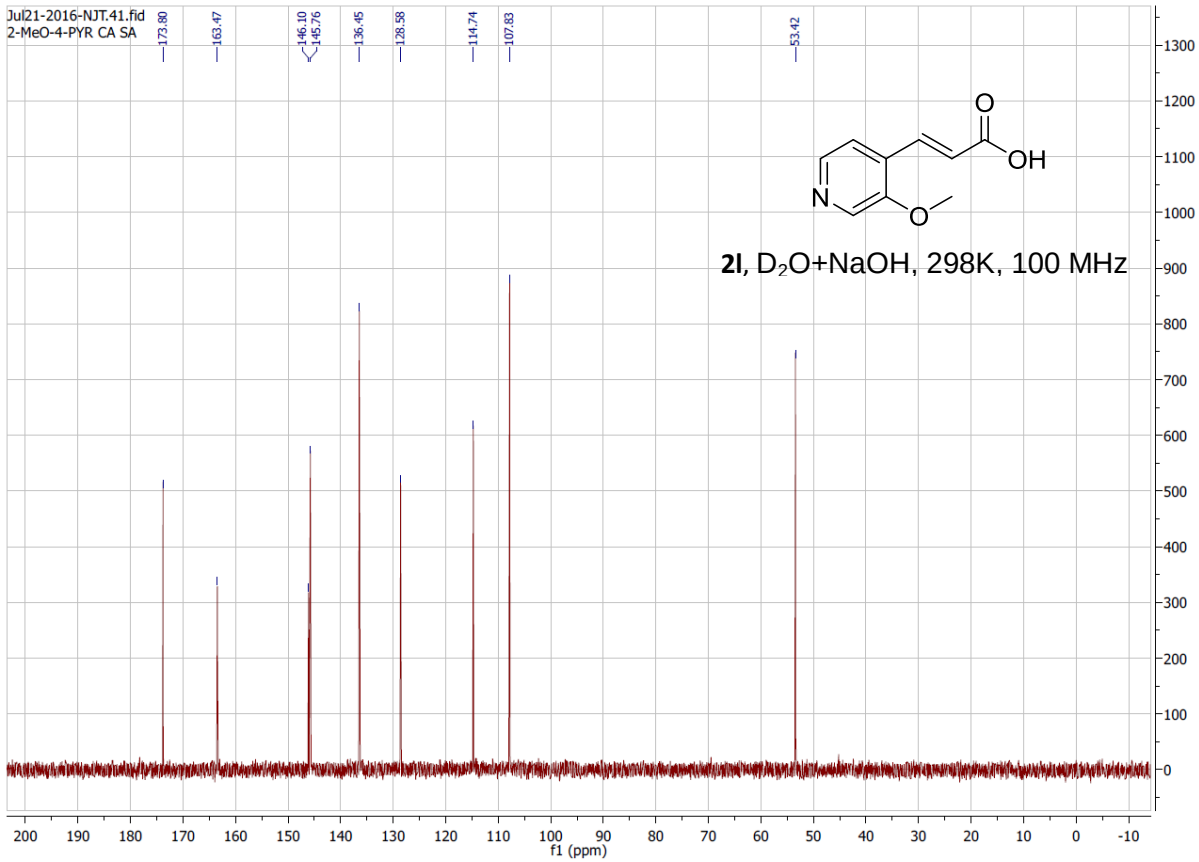

2l, D_2O+NaOH, 298K, 100 MHz

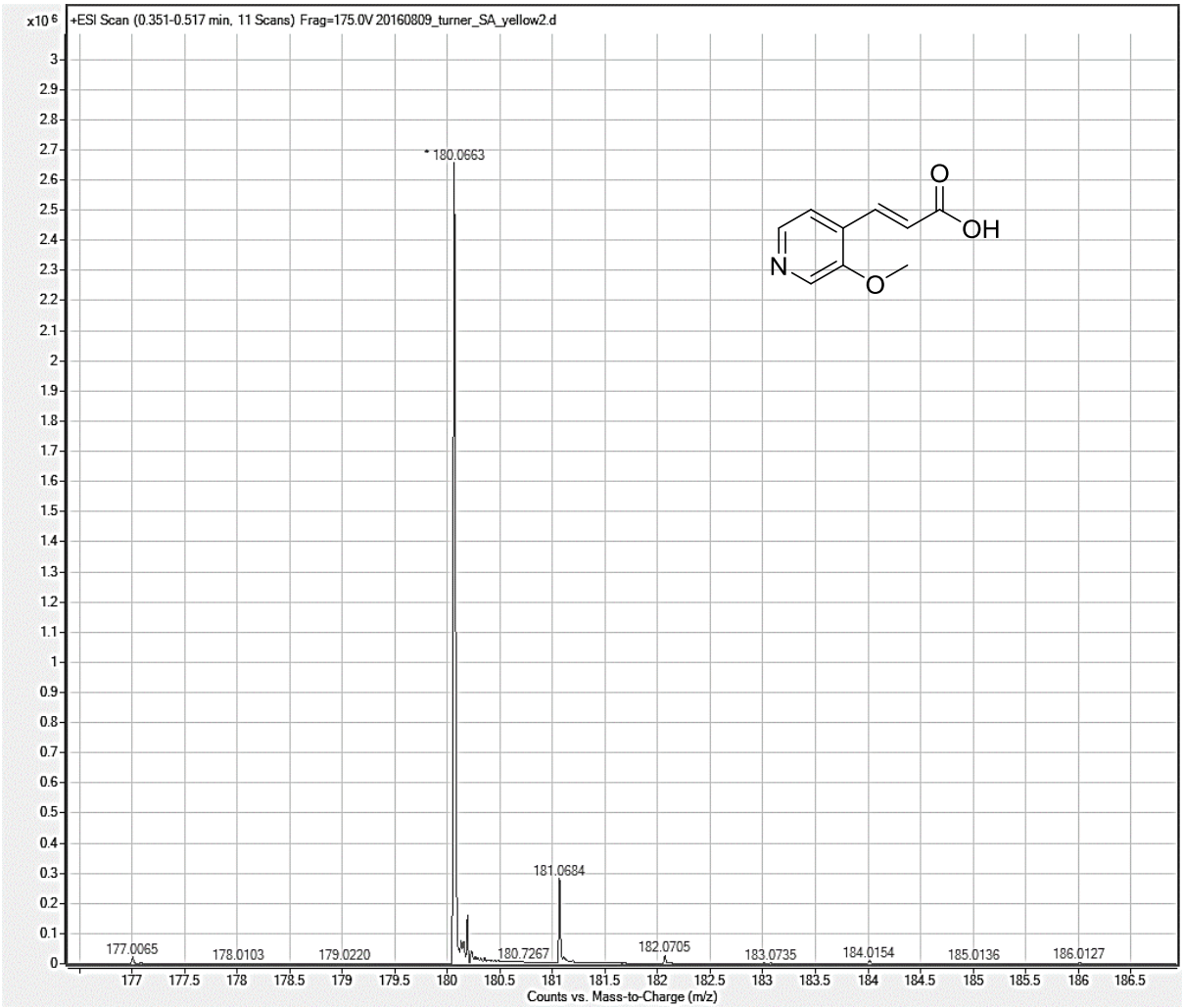
x10 6
+ESI Scan (0.351-0.517 min, 11 Scans) Frag=175.0V 20160809_turner_SA_yellow2.d
180.0663
181.0684
177.0065
178.0103
179.0220
180.7267
182.0705
183.0735
184.0154
185.0136
186.0127
O
OH
N
O
Counts vs. Mass-to-Charge (m/z)

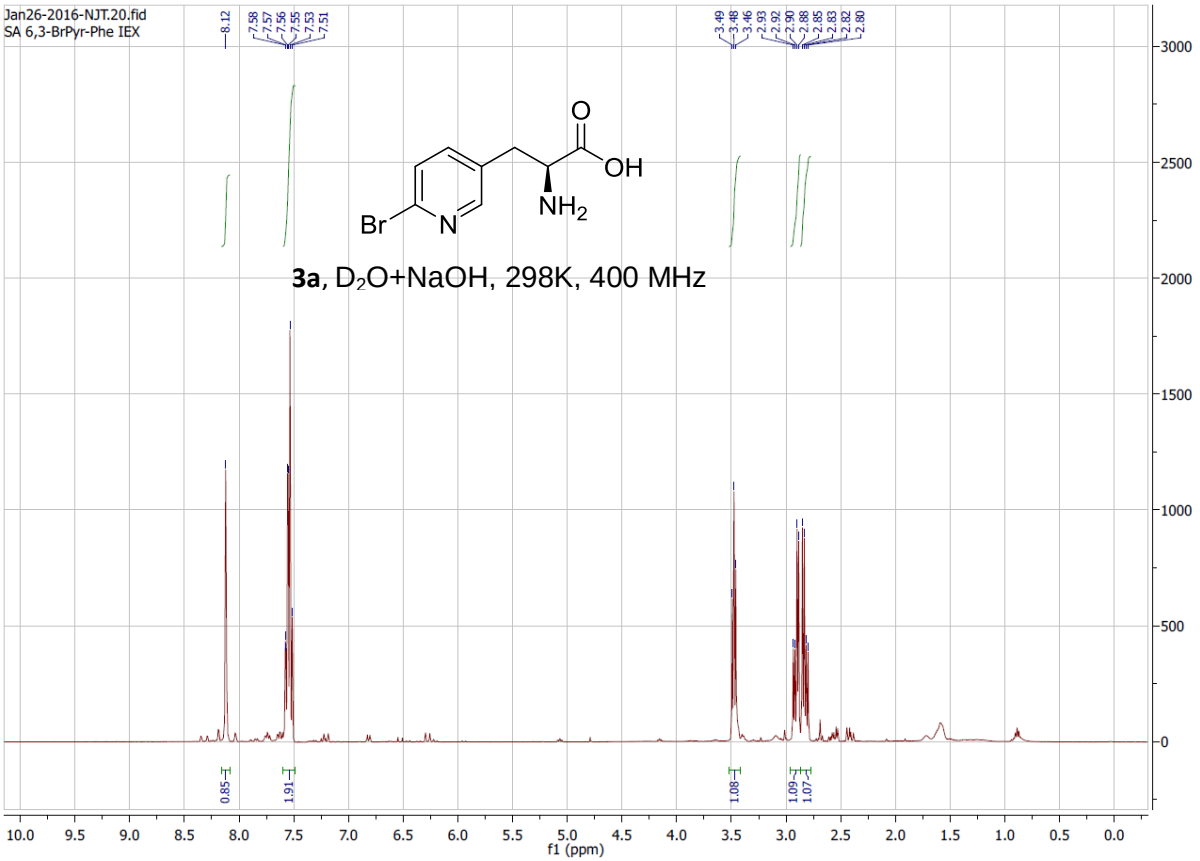
Jan26-2016-NJT.20.fid
SA 6,3-BrPyr-Phe IEX
8.12
7.58
7.57
7.56
7.55
7.53
7.51
3.49
3.48
3.46
2.93
2.92
2.90
2.88
2.85
2.83
2.82
2.80
O
OH
NH2
Br
N
3a, D2O+NaOH, 298K, 400 MHz
0.85
1.91
1.08
1.09
1.07
f1 (ppm)

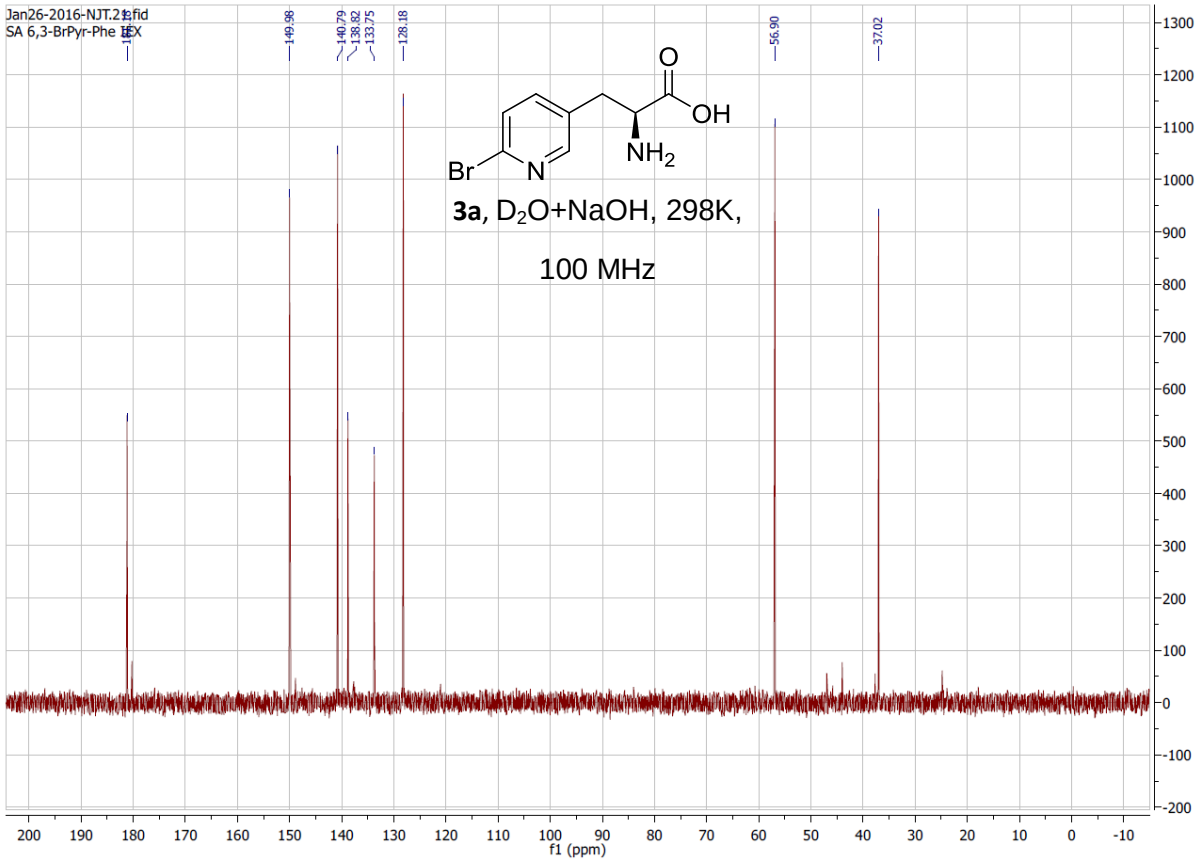
Jan26-2016-NJT.21.fid
SA 6,3-BrPyr-Phe IEX
149.98
140.79
138.82
133.75
128.18
56.90
37.02
O
OH
NH2
Br
N
3a, D2O+NaOH, 298K,
100 MHz
f1 (ppm)

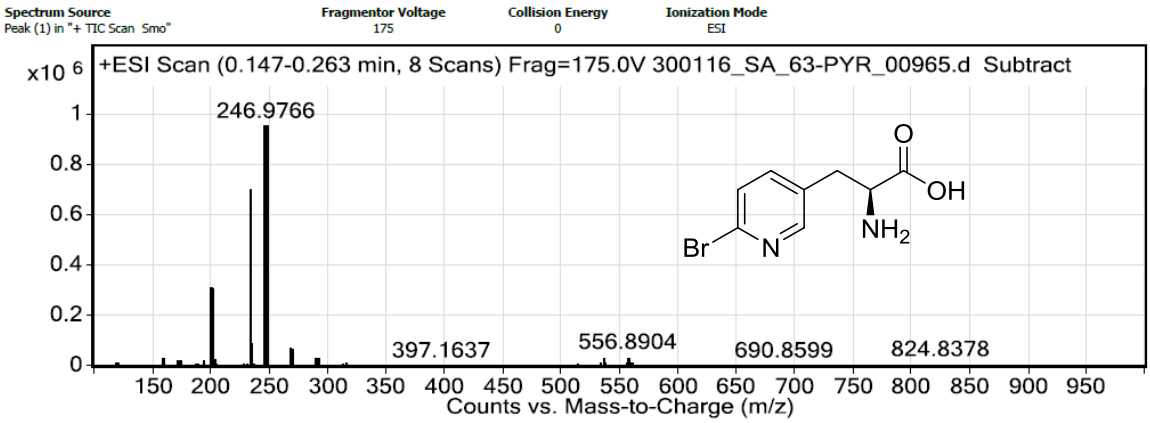
Spectrum Source
Peak (1) in "+ TIC Scan Smo"
Fragmentor Voltage
175
Collision Energy
0
Ionization Mode
ESI
+ESI Scan (0.147-0.263 min, 8 Scans) Frag=175.0V 300116_SA_63-PYR_00965.d Subtract
x10 6
246.9766
397.1637
556.8904
690.8599
824.8378
Br
N
NH2
OH
O
Counts vs. Mass-to-Charge (m/z)

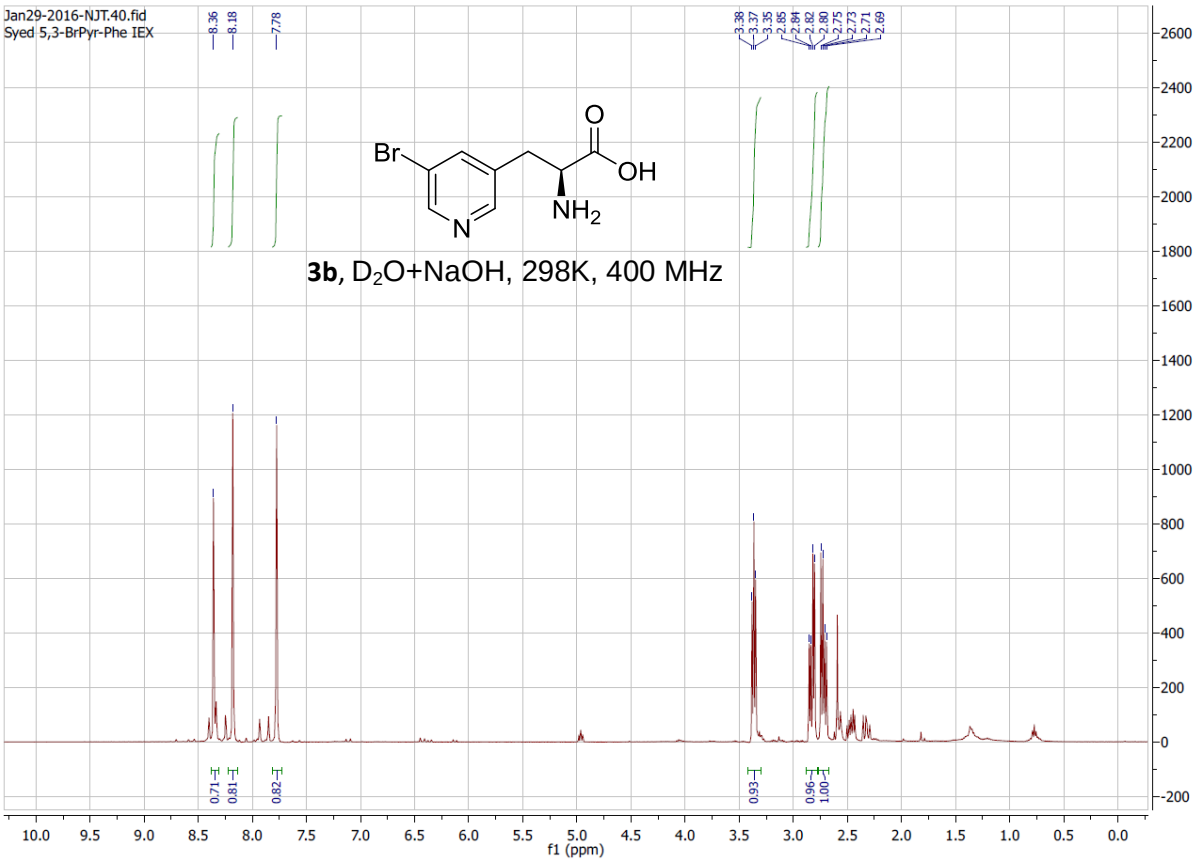

3b, D_2O+NaOH, 298K, 400 MHz

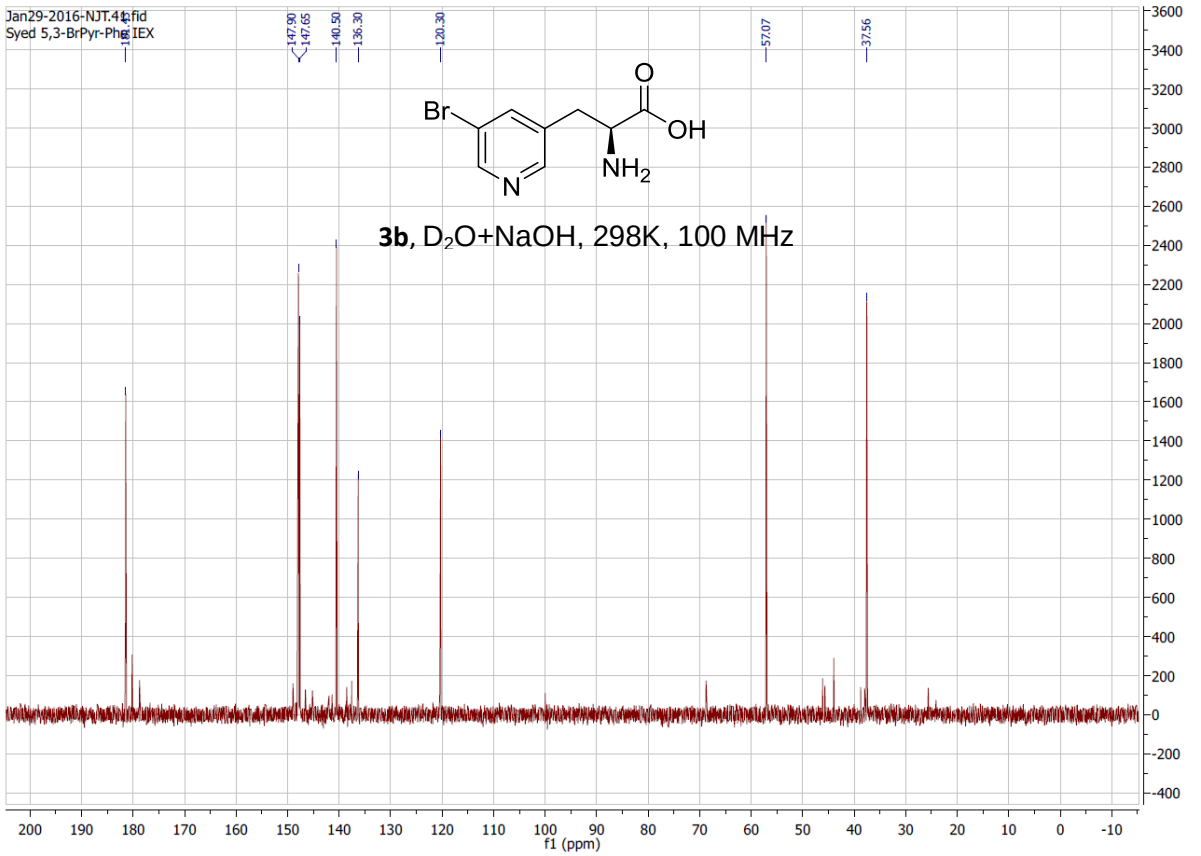

3b, D_2O+NaOH, 298K, 100 MHz

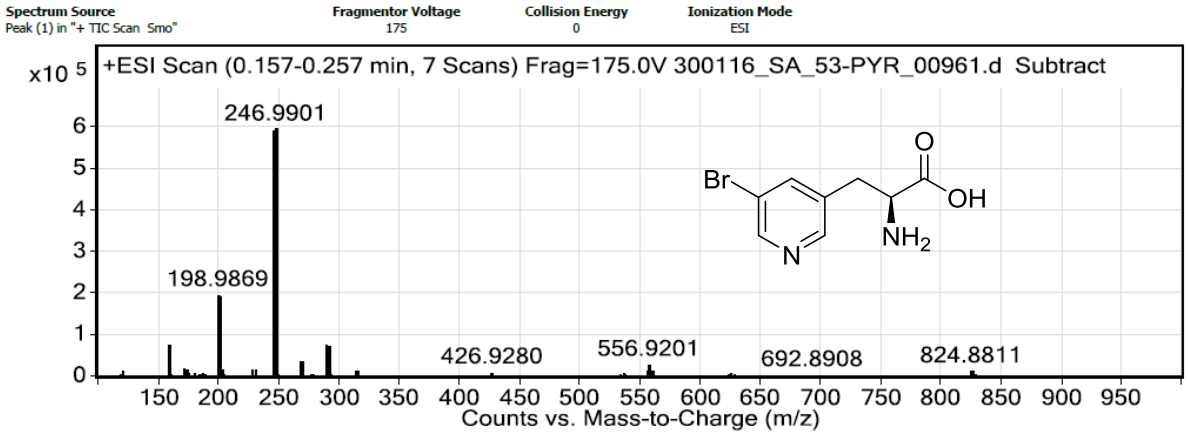
Spectrum Source
Peak (1) in "+ TIC Scan Smo"
Fragmentor Voltage
175
Collision Energy
0
Ionization Mode
ESI
+ESI Scan (0.157-0.257 min, 7 Scans) Frag=175.0V 300116_SA_53-PYR_00961.d Subtract
x10 5
246.9901
198.9869
426.9280
556.9201
692.8908
824.8811
Br
O
OH
NH2
N
Counts vs. Mass-to-Charge (m/z)

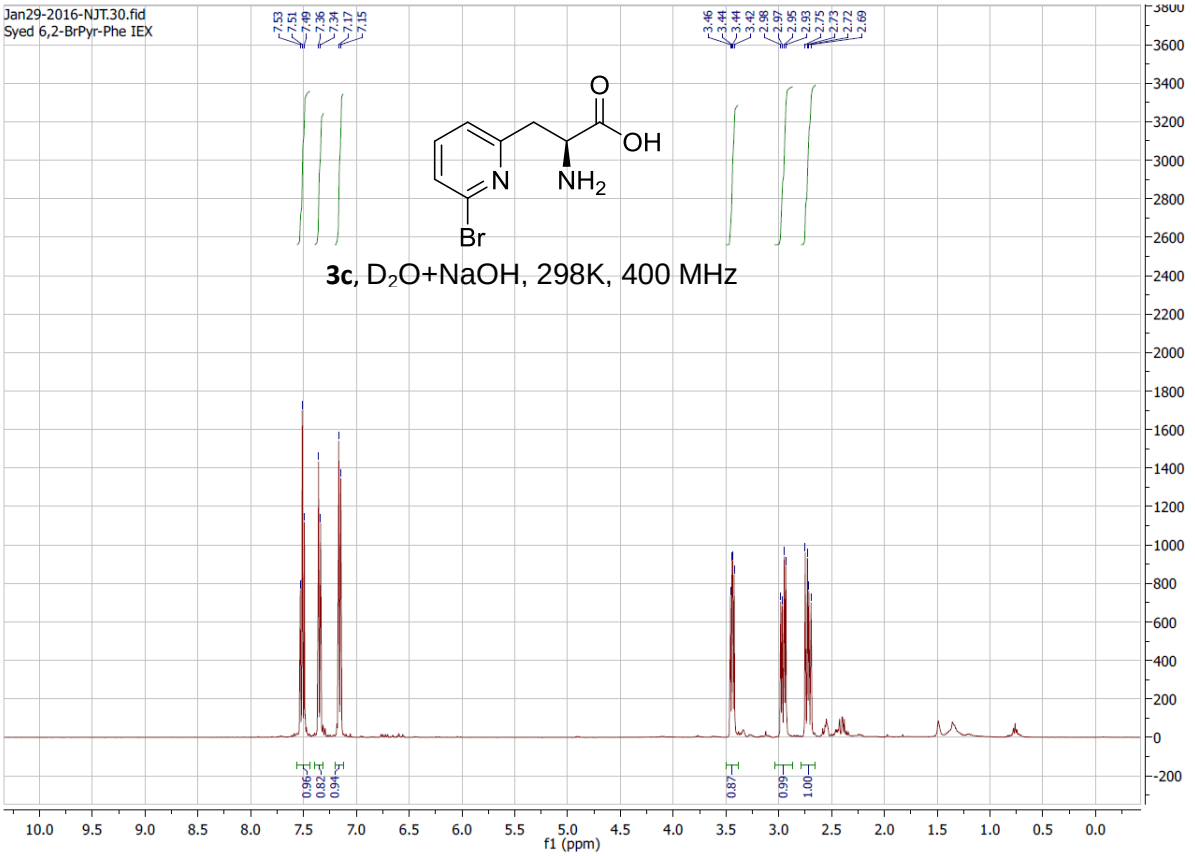

3c, D_2O+NaOH, 298K, 400 MHz

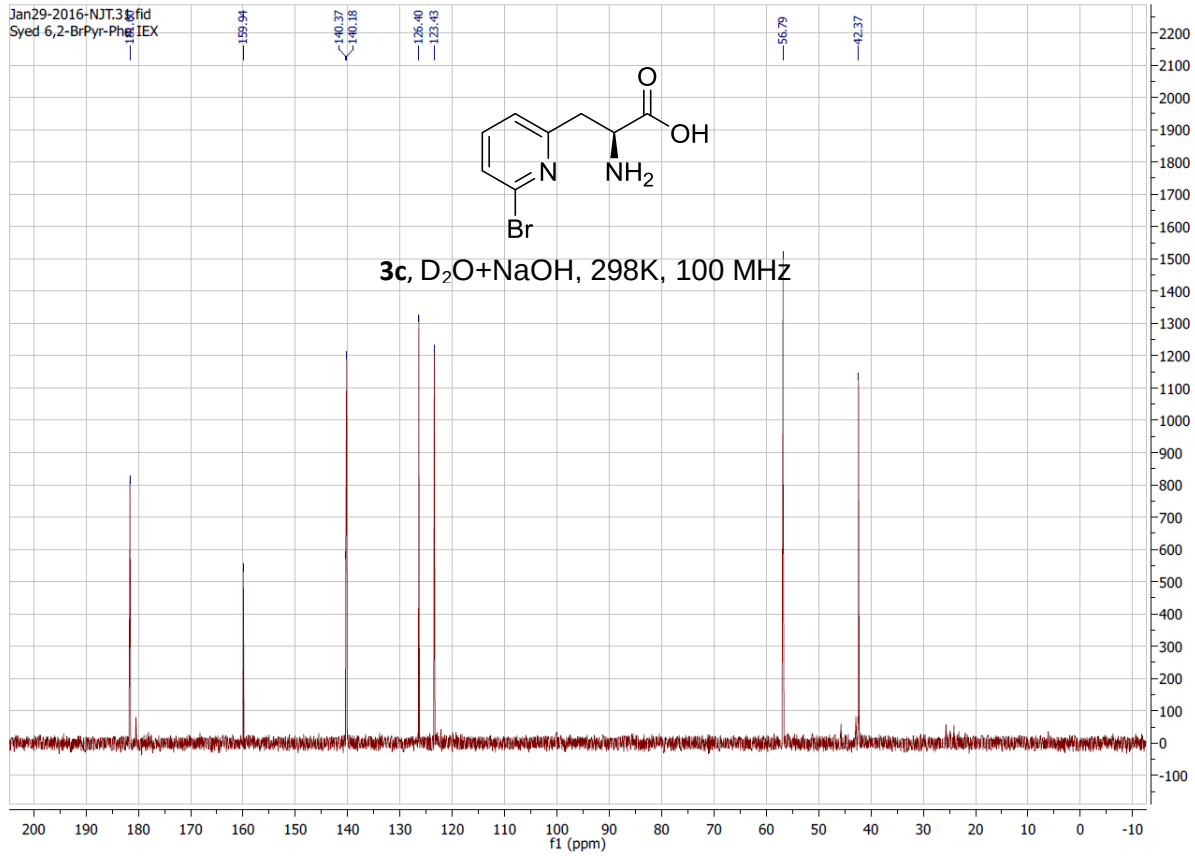

3c, D_2O+NaOH, 298K, 100 MHz

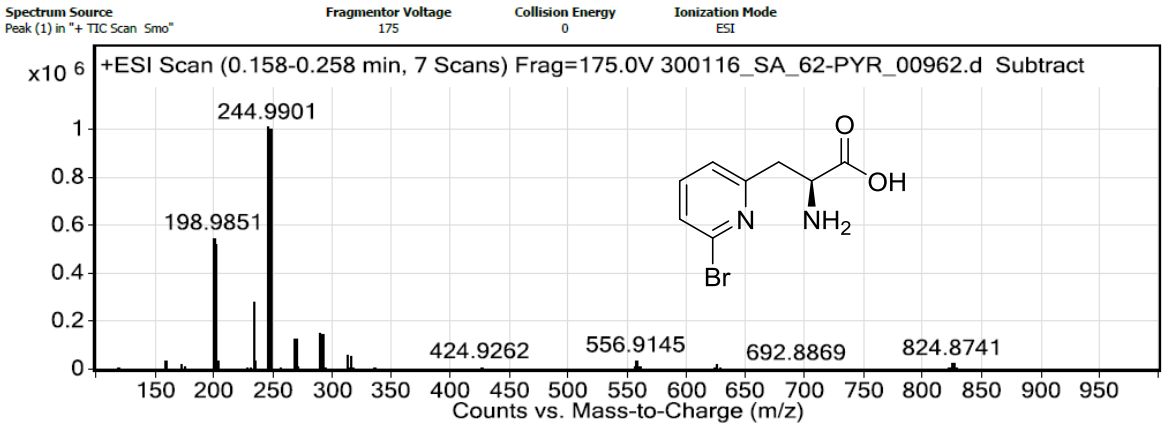
Spectrum Source
Peak (1) in "+ TIC Scan Smo"
Fragmentor Voltage
175
Collision Energy
0
Ionization Mode
ESI
+ESI Scan (0.158-0.258 min, 7 Scans) Frag=175.0V 300116_SA_62-PYR_00962.d Subtract
x10 6
244.9901
198.9851
424.9262
556.9145
692.8869
824.8741
O
OH
N
NH2
Br
Counts vs. Mass-to-Charge (m/z)

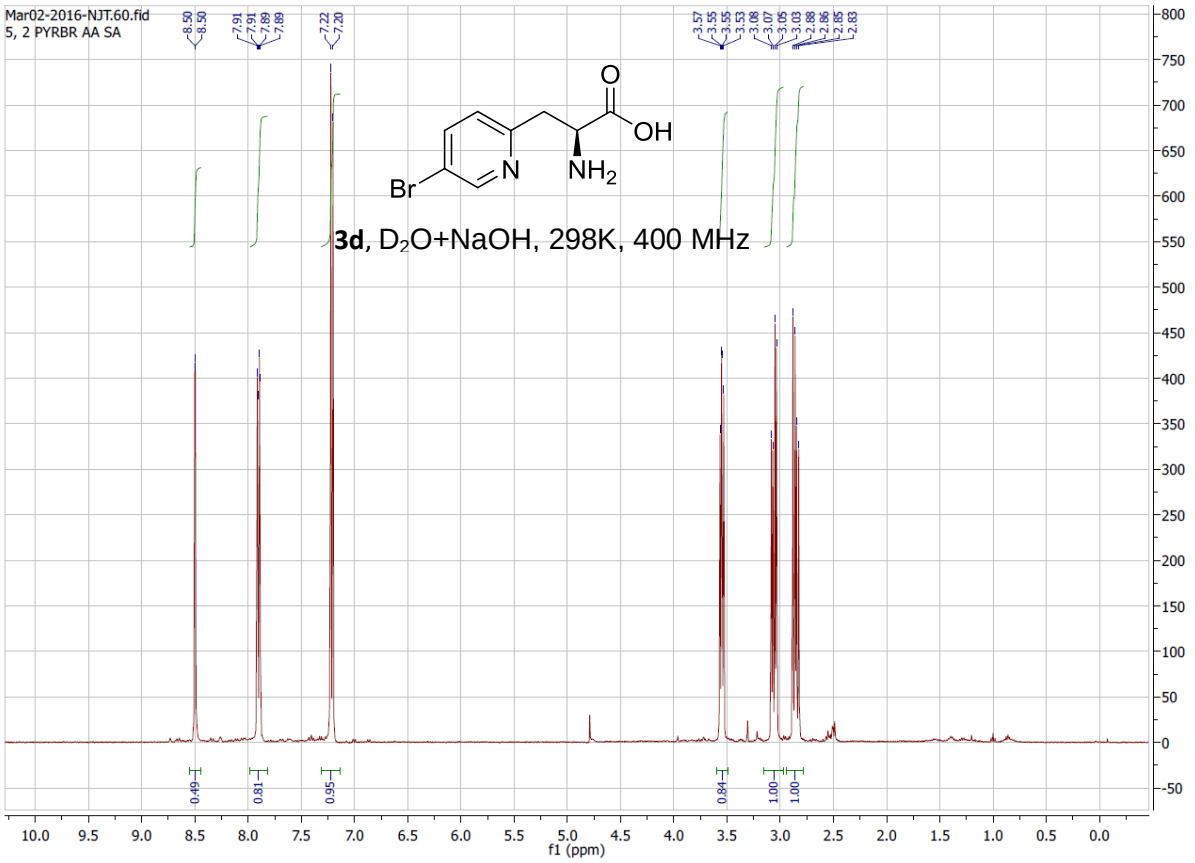
Mar02-2016-NJT.60.fid
5, 2 PYRBR AA SA
O
OH
N
NH2
Br
3d, D2O+NaOH, 298K, 400 MHz
f1 (ppm)

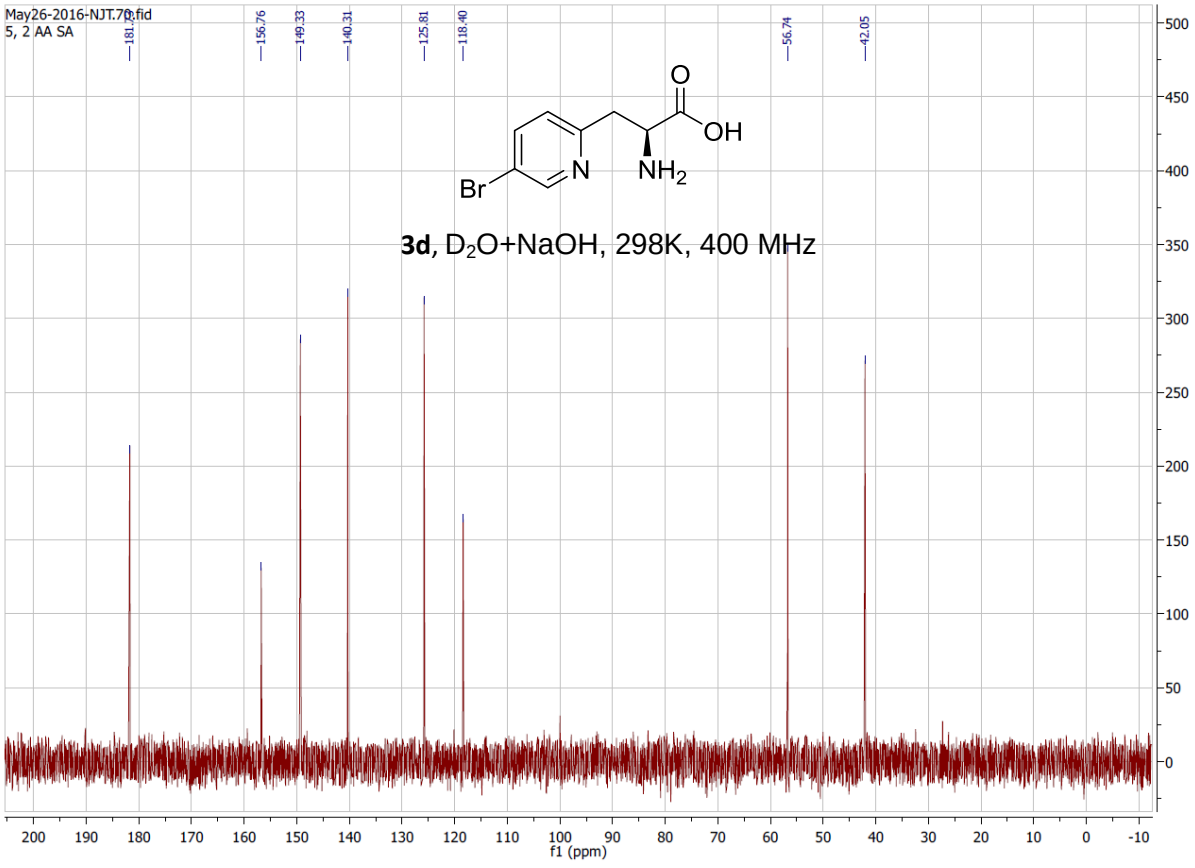
May26-2016-NJT.70.fid
5, 2 AA SA
O
OH
N
NH2
Br
3d, D2O+NaOH, 298K, 400 MHz
f1 (ppm)

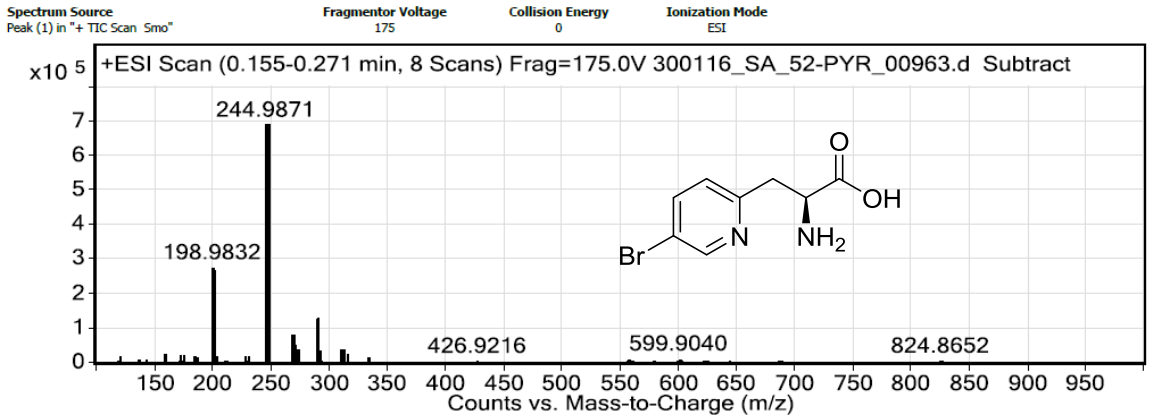
Spectrum Source
Peak (1) in "+ TIC Scan Smo"
Fragmentor Voltage
175
Collision Energy
0
Ionization Mode
ESI
+ESI Scan (0.155-0.271 min, 8 Scans) Frag=175.0V 300116_SA_52-PYR_00963.d Subtract
x10 5
244.9871
198.9832
426.9216
599.9040
824.8652
Br
N
NH2
OH
O
Counts vs. Mass-to-Charge (m/z)

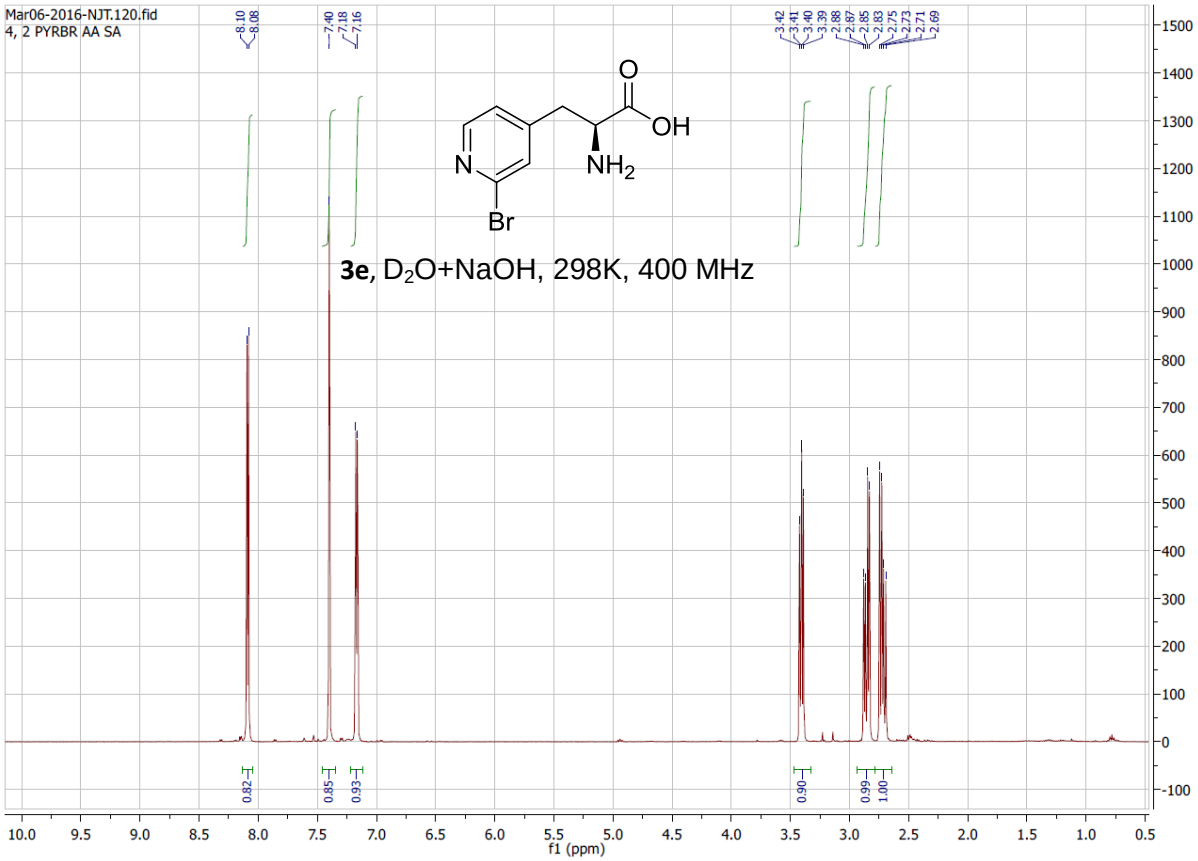
Mar06-2016-NJT.120.fid
4, 2 PYRBR AA SA
8.10
8.08
7.40
7.18
7.16
3.42
3.41
3.40
3.39
2.88
2.87
2.85
2.83
2.75
2.73
2.71
2.69
O
OH
N
NH2
Br
3e, D2O+NaOH, 298K, 400 MHz
0.82
0.85
0.93
0.90
0.99
1.00
f1 (ppm)

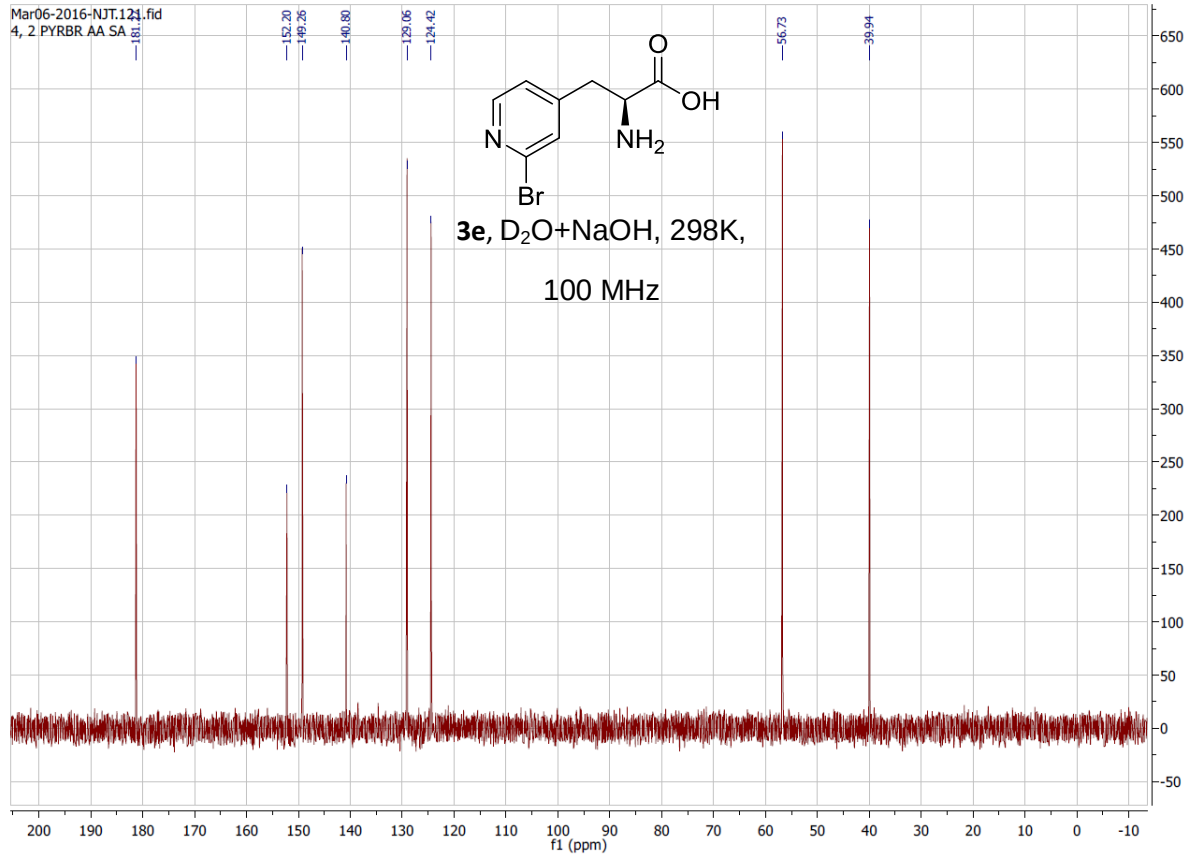
Mar06-2016-NJT.121.fid
4, 2 PYRBR AA SA
181.41
152.20
149.26
140.80
129.06
124.42
56.73
39.94
O
OH
N
NH2
Br
3e, D2O+NaOH, 298K,
100 MHz
f1 (ppm)

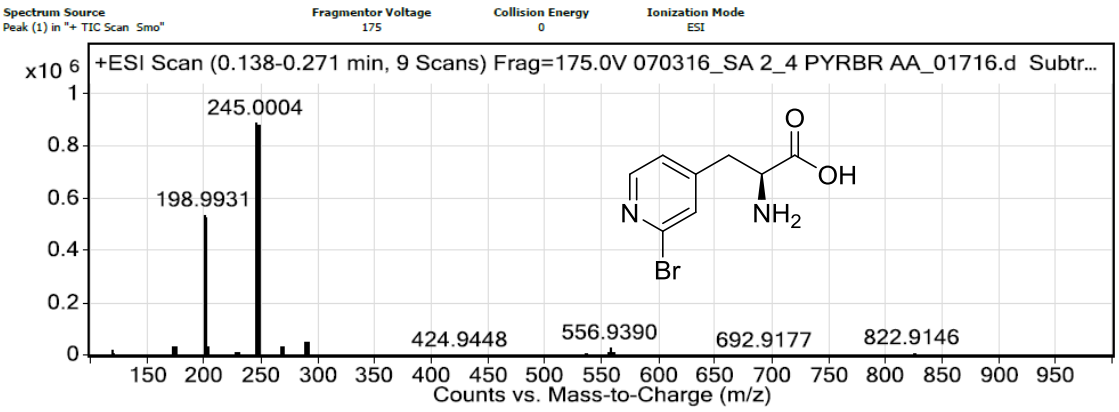
Spectrum Source
Peak (1) in "+ TIC Scan Smo"
Fragmentor Voltage
175
Collision Energy
0
Ionization Mode
ESI
+ESI Scan (0.138-0.271 min, 9 Scans) Frag=175.0V 070316_SA 2_4 PYRBR AA_01716.d Subtr...
x10 6
245.0004
198.9931
424.9448
556.9390
692.9177
822.9146
O
OH
N
NH2
Br
Counts vs. Mass-to-Charge (m/z)

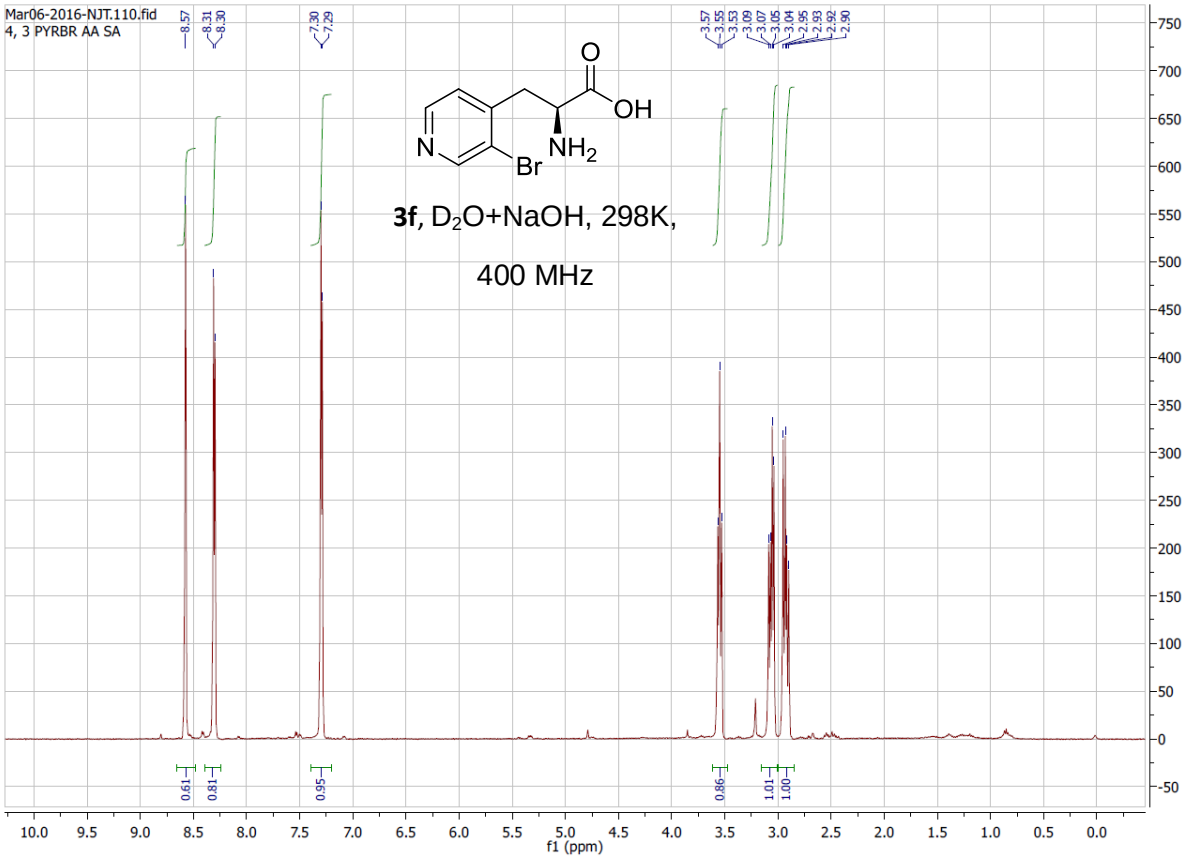
Mar06-2016-NJT.110.fid
4, 3 PYRBR AA SA
8.57
8.31
8.30
7.30
7.29
3.57
3.55
3.53
3.09
3.07
3.05
3.04
2.95
2.93
2.92
2.90
O
OH
N
Br
NH2
3f, D2O+NaOH, 298K,
400 MHz
0.61
0.81
0.95
0.86
1.01
1.00
f1 (ppm)

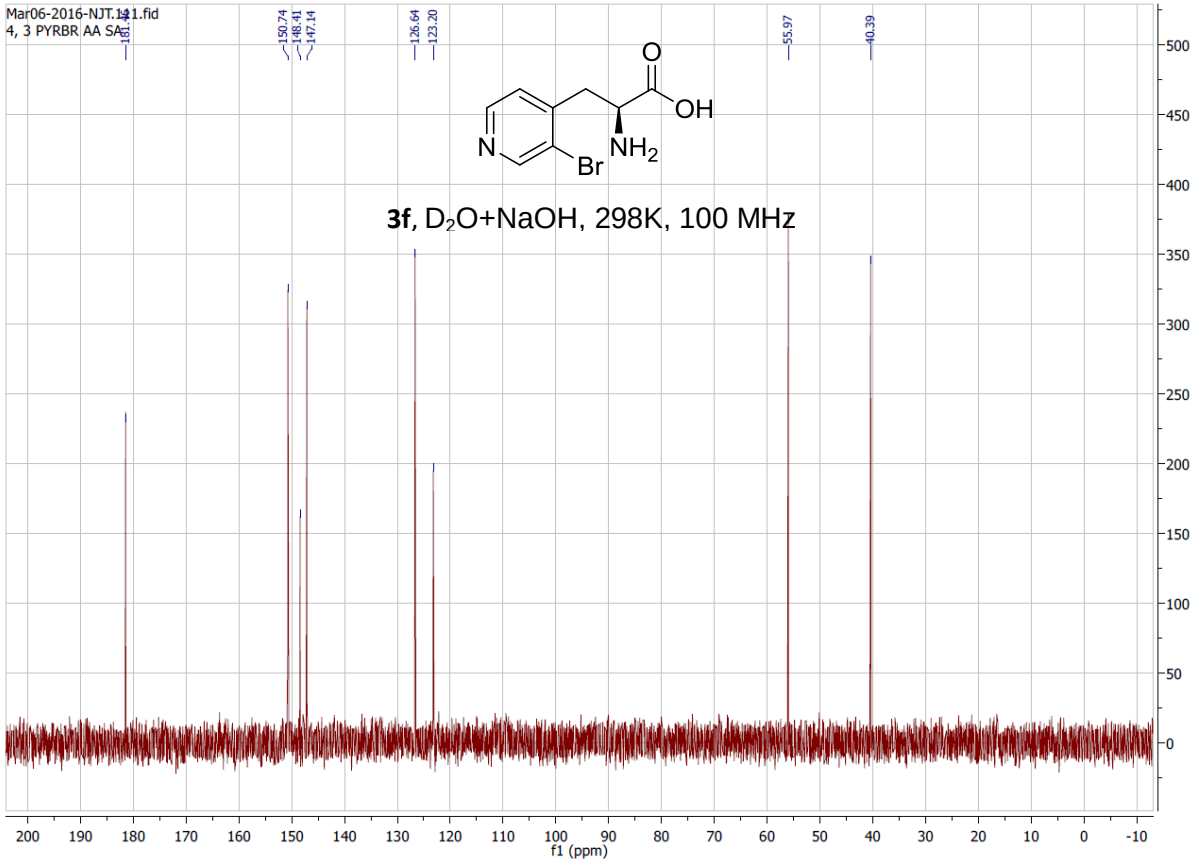
Mar06-2016-NJT.111.fid
4, 3 PYRBR AA SA
150.74
148.41
147.14
126.64
123.20
55.97
40.39
O
OH
N
Br
NH2
3f, D2O+NaOH, 298K, 100 MHz
f1 (ppm)

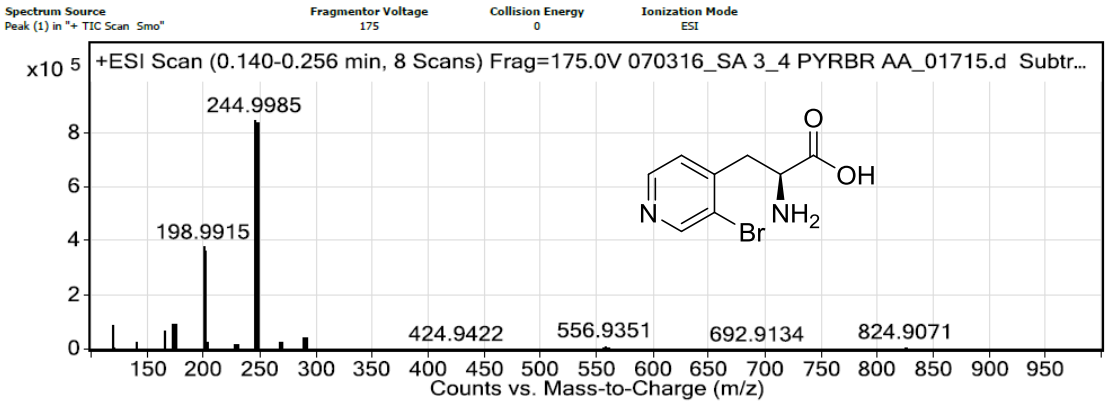
Spectrum Source
Peak (1) in "+ TIC Scan Smo"
Fragmentor Voltage
175
Collision Energy
0
Ionization Mode
ESI
+ESI Scan (0.140-0.256 min, 8 Scans) Frag=175.0V 070316_SA 3_4 PYRBR AA_01715.d Subtr...
x10 5
244.9985
198.9915
424.9422
556.9351
692.9134
824.9071
O
OH
N
NH2
Br
Counts vs. Mass-to-Charge (m/z)

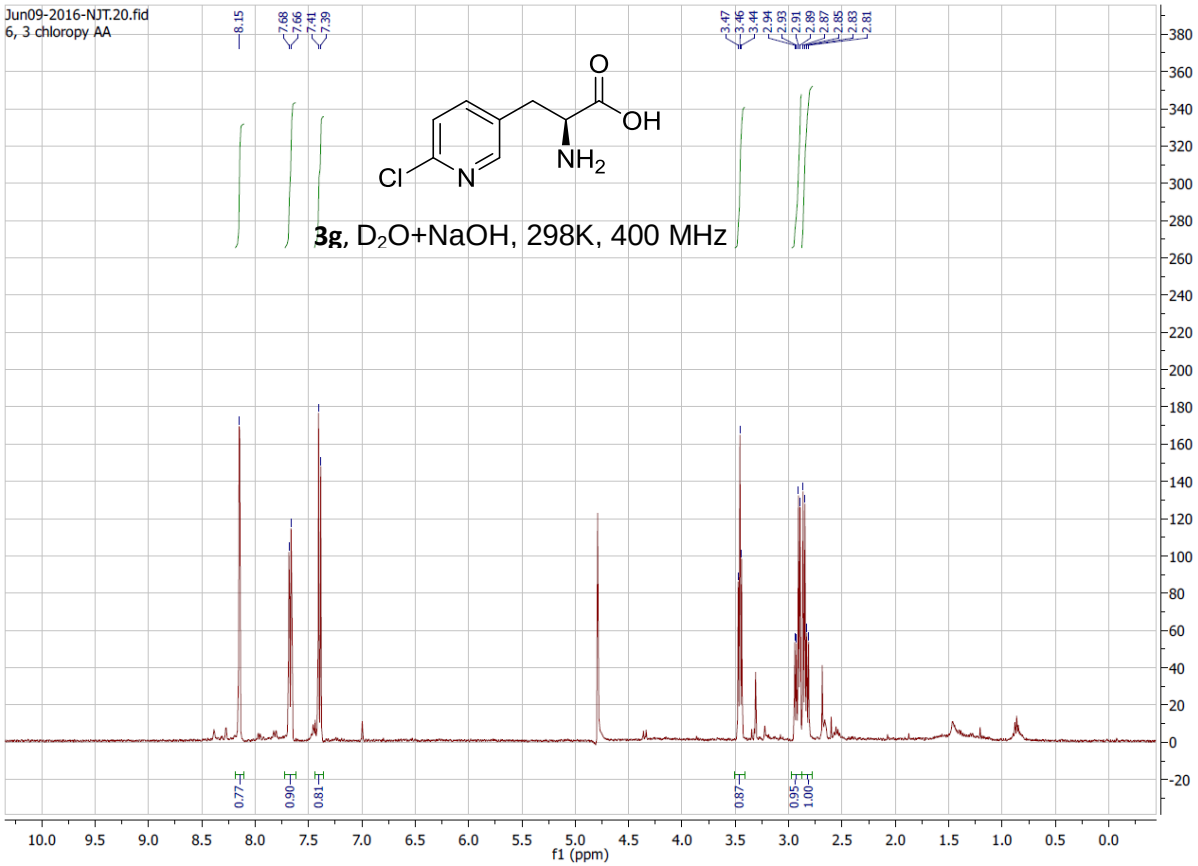
Jun09-2016-NJT.20.fid
6, 3 chloropy AA
8.15
7.68
7.66
7.41
7.39
3.47
3.46
3.44
2.94
2.93
2.91
2.89
2.87
2.85
2.83
2.81
O
OH
NH2
Cl
N
3g, D2O+NaOH, 298K, 400 MHz
0.77
0.90
0.81
0.87
0.95
1.00
f1 (ppm)

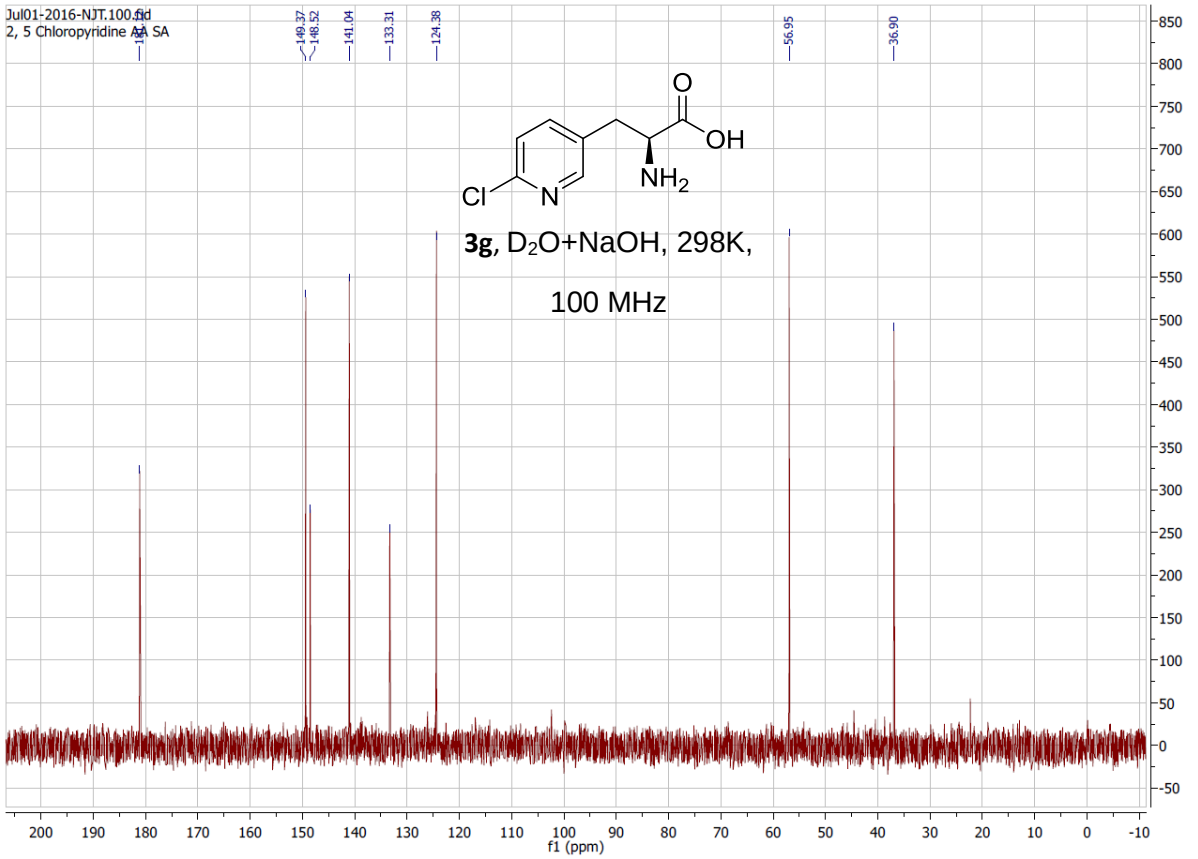
Jul01-2016-NJT.100.fid
2, 5 Chloropyridine AA SA
149.37
148.52
141.04
133.31
124.38
56.95
36.90
O
OH
NH2
Cl
N
3g, D2O+NaOH, 298K,
100 MHz
f1 (ppm)

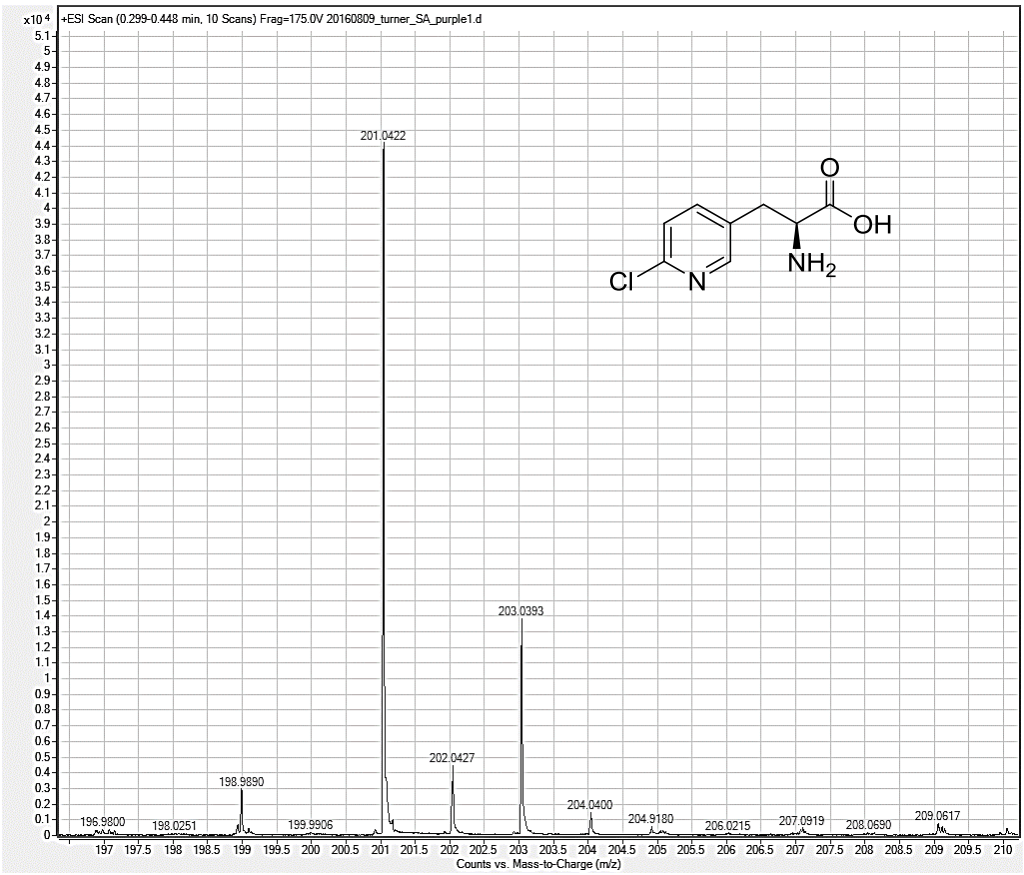
+ESI Scan (0.299-0.448 min, 10 Scans) Frag=175.0V 20160809_turner_SA_purple1.d
x10 4
201.0422
203.0393
202.0427
198.9890
204.0400
196.9800
198.0251
199.9906
204.9180
206.0215
207.0919
208.0690
209.0617
Counts vs. Mass-to-Charge (m/z)
O
OH
NH2
Cl
N

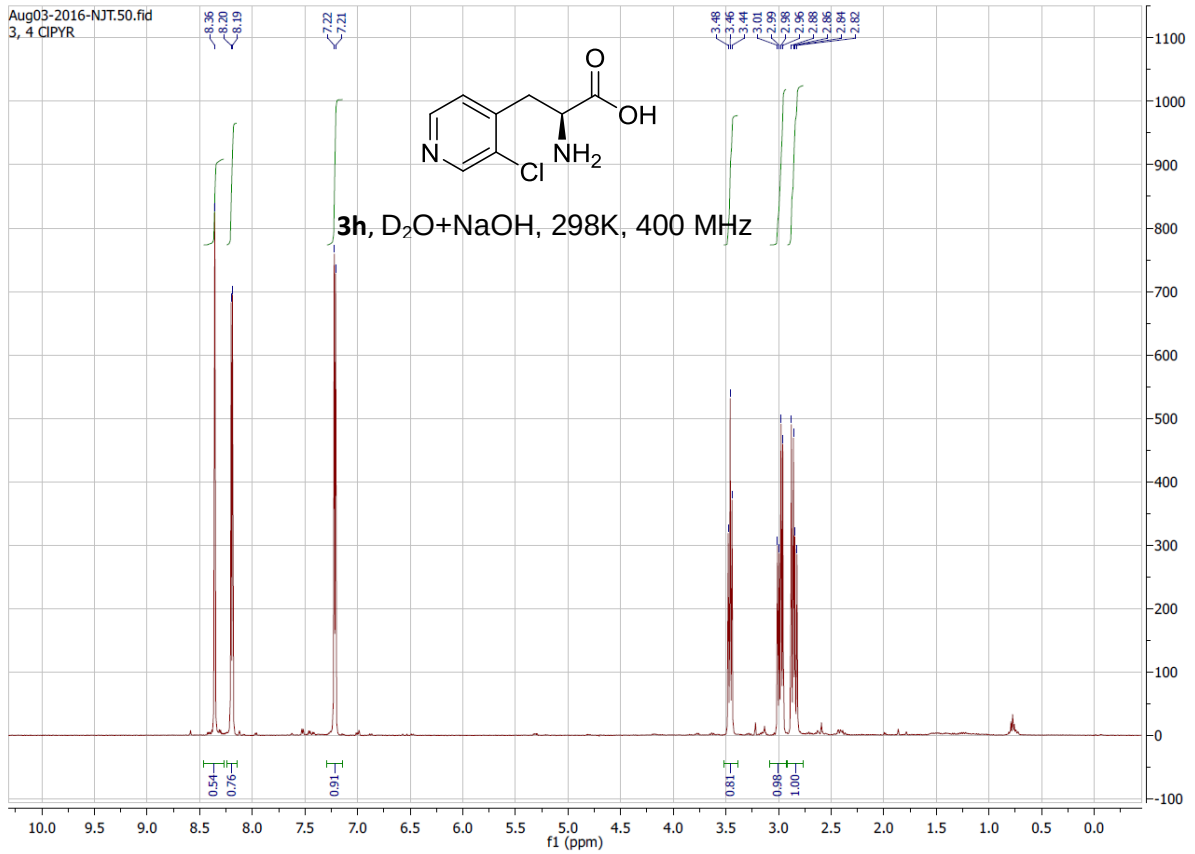

3h, D_2O+NaOH, 298K, 400 MHz

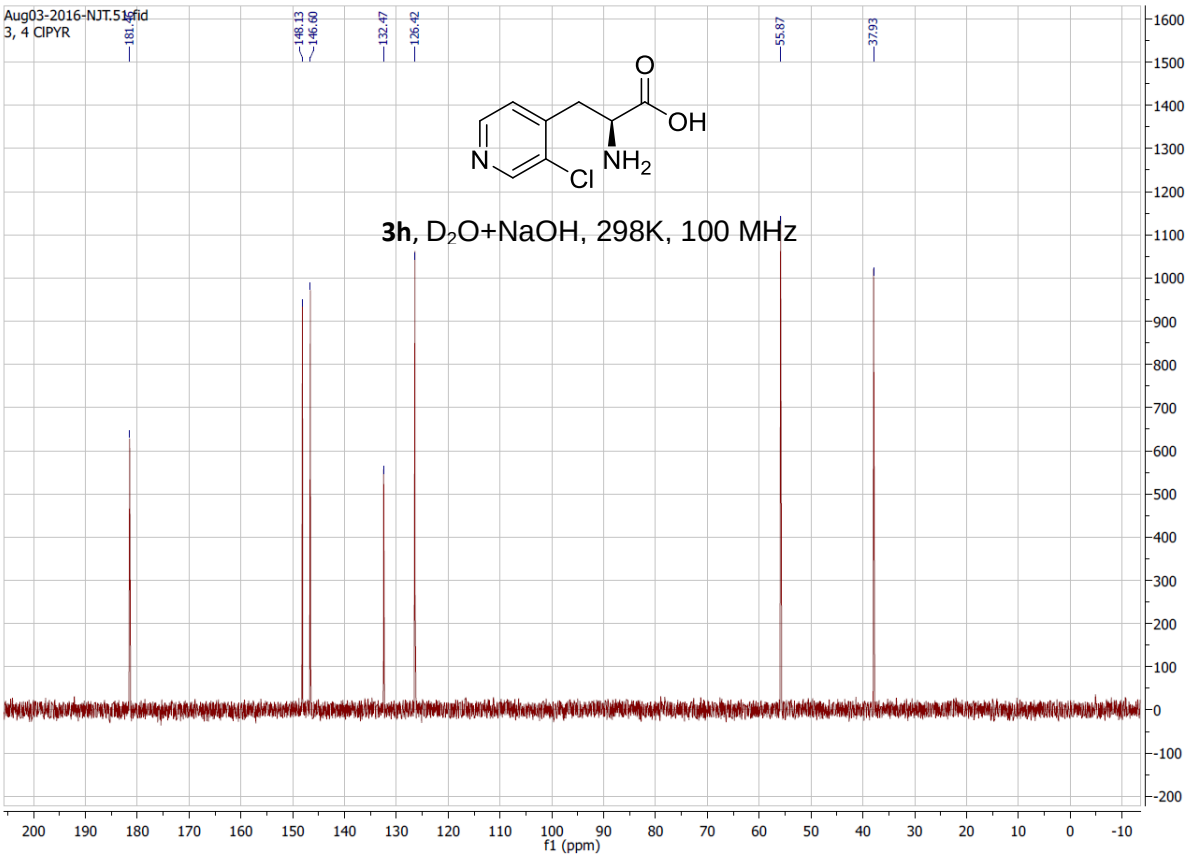

3h, D_2O+NaOH, 298K, 100 MHz

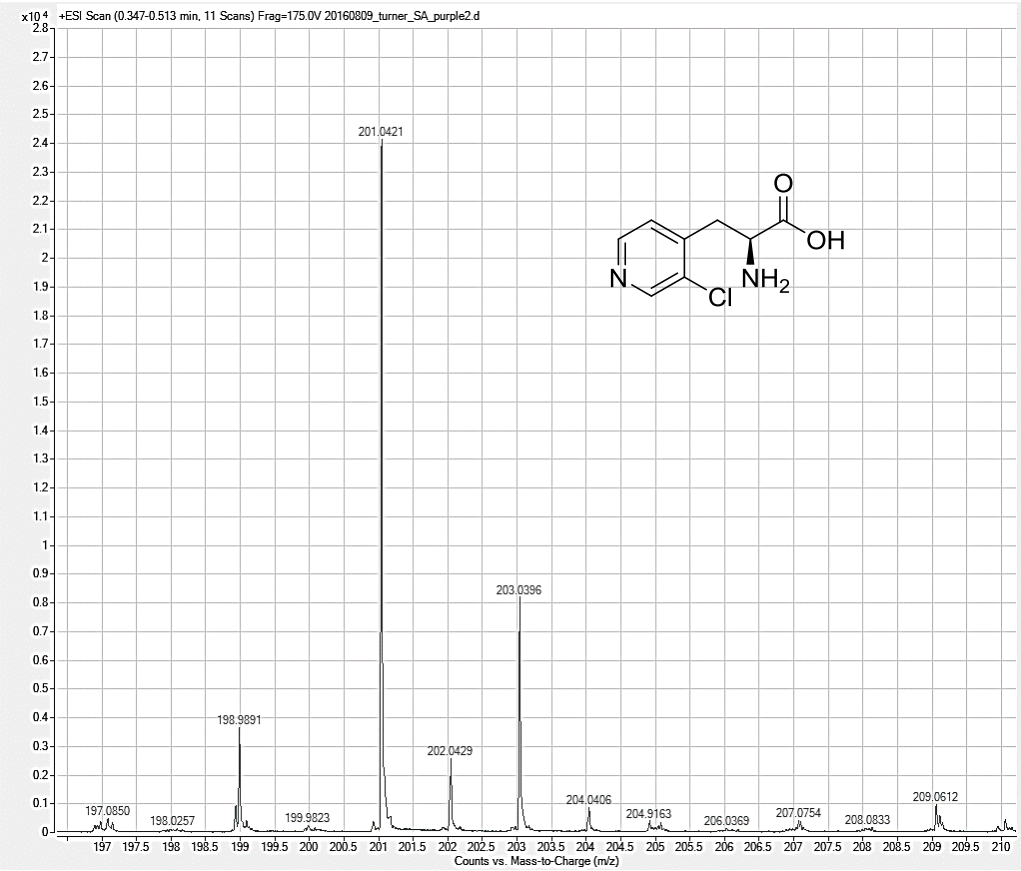
x10 4
+ESI Scan (0.347-0.513 min, 11 Scans) Frag=175.0V 20160809_turner_SA_purple2.d
201.0421
203.0396
198.9891
202.0429
204.0406
209.0612
197.0850
198.0257
199.9823
204.9163
206.0369
207.0754
208.0833
O
OH
N
NH2
Cl
Counts vs. Mass-to-Charge (m/z)

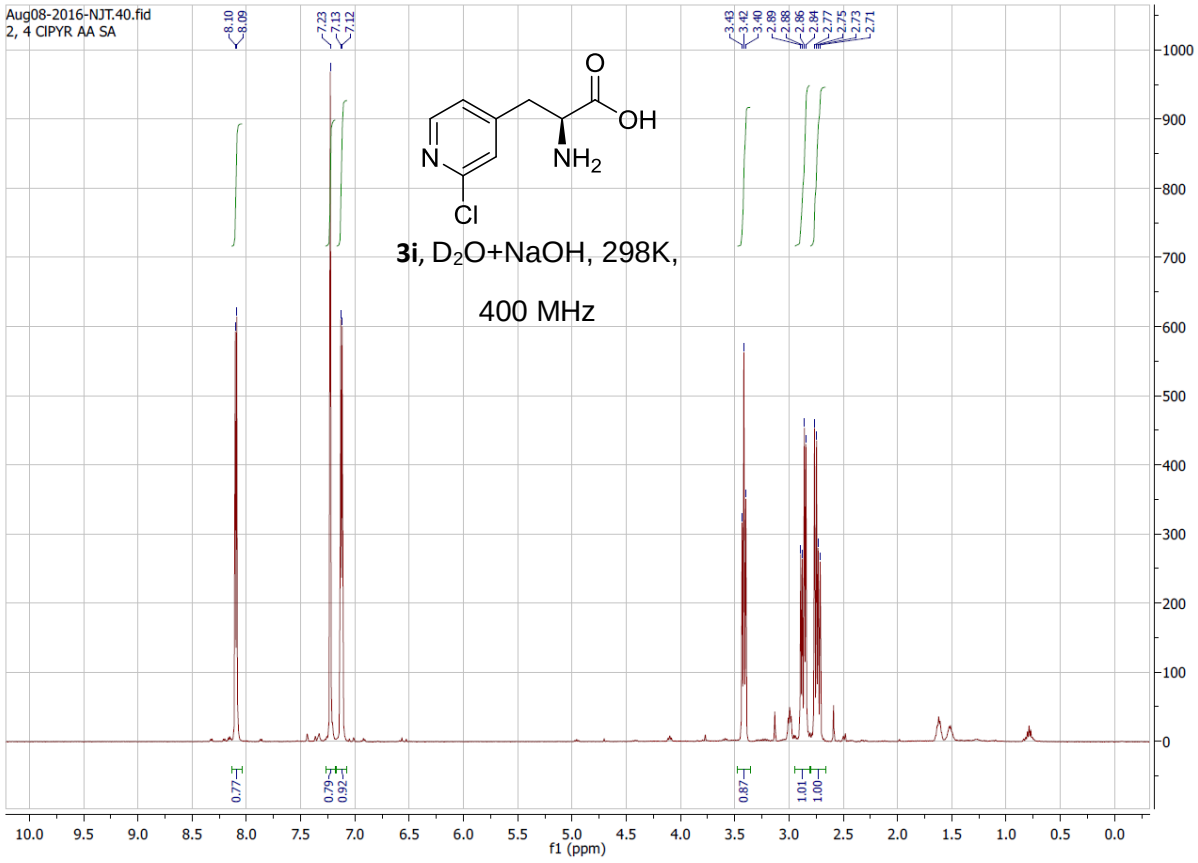
Aug08-2016-NJT.40.fid
2, 4 ClPYR AA SA
8.10
8.09
7.23
7.13
7.12
3.43
3.42
3.40
2.89
2.88
2.86
2.84
2.77
2.75
2.73
2.71
O
OH
N
NH2
Cl
3i, D2O+NaOH, 298K,
400 MHz
0.77
0.79
0.92
0.87
1.01
1.00
f1 (ppm)

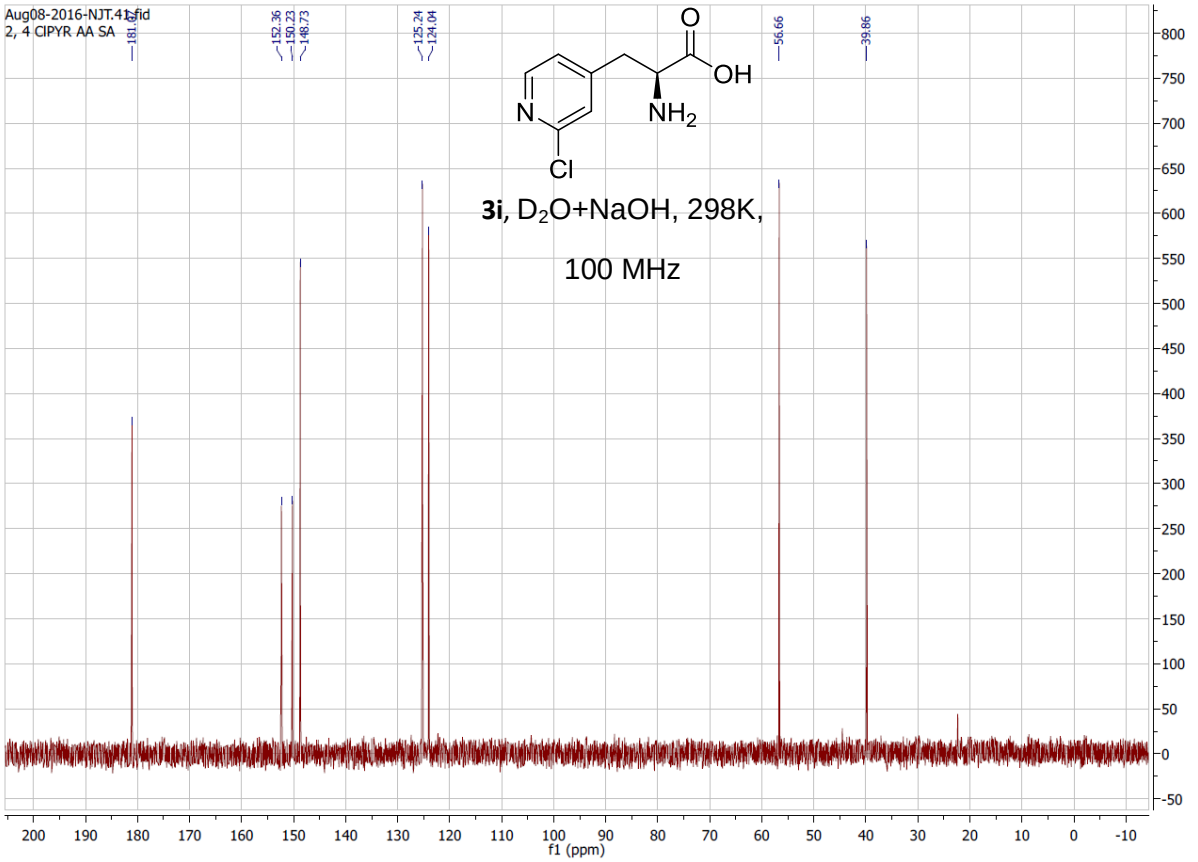
Aug08-2016-NJT.41.fid
2, 4 ClPYR AA SA
181.57
152.36
150.23
148.73
125.24
124.04
56.66
39.86
O
OH
N
NH2
Cl
3i, D2O+NaOH, 298K,
100 MHz
f1 (ppm)

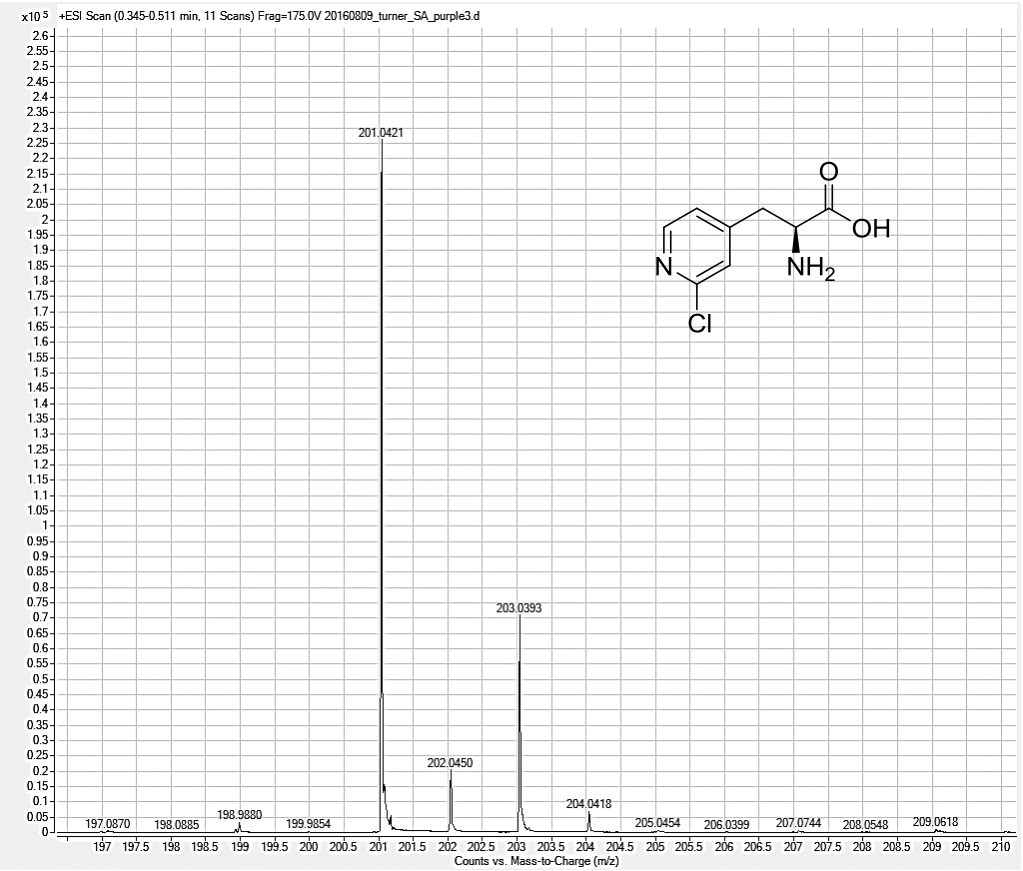
x10 5 +ESI Scan (0.345-0.511 min, 11 Scans) Frag=175.0V 20160809_turner_SA_purple3.d
201.0421
203.0393
202.0450
204.0418
197.0870
198.0885
198.9880
199.9854
205.0454
206.0399
207.0744
208.0548
209.0618
Counts vs. Mass-to-Charge (m/z)
O
OH
N
NH2
Cl

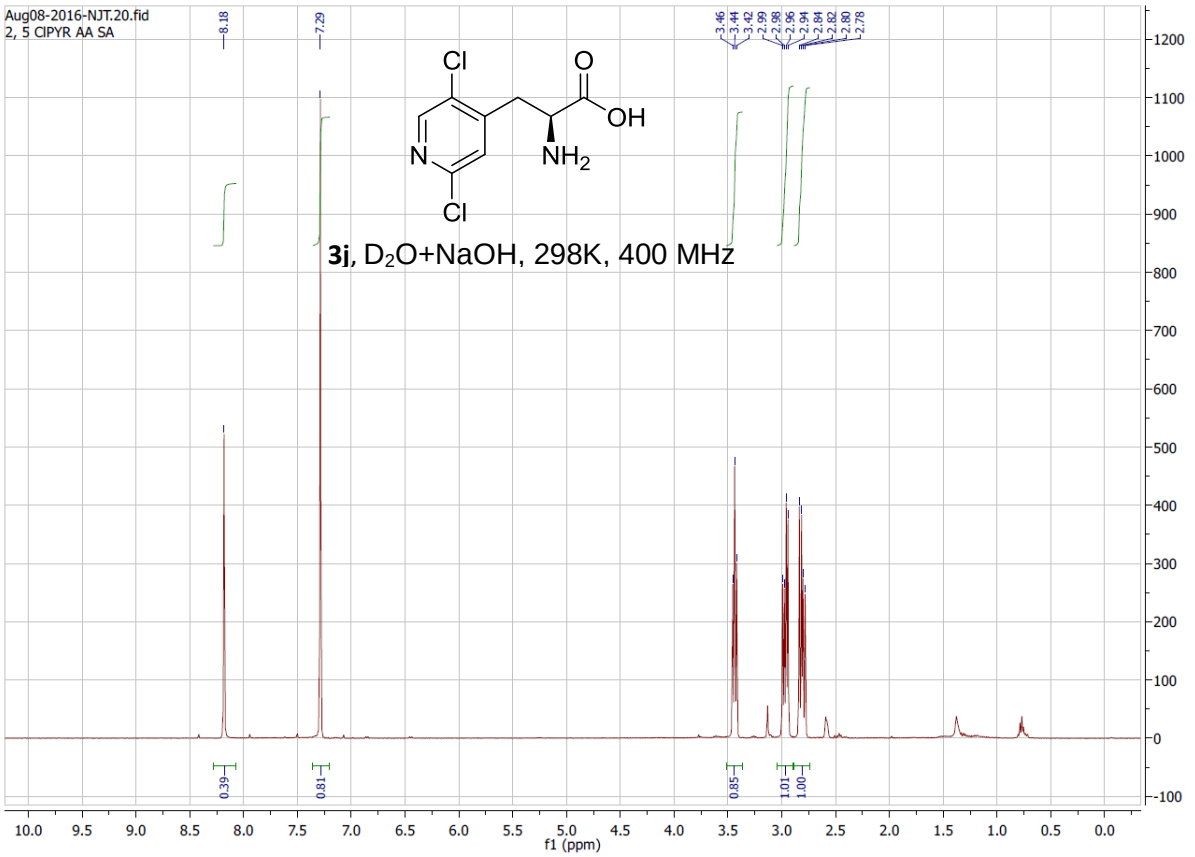

3j, D_2O+NaOH, 298K, 400 MHz

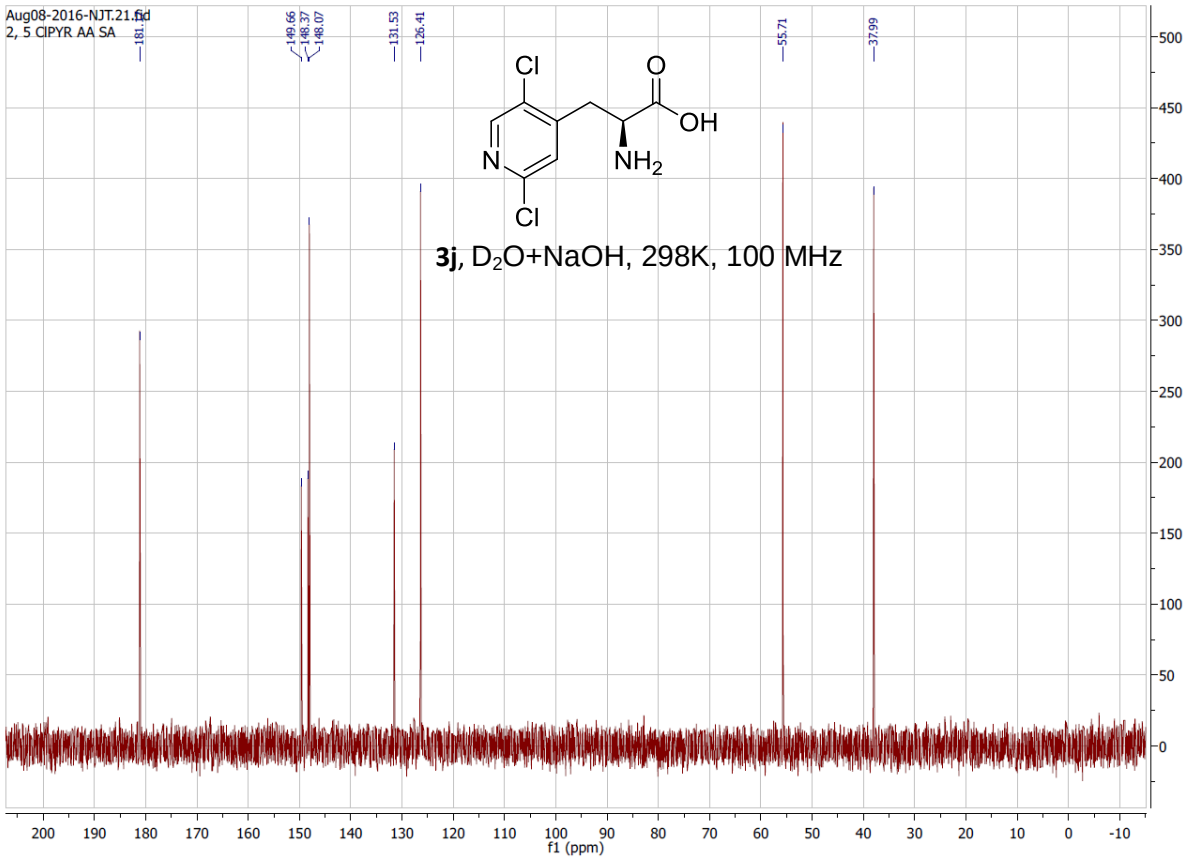

3j, D_2O+NaOH, 298K, 100 MHz

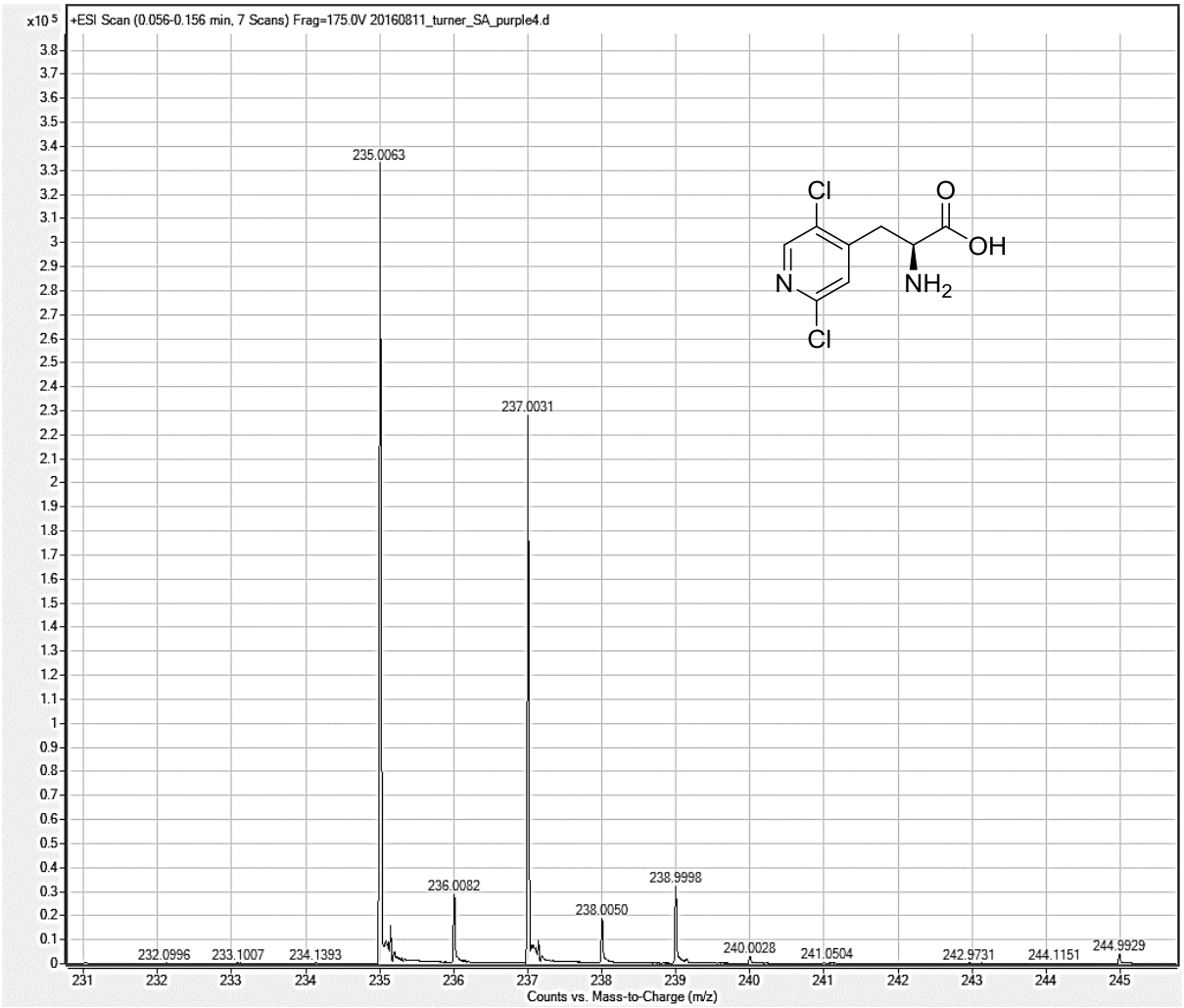
+ESI Scan (0.056-0.156 min, 7 Scans) Frag=175.0V 20160811_turner_SA_purple4.d
x10 5
235.0063
237.0031
236.0082
238.9998
238.0050
240.0028
241.0504
242.9731
244.1151
244.9929
232.0996
233.1007
234.1393
Cl
O
OH
N
NH2
Cl
Counts vs. Mass-to-Charge (m/z)

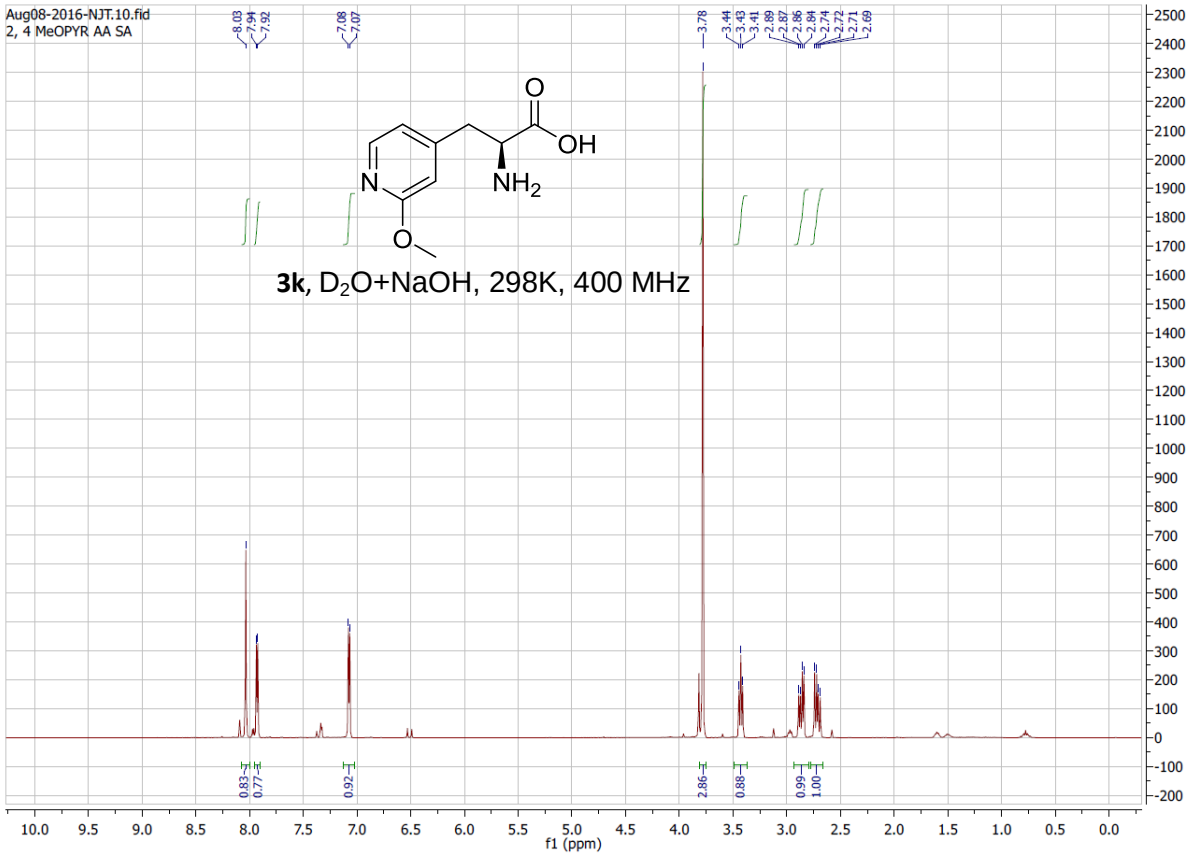

3k, D_2O+NaOH, 298K, 400 MHz

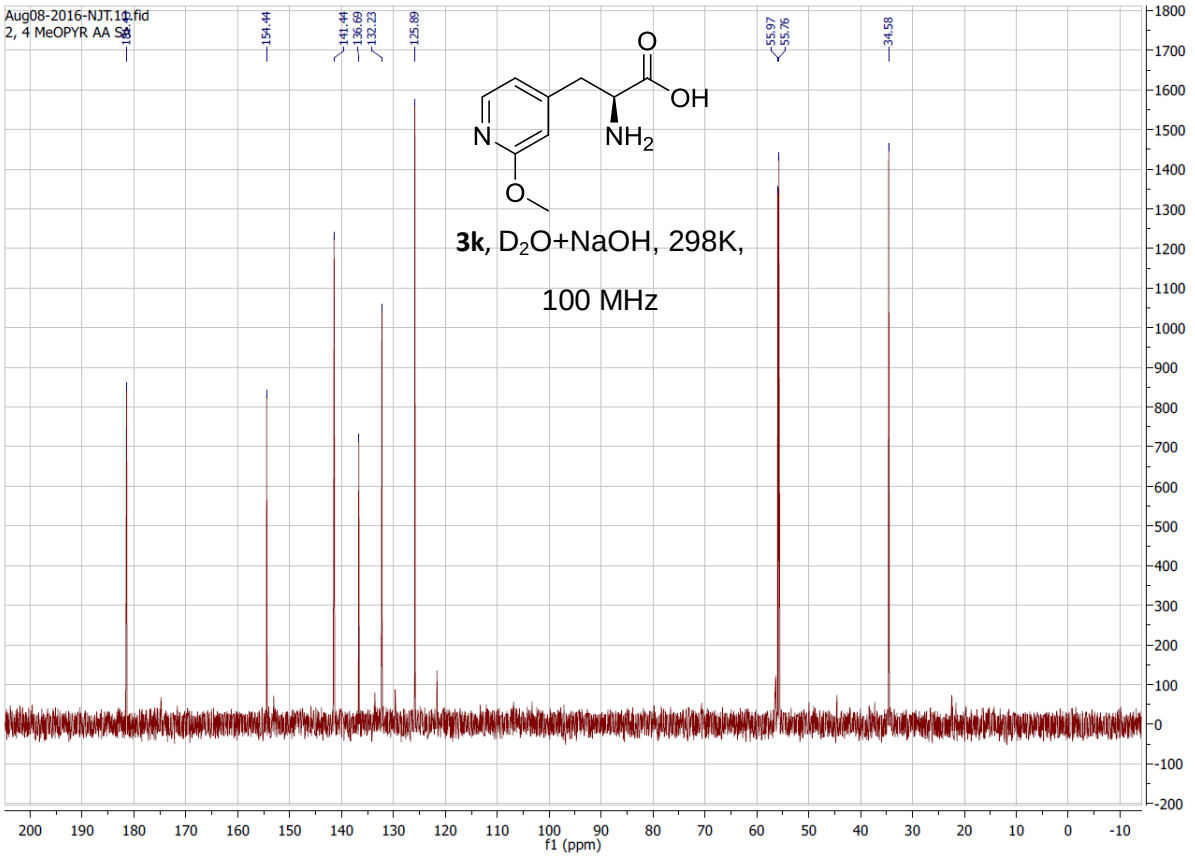

3k, D_2O+NaOH, 298K,

100 MHz

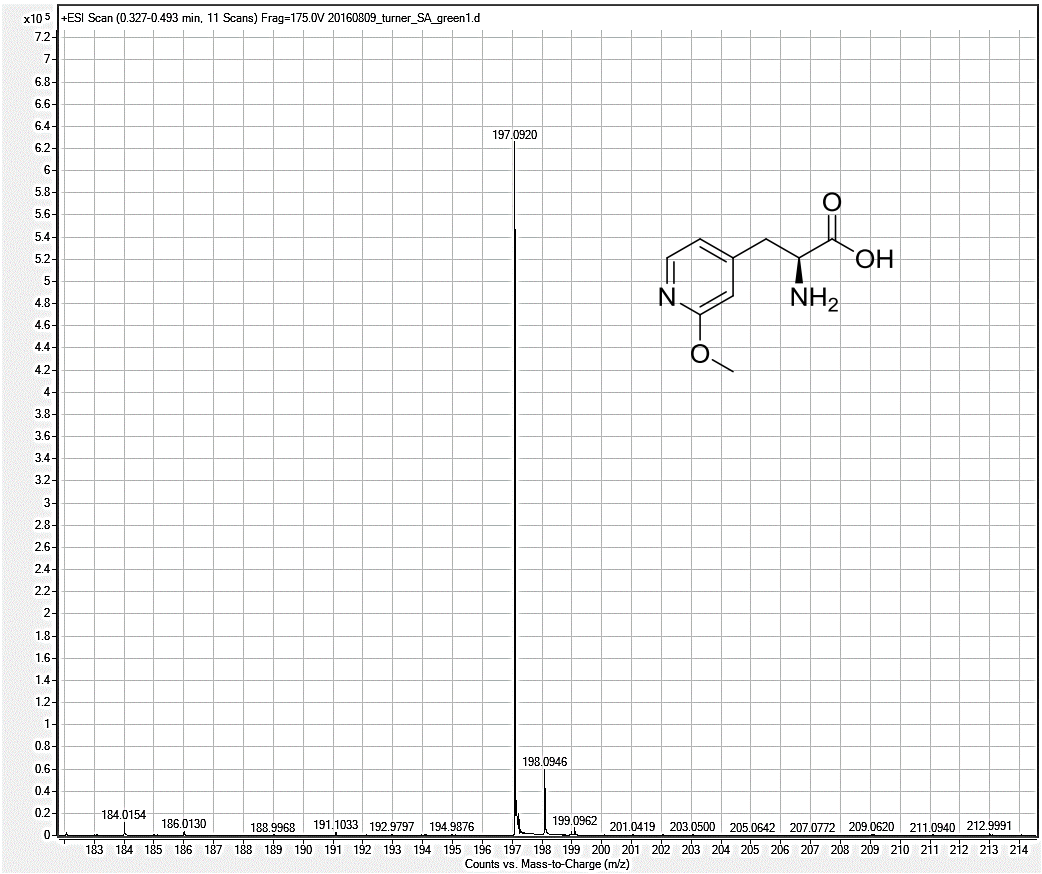
x10 5
+ESI Scan (0.327-0.493 min, 11 Scans) Frag=175.0V 20160809_turner_SA_green1.d
197.0920
198.0946
184.0154
186.0130
188.9968
191.1033
192.9797
194.9876
199.0962
201.0419
203.0500
205.0642
207.0772
209.0620
211.0940
212.9991
O
OH
N
NH2
O
Counts vs. Mass-to-Charge (m/z)

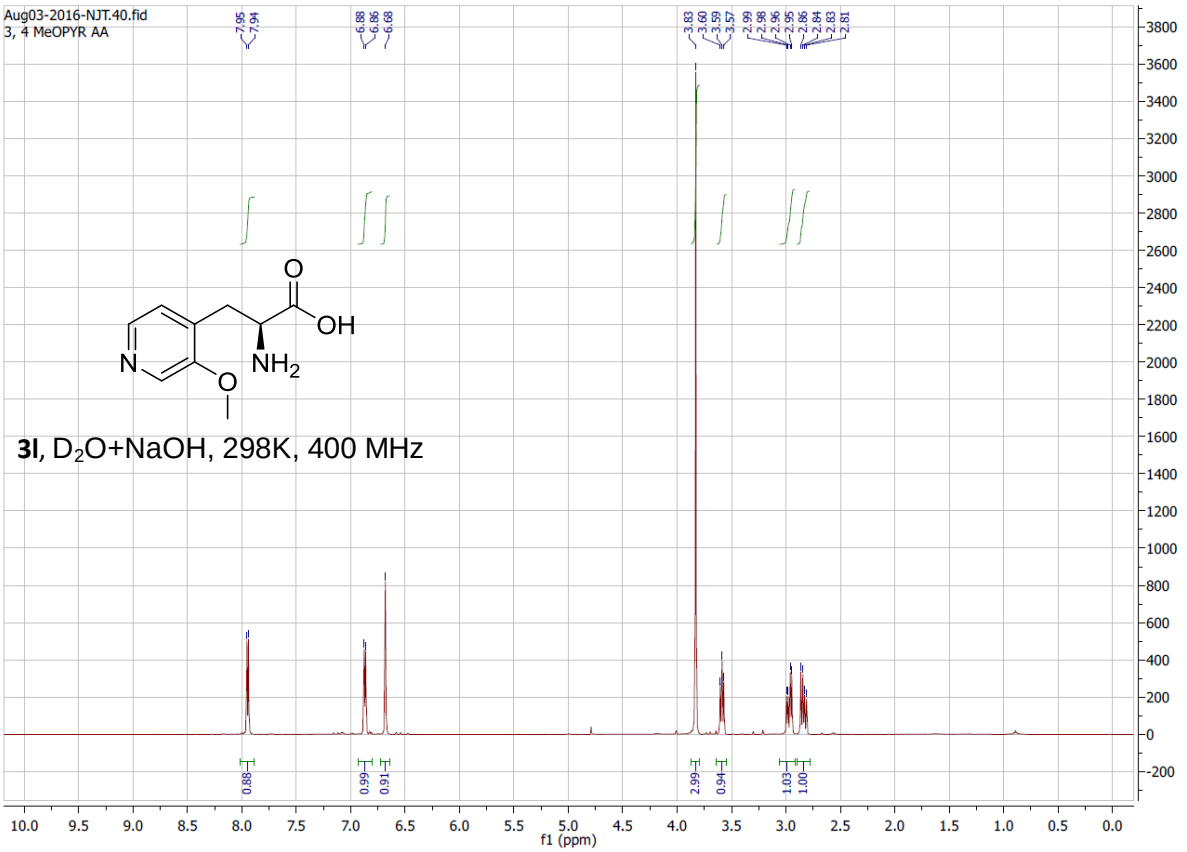

3l, D_2O+NaOH, 298K, 400 MHz

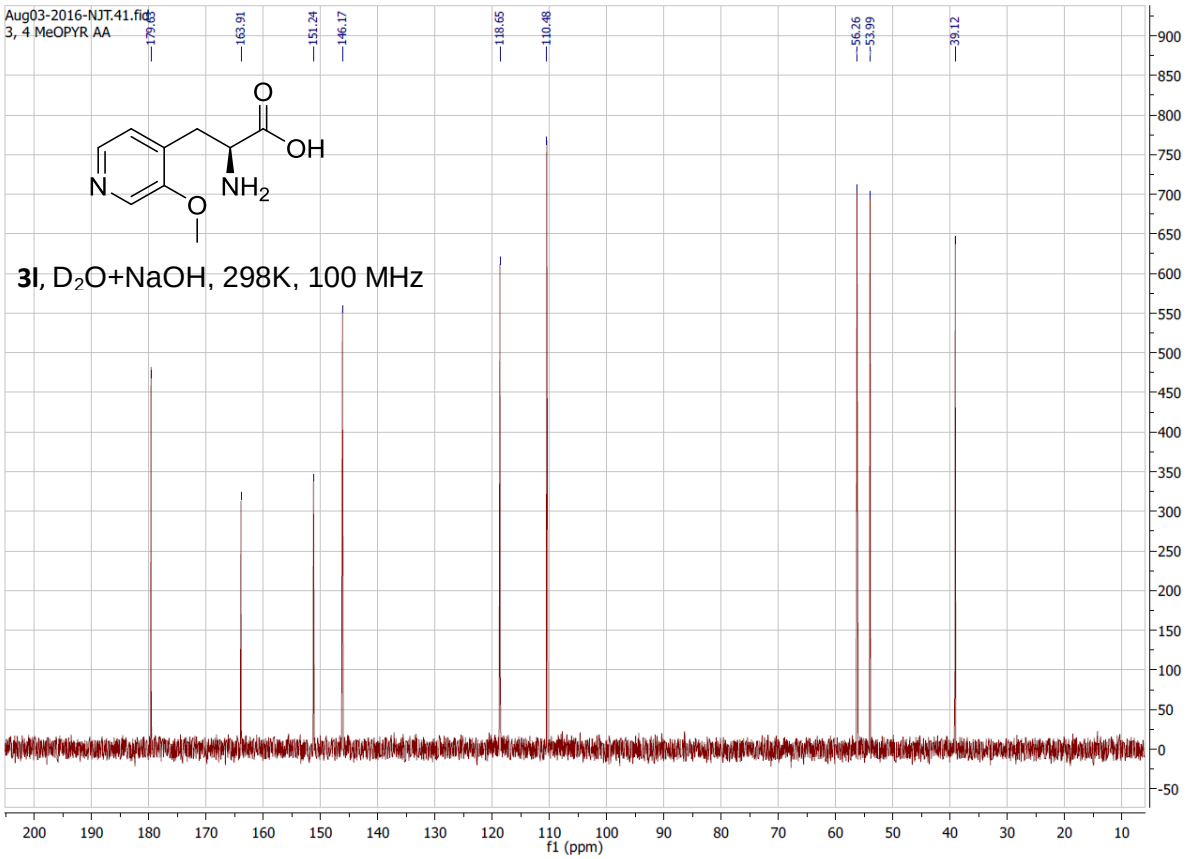

3l, D_2O+NaOH, 298K, 100 MHz

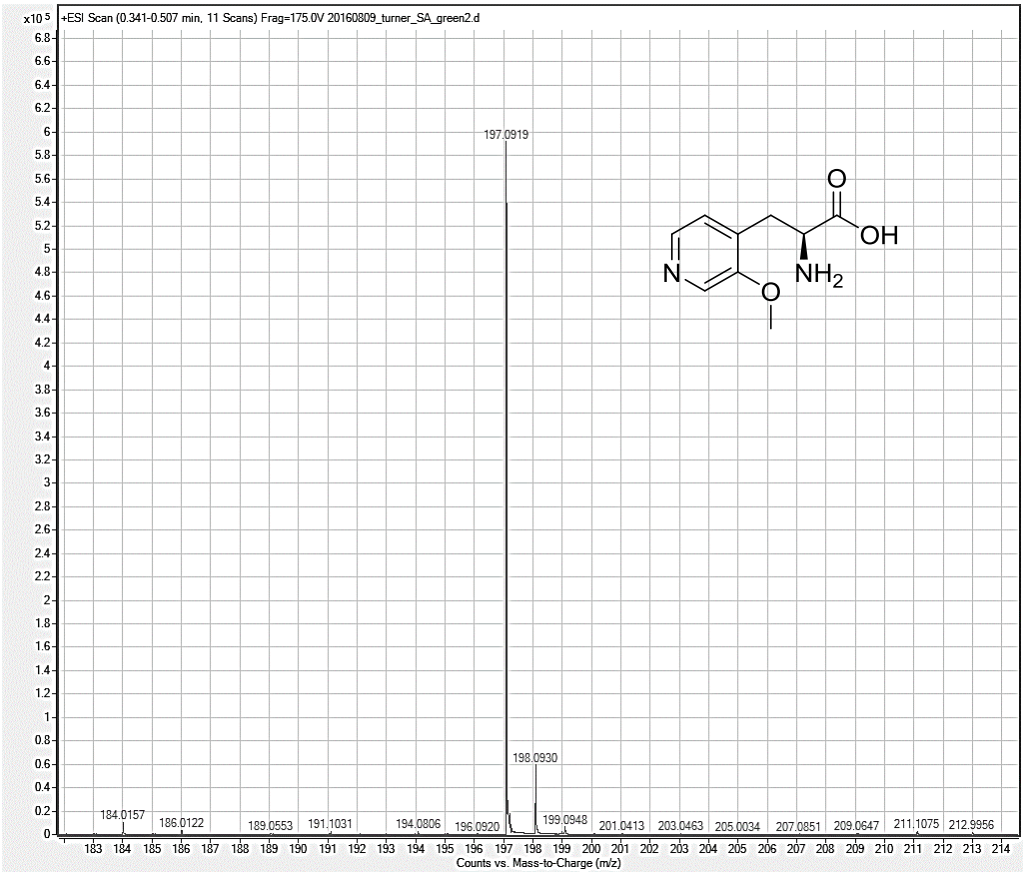
x10 5
+ESI Scan (0.341-0.507 min, 11 Scans) Frag=175.0V 20160809_turner_SA_green2.d
197.0919
198.0930
184.0157
186.0122
189.0553
191.1031
194.0806
196.0920
199.0948
201.0413
203.0463
205.0034
207.0851
209.0647
211.1075
212.9956
O
OH
N
NH2
O
Counts vs. Mass-to-Charge (m/z)

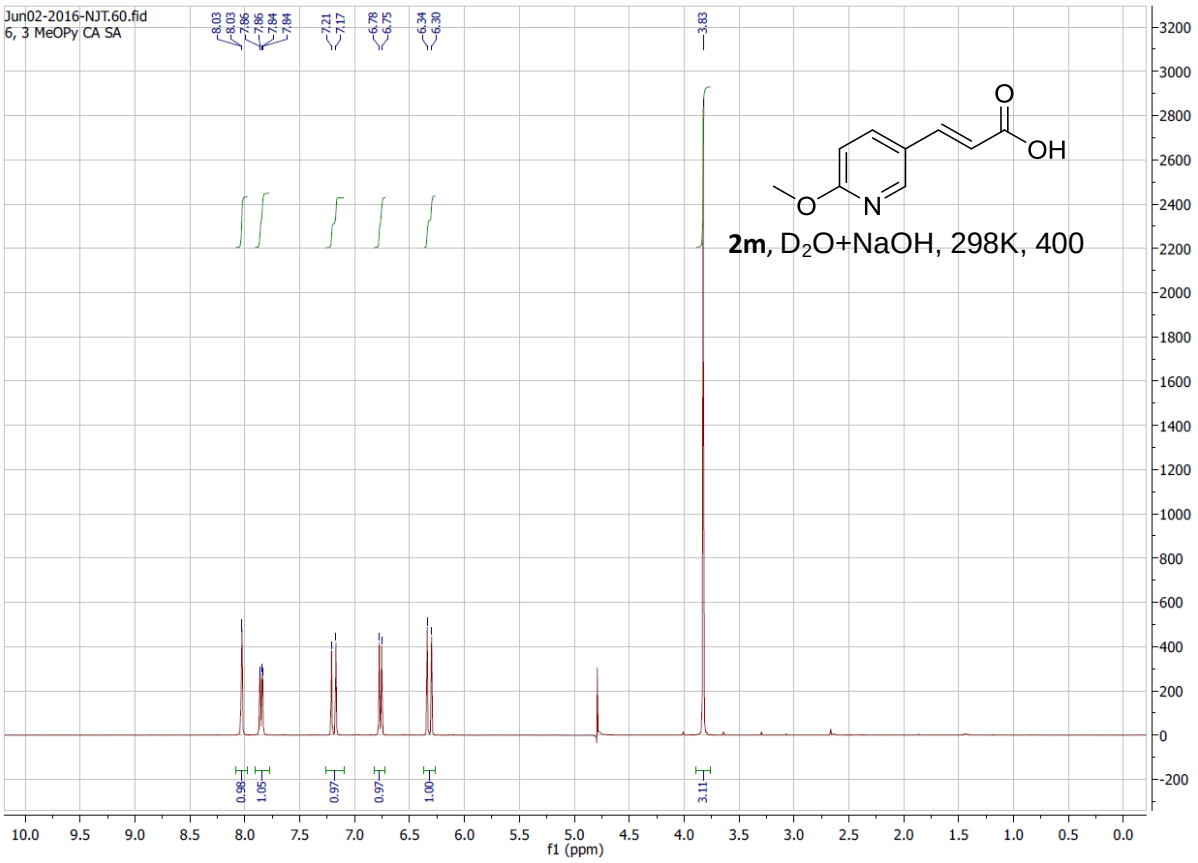

2m, D_2O+NaOH, 298K, 400

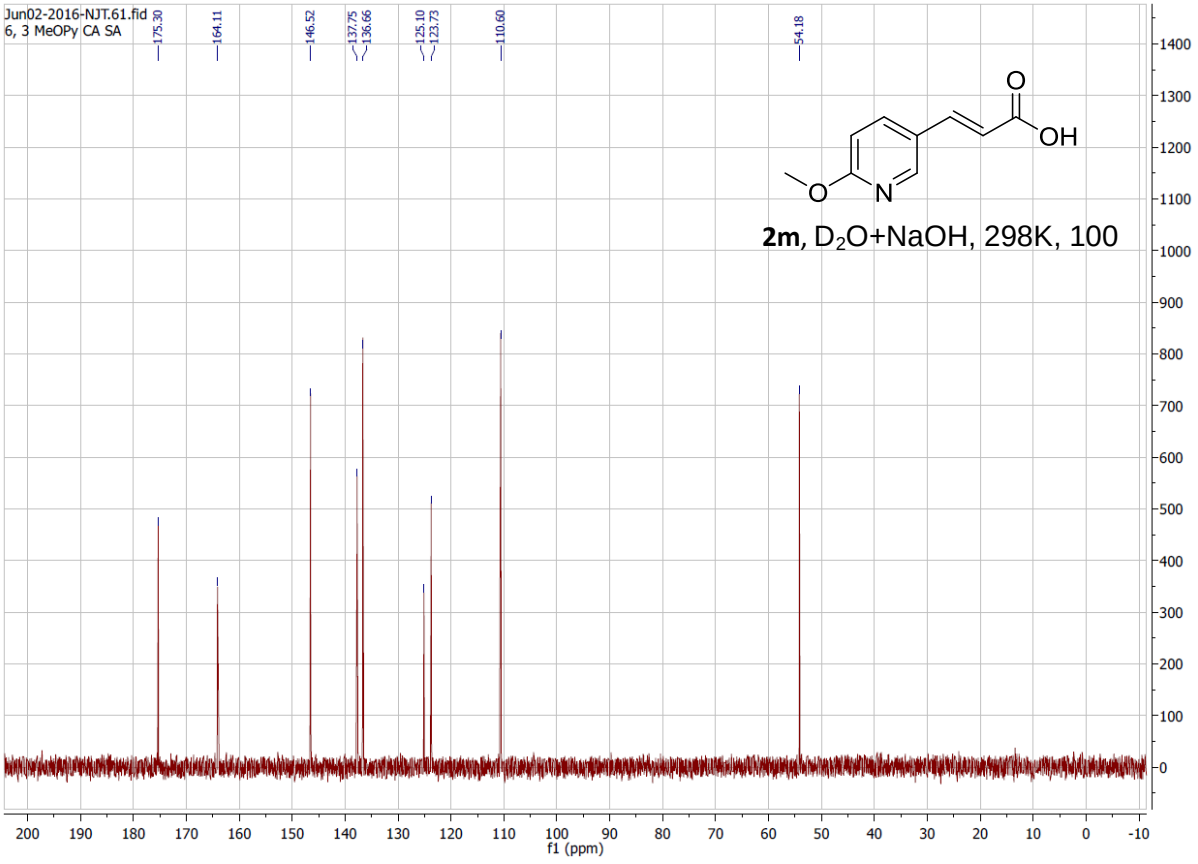

2m, D_2O+NaOH, 298K, 100

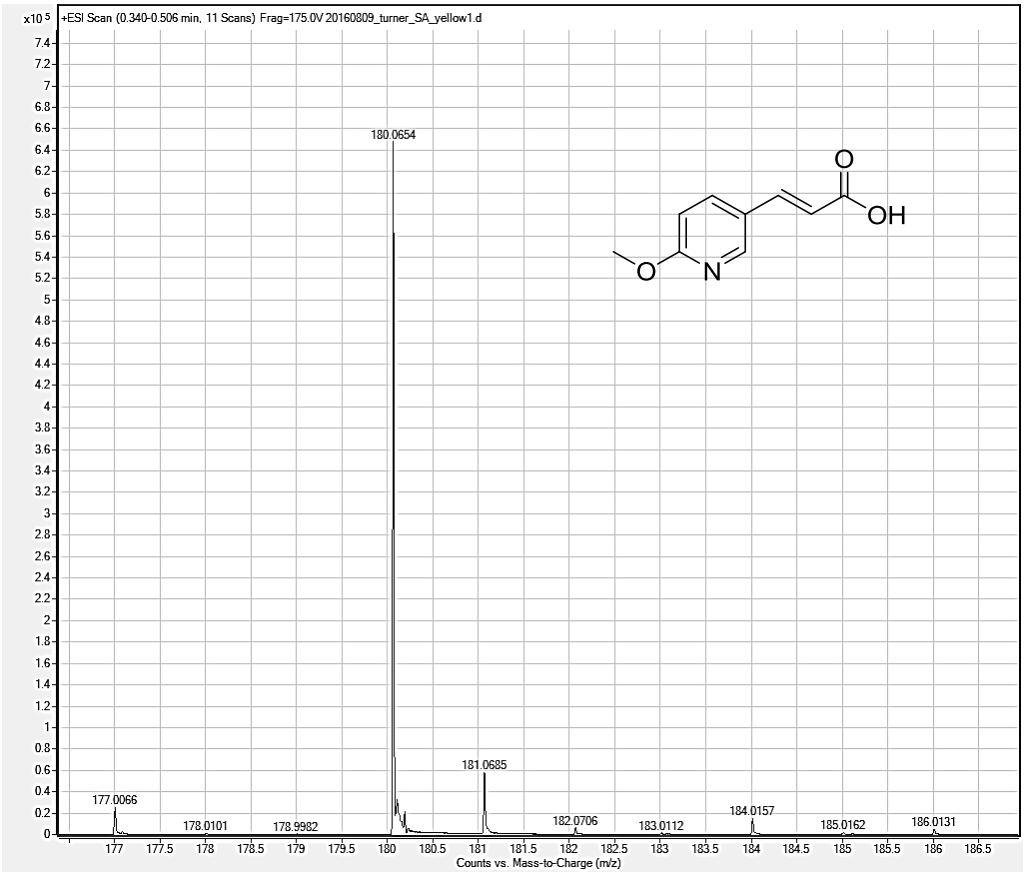
x10 5
+ESI Scan (0.340-0.506 min, 11 Scans) Frag=175.0V 20160809_turner_SA_yellow1.d
180.0654
181.0685
177.0066
178.0101
178.9982
182.0706
183.0112
184.0157
185.0162
186.0131
O
OH
O
N
Counts vs. Mass-to-Charge (m/z)

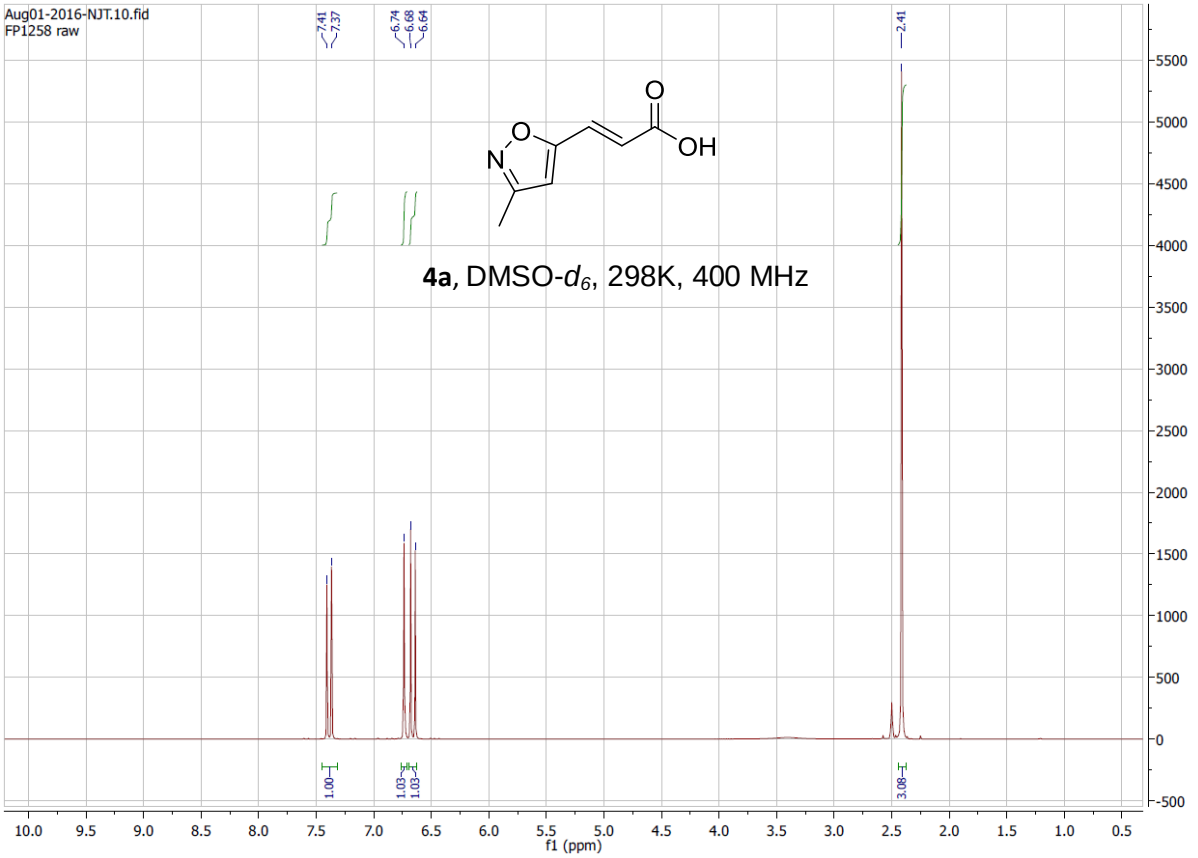

4a, DMSO-d_6, 298K, 400 MHz

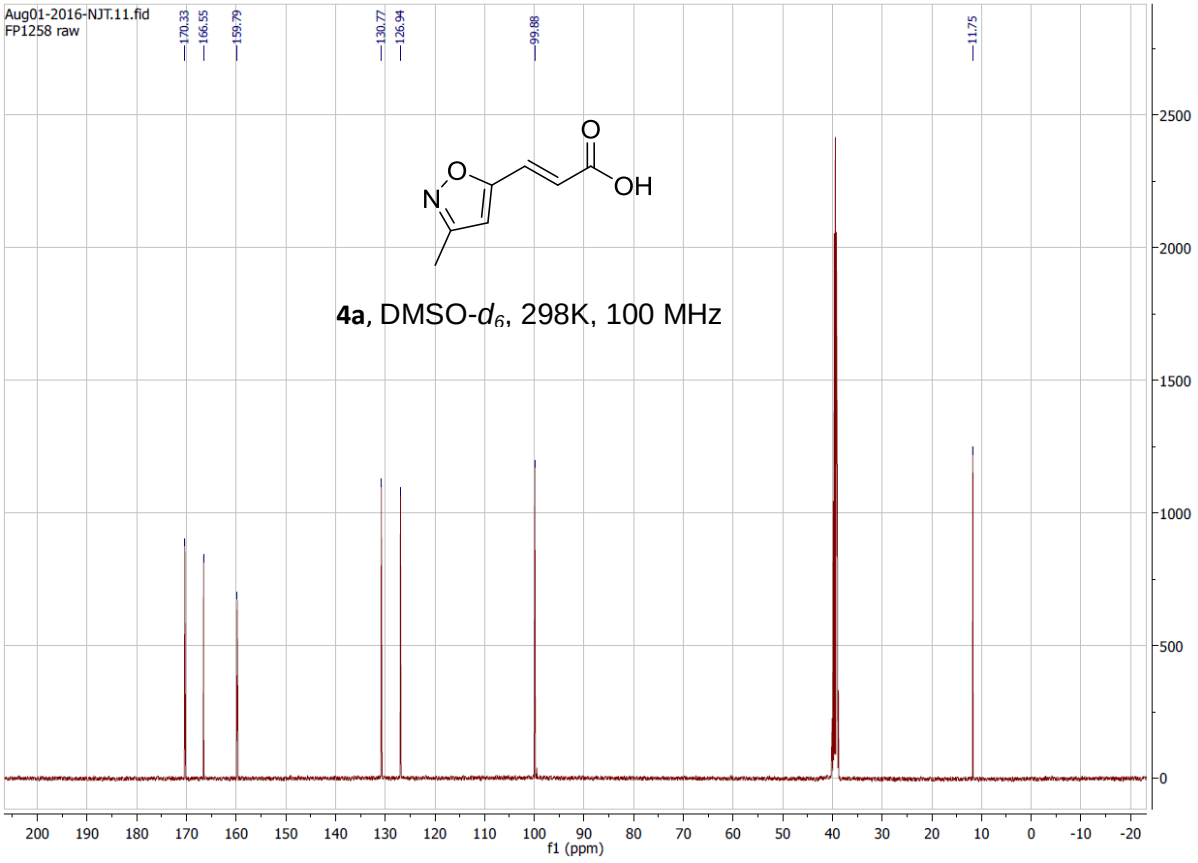

4a, DMSO-d_6, 298K, 100 MHz

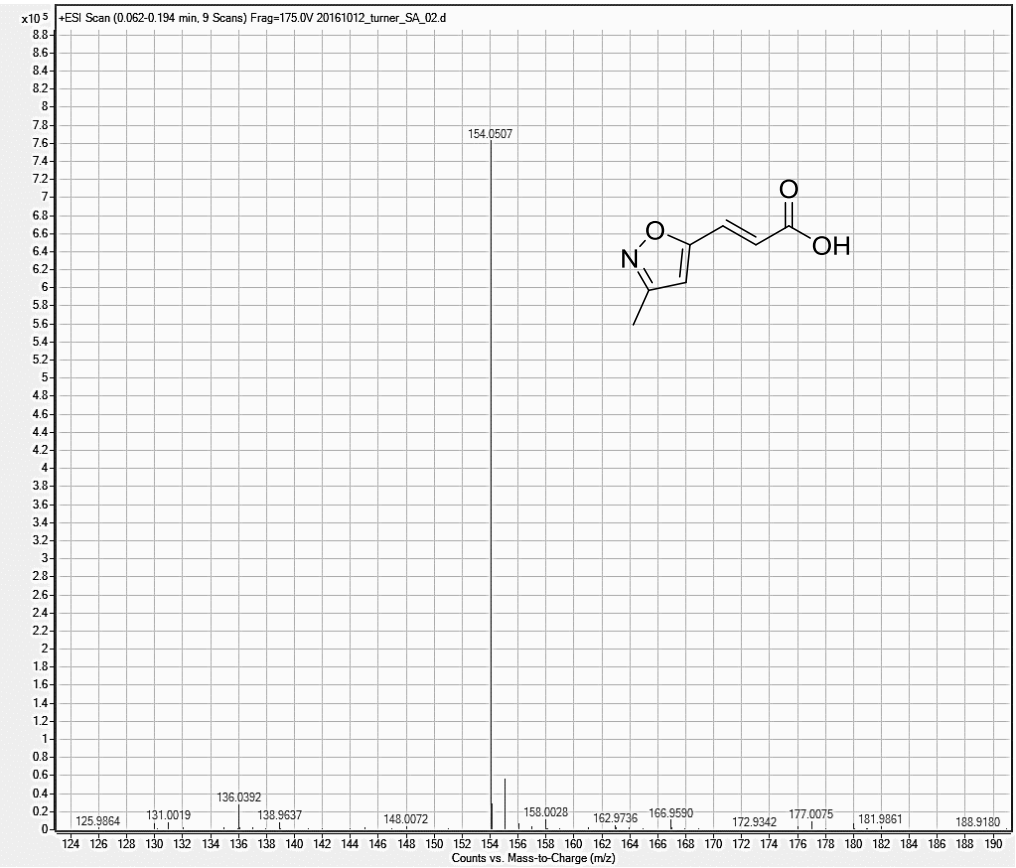
x10 5
+ESI Scan (0.062-0.194 min, 9 Scans) Frag=175.0V 20161012_turner_SA_02.d
154.0507
136.0392
125.9864
131.0019
138.9637
148.0072
158.0028
162.9736
166.9590
172.9342
177.0075
181.9861
188.9180
Counts vs. Mass-to-Charge (m/z)
O
N
O
OH

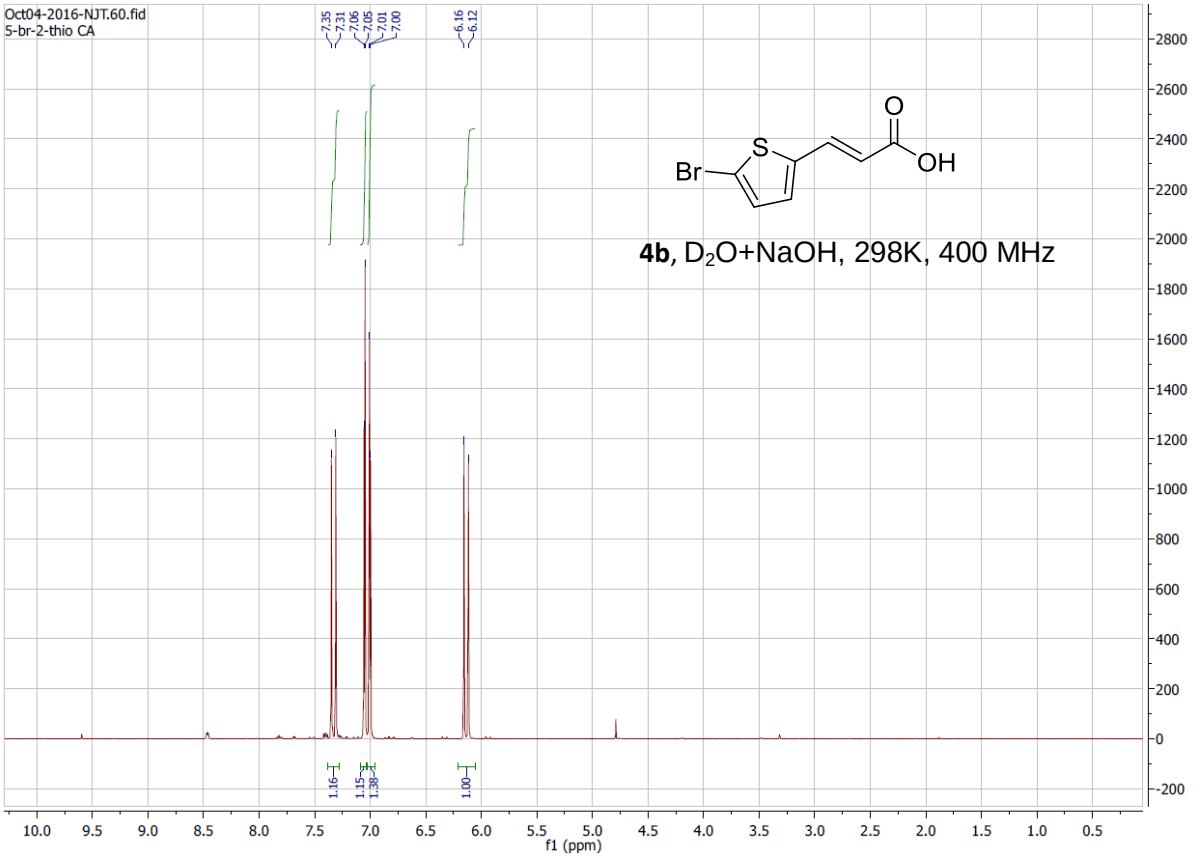

4b, D_2O+NaOH, 298K, 400 MHz

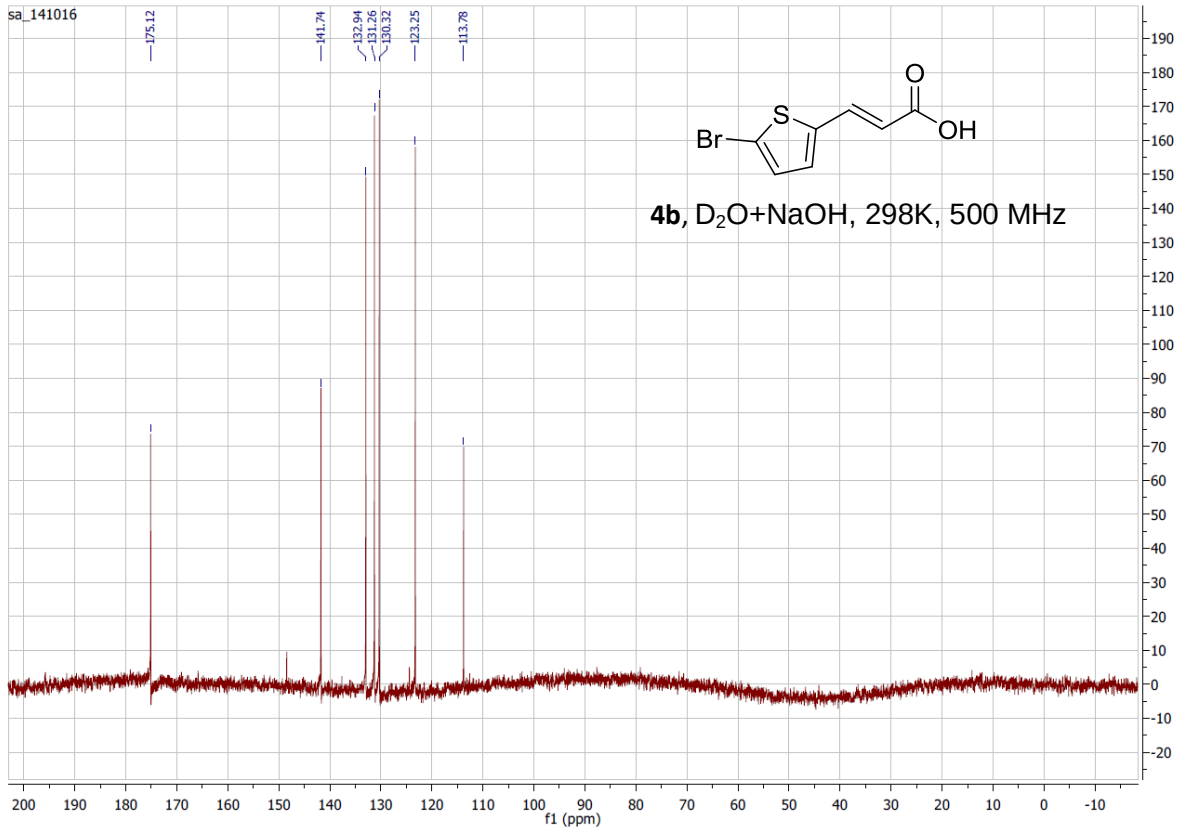

4b, D_2O+NaOH, 298K, 500 MHz

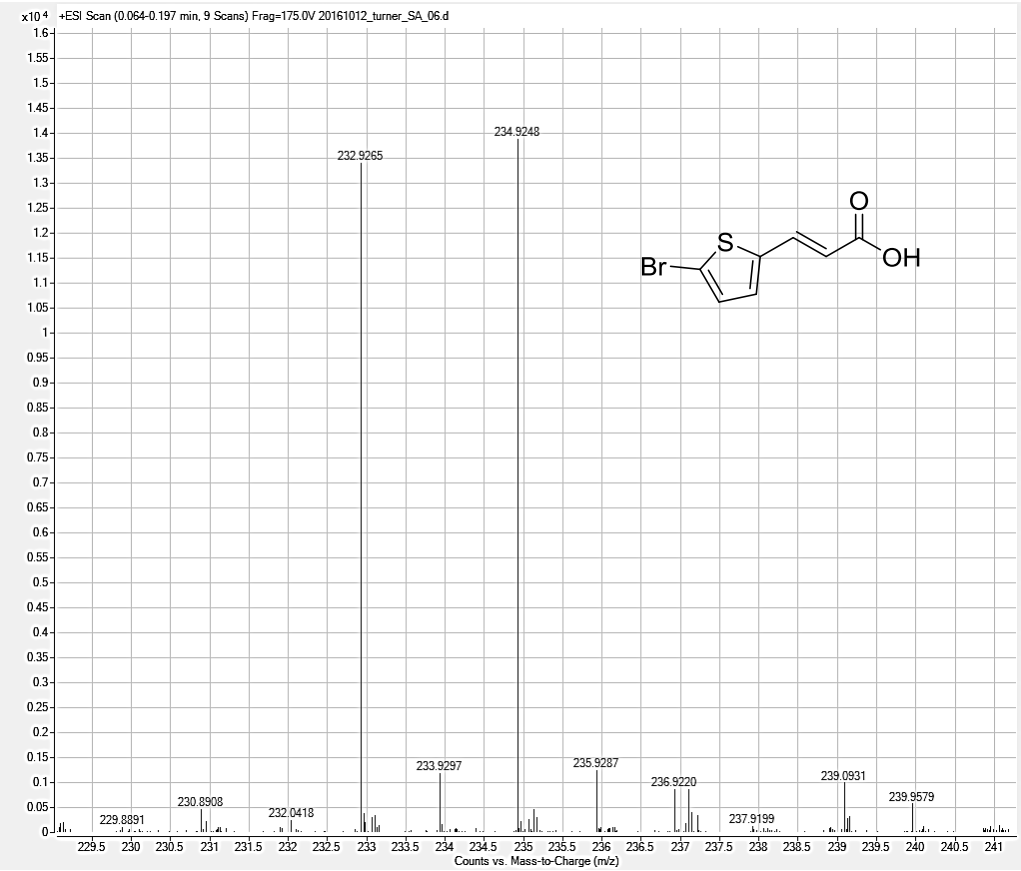
x10 4 +ESI Scan (0.064-0.197 min, 9 Scans) Frag=175.0V 20161012_turner_SA_06.d
232.9265
234.9248
233.9297
235.9287
236.9220
239.0931
239.9579
230.8908
229.8891
232.0418
237.9199
Br
S
O
OH
Counts vs. Mass-to-Charge (m/z)

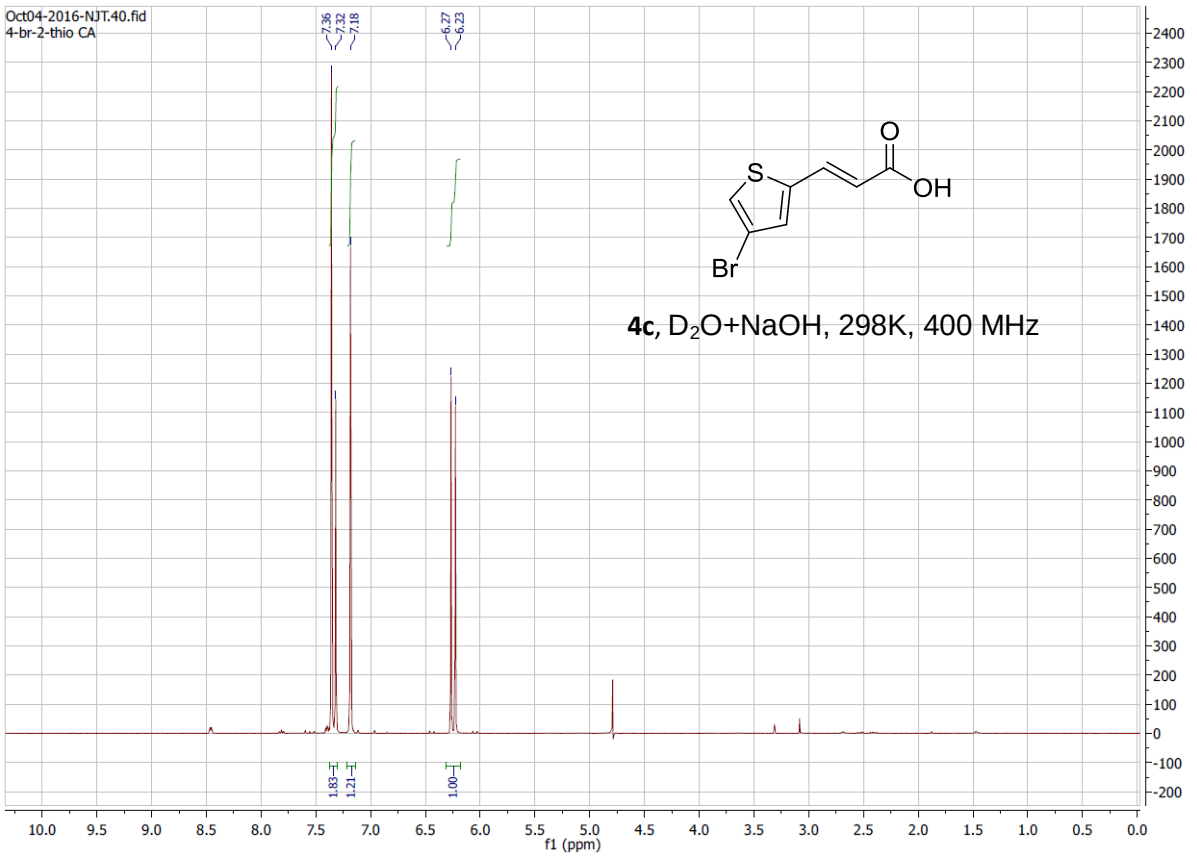

4c, D_2O+NaOH, 298K, 400 MHz

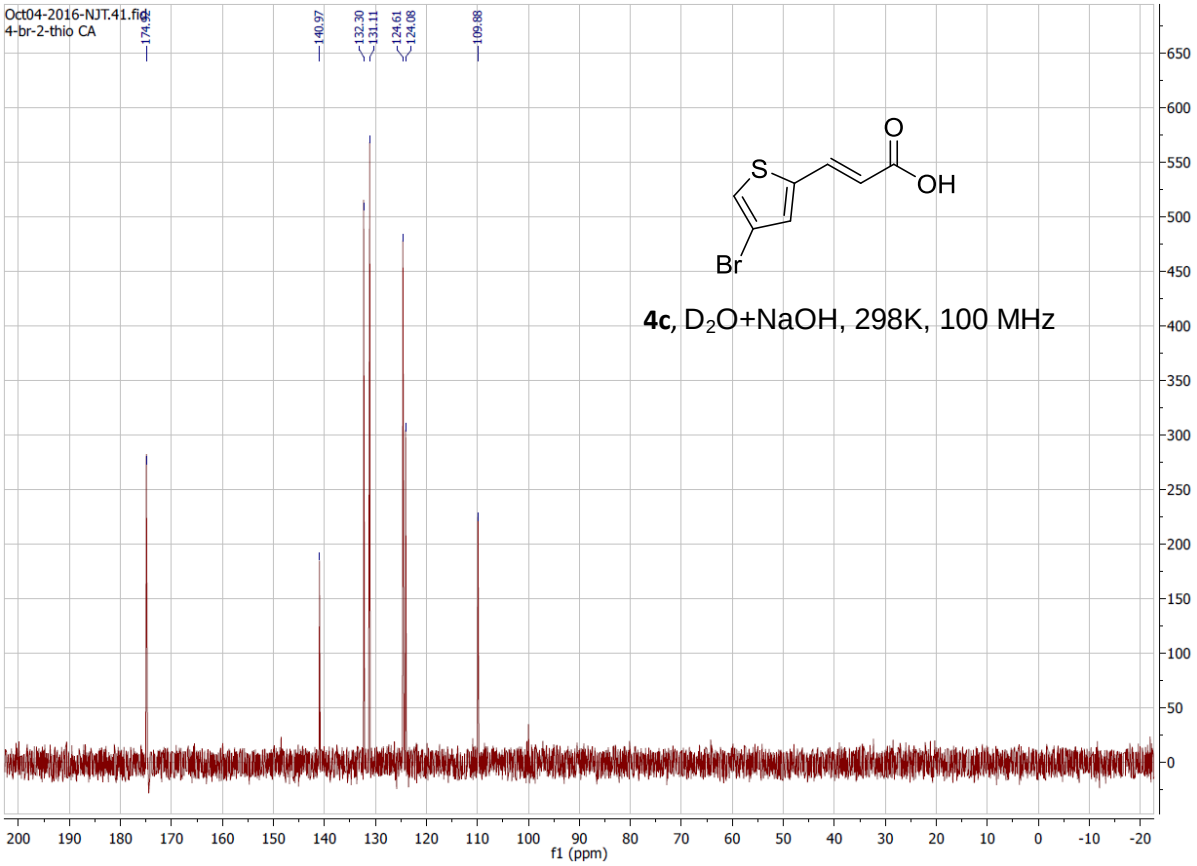

4c, D_2O+NaOH, 298K, 100 MHz

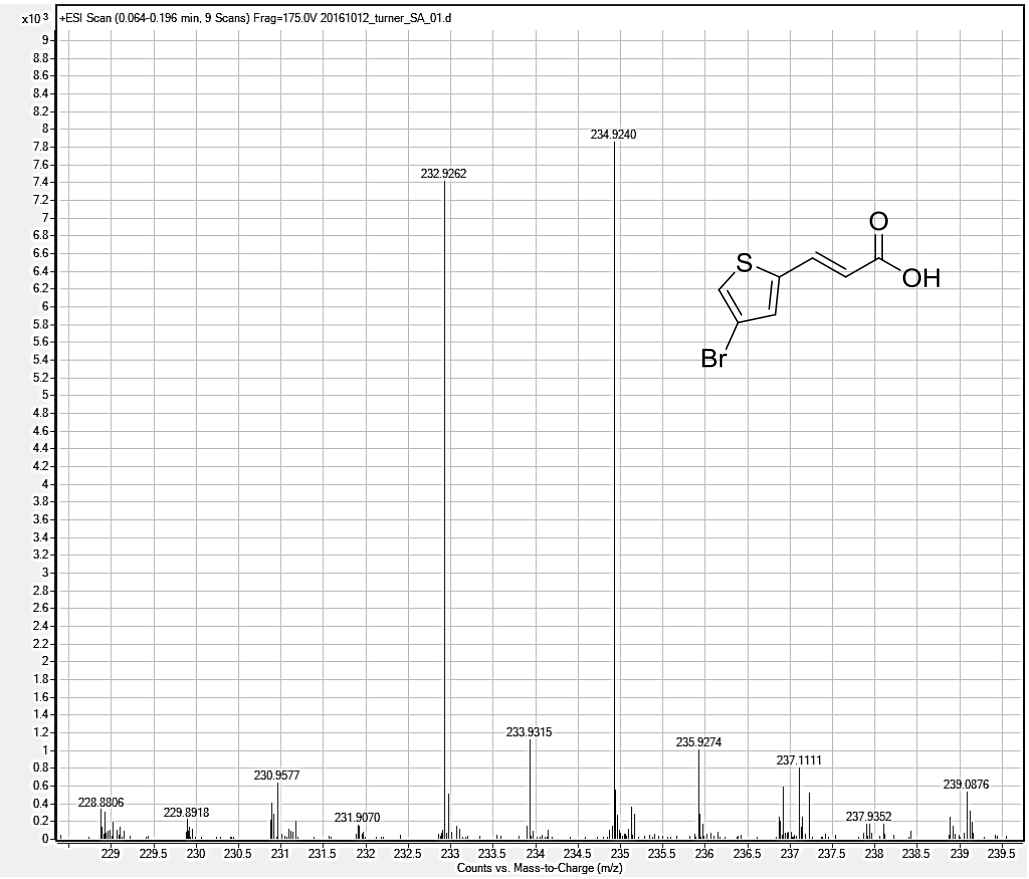
x10 3
+ESI Scan (0.064-0.196 min, 9 Scans) Frag=175.0V 20161012_turner_SA_01.d
234.9240
232.9262
233.9315
235.9274
237.1111
230.9577
239.0876
228.8806
229.8918
231.9070
237.9352
O
S
OH
Br
Counts vs. Mass-to-Charge (m/z)

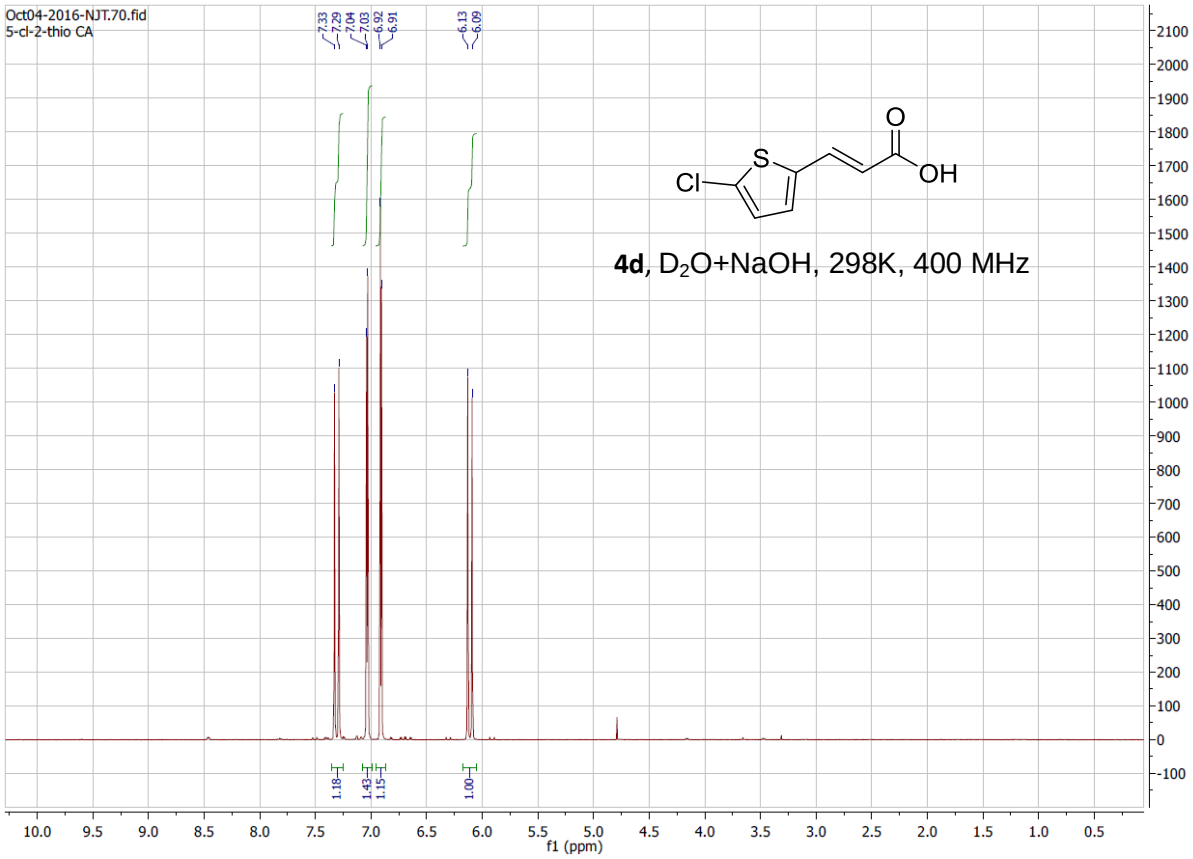

4d, D_2O+NaOH, 298K, 400 MHz

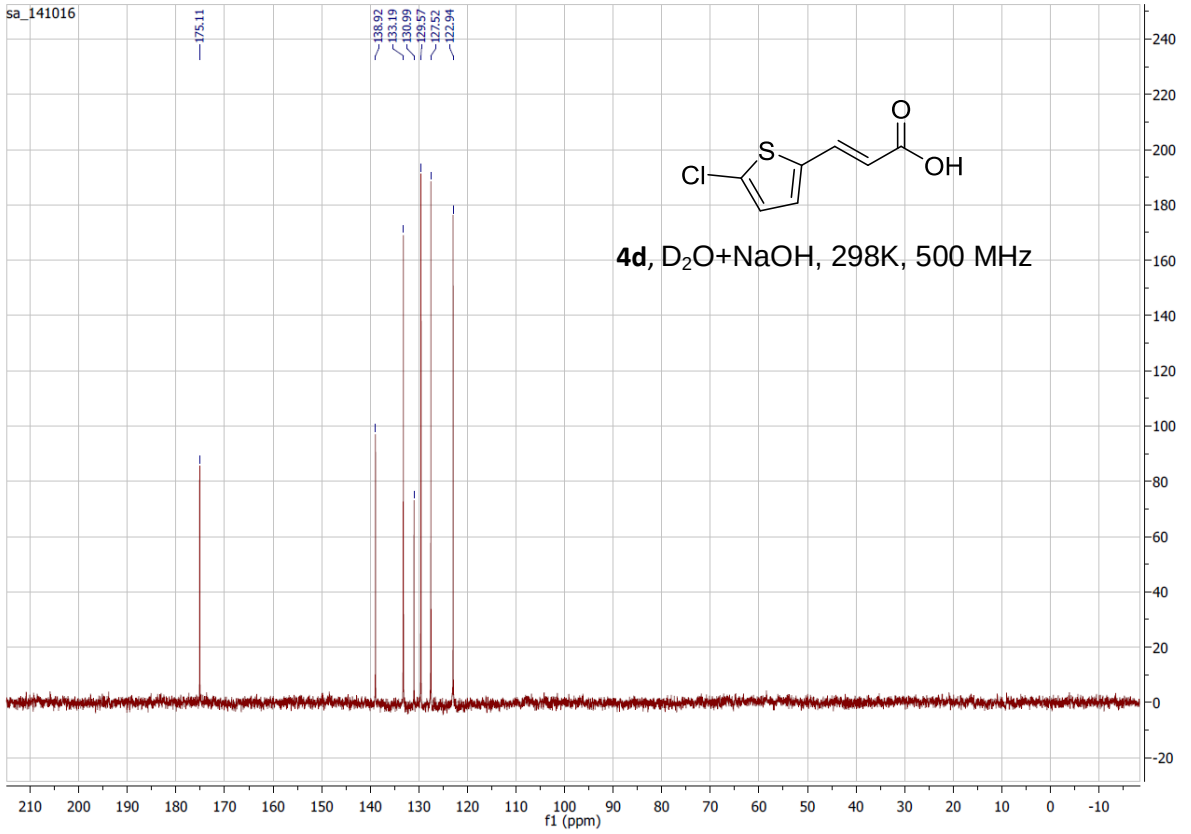

4d, D_2O+NaOH, 298K, 500 MHz

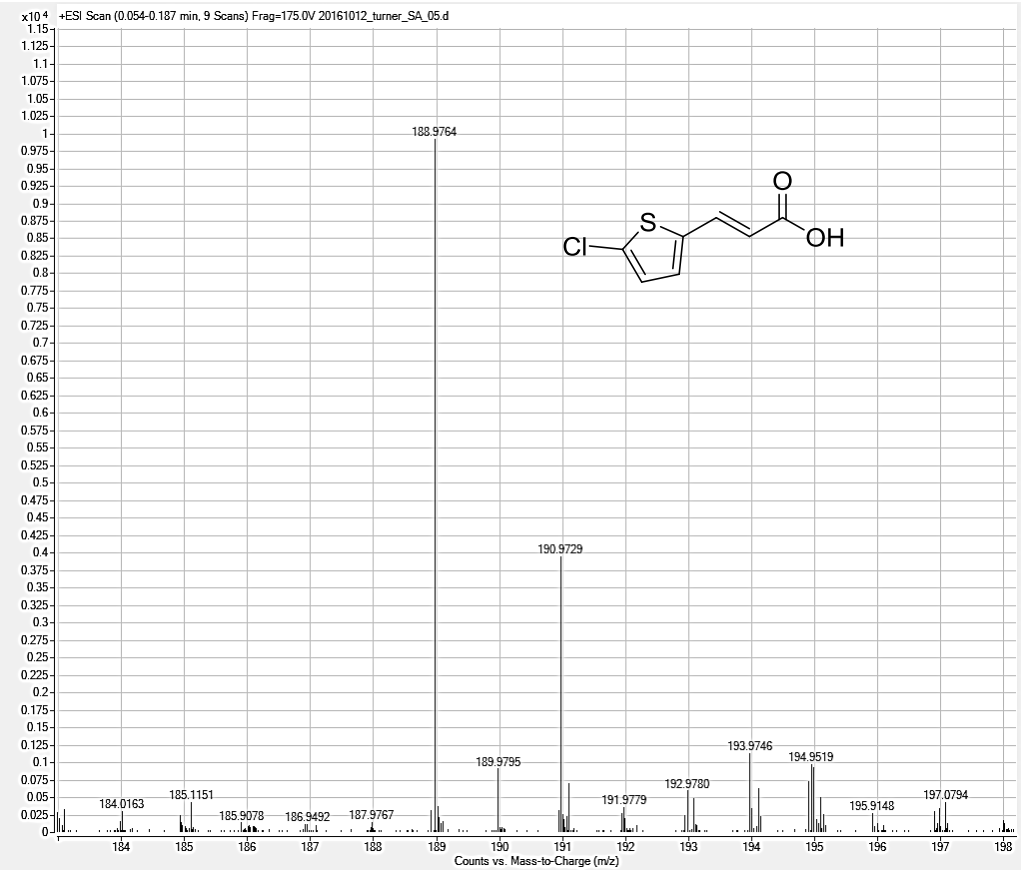
x10 4 +ESI Scan (0.054-0.187 min, 9 Scans) Frag=175.0V 20161012_turner_SA_05.d
188.9764
190.9729
189.9795
193.9746
194.9519
192.9780
191.9779
184.0163
185.1151
185.9078
186.9492
187.9767
195.9148
197.0794
Cl
S
O
OH
Counts vs. Mass-to-Charge (m/z)

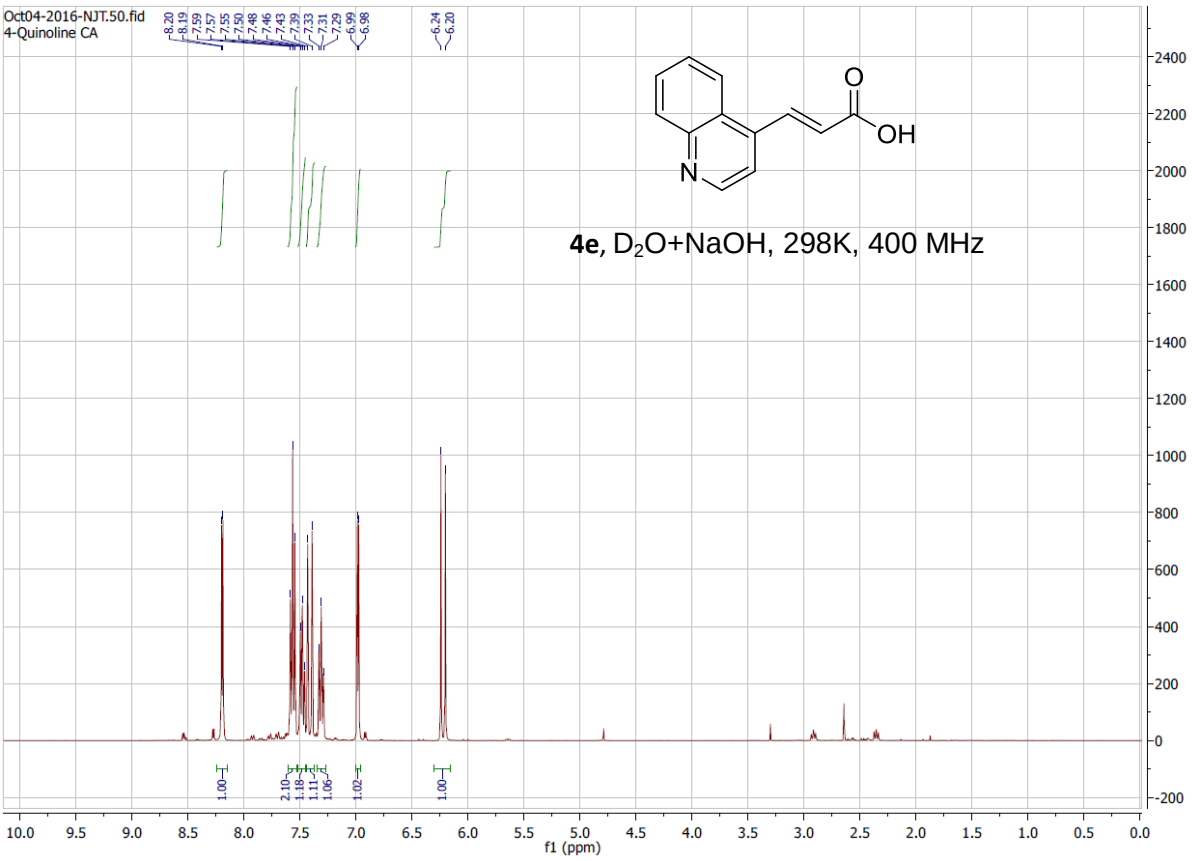

4e, D_2O+NaOH, 298K, 400 MHz

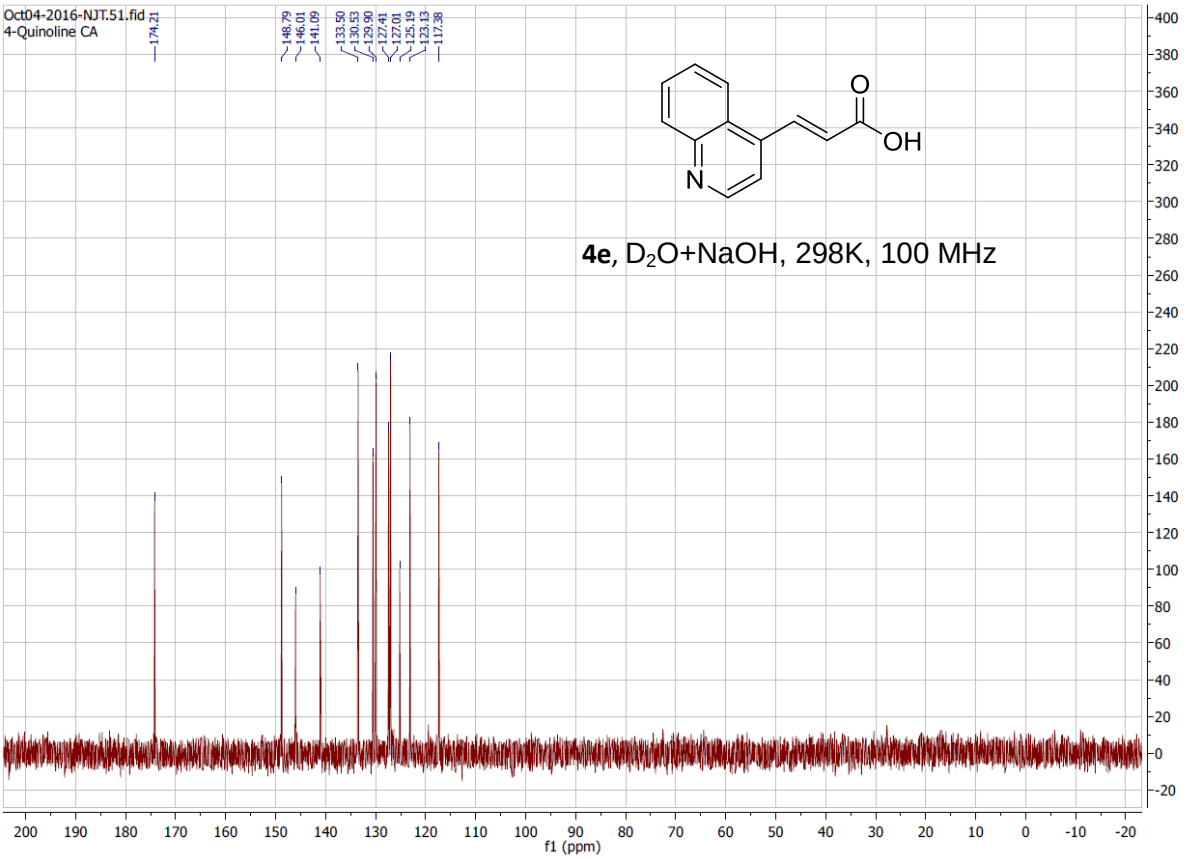

4e, D_2O+NaOH, 298K, 100 MHz

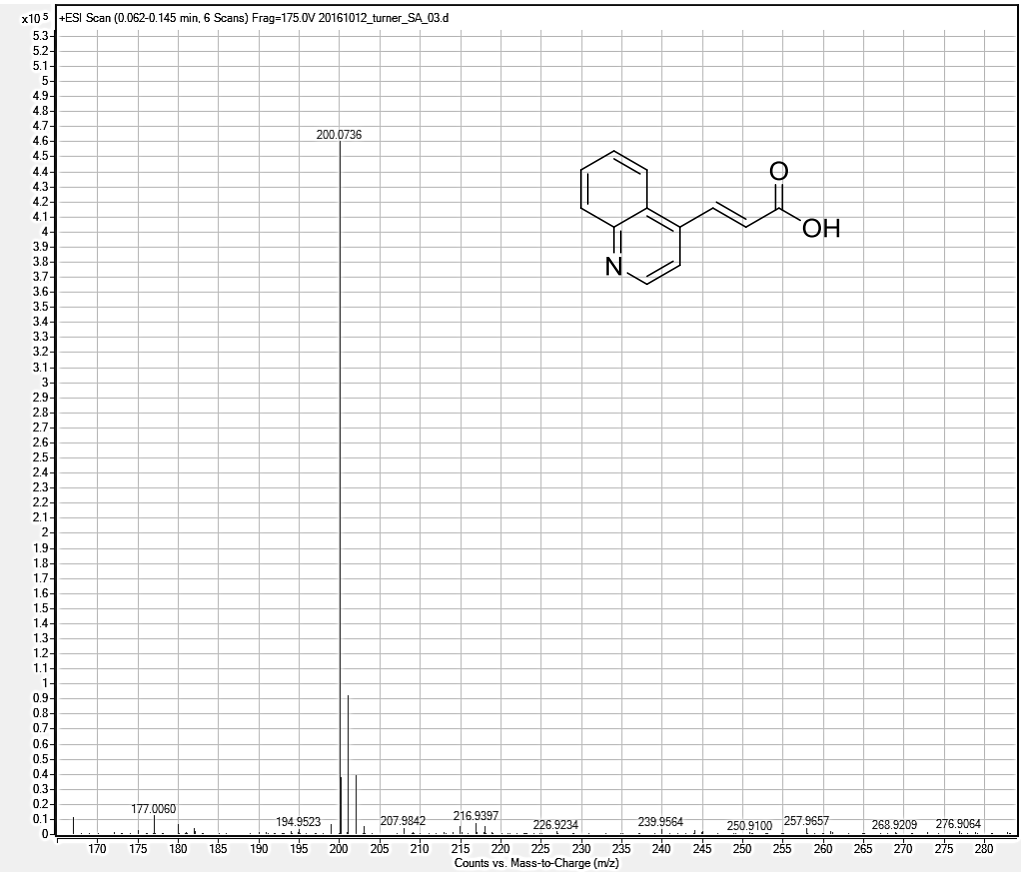
x10 5
+ESI Scan (0.062-0.145 min, 6 Scans) Frag=175.0V 20161012_turner_SA_03.d
200.0736
177.0060
194.9523
207.9842
216.9397
226.9234
239.9564
250.9100
257.9657
268.9209
276.9064
O
OH
N
Counts vs. Mass-to-Charge (m/z)

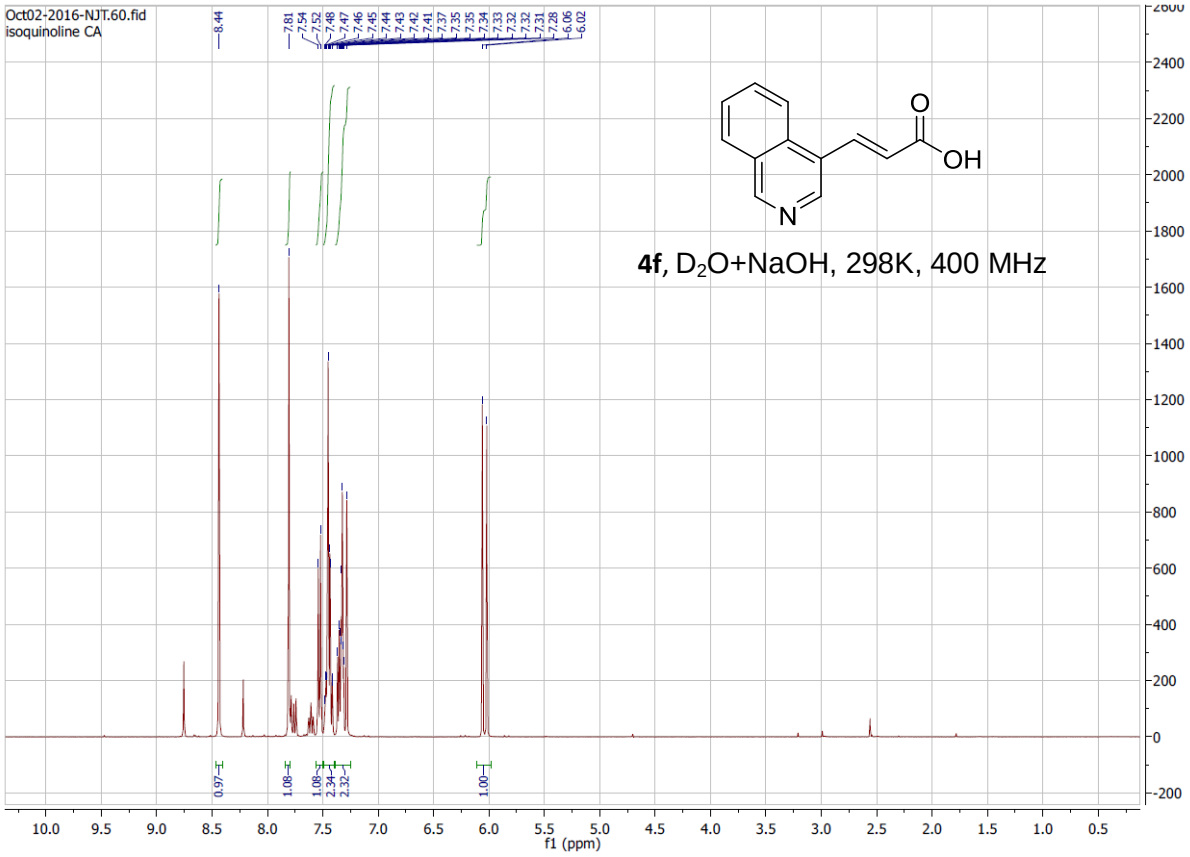
Oct02-2016-NJT.60.fid
isoquinoline CA
O
OH
N
4f, D2O+NaOH, 298K, 400 MHz
f1 (ppm)

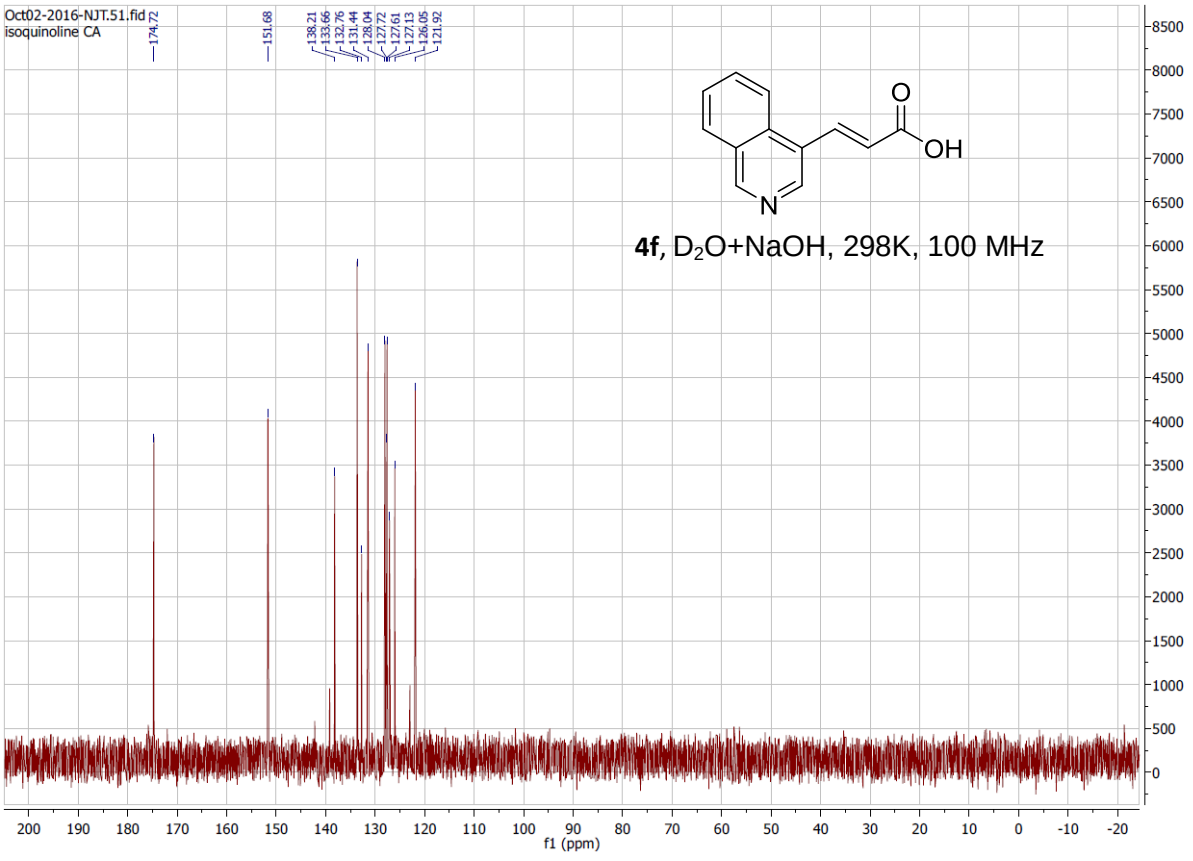
Oct02-2016-NJT.51.fid
isoquinoline CA
O
OH
N
4f, D2O+NaOH, 298K, 100 MHz
f1 (ppm)

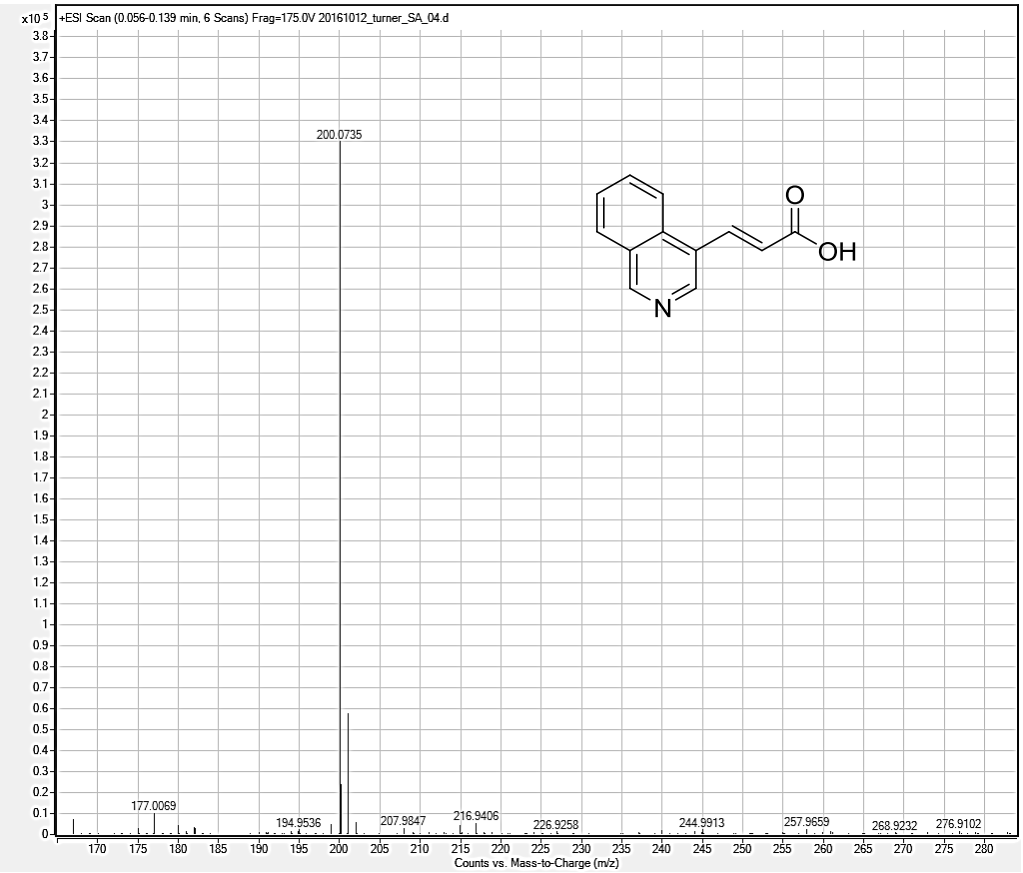
x10 5
+ESI Scan (0.056-0.139 min, 6 Scans) Frag=175.0V 20161012_turner_SA_04.d
200.0735
177.0069
194.9536
207.9847
216.9406
226.9258
244.9913
257.9659
268.9232
276.9102
O
OH
N
Counts vs. Mass-to-Charge (m/z)

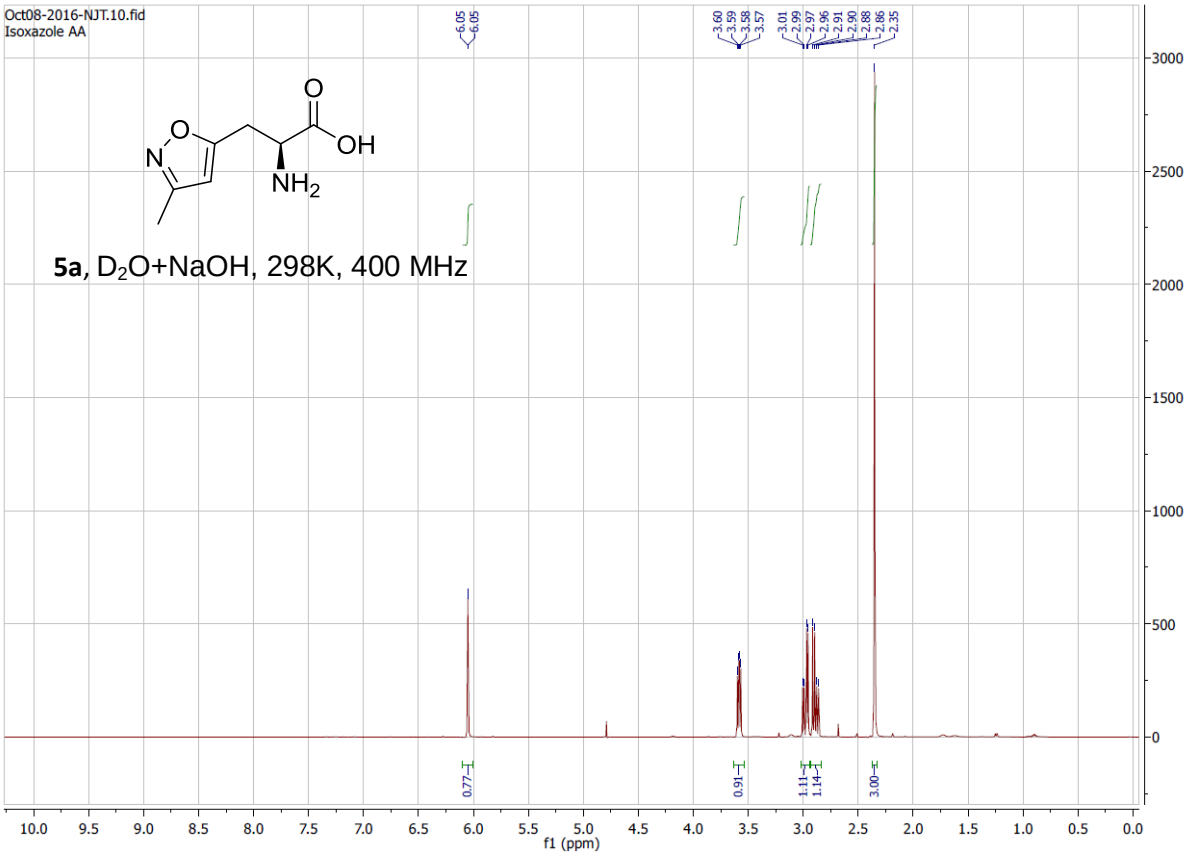

5a, D_2O+NaOH, 298K, 400 MHz

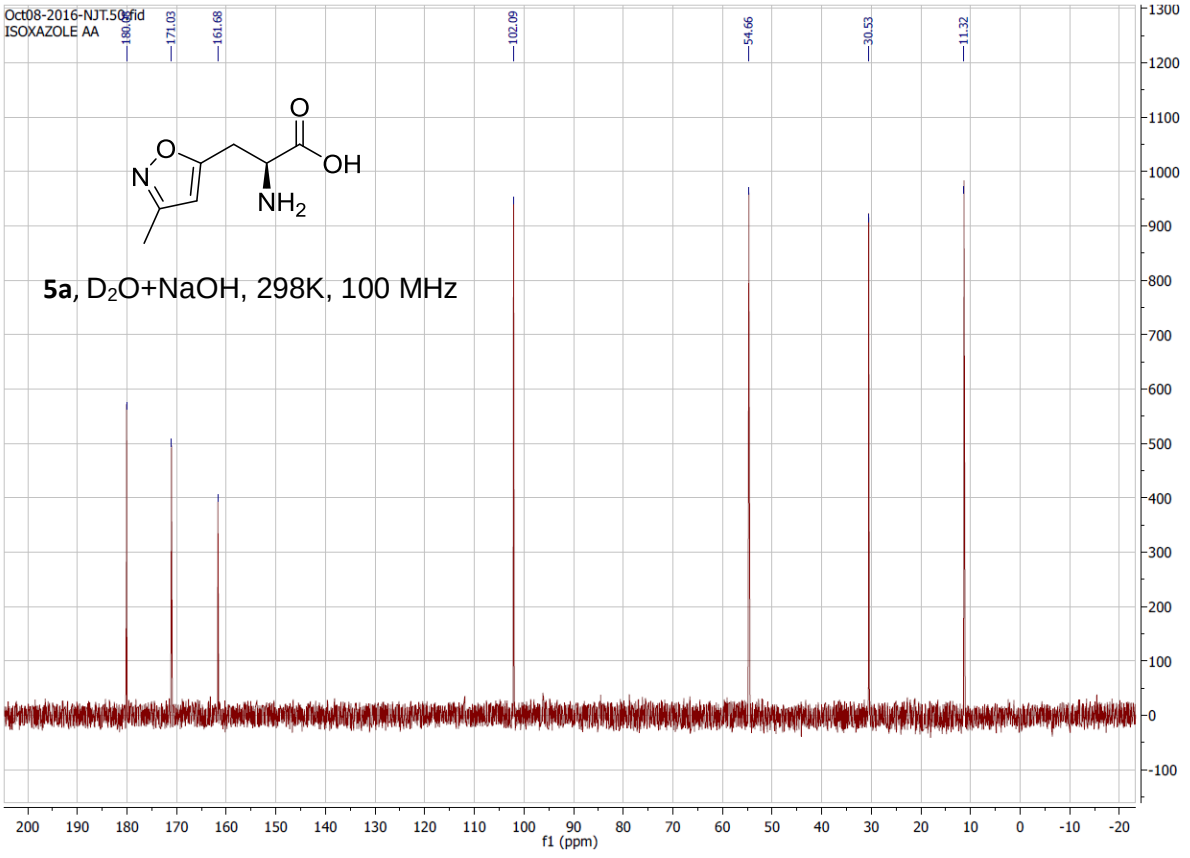

5a, D_2O+NaOH, 298K, 100 MHz

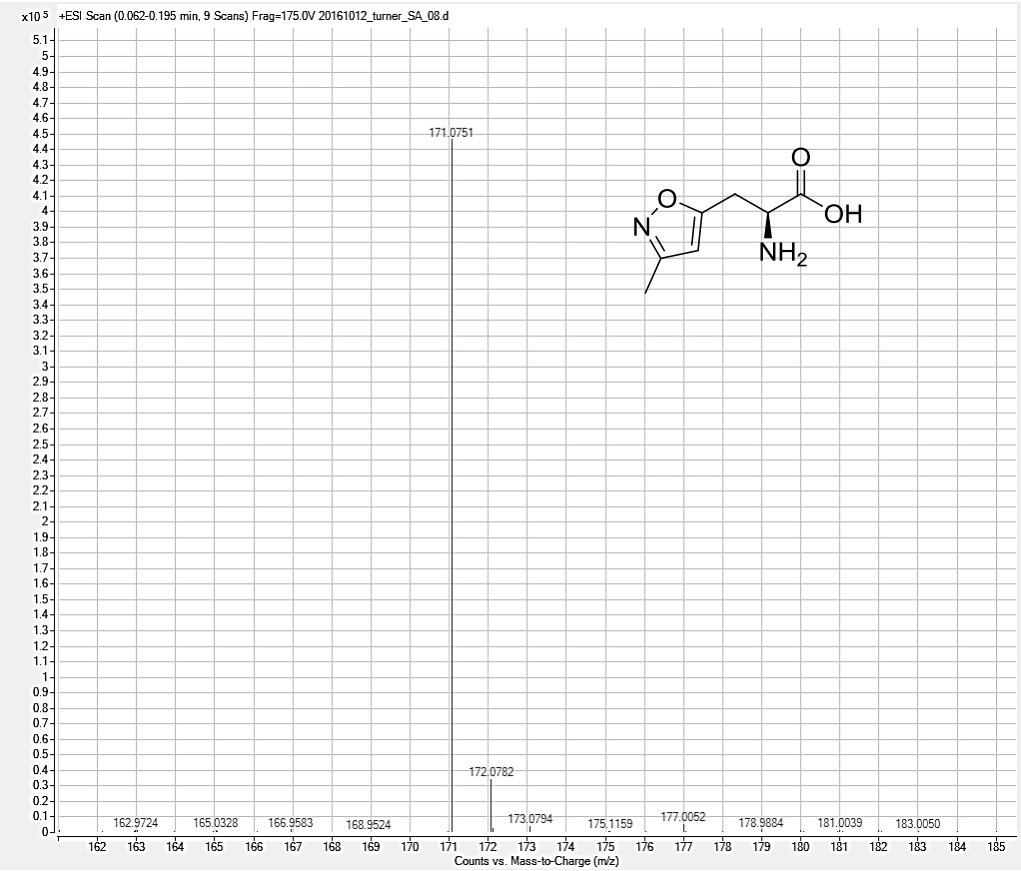
x10 5
+ESI Scan (0.062-0.195 min, 9 Scans) Frag=175.0V 20161012_turner_SA_08.d
171.0751
172.0782
162.9724
165.0328
166.9583
168.9524
173.0794
175.1159
177.0052
178.9884
181.0039
183.0050
O
O
N
OH
NH2
Counts vs. Mass-to-Charge (m/z)

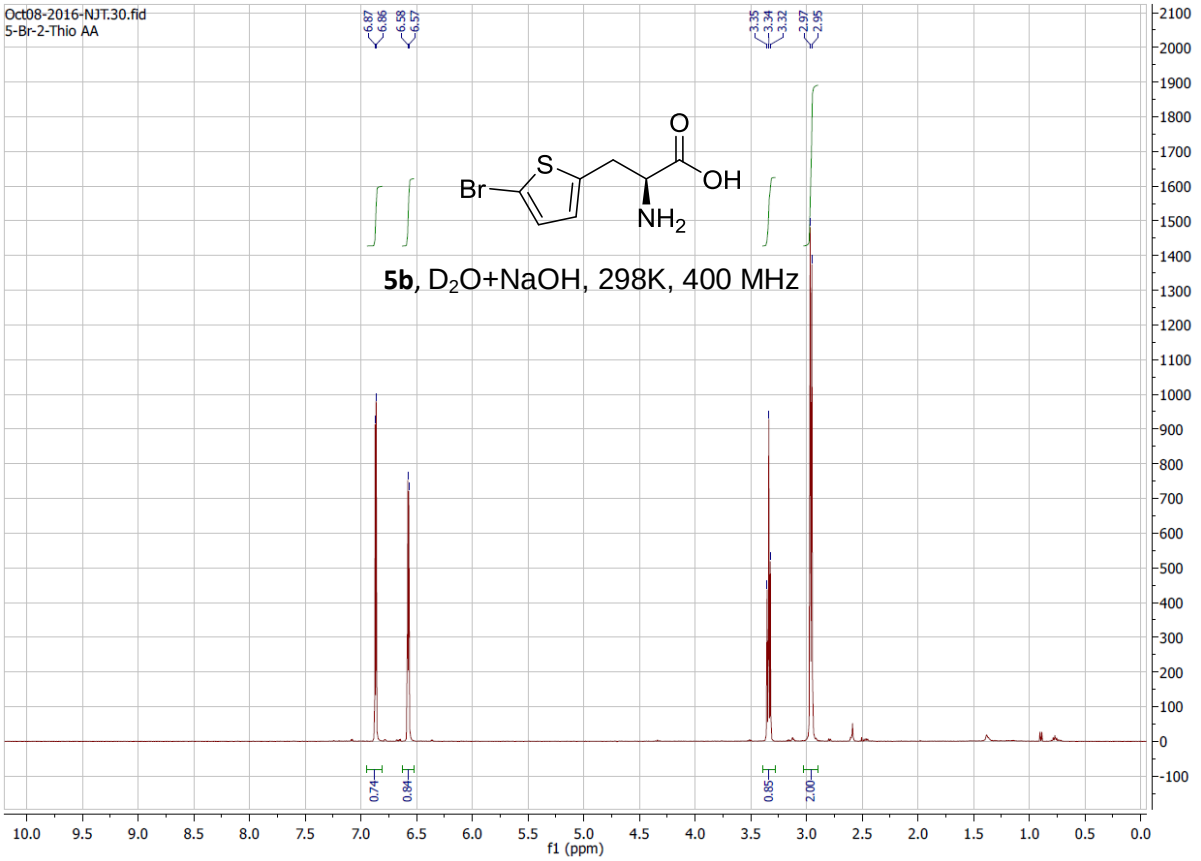

5b, D_2O+NaOH, 298K, 400 MHz

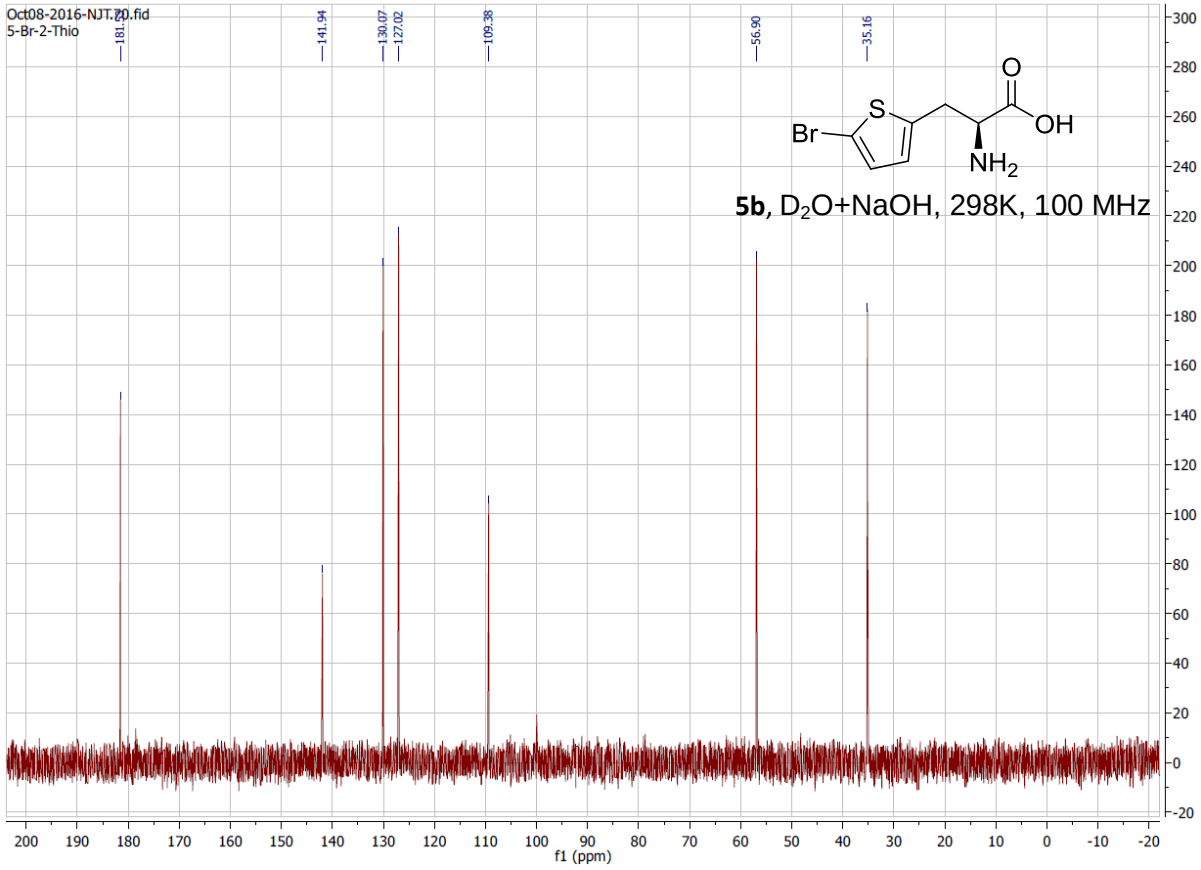

5b, D_2O+NaOH, 298K, 100 MHz

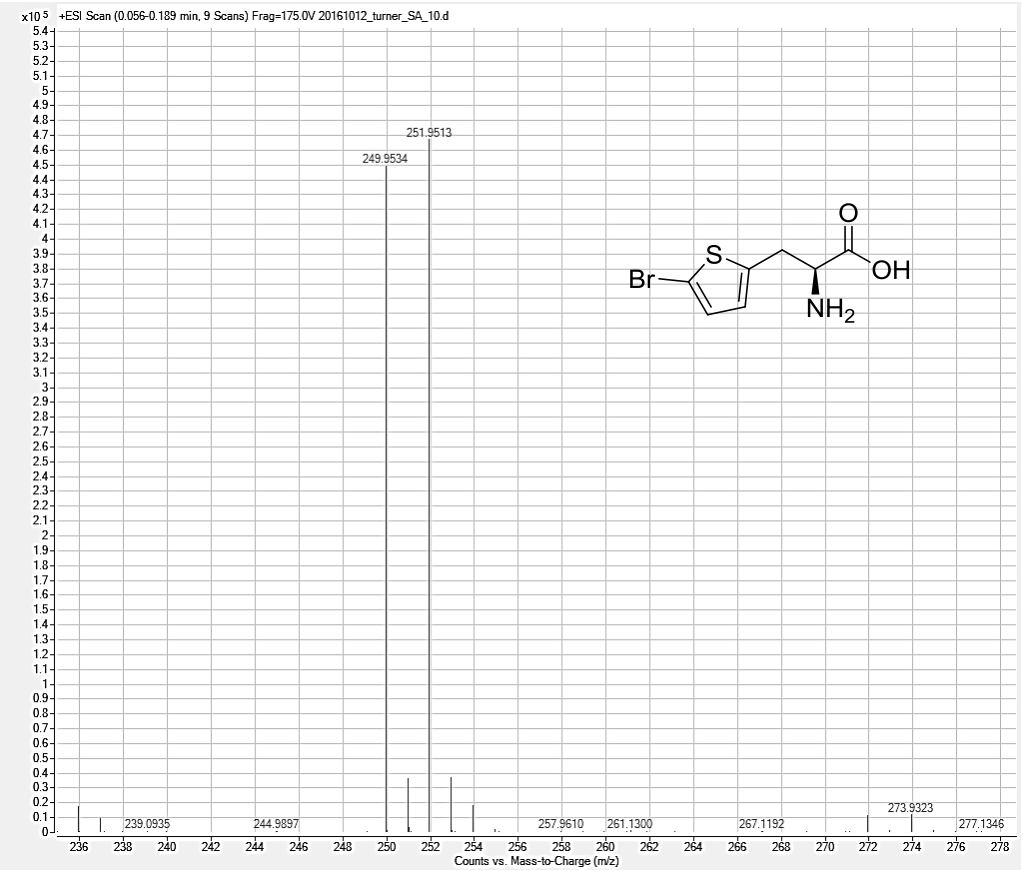
x10 5 +ESI Scan (0.056-0.189 min, 9 Scans) Frag=175.0V 20161012_turner_SA_10.d
251.9513
249.9534
239.0935
244.9897
257.9610
261.1300
267.1192
273.9323
277.1346
Counts vs. Mass-to-Charge (m/z)
Br
S
O
OH
NH2

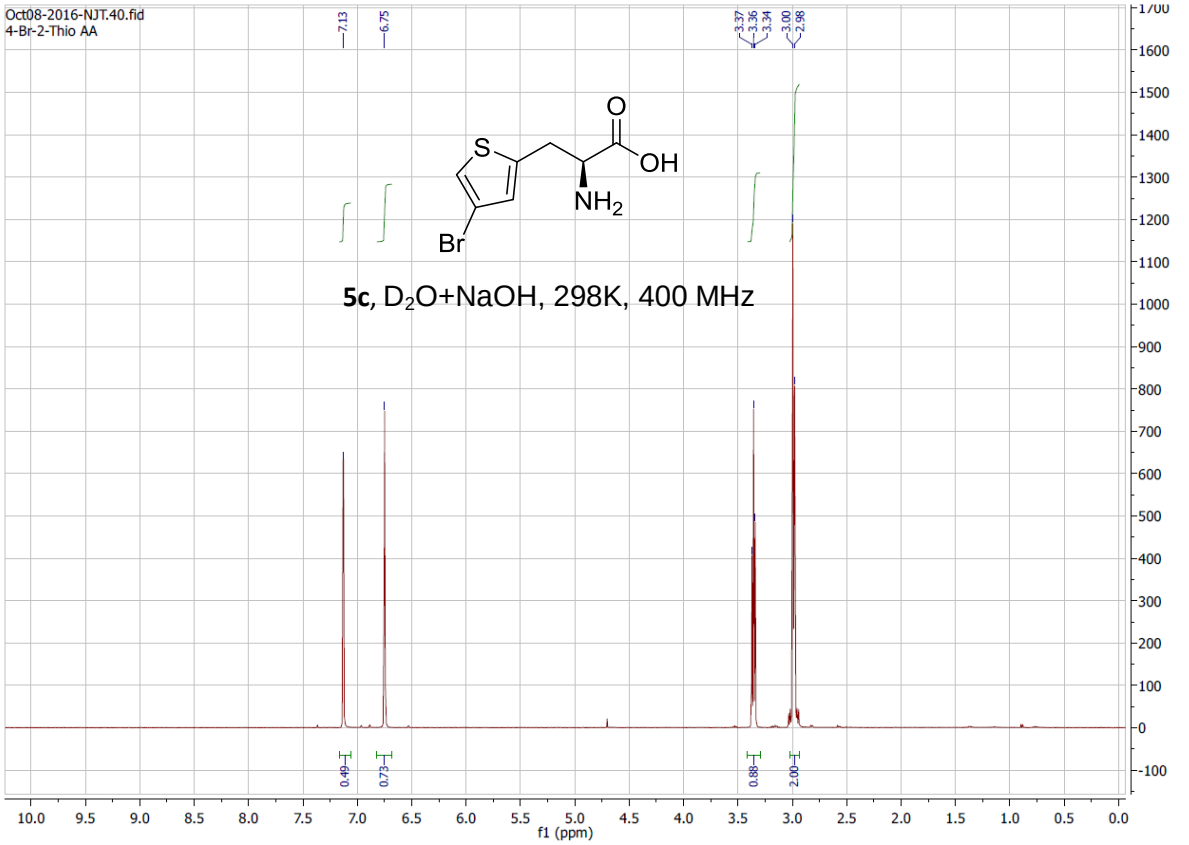

5c, D_2O+NaOH, 298K, 400 MHz

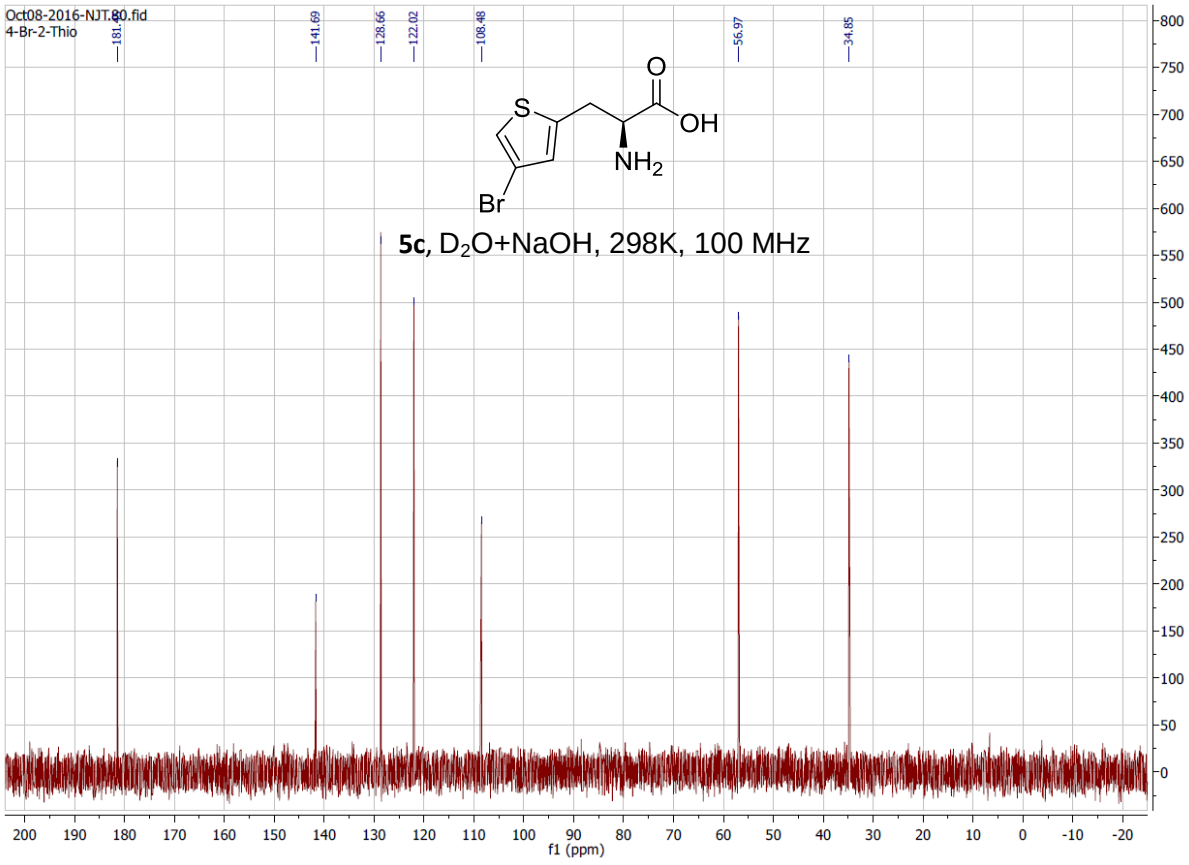

5c, D_2O+NaOH, 298K, 100 MHz

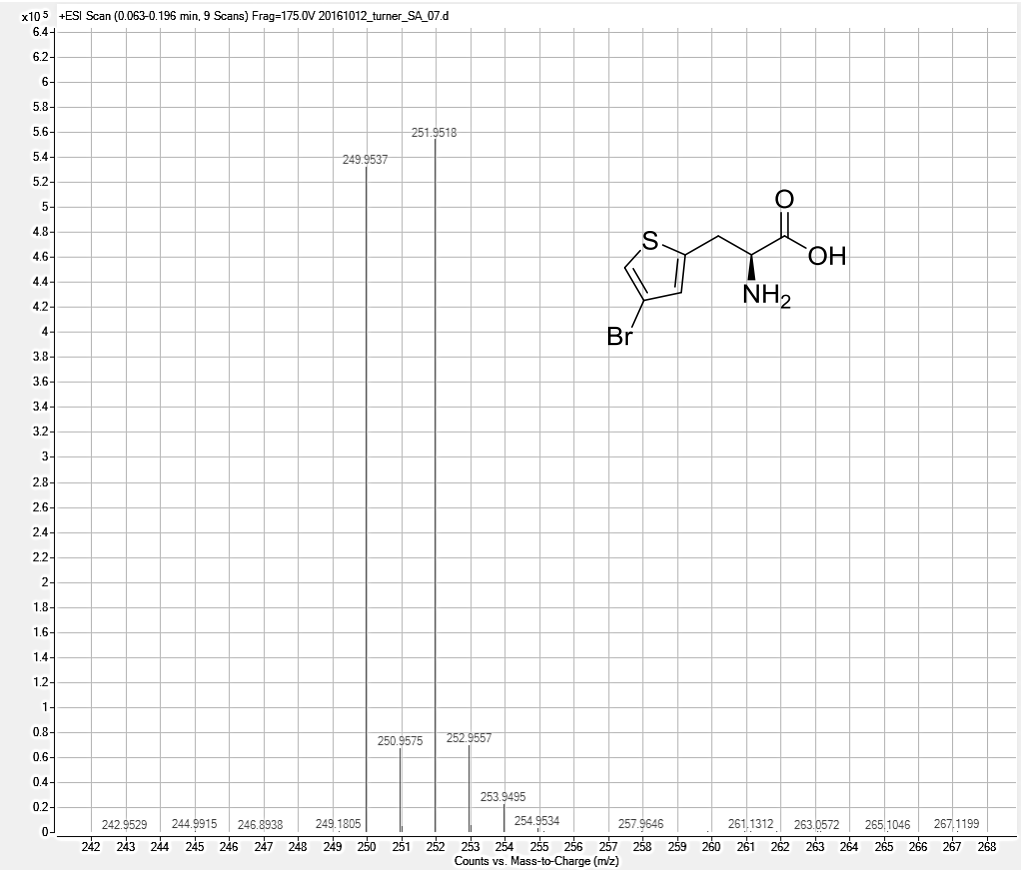
x10 5
+ESI Scan (0.063-0.196 min, 9 Scans) Frag=175.0V 20161012_turner_SA_07.d
249.9537
251.9518
250.9575
252.9557
253.9495
254.9534
242.9529
244.9915
246.8938
249.1805
257.9646
261.1312
263.0572
265.1046
267.1199
Counts vs. Mass-to-Charge (m/z)
S
O
OH
NH2
Br

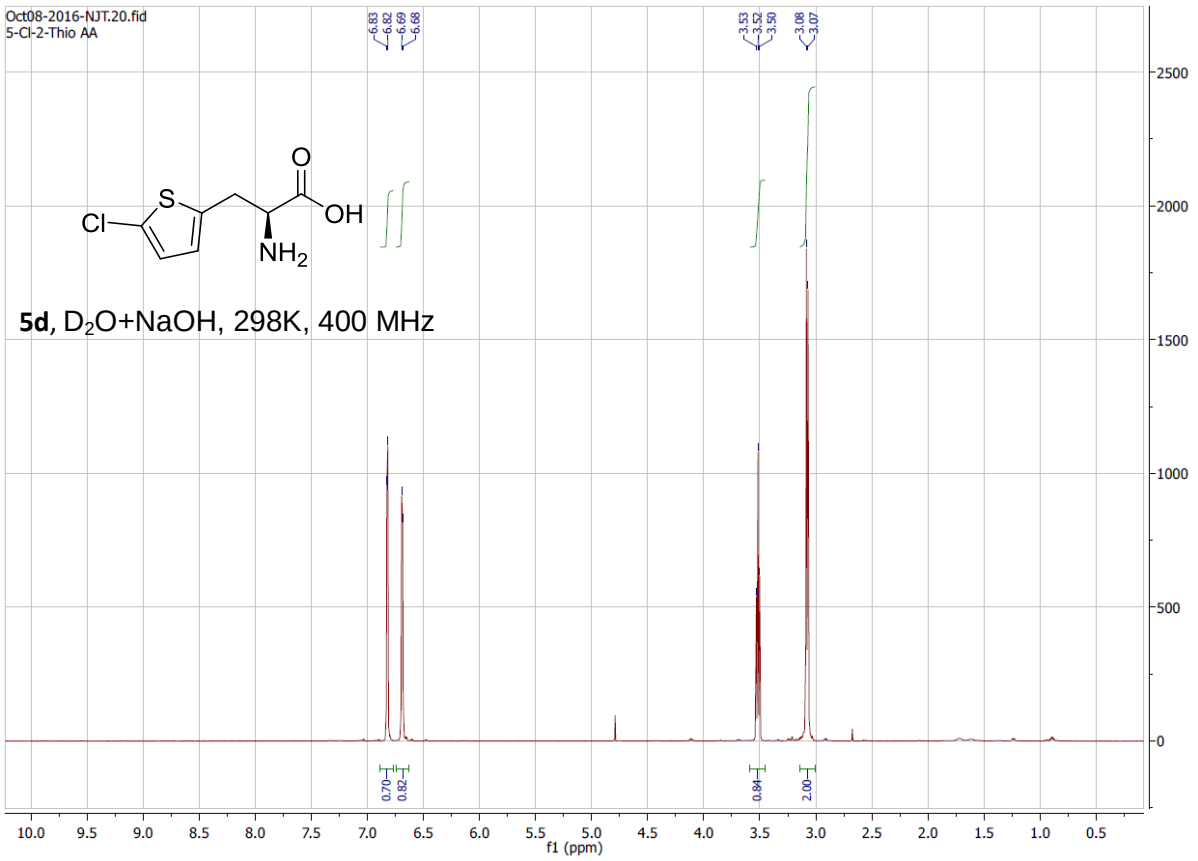
Oct08-2016-NJT.20.fid
5-Cl-2-Thio AA
6.83
6.82
6.69
6.68
3.53
3.52
3.50
3.08
3.07
Cl
S
O
OH
NH2
5d, D2O+NaOH, 298K, 400 MHz
0.70
0.82
0.84
2.00
f1 (ppm)

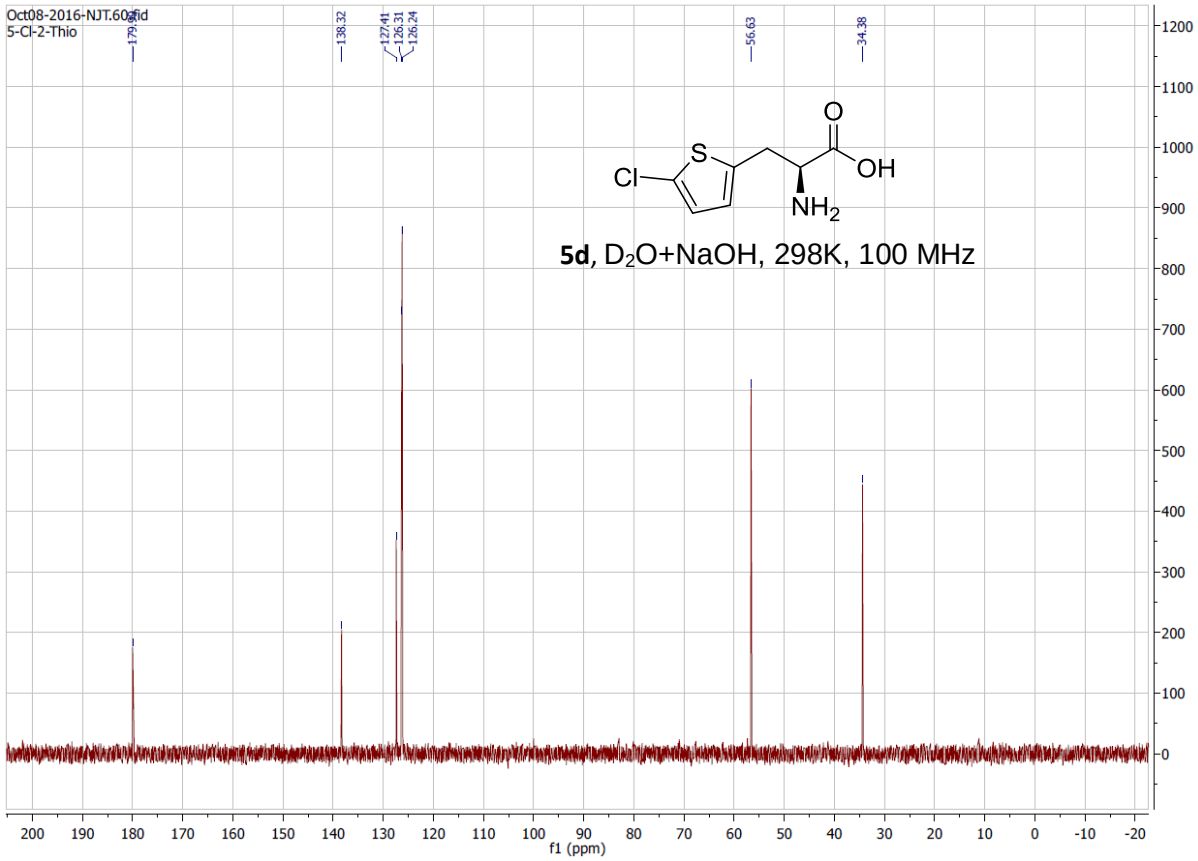
Oct08-2016-NJT.60.fid
5-Cl-2-Thio
179.80
138.32
127.41
126.31
126.24
56.63
34.38
Cl
S
O
OH
NH2
5d, D2O+NaOH, 298K, 100 MHz
f1 (ppm)

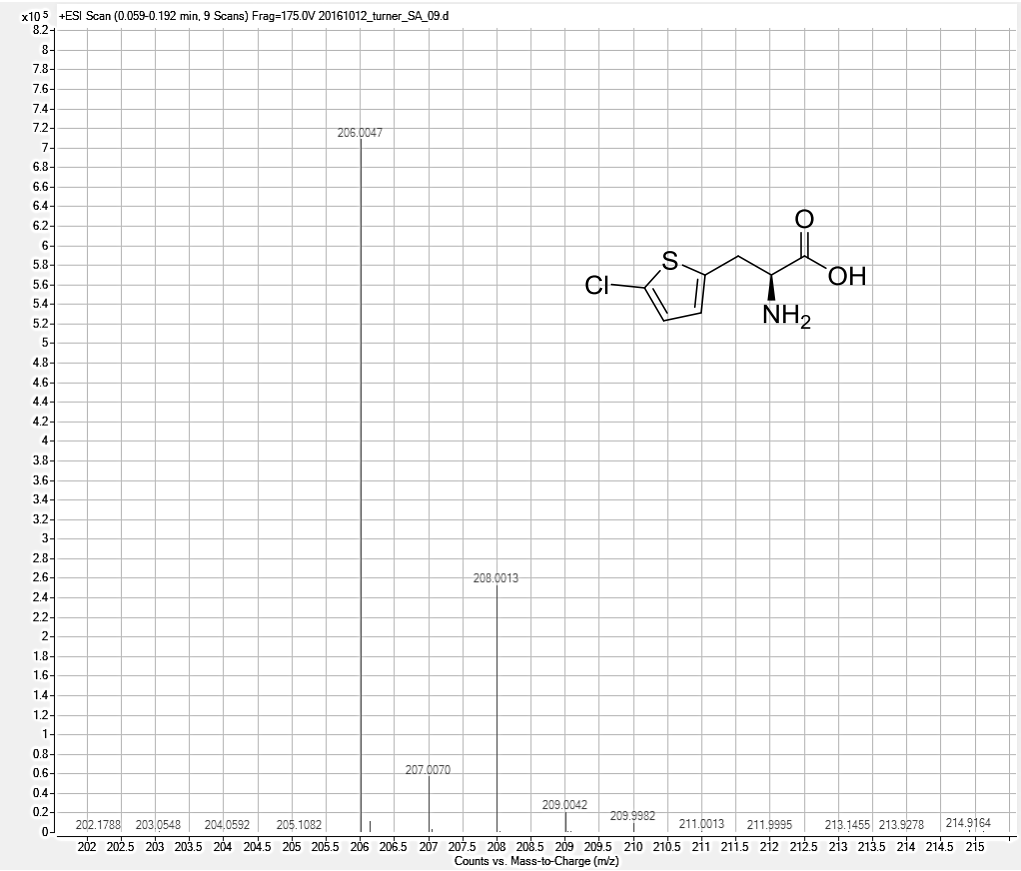
x10 5 +ESI Scan (0.059-0.192 min, 9 Scans) Frag=175.0V 20161012_turner_SA_09.d
206.0047
208.0013
207.0070
209.0042
209.9982
202.1788
203.0548
204.0592
205.1082
211.0013
211.9995
213.1455
213.9278
214.9164
Counts vs. Mass-to-Charge (m/z)
Cl
S
O
OH
NH2

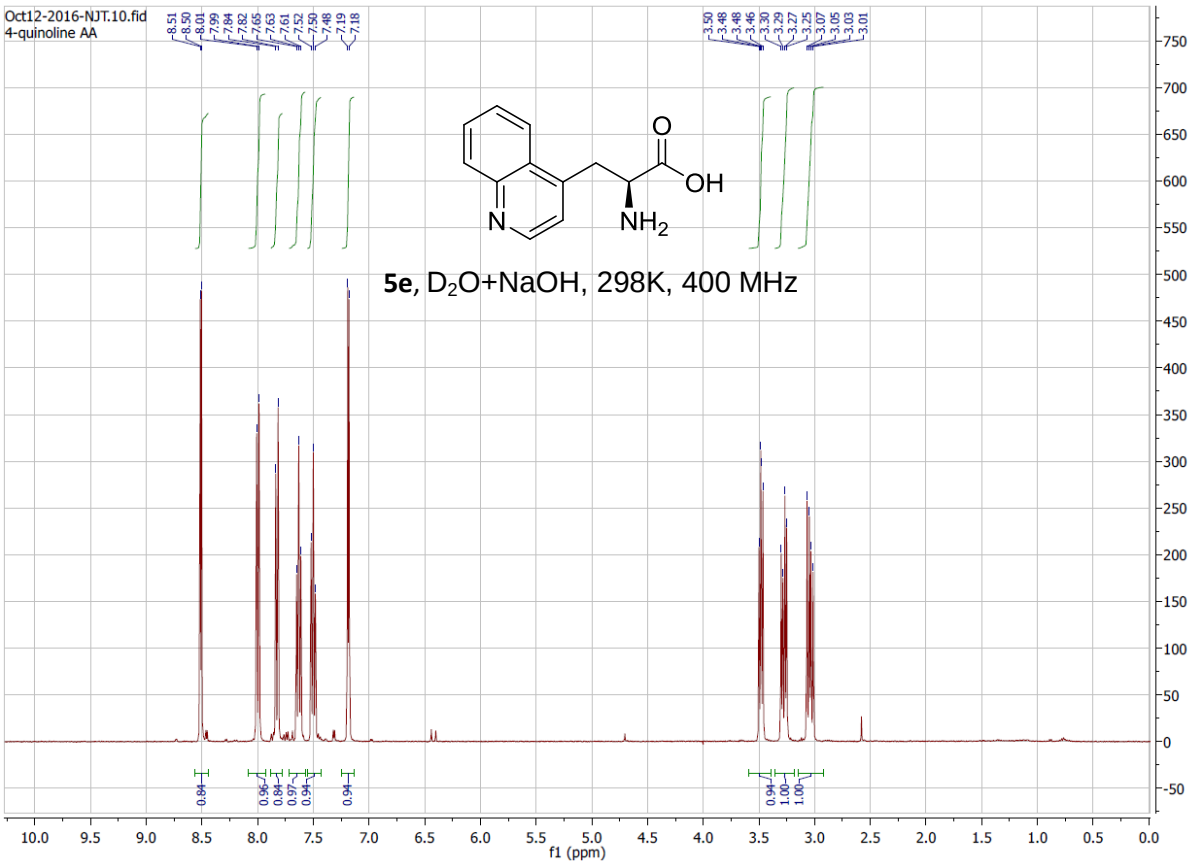
Oct12-2016-NJT.10.fid
4-quinoline AA
O
OH
N
NH2
5e, D2O+NaOH, 298K, 400 MHz
f1 (ppm)

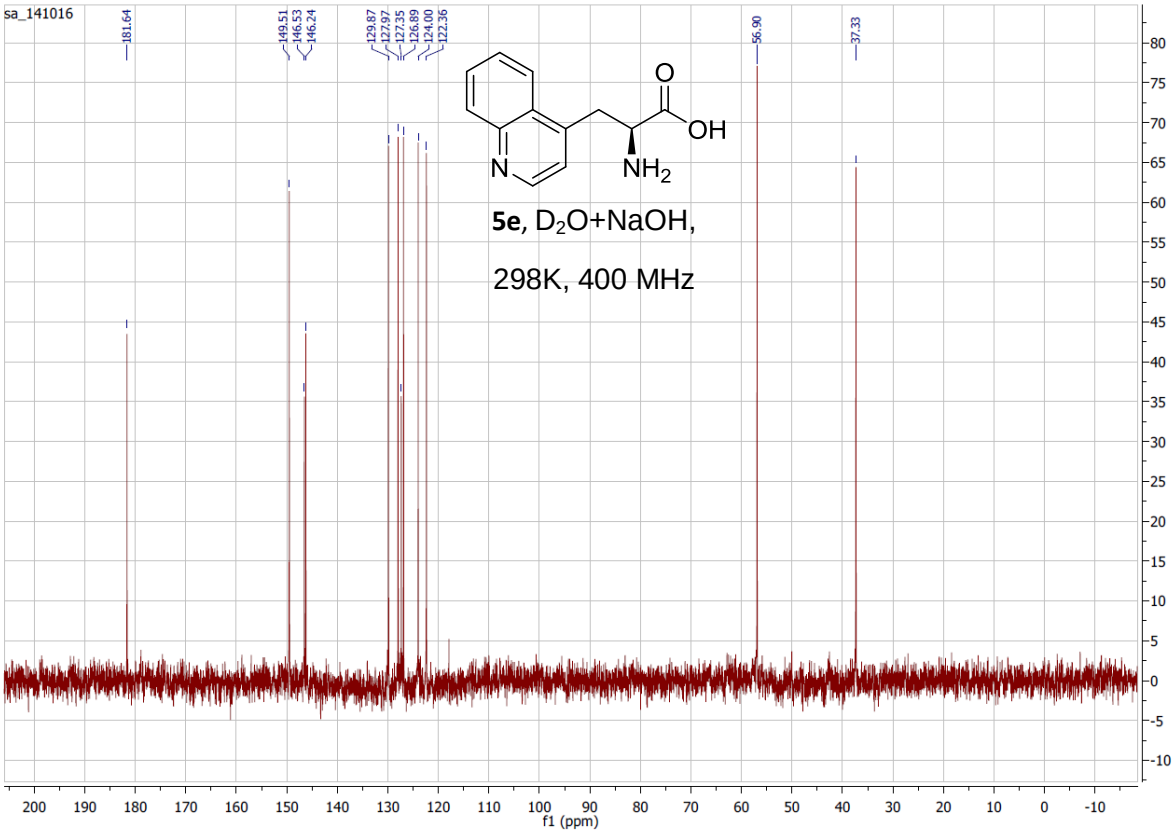
sa_141016
O
OH
N
NH2
5e, D2O+NaOH,
298K, 400 MHz
f1 (ppm)

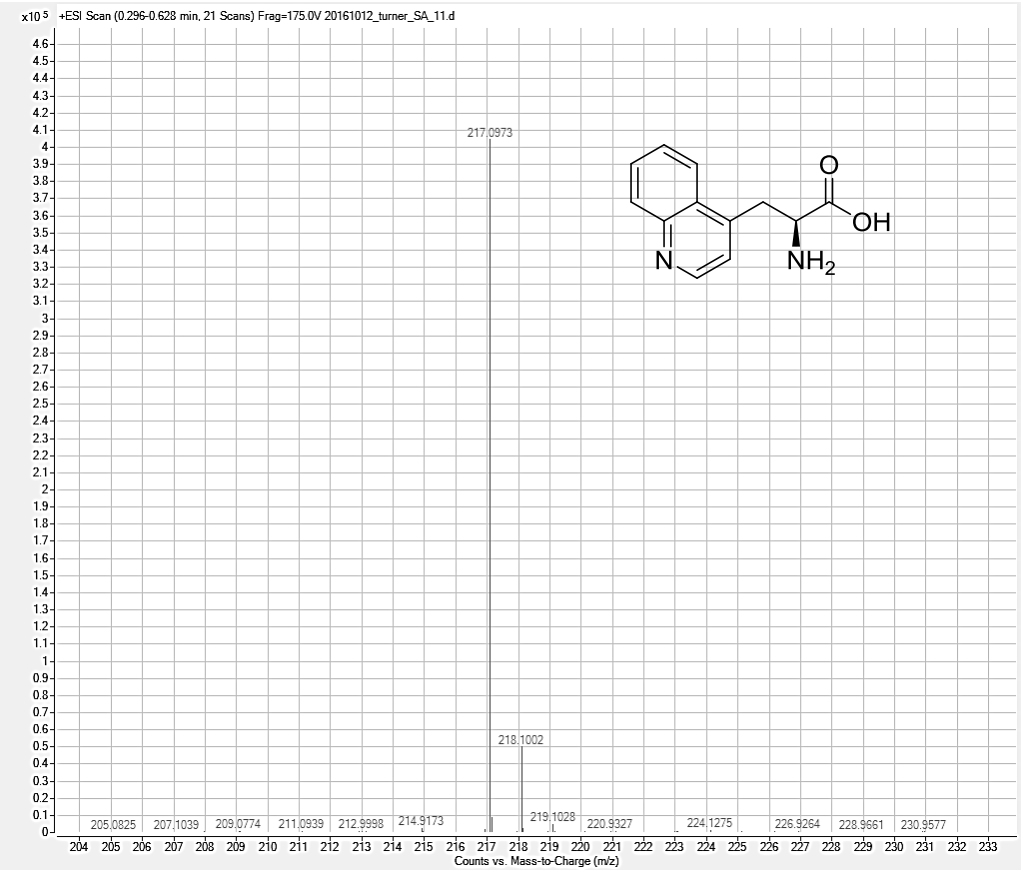
x10 5 +ESI Scan (0.296-0.628 min, 21 Scans) Frag=175.0V 20161012_turner_SA_11.d
217.0973
218.1002
205.0825
207.1039
209.0774
211.0939
212.9998
214.9173
219.1028
220.9327
224.1275
226.9264
228.9661
230.9577
O
OH
N
NH2
Counts vs. Mass-to-Charge (m/z)

References

1. Lovelock, S. L.; Lloyd, R. C.; Turner, N. J. *Angew. Chem. Int. Ed.* **2014**, *53*, 4652-4656.
2. Studier, F. W. *Prot. Expr. Purif.* **2005**, *41*, 207-234.
3. Alexandre, F.-R.; Pantaleone, D. P.; Taylor, P. P.; Fotheringham, I. G.; Ager, D. J.; Turner, N. J. *Tetrahedron Lett.* **2002**, *43*, 707-710.